



RESEARCH & DEVELOPMENT

Compare NCDOT Bridge Scour Calculations to USGS SIR 2016-5121 South Carolina (SC) Scour Envelope Curves Results

Brina Montoya, Ph.D., PE
Mohammed Gabr, Ph. D., PE

Graduate Students:

Azmayeen Shahriar
Hanieh Mohamadi Moghadam

**Department of Civil, Construction, and Environmental Engineering
North Carolina State University**

Alejandra C. Ortiz, Ph. D.
Undergraduate Student:
Lottie Franck

**Department of Geology
Colby College**

**NCDOT Project 2020-06
September 2022**

Compare NCDOT Bridge Scour Calculations to USGS SIR 2016-5121 South Carolina (SC) Scour Envelope Curves Results

DRAFT FINAL REPORT

Prepared by:

Brina Montoya, Ph.D., PE
Mohammed Gabr, Ph. D., PE
Alejandra C. Ortiz, Ph. D.
Azmayeen Shahriar
Hanieh Mohamadi Moghadam
Lottie Franck

A report on research sponsored by:

THE NORTH CAROLINA DEPARTMENT OF TRANSPORTATION

June 2022

1. Report No. 2020-06	2. Government Accession No. ...leave blank...	3. Recipient's Catalog No. ...leave blank...	
4. Title and Subtitle Compare NCDOT Bridge Scour Calculations to USGS SIR 2016-5121 South Carolina (SC) Scour Envelope Curves Results		5. Report Date June 2022	6. Performing Organization Code ...leave blank...
		8. Performing Organization Report No. ...leave blank...	
7. Author(s) Brina Montoya, Mohammed Gabr, Alejandra C. Ortiz, Azmayeen Shahriar, Hanieh Mohamadi Moghadam, Lottie Franck		10. Work Unit No. (TRAIS) ...leave blank...	
9. Performing Organization Name and Address NORTH CAROLINA STATE UNIVERSITY Department of Civil, Construction, and Environmental Engineering Campus Box 7908, Raleigh, NC 27695-7908		11. Contract or Grant No. ...leave blank...	
		13. Type of Report and Period Covered Final Report August 1, 2019 - May 15, 2022	
12. Sponsoring Agency Name and Address North Carolina Department of Transportation Research and Development Unit 104 Fayetteville Street Raleigh, North Carolina 27601		14. Sponsoring Agency Code NCDOT Project #2020-06	
		Supplementary Notes: ...leave blank...	
<p>Abstract: In the research herein we focus on estimating the magnitude of scour at bridge sites using three different approaches: the SC Scour Envelope Curves, four simple analytical models in literature including HEC-18, and the use of advanced numerical model (Delft3D.) Field work is performed at four bridge sites and measurements of flow, bathymetry, and geometry data are obtained for calibration of the numerical modeling approach. Results from the various approaches are compared to provide the NCDOT with model performance data that are focused on assessing the magnitude of scour at bridge sites. Five scour analytical prediction models are assessed in terms of two statistical parameters, termed Mean Absolute Percentage Error (MAPE,) as a measure of accuracy of the prediction, and “level of conservatism” (as a measure of percent of cases where scour estimates from a given approach exceeded measured values.) Analyses performed using clear water data collected by Benedict and Caldwell (2014) indicated values of MAPE ranged from 238% to 336%, whereas conservatism ranged from 77% to 97.8%. Briaud (2014) model presented the least error (238%), and SC Envelope (2018) model presented the highest error (336%). The use of the SC Envelope model provided the most conservative scour depth (97.8%), whereas Briaud (2014) model presented the least conservatism (77%). In parallel when the live bed laboratory data collected in Benedict and Caldwell (2014) were used, values of MAPE ranged from 23.5% to 1218% with the SC envelope approach yielding the higher end of the MAPE, whereas conservatism ranged from 28.4% to 100%. The accuracy and conservatism of a specific model can however be adjusted by multiplying the scour depth by proposed modification factors. Focusing on the Roanoke River bridge site, the scour prediction from the deterministic approaches provided a scour depth in the range of 2.37 m to 3.24 m. These values are one order of magnitude higher than the scour estimated from the Delft 3D numerical approach. The scour estimates from Delft 3D were however obtained using the temporal hydrograph of 100-year flood event (where the water depth and velocities varied over a period of 30 days), while the scour estimates from the analytical model equations provide pier scour at equilibrium, assuming the water depth and velocities corresponding to the 100-year flood at the structure. A relationship between reliability index and scour factors is introduced herein. These “scour factors” are proposed for application to the deterministic scour predictions to account for uncertainty and inherent model bias.</p>			
17. Key Words Scour, bridge pier, abutment scour, numerical modeling		18. Distribution Statement ...leave blank...	
19. Security Classif. (of this report) Unclassified	20. Security Classif. (of this page) Unclassified	21. No. of Pages	22. Price ...leave blank...

DISCLAIMER

The contents of this report reflect the views of the author(s) and not necessarily the views of the University. The author(s) are responsible for the facts and the accuracy of the data presented herein. The contents do not necessarily reflect the official views or policies of either the North Carolina Department of Transportation or the Federal Highway Administration at the time of publication. This report does not constitute a standard, specification, or regulation.

ACKNOWLEDGMENTS

The authors would like to acknowledge the support of the North Carolina Department of Transportation Office of Research and Development. A special “thank you” is expressed to the Project’s steering committee members for their valuable technical input, including providing site data and facilitating site visit, throughout the project period. The technical support provided by Mr. Jerry Snead (deceased,) Brian Radakovic, Matt Lauffer, Stephen Benedict, Corey Cavalier, is greatly acknowledged. Additionally, the authors would like to thank Mr. Dave Langston, Mr. Walter Hunt, and Mr. Stephen Sykes for their planning and on-site support of the project fieldwork activities.

EXECUTIVE SUMMARY

At present, there are more than twenty pier-scour analytical models available in literature. These models are developed in most cases from extensive laboratory testing data or based on limited field data. In parallel, representative approaches for estimating first order scour magnitude can be used for comparative classification of “scour- critical” hydraulic structures and for providing an upper bound of scour depth. The South Carolina (SC) Bridge-Scour Envelope criteria were developed for such first order estimate of scour. The robustness and limitation of the first order scour estimates obtained by applying the SC criteria are the focus herein. The research aims at assessing the accuracy of the scour predictions using the Scour Envelope for use by the North Carolina Department of Transportation (NCDOT). We estimate bridge scour using three different approaches: the SC Scour Envelope Curves, simple analytical models in literature including HEC-18, and the use of advance numerical model (Delft3D.) In addition, field work is performed at four sites provided measurements of flow, bathymetry, and bridge geometry data for calibration of the numerical modeling. We then compare the results from the methodologies/approaches to provide the NCDOT with comparative results regarding options for estimation of the magnitude of scour at bridge sites.

Five bridge scour prediction models including Wilson (1995) model, Melville (1997) model, Hydraulic Engineering Circular (HEC) No. 18 (2012) model (HEC 18), Briaud (2014) model, and the SC Bridge-Scour Envelope (SC) are assessed in terms of two statistical parameters, termed Mean Absolute Percentage Error (MAPE,) as a measure of accuracy of the prediction, and “level of conservatism” (as a measure of percent of cases where scour estimates from a given approach exceeded measured values.) Analyses performed using clear water data collected by Benedict and Caldwell (2014) indicated values of MAPE ranged from 238% to 336%, whereas conservatism ranged from 77% to 97.8%. Briaud (2014) model presented the least error (238%), and SC Envelope (2018) model presented the highest error (336%). The use of the SC Envelope (2018) model provided the most conservative scour depth (97.8%), whereas Briaud (2014) model presented the least conservatism (77%). In parallel when the live bed laboratory data collected in Benedict and Caldwell (2014), were used, values of MAPE ranged from 23.5% to 1218% with the SC envelope approach yielding the higher end of the MAPE, whereas conservatism ranged from 28.4% to 100%. Utilizing live bed field data, MAPE ranged from 205.6% to 322% for the five models considered herein. In this case, the SC envelope model also provided the most conservative estimate (97.5%), while HEC 18 (2012) model provided the least conservative scour depth estimate (93.3%). When the limitation of SC envelope curve approach of nominal pier width ≤ 6 ft is imposed, the level of conservatism does not differ significantly (less than 1%) and the MAPE for the SC approach slightly increased from 322% to 349%.

The scour magnitudes estimated from Delft3D were compared to data from the scour estimation approaches suggested by South Carolina envelope (2018) model, Wilson (1995) model, Melville (1997) model, HEC 18 (2012) model and Briaud (2014) model. The scour prediction from the deterministic approaches provides a scour depth of 237 cm to 324 cm, which is one order of magnitude higher than the scour estimated from the numerical approach. However, while the scour estimates from the numerical model using Delft 3D were obtained using the temporal hydrograph of 100-year flood event (where the water depth velocities varied over a period of 30 days), the

estimates from the simple analytical model equations provide pier scour at equilibrium assuming water depth and velocities corresponding to the 100-year flood.

The numerical analyses using Delft 3D proceeded by first establishing equilibrium morphology then inducing the 100-year flood transient flow rate to assess the change in morphology and discern the scour magnitude. Utilizing the Roanoke River morphology and flood parameters with 100-year return period yielded pier scour magnitude slightly higher than the case in which 200-year flood constant discharge was used. This is due to overland flow and less channelized flow toward the pier. Results from the Delft3D numerical approach are insightful and field spatial morphology can be reasonable represented. However the use of such advanced numerical analyses is best utilized when simulating larger river systems as such modeling is time intensive both in the creation of the discretized global mesh and the running of various scenarios including simulating a realistic flood event with temporally changing upstream discharge conditions.

As AASHTO (2007) bridge design specification suggests different target reliability index for the load factors and resistance factors, based on the redundancy and non-redundancy of a structure, a relationship between reliability index and scour factors is introduced herein. These “scour factors” are proposed for application to the deterministic predictions to account for input parameter uncertainty and inherent model bias and are applicable for local scour assessment in riverine flow under clear water and live bed conditions.

While we provide NCDOT with the comparative data, the use of a specific approach for scour assessment is related to the importance of the structure and the level of accuracy needed for such assessment. As demonstrated herein, the estimates from the five analytical approaches are conservative in comparison to the results from Delft 3D. The numerical results from Delft 3D proceeded by first establishing equilibrium morphology under mean flow conditions, and then inducing the 100-year flood transient flow rate to assess the change in morphology and discern the scour magnitude. Information presented in this report enables engineers to decide the level of scour estimation reliability desired per the importance of the structure and facilitate the development of integral risk-based design approach for bridge structures.

The use of SC envelope (2018) model is recommended for first order estimate of scour with the understanding of the inherent bias and level of conservatism. The use deterministic models, e.g., Wilson (1995) model, Melville (1997) model, HEC 18 (2012) model, Briaud (2014) model is predicated upon having sufficient data to develop the required input parameters. The results from these deterministic approaches can be adjusted using the proposed modification factors in order to obtain a the desired “level of conservatism” with a known Mean absolute percentage error. For an approach that is consistent with the LRFD, the use of the introduced reliability-based scour factors is recommended in order to achieve a level of reliability of the scour magnitude estimates that is consistent with the reliability index of the bridge super-and sub-structure components. This is necessary for the development of integral risk-based design approach for bridge structures.

This page left intentionally blank

Table of Contents

1. Introduction 10

2. Research Objectives 13

3. Literature Review 14

4. Application of South Carolina (Sc) Scour Envelope Curves to the Collected Data..... 22

5. Site Selection and Monitored Data..... 35

6. Numerical Modeling..... 45

7. Comparative Assessment of Various Scour Estimation Approaches 55

8. Findings and Recommendations..... 62

 Recommendations 64

9. References 65

Appendix A: Literature Review..... 69

Appendix B: Bridge Pier Scour: Analyses Using Clear Water Data 118

Appendix C: Bridge Pier Scour: Analyses Using Live-Bed Data 147

Appendix D: Development of Reliability Index Based Framework for Bridge Pier Scour
Analyses..... 197

Appendix E: Application Assessment of Reliability-Index Based Scour Approach and
Corresponding Impact on Pile Foundation System 225

Appendix F: Bridge Abutment Scour: Analyses Using Sturm (2004) Data..... 247

Appendix G: Preliminary List and Map of Potential Bridge Sites to Study In Collaboration with
Rp 2020-03..... 256

Appendix H: Numerical Modeling of Monitored Sites Data..... 258

Appendix I: Scour Depth Analysis by Numerical Modeling for Roanoke River 269

1. Introduction

The Federal Highway Administration (FHWA) requires that all bridges over water be assessed for scour susceptibility. If the assessment shows that the bridge is scour- susceptible they require the bridge to be coded as scour critical. For bridges coded as scour critical, the FHWA requires State Departments of Transportation to develop an action plan for each bridge. According to the FHWA policy, the action can include replacement or the installation of scour counter measures. Assessment of scour and erosion magnitudes is a major challenge for the functional sustainability of bridge foundation system over waterways. As shown in Figure 1 by Briaud et al (2014,) hydraulic aspects including scour represent a leading cause of bridge failure over the period of five decades. The occurrence of scour has a large impact on the cost of maintaining existing bridges as well as construction of new bridges.

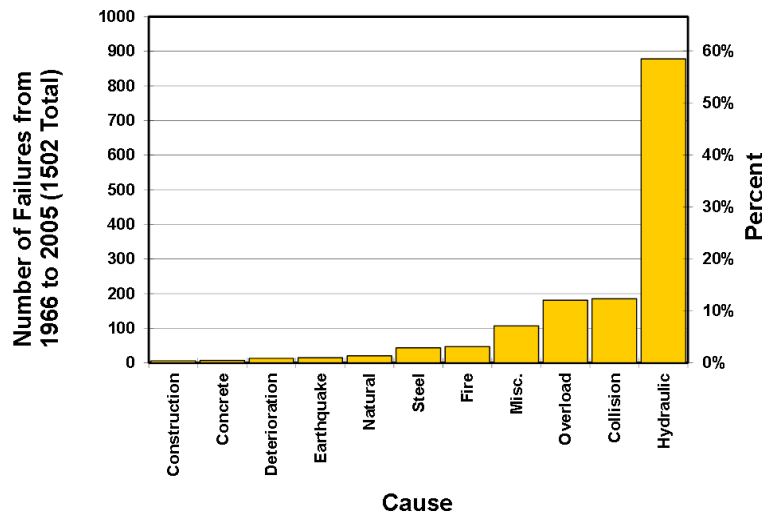


Figure 1. The Percent and pause of Bridge Failure in the US (Briaud et al 2014)

There are mainly four general approach that are currently used for assessment of scour potential. These are classified as:

- i. The use of deterministic analytical equations based on observational approaches mainly from flume testing, as presented for example in HEC-18 which is a main guidance for calculating depth of scour at bridge sites. There have been several scour related research projects to improve the accuracy of the approach developed in HEC -18, and there are many other models in literature to compute equilibrium scour.
- ii. The extension of deterministic model probabilistic approaches. To the authors' knowledge, the first probability-based pier scour model was introduced by Johnson (1992). The Johnson (1992) study was focused on the relationship between probability of bridge failure and safety factors. Johnson and Dock (1998), using a Monte-Carlo

- simulation technique, developed probabilistic bridge scour depth estimates. They considered model error statistics, and hydraulic and geometrical parameters uncertainty. With the adoption of the Load Resistance Factor Design (LRFD) by Department of Transportations across the country for the design super-and sub bridge structures, more focus is currently placed on probabilistic scour assessment as a mean of have consistent risk for a given bridge structure, and to allow for performing risk assessment considering highway assets at a given location as an integrated system.
- iii. The retrieval of samples from the field and the performance of laboratory testing to estimate erosion parameter, such as, for example, the use of the Erosion Function Apparatus (EFA) approach by Briaud et al (2001) and the Rotating Erosion Test Apparatus (RETA) by Bloomquist et al (2012). This approach requires the use of specialized equipment and is only applicable to soils with sufficient plasticity such that the sample does not disintegrate during testing.
 - iv. The use of in situ testing approaches such as the In-Situ Erosion Evaluation Probe (ISEEP) by Gabr et al (2012) and In-Situ Scour Testing Device (ISTD) by Turner-Fairbank Highway Research Center. These approaches seek to assess the scour rate per applied level of water velocity (or shear stresses.) It is however the case that the mode of applied flow during testing is significantly different from the flow regime and the boundary conditions occurring at a given site. Therefore, there is a need to better understand the meaning of the data obtained from such testing before their results are widely used in practice.
 - v. The compilation of soil erosion data and synthetizing such data into erosion threshold charts, such as for example the approach presented by Benedict el al (2018). In this case, the authors developed envelope curves for clear water and live bed components of scour at sites in South Carolina.

The use of the approach of compilation of a soil erosion database and the development of threshold scour charts for first order estimation of scour potential is attractive for its simplicity and by necessity needs to be overly conservative. Such charts are developed using regression analyses and correlations mainly utilizing measured laboratory and field data.

South Carolina Scour Envelope Curves (SC-SEC)

The approach followed by the U.S. Geological Survey, in developing the South Carolina Bridge-Scour Envelope Curves was based on a collection of historical riverine bridge-scour data in the Piedmont and Coastal Plain geologic regions of South Carolina (Benedict et al 2018). The approach provides an upper limit of observed historical scour depth based on clear-water and live-bed scour data from 231 riverine bridges. Figure 2 shows an example of the defined upper bound of clear-water contraction scour for sites at the Piedmont and Coastal Plain geologic regions (Benedict and Caldwell, 2006). Similar graphs were presented for clear-water abutment and pier scour, as well as live-bed contraction and pier scour. The developed criteria were validated using data from 569 laboratory and 1,858 field measurements of clear-water and live-bed pier scour data that is implemented in a data base (referred to as PSDb-2014) by Benedict and Caldwell (2014).

Benedict et al (2018) presented several modifications to the specified 2006 criteria with such modifications accounting for estimate of the drainage area, adjustment for the 500-Year flow level, and update of the criteria in the bases of data from PSDb-2014 by Benedict and Caldwell (2014). Figure 3 shows comparison between the specified Piedmont and Coastal Plain envelope curves and the field data expressed in terms of the embankment length. The majority of the data is for embankment length smaller than 1500 ft. While the scale of “800 ft” on the x-axis is obscuring the clarity of the presentation, it seems that two different envelope curves for the Piedmont and Coastal Plain regions are more appropriate since the majority of data from the Piedmont area show scour below 10 ft versus 15 ft for the Coastal Plain region. Most of the data fall within the envelope curves, providing support for the curves.

There are several limitations associated with the South Carolina Bridge-Scour Envelope Curves as was identified by Benedict et al (2018). These include the need to apply the criteria to sites with similar flow and structure geometric characteristics to those used to develop the envelope.

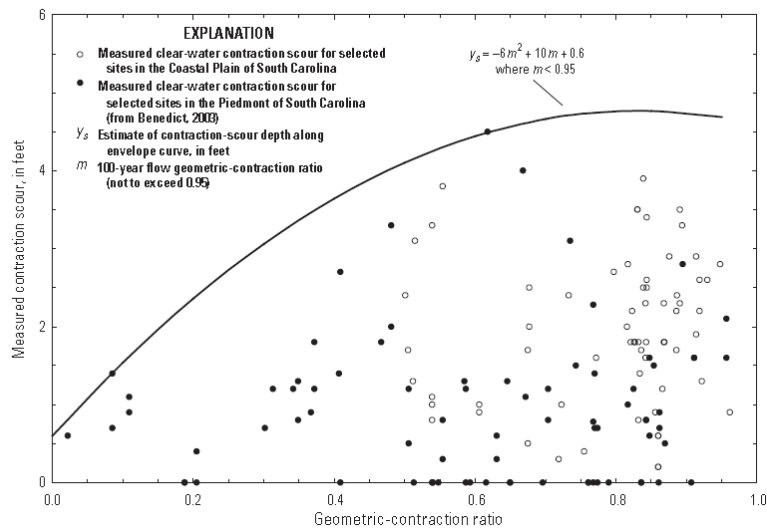


Figure 2. The South Carolina clear-water contraction-scour envelope curve combining sites from the Piedmont and Coastal Plain (from Benedict and Caldwell, 2006)

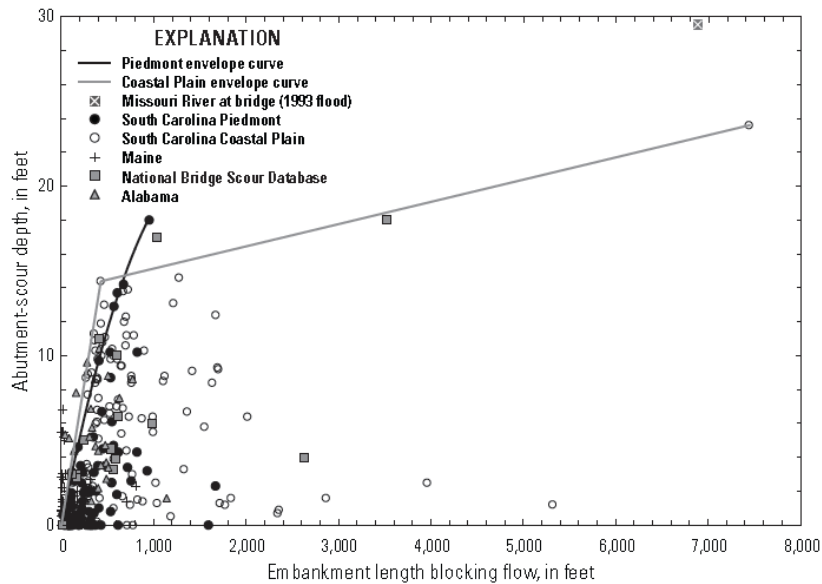


Figure 3. Comparison between Proposed Criteria and Collected Field Data (Benedict et al, 2018)

The authors also recommend the application of “safety factor” to the estimated scour depth. The authors also stated that “the uncertainty associated with the envelope curves increases near the limits of the data range” with live bed scour data having the largest uncertainty. Six factors were identified as “unusual site conditions” which were not considered during the development of the envelope curves. These are related to severe channel bends, unusual flow distribution, pier proximity to abutment, debris accumulation, vegetation within the floodplain, and tidally influenced waterways.

2. Research Objectives

The overall objective of this study is to assess the SC-SEC and the ability to predict the scour magnitude at bridge sites including pier, abutment, and embankment scour. The work scope included assessing the results obtained using SC-SEC in view of existing deterministic approaches reported in the literature. The study objective also included quantifying the conservatism and accuracy of the various scour assessment models including SC-SEC. The specific objectives include the following:

- i. Performance of literature review with a focus on understanding the development of the South Carolina SC-SEC as well as existing deterministic models for scour assessment at bridge sites.
- ii. Assessment of the applicability of South Carolina (SC) Scour Envelope Curves to estimating scour in comparison to several published deterministic models including HEC-18.

- iii. Field monitoring and GIS mapping at four selected North Carolina bridge sites, including characterizing site-specific flow conditions, flow profiles upstream, downstream, and at the bridge. Mapping data spatially within GIS software (ArcGIS) at each site to analyze the spatial variability and site feature to be utilized in modeling. Data from the monitored sites will be used in Delft 3D (a three dimensional hydrodynamic and morpho dynamic model) to assess the scour at the bridge sites. The results from Delft3D are compared to those obtained using the FHWA HEC-18 procedure and the SC scour envelope curves.
- iv. Compilation of the modeling and experimental results to suggest procedures applicable for scour assessment at bridge sites. Work in this objective includes comparing the accuracy and conservatism of various models including SC-SEC. This objective includes assessing the benefit of using SC-SEC versus the of HEC 18 approach.

3. Literature Review

The review presented herein is focused on summarizing the current state of knowledge on erodibility, geotechnical aspects of erodibility, factors influencing pier scour, factors complicating pier scour, and databases available on erodibility and pier scour measurements. A summary of the deterministic pier scour models developed since 1990, and whether the models consider the factors affecting pier scour, are presented. In addition, developments in probabilistic pier scour analyses, and observation-based models are summarized. Four fundamentally different and widely used pier scour models, namely the Wilson (1995) model, Melville (1997) model, Hydraulic Engineering Circular (HEC) No. 18 (2012) model, and Briaud (2014) model were further chosen for the comparative study. These four models were developed with each relying on a different mode of collected data. The laboratory live bed and clear water data, as summarized by Benedict and Caldwell (2014,) were used in the analyses. Error statistics were computed and included in discussion on accuracy, precision, and probabilistic distribution of predictions from these four models. Conclusions were drawn based on the understanding of the literatures and critical analyses presented. The details of the literature review are presented in Appendix A, while a summary of the scour process, factors influencing pier scour, and scour prediction models are presented below.

Scour Process

Macro perspective

Scour can be defined as the removal of materials from bed and banks of streams, around the piers and abutment of bridges. Bed materials may consist of granular or cohesive deposits or a combination of the two. Under similar hydraulic conditions, loose granular soil will scour at a rate different from cohesive deposits. Information in literature suggest that the detachment of particle from bed can be related to the upstream flow velocity and scour can be classified as clear-water or live-bed conditions. If the flow velocity is such that there is no transport of bed material from the upstream of the crossing, the condition is considered as *clear water*. In contrast, if the transport of bed material occurs from the upstream area, the condition is *live bed*. It is important to note that

there are three main sources of scour which contributes to the total scour estimate. These are, i) Long-term degradation, ii) Contraction scour, and iii) Local scour. Long-term degradation is a type of scour that occurs due deficit in sediment supply from upstream over relatively long reaches (Arneson et al. 2012). Contraction scour occurs due to the geometric contraction of flow resulting in removal of materials from the bed. The difference between long term degradation and contraction scour is that the latter is associated with any constriction of flow. Local scour takes place when the flow is obstructed by a structure such as pier, abutment, spurs, or embankment. Arneson et al. (2012) considered local scour as the combined effect of flow acceleration and the vortices induced by the obstruction. Three principal flow features were described in this case, these are, i) down flow at the face of pier, ii) the horseshoe vortex at the base of the pier, and iii) the wake vortices formed at the downstream direction of the pier (Arneson et al. 2012, Melville and Coleman 2000). The down flow at the pier face erodes the bed material which are then transported past the pier by horseshoe vortex, and wake vortices thereafter. The mechanism is presented schematically in Figure 4. Deng and Cai (2010) reported that the strength of the horseshoe vortex is reduced as the depth of scour increases. Thereby, with time, reducing the transport rate of bed material past the bridge pier. As the scouring process ceases, a re-equilibrium is established between bed material inflow and outflow.

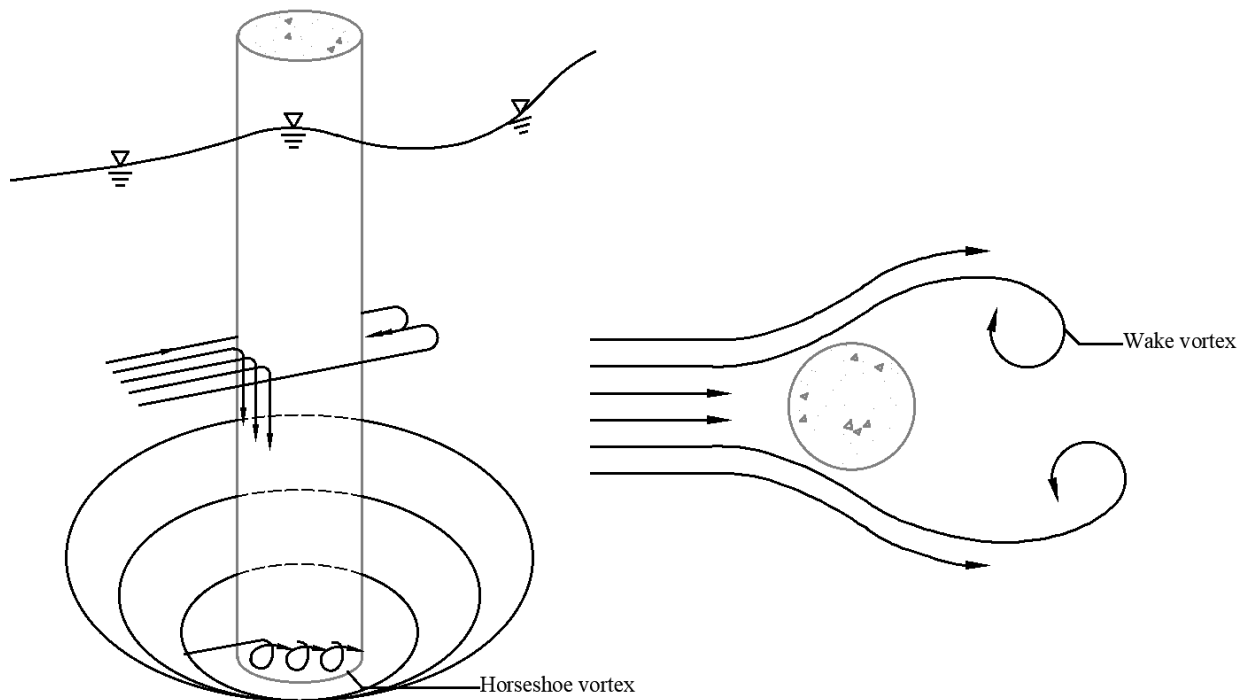


Figure 4. Illustration of the flow around a circular pier in a scour hole (from Arneson et al. 2012)

Micro perspective

Soil erodes if the applied hydraulic shear stress exceeds the critical shear stress. The key forces acting on a soil particle are weight of the particle, electrical forces between the particles,

forces at contact point of the particles, and water pressure around the particle. Briaud (2008) noted that flow of water exerts a pressure around the particles, and the normal stress at the base of the particle will be higher than that acting at the top of the particle, resulting in a buoyant force. In addition, the velocity head increases, and pressure head drops at the interface according to Bernoulli's conservation of energy principle. Conventionally, the shear stress acting on the soil-water interface is considered as the parameter influencing the erodibility of the soil. Briaud (2008) suggested that the constitutive law of the erosion process can be given as in Eq. (1).

$$\dot{z} = f(\tau) \quad (1)$$

Where, \dot{z} is erosion rate and τ is hydraulic shear stress at the interface of soil and water. To normalize Eq. (1), Shafii et al. (2016) proposed Eq. (2), which can be expressed as-

$$\frac{\dot{z}}{v_c} = \alpha' \left(\frac{\tau - \tau_c}{\tau_c} \right)^m \quad (2)$$

Where, α' and m are unitless erosion model parameters depending on soil properties. v_c and τ_c are critical velocity and critical shear stress respectively (below which no erosion occurs.) Hofland et al. (2005) through an experimental investigation on granular beds showed that the forces exerted on the soil particle due to turbulent stress fluctuation at the bed level is sufficient to dislodge the soil particle. The turbulent stress fluctuations acting on the soil particles surrounding an obstruction may result in suction pressures, which affects the erosion of the bed material. Shafii et al. (2019), through hydrodynamic analysis to discern the forces acting on the gravel particles, identified that critical normal stress on the soil particle as also an important parameter which influences erosion rate. The developed model is presented in Eq. (3),

$$\frac{\dot{z}}{0.1} = \left(\frac{\tau}{\tau_c} \right)^\alpha \left(\frac{\sigma}{\sigma_c} \right)^\beta \quad (3)$$

Where, \dot{z} is erosion rate (mm/hr), τ_c and σ_c are critical shear stress (Pa) and critical normal stress associated with an erosion rate of 0.1 mm/hr respectively, σ is the normal stress (Pa) acting on the particle at bed level, α and β are unitless erosion model parameters. Briaud et al. (2019) indicated that parameters α and β cannot be determined definitively with the existing state of knowledge and it would be cumbersome to estimate the parameters on a site specific basis.

Numerical analyses are also used to understand the interaction between flow and obstacles. Recently, Zhang et al. (2016) conducted a Molecular Dynamic (MD) to explain the interaction occurring at soil-water interface. Joseph and Hunt (2004), Kloss et al. (2012), Ni et al. (2015) introduced the approach of coupled Computational Fluid-Dynamics-Discrete Element Modeling (CFD-DEM) to investigate various hydromechanical problems associated with granular media. CFD was used to model the interstitial fluid flow and DEM was used to simulate the particles assembly. Their successful introduction of the CFD-DEM technique led researchers, including Huang et al. (2014), Ni et al. (2015), Chang et al. (2016), Guo and Yu (2017), Kawano et al. (2017), Tao and Tao (2017), Guo et al. (2018), to incorporate CFD-DEM approach into

understanding soil erosion. Although soil erosion was modeled in those studies, none have focused on erosion rate.

Factors Influencing Pier Scour

Ettema et al. (2011) classified factors influencing pier scour into two broad categories, a) primary factors and b) secondary factors. It was suggested that primary factors are those parameters defining the structure and geometric scale of the pier flow field, thus, influencing the maximum scour depth. Parameters included in the primary factors' category are flow depth to pier width ratio, pier width to d_{50} ratio, pier face shape, pier aspect ratio, and skew angle of pier. In contrast, secondary factors are those which influence the computed scour depth sensitivity within a specific geometric scale limit. These include Flow intensity, Euler number or Reynolds number, sediment non-uniformity, and the temporal rate of scour. Ettema et al. (2011) suggested that consideration of secondary factors will lead to a scour depth estimation less than the potential maximum scour obtained from only considering the primary parameters, thus reducing the conservativeness of the estimate. Figure 5 presents a conceptual sketch of the primary and secondary factors influencing pier scour magnitude.

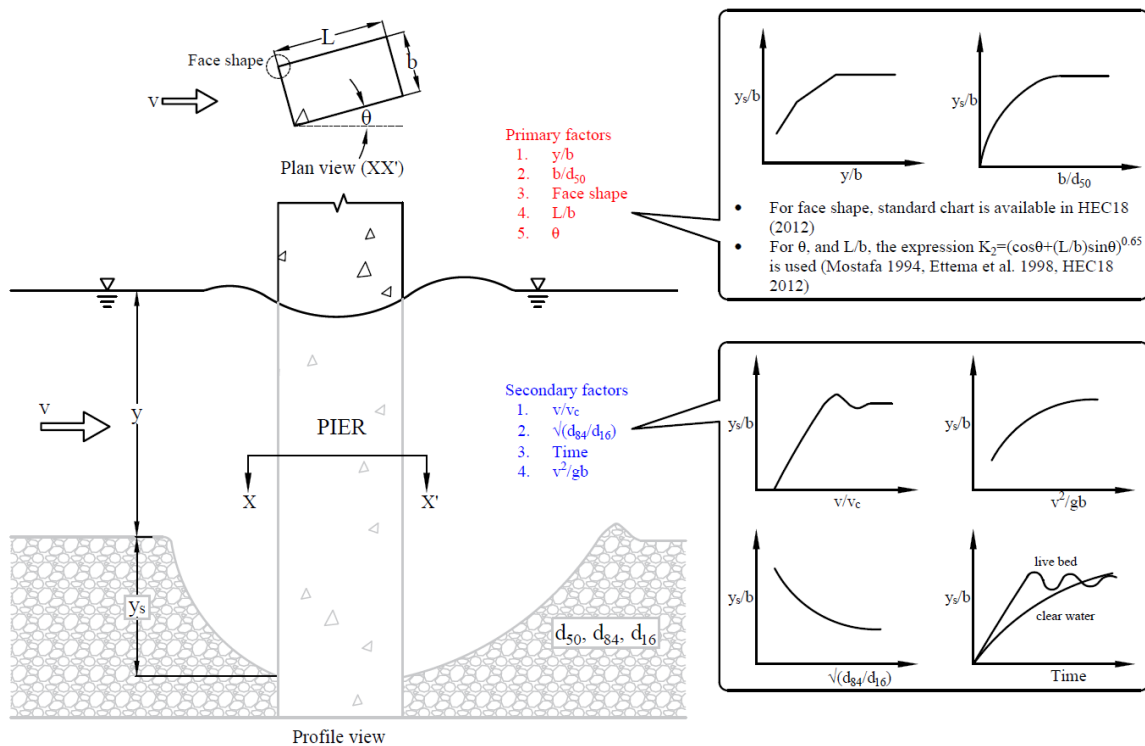


Figure 5. A conceptual sketch showing the primary and secondary factors influencing pier scour

Primary factors

Melville and Coleman (2000) and Sheppard and Melville (2011) identified the water depth to pier width ratio (y/b), also termed as the geometric scale of the pier flow field, as one of the most important parameters driving the maximum scour depth. Based on experimental and numerical studies, Melville and Coleman (2000) classified the pier scour flow field into three

categories. Table 2 (Appendix A) shows such classification based on y/b and summarizes the type of turbulent structures developed due to the presence of obstacles for the three categories of piers.

Sheppard et al. (2004) and Sheppard and Miller (2006) observed that scour depth is dependent on the ratio of pier width to sediment size, b/d_{50} . Lee and Sturm (2009) experimentally observed that smaller values of b/d_{50} can impede the scour progression and subsequently confine the scour depth. They further suggested that scour depth to pier width ratio increases logarithmically in the range $b/d_{50} \leq 25$, while it decreases for $b/d_{50} > 25$, and eventually remains constant if b/d_{50} exceeds 400. Ettema et al. (2011) suggested that if $b/d_{50} \leq 8$, individual particles are large relative to the groove excavated by the down flow and erosion is impeded because the rough and porous bed dissipates some of the down flow energy.

In general, piers are constructed in a variety of shapes that include cylindrical, oblong or rectangular configurations. As pier shape influences the flow field surrounding a pier, the magnitude of scour is also affected in the process. The deterministic pier scour models by Melville (1997), HEC 18 (2012), and Briaud (2014a) adopt a multiplication factor to consider pier shape varieties. From an experimental investigation, Mostafa (1994) observed a variation of scour depth as a function of the magnitude of the aspect ratios; such variation was attributed to the change in formation and spacing of turbulence structures at different aspect ratios. Pier skewness to flow leads to altering the effective pier width and influencing the flow field, and consequently the scour depth. Yang et al. (2017) observed that when skewness exceeds 30° , irrespective of the undisturbed bed level, the bottom of the equilibrium scour hole reaches the same depth below the pile cap in clear water conditions. Nevertheless, it is a common practice to combine the effects of pier skewness, shape, and pier width in terms of expressing an effective pier width (Mostafa 1994, Ettema et al. 1998, and Arneson et al. 2012).

Secondary factors

Sediment's non-uniformity, presented in Eq. (4) is one of the secondary factors influencing bridge pier scour.

$$\sigma_g = \sqrt{\frac{d_{84}}{d_{16}}} \quad (4)$$

Where, d_{84} and d_{16} are the particle diameters corresponding to 84% and 16% finer. Until recently, the effect of sediment non-uniformity was omitted or not considered. For example, in the Pier Scour Database, PSDb (Benedict and Caldwell, 2014), only in 30% of the cases was the sediment non-uniformity reported. However, in most of the cases (96%), the median particle size was reported. For clear water condition, the scour depth decreases with the increase in sediment non-uniformity (Ettema 1980; Melville 1997; Raikar and Dey 2005). In the case of non-uniform sediments ($\sigma_g > 1.3$), it is possible to form an armor layer surrounding the pier. The armor layer resists the subsequent development of the scour depth due to the progressively increasing critical shear stress with the presence of the larger grain sizes.

The energy associated with turbulence structures is determined in terms of the pier Euler number ($\frac{v^2}{gb}$; where v is the upstream flow velocity, g is the gravitational acceleration, and b is the pier width) and pier Reynolds number ($\frac{\rho Vb}{\mu}$; where ρ and μ are the density and viscosity of water respectively). Ettema et al. (1998) and Ettema et al. (2006) observed that scour depth increases significantly as the pier Euler number increases, suggesting the consideration of a correction factor accounting for Euler number impacts. It is interesting to note that most of the scour prediction equations (Wilson 1995; Melville 1997; HEC 18 2012) available in the literature do not consider the effect of the power of turbulence structures.

Pier scour is also affected by the flow intensity, expressed as a ratio of upstream flow velocity, v to the sediment critical velocity, v_c . The effect of uniformity of sediments, size and steepness of bed features in relation to v/v_c has been studied extensively in the literature (Chee 1982; Chiew 1984; Melville 1984; Melville and Sutherland 1988). Temporal evolution of scour has been studied by Shen et al. (1969), Ettema (1980), Melville and Chiew (1999), Oliveto and Hager (2002, 2005), Miller (2003), and Kothyari et al. (2007). However, Ettema et al. (2010) pointed out that data on the time development of local scour at wide piers or piers with complex geometry is scarce; therefore, the validity of the temporal evolution theory when applied to wide piers or long skewed piers is questionable.

Scour Prediction Models

The available scour prediction studies can be broadly classified into three different categories. These are, i) Deterministic, ii) Probabilistic, and iii) Observation-based.

Deterministic models

Ettema et al. (2011) and Sheppard et al. (2011) compiled the pier-scour prediction models developed since 1949. At present, there are more than 20 pier-scour models available in the literature. These models are developed in most cases based on either extensive laboratory testing data, from field data, or from both. However, as a part of the review herein the scour prediction models developed since 1990 are presented in Table 4 (Appendix A), albeit this list is not exhaustive. Gao et al. (1990) model was developed from local scour data collected in China and consisting of 137 live bed and 115 clear water data points. Wilson (1995) model is based on field data collected from 22 bridges in Mississippi. Melville (1997) model is based on extensive laboratory and field data collected over a period of 25 years. Sheppard and Miller (2006) model was developed primarily based on laboratory data and few field observations. Oliveto and Hager (2002, 2005), Kothyari et al. (2007) model is based on experiments performed on pier width ranging from 0.02-0.50 m, d_{50} ranging from 0.55-5.3 mm. The latest update of HEC-18 model by Arneson et al. (2012) is the most widely used pier-scour prediction model. It is developed based on data from laboratory testing on sediments with median grain size, d_{50} ranging from 0.24-0.52 mm. Briaud (2014a) model is based on data from large scale laboratory flume testing (d_{50} ranged from 0.10-0.60 mm).

To provide a comparative assessment of the influencing parameters on computing scour magnitude, Table 5 (Appendix A) is provided, listing the parameters considered in each of the models in Table 4 (Appendix A). Sheppard et al. (2011) considered 23 different scour prediction models and investigated the performance of the models when compared to 928 field and 569 laboratory data. Their conclusion suggested that results from Sheppard and Miller (2006) and Melville (1997) models provided reasonable values when compared with field data. Careful observation of Table 5 (Appendix A) suggests that these two models incorporated all the primary variables, in contrast to the remaining listed models in Table 5 (Appendix A). Sheppard et al. (2011, 2014) melded and empirically modified Sheppard and Miller (2006) and Melville (1997) models to obtain a refined estimate of scour for wide piers, as the existing deterministic models cannot predict the scour depth for wide piers with accuracy (compared to narrow, and intermediate piers).

Probabilistic approach

Although there seems to be a significant number of studies that were focused on developing deterministic pier scour equations, focus on probabilistic approaches is limited. To the authors' knowledge, the first probability-based pier scour model was introduced by Johnson (1992). The Johnson (1992) study was focused on the relationship between probability of bridge failure and safety factors. Johnson and Dock (1998), using a Monte-Carlo simulation technique, developed probabilistic bridge scour depth estimates, considering hydraulic and geometrical parameter uncertainty. Probabilistic framework was also developed for assessing the likelihood of achieving a specific scour depth, probability of exceedance, as well as adequate pile depth. Briaud et al. (2007) developed a probabilistic bridge scour model that considered the uncertainty of hydrologic conditions; however, uncertainties associated with input parameters (geometry of obstacle, soil erodibility) were not considered. Bolduc et al. (2008) introduced a probabilistic model based on the bias and scatter around the mean. Bias was defined as the ratio between the mean-measured value to the mean-predicted value. Johnson et al. (2014) examined the overall uncertainty in local pier or abutment scour in combination with contraction scour. As a part of the study, reliability-based scour design factors were suggested. Briaud et al. (2014) developed a reliability-based pier scour model focusing on the risk associated with failure of shallow and deep foundations subjected to scour. It was demonstrated that the scour depth prediction from HEC-18 should be multiplied by the factor 2.05 to ensure a probability of exceedance of 0.001 for shallow foundations in sand subjected to scour. While the HEC-18 scour prediction model is considered to be highly conservative, yet per Briaud et al. (2014), the scour predictions from HEC-18 did not correspond to sufficiently low probability of failure.

Observation-based approach

The designation of a bridge pier as “*scour critical*” highly depends on the method used to estimate the scour. Most scour prediction models do not take into account the key physical and engineering parameters of soils being eroded, such as plasticity, density and shear strength.

Although scour prediction models such as Briaud et al. (2008) and Briaud (2014b) are based on using erodibility parameters, the use of such models necessitates performing site-specific erosion testing. To address this issue, Govindasamy et al. (2013) developed a model that is referred to as the Observation Method for Scour (OMS). One point of subjectivity in the OMS technique is if one soil classification falls into two different categories, the same structure can be classified as scour-critical or non-critical based on the erosion category that was assigned to the soil. Nevertheless, Govindasamy (2009) demonstrated successful application of OMS to 16 Texas bridges. Results however revealed that some of the scour-critical bridges are not scour critical based on the OMS analyses. The OMS technique has been automated for the state of Texas and is used for first order approximation of scour criticality (Govindasamy et al., 2013).

4. Application of South Carolina (SC) Scour Envelope Curves to the Collected Data

The deterministic models commonly used in practice do not indicate the inherent biasness (conservativeness/ unconservativeness) in scour predictions. Knowledge of biasness while using a given deterministic model is necessary to properly evaluate the factor of safety to be applied to the predicted scour depth. The research team has focused on assessment of five scour prediction models, viz. Wilson (1995) model, Melville (1997) model, HEC-18 (2012) model, Briaud (2014) model, and SC Envelope (2018) approach. The assessment includes investigation of Accuracy and conservatism of a given model within the context of comparing the models' results with measured clear-water field scour-depth data. Accuracy is measured in terms of Mean Absolute Percentage Error (MAPE), while conservatism is defined as the ratio of the number of cases the model-computed scour depth being more than the measured scour depth, expressed as percentage of the total number of data sets. The database reported in Benedict and Caldwell (2014) is used except for some data points for which insufficient information was reported to be able to apply the predictive models. The data screening processes and the details of analyses are found in Appendices B and C. An excerpt of the results obtained are presented in the following sections.

Analyses with clear water and live bed data

The analyses were divided into two categories. At first, analyses were performed using clear water data, followed by analyses using live bed data. Following results are obtained when clear water data collected by Benedict and Caldwell (2014) was used. Values of MAPE ranged from 238% to 336%, whereas conservatism ranged from 77% to 97.8%. The SC Envelope (2018) model provided the most reliable scour depth, whereas Briaud (2014) model presented the least conservatism. In regard to MAPE, Briaud (2014) model presented the least error, and SC Envelope (2018) model presented the highest error. An approach to alter the accuracy and conservatism of a given model is demonstrated as well. In order to evaluate and quantify the scatter and uncertainty associated with scour prediction, the performance of several statistical approaches are assessed and the appropriate approaches are proposed. Finally, a relationship between probability of

decedance of a given measured scour depth and a modification factor (that is applied onto the deterministic prediction) is devised. A probability of decedance is defined as the probability that the computed scour magnitude will be less than the most likely to occur in the field. Please refer to Appendices B and C for more detail on the analysis procedure.

When the live bed data collected in Benedict and Caldwell (2014) was used, the following results are obtained. Except for the SC envelope (2018) model, values of MAPE ranged from 23.5% to 59.8% when live bed laboratory data is considered. The SC envelope (2018) model presented a MAPE of 1218%. For live bed field data, MAPE ranged from 205.6% to 322% for the five models considered herein. Considering the live bed laboratory data, SC envelope model's estimates provided the highest conservatism factor, whereas Wilson's (1995) model yielded the least conservatism factor. When the live bed field data are considered, SC envelope model provided the most reliable estimate, while HEC 18 (2012) model provided the least reliable scour depth estimate. When the limitation of SC envelope curve approach, which is nominal pier width should be ≤ 6 ft, is imposed, the conservatism values do not differ much (less than 1%). In regard to MAPE, when the limit on SC envelope model is applied (Case with 641 data sets), the MAPE rather increased from 322% to 349%. The accuracy and conservatism of a specific model are adjusted by multiplying the scour depth computed using a given deterministic model by a modification factor. The proposed modification factors necessary to attain certain conservatism level for the five models considered herein are presented. Deterministic models used for bridge pier scour do not account for inherent model's uncertainties. The scatter associated with the scour prediction produces heteroscedasticity, and non-normal errors. As shown, statistical measures can be developed to reduce the error associated with data distribution. Utilizing both laboratory and field databases, a relationship between probability of decedance of a given measured scour depth and a modification factor (that is applied into the deterministic prediction) is proposed. The modification factor allows for the use of the deterministic models while quantifying the probability of the computed scour depth being less than or more than the most likely value per measurements reported in the utilized databases.

The relationship between probability of decedance of a given measured scour depth and a modification factor is presented in Figure 6. Figure 6 suggests that as the POD decreases, the modification factor increases. The rate of increase of modification factor increases significantly at $POD < 0.1$ for based on applying the five deterministic models to both laboratory and field data. For comparison, the modification factors proposed in Shahriar et al. (2021b) are also presented in Figure 6. Clear water scour measurements reported in Benedict and Caldwell (2014) was utilized in Shahriar et al. (2021b). Figure 6(a) suggests that the factors proposed for clear water laboratory scour measurements are comparatively higher than the live bed laboratory scour measurements throughout the POD range. The reason can be attributed to the fact that the live bed estimates of the scour depth using the models proposed herein are inherently more conservative than the clear water scour estimates obtained from Shahriar et al. (2021b) model. An additional possible factor, is soil type and approach velocities at clearwater sites may differ from the live-bed conditions. Clearwater conditions often occur on the floodplains where soils may have varying degrees of clays that are more scour resistant reducing scour potential. Additionally, floodplains

often have lower velocities that will not produce as large a scour depth as the higher velocities in the main channel. These lower velocities may tend to produce smaller theoretical scour depths as well. In contrast, live-bed scour more typically occurs in the main channel where there are often sandy soils more susceptible to scour and channels typically have higher velocities than the floodplain, creating a larger potential for deeper scour depths. Accordingly, to attain a similar POD, the scour estimates from the clear water models need to be multiplied with a higher factor than the one corresponding to the live-bed case. In addition, for the live bed analyses, a μ_{POD} of 1.85 ensure a $POD \leq 0.1$ for all the four models (except SC model), while to ensure $POD \leq 0.1$, a factor ranging from 2.2-2.6 is required for the clear water analyses based statistics suggested in Shahriar et al. (2021b). A development of POD chart for SC envelope model was not approached owing to the fact that all the scour predictions were conservative while SC model is used (refer to Figure 5a of Appendix C). For rest of the four models corresponding to clear water analyses, the μ_{POD} continued to increase until a $\mu_{POD} = 5$, while for the live bed case, an increase in μ_{POD} beyond a $\mu_{POD} = 3.2$ was not noticed. Interpretation of Figure 6(b) does not suggest a discernible difference between the clear water and live bed μ_{POD} except for HEC 18, Briaud, and SC envelope models in the POD range of 0.10-0.65. The modification factors reported herein for field measurement based statistics are comparatively higher than the modification factors proposed for laboratory measurement based statistics. The higher modification factor, to some extent, can be attributed to the limitation of the field scour measurements. While the laboratory measurements provide a relatively accurate measurements of downscaled parameter associated scour, field measurements may not represent an equilibrium scour depth. Although, through the screening process, the extreme outliers were eliminated from the dataset, there are still possibilities that a non-equilibrium scour measurement remain in the dataset utilized herein, which increased the inherent uncertainty of the model (refer to Figure 1 of Appendix C, frequent occurrence of comparatively high errors); thereby increased the value of the developed modification factor, based on the measured field scour data.

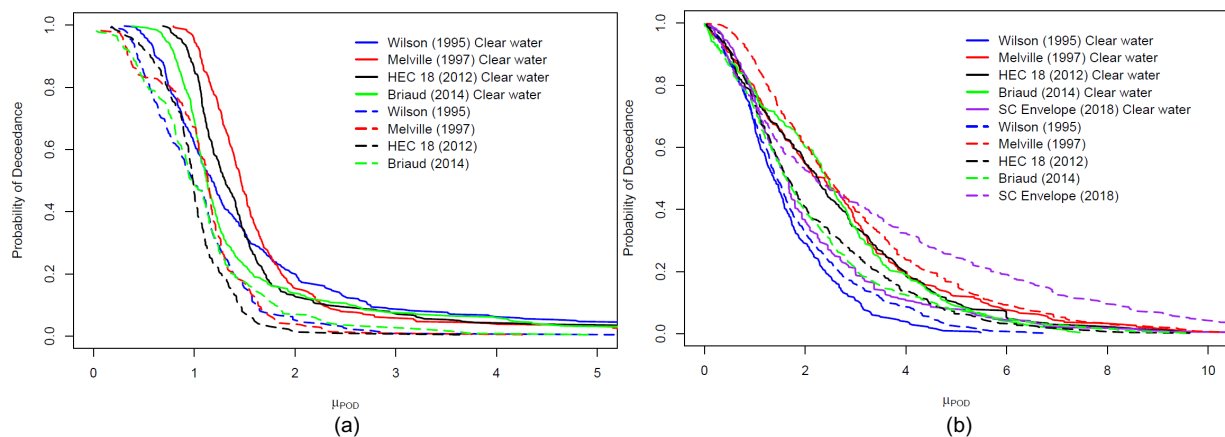


Figure 6. Probability of deceedance-modification factor relation for different models using (a) laboratory live bed dataset (Data count: 229), (b) field live bed dataset (Data count: 758). Clear water data points are from Shahriar et al. (2021b).

Reliability Based Pier Scour Estimation

Realizing the importance of parameters influencing the scour estimation using different scour prediction models, the research team then focused on developing a reliability based scour estimation approach. A reliability-based pier scour estimation methodology was presented accounting for input parameter uncertainty and inherent model bias. The methodology is applicable for local scour calculation in riverine flow under clear water and live bed condition using four deterministic scour prediction models: Wilson (1995) model, Melville (1997) model, HEC-18 (2012) model, and Briaud (2014) model. A relationship between scour factor, which is the ratio of the depth from average bed level to the bottom of the footing, to the scour depth predicted from different scour prediction models and probability of exceedance of the measured scour depth is proposed. It was observed that the proposed relationship is dependent on the pier type (e.g., narrow pier, intermediate pier, and wide pier), upstream sediment transport condition (e.g., clear water and live bed), and the deterministic model being used (e.g., Wilson (1995) model, Melville (1997) model, HEC-18 (2012) model, and Briaud (2014) model). AASHTO (2007) bridge design specification suggests different target reliability index, β_T , based on the redundancy and non-redundancy of the structure. A relationship between reliability index and scour factor is devised, enabling engineers to decide the level of reliability index desired per the importance of the structure. The proposed method will help mitigating the inconsistency posed by adopting a β -based approach for the design of various superstructure bridge components as opposed to a deterministic approach for assessing the scour magnitude at the foundation system. Having a uniform level in the reliability index of the bridge components will facilitate the development of integral risk-based design approach for bridge structures. A detail of the methodology and results are presented in Appendix D.

In the following section, focus was put on demonstrating the implications of the β -based scour assessment approach on the response of pile groups supporting bridge piers. To facilitate illustrating the applicability of β based approach, parameters from the Woodrow Wilson bridge pier in Prince George County, Alexandria, Virginia carrying traffic of I-95 and I-485 was considered in the analyses. A relationship between the probability of exceedance over the design life and the scour depth is presented to demonstrate the risk associated with utilizing HEC 18 (Arneson et al. 2012) in the analysis. Scour depth was estimated using both traditional HEC 18 procedure and the β -based procedure. The estimated scour depth using both approaches was then applied to the Woodrow Wilson bridge foundation system and the corresponding displacement (transverse, longitudinal, axial) components and moments of the pile foundation under AASHTO loading condition were studied. The analyses were extended by conducting a parametric study by varying the pile length and pile diameter to explore the effect on the transverse, longitudinal, and axial displacement components of the pile foundation system. Finally, risk (the product of probability of failure and the cost of the consequences) analysis was presented to show how the consideration of β -based approach is advantageous in assessing the potential of economic loss.

The Woodrow Wilson Bridge Site

The Woodrow Wilson bridge on the Potomac River is located in Prince George County, Alexandria, Virginia, and crosses over to Washington D.C. The bridge carries traffic through I-95 and I-485 and the relatively recent construction was built due to the fact that the previous Woodrow Wilson bridge reached its capacity (75,000 vehicles per day) within 8 years of its construction in 1969. The overall cost of the project including the approach embankment, and interchanges was estimated at 2.2 billion dollars (Kwak 2000; Kwak and Briaud 2002). The drawbridge is supported by two bascule piers (Jones 2000), which are located on the main channel of the Potomac River. The foundation system of the bascule piers consists of exposed pile foundation that is capped near the water surface. The soil stratigraphy in the main channel is made of soft clay overlying on thin layer of loose sand. Below the loose sand layer, a clay layer persists. The profile view, and pile cap section along with the soil stratigraphy for the pier M1, which supports the drawbridge, is presented in Figure 7. The soil properties, pile and pile cap properties are from Kwak and Briaud (2002) and Briaud (2008).

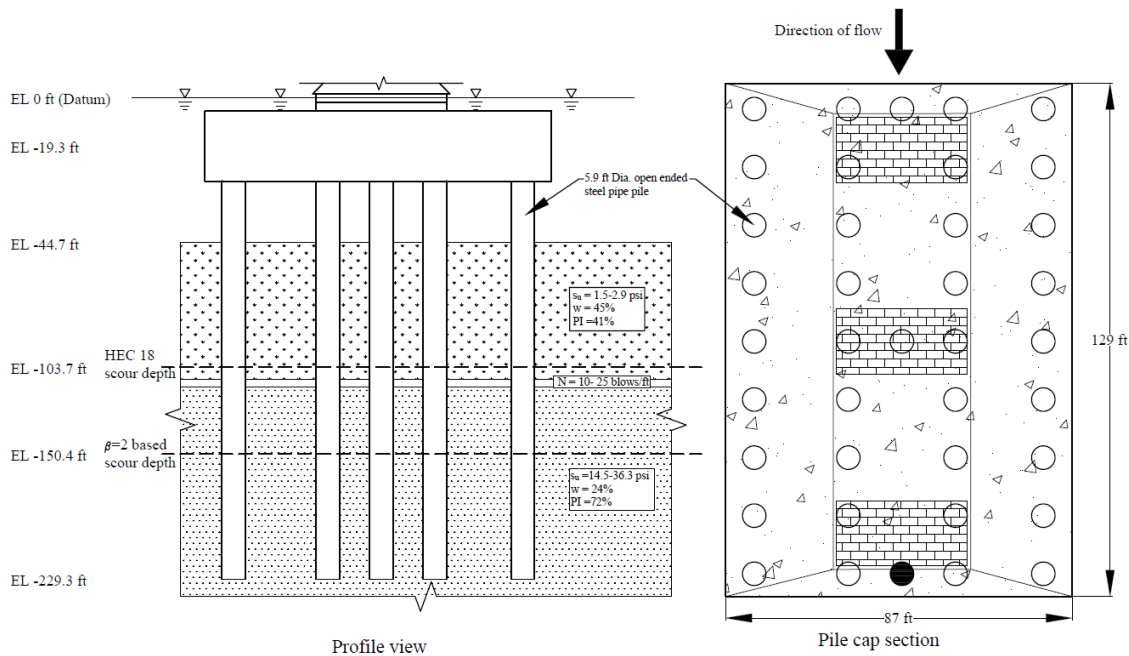


Figure 7. Profile view and pile cap section along with the soil stratigraphy for the bascule pier M1 of Woodrow Wilson bridge (After Kwak and Briaud 2002; Briaud 2008).

Scour Estimation

The Woodrow Wilson bridge pier consists of three complex geometrical shapes of columns resting on a pile cap, supported by the pile groups. HEC 18 (2012) classifies such pier as complex pier and provides guidance on the calculation of scour depth. Jones and Sheppard (2000) suggested that a superposition of the scour depth component from the pier stem (y_{s-pier}), pile cap

($y_{s-pile\ cap}$) and the pile group ($y_{s-pile\ group}$) is necessary to estimate the total local scour depth, y_s (Equation 5).

$$y_s = y_{s-pier} + y_{s-pile\ cap} + y_{s-pile\ group} \quad (5)$$

The scour depth estimated from the HEC 18-suggested approach was 62.3 ft (19 m). Sheppard et al. (2004) reported experimental results of large-scale model bridge study in a 22 × 125 ft (6.7 × 38.1 m) long concrete channel at the USGS BRD Conte Research Center in Turners Falls, Massachusetts. The geometric scale considered was 1:50, the sediment had a median grain size of $d_{50} = 0.8$ mm and sediment non-uniformity, $\sigma = \sqrt{d_{84}/d_{16}} = 1.3$ (d_{84} and d_{16} are particle diameters corresponding of 84% and 16% finer respectively). The sand bed was 6 ft (1.83 m) thick. The estimated scour depth was 54 ft (16.5 m). Jones and Davis (2007) further reported the results of small-scale flume study in a 6 × 70 ft (1.83 × 21.3 m) long flume at the FHWA hydraulics lab at the Turner Fairbanks Highway Research Center in McLean, Virginia. The geometric scale considered was 1:100, the used sediment had a $d_{50} = 0.30$ mm, the sediment standard deviation was not reported. The scour depth was estimated to be 53.2 ft (16.2 m).

Although large-scale and small-scale model experiments are important to understand the underlying scour mechanisms, Ettema et al. (2017) and Link et al. (2019) suggested that the incapability of the laboratory scale models to maintain a geometric similitude among the three length scales (pier width, flow depth, and bed sediment size) results in differences in scour estimations from laboratory test-based models and field observed scour magnitude. In addition, the uncertainty inherent in the hydraulic, hydrologic, and geotechnical parameters might result in a different scour depth compared to what has been observed in the flume experiments and estimated from deterministic models.

Jones and Davis (2007) computed the contraction scour in the main channel of the Potomac River using the Laursen (1960) model, and concluded that the contraction scour magnitude is insignificant, thereby suggesting that total scour entails only local scour around the bridge pier for the Woodrow Wilson bridge case. Subsequently, analyses in this study were conducted using a total scour magnitude of 62.3 ft (19 m), obtained from HEC 18 (2012) model (as currently FHWA suggests using HEC 18 (2012) model for scour assessment while designing bridge foundation).

Reliability Index-Based Scour Estimation

The reliability index incorporated in the LRFD methodology accounts for the uncertainties of loads and resistances while evaluating the safety of a system. In LRFD, safety is expressed by the level of desired reliability (e.g., Lagasse et al. 2013; Nowak and Collins 2000). The methodology to develop a reliability index based on scour estimation entails consideration of statistical attributes (mean, coefficient of variation, probabilistic distribution) of the input parameters in scour analyses (e.g., upstream flow velocity, upstream flow depth, median grain size of the bed material, Manning's roughness coefficient, channel bed slope) to analyze the limit state function that defines the foundation safety. The limit state function, L , can be expressed through Equation (6).

$$L = D_p - D_s \quad (6)$$

Where, D_p is the depth that will lead to a foundation failure from current bed level (as defined by geotechnical analyses), and D_s is the scour depth predicted from HEC 18 (2012) scour prediction model. The probability of exceedance of L when HEC 18 model is considered can be expressed as in Equation (7).

$$P_e = P\left(D_p < \lambda 2K_1K_2K_3\left(\frac{y}{b}\right)^{0.35}F^{0.43}\right) \quad (7)$$

Where, K_1 , K_2 , and K_3 are pier nose shape factor, pier alignment factor, and bed condition factor respectively; y , b , and F are flow depth upstream of the pier, pier width and Froude number respectively; λ is the bias factor. In Equation (7), flow depth, flow velocity, and bias factor are random variables, while pier width, skew angle, pier face shape, and aspect ratio are deterministic, as these parameters are not subjected to any inherent temporal or spatial variability. The Coefficient of Variation (COV) of y is dependent on the statistical distribution of Manning's roughness coefficient, n and channel bed slope, S and can be estimated based on the uncertainty analyses presented by the U.S. Army Corps of Engineers (HEC 1986). The COV of flow velocity is also dependent on the distribution properties of n and S , and can be estimated based on the hydrologic uncertainty analyses presented in Johnson (1992), and Lagasse et al. (2013). The λ is defined as the ratio of the measured to the predicted scour depth; the estimation procedure of λ being dependent on the database being used. Data reported in Benedict and Caldwell (2014), who compiled laboratory scour measurements conducted since 1956, are utilized herein. Although the database entails a wide range of data, laboratory live bed data under narrow pier condition was considered for the estimation of λ since the site condition of the Woodrow Wilson bridge falls in such category. Based on the definition of Melville and Coleman (2000), if $y/b > 1.4$, then a narrow pier condition exists. The distribution of λ was observed to be normally distributed. Figure 8 shows the observed distribution of λ for the laboratory live bed data under narrow pier condition when the HEC 18 model is used. Table 1 shows the list of deterministic and random variables and the associated statistical characteristics considered herein.

Owing to the non-linear nature of Equation (7), a Monte Carlo simulation approach was considered to compute the probability of exceedance. A total of 10,000 simulation cycles were used to estimate P_e . If the limit state function follows normal probability distribution, β can be related to P_e using Equation (8).

$$P_e = \Phi(-\beta) \quad (8)$$

Where, Φ is a probability function representing the probability that the normalized random variable is below a given value. A *scour factor* is defined as the ratio of D_p to D_s . The Monte Carlo simulation was run for a scour factor ranging from 1 to 3, subsequently, a relationship between the reliability index and scour factor was devised. The concept is very similar to *resistance factors* in the LRFD approach as it develops *scour factors* to be applied to the deterministically-evaluated scour magnitudes.

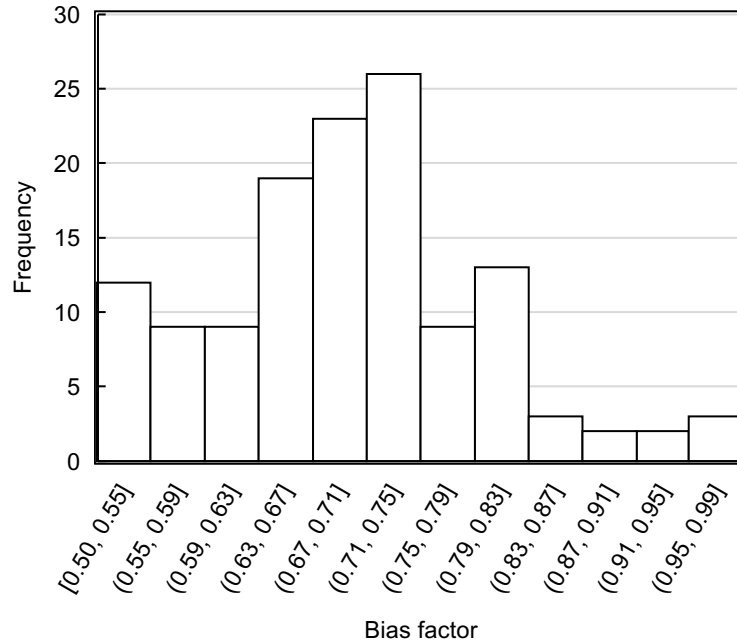


Figure 8. Statistical distribution of bias factor, λ for narrow pier under live bed condition when HEC 18 (2012) model is used. (Normally distributed with skewness = 0.34)

Table 1. Distribution properties of utilized deterministic and random variables in Monte Carlo simulation

Variables	Live bed		Distribution
	Mean	COV	
Pier width	0.6 ft		Deterministic
Pier face shape	Circular		Deterministic
Skew angle	0 degree		Deterministic
Aspect ratio (Length to width)	1		Deterministic
Flow velocity	1.55 ft/s	0.186	Log-normal
Flow depth	1.24 ft	0.2	Normal
Median grain size	0.3 mm	0.081	Normal
Bias factor – HEC 18 (2012)	0.67	0.21	Normal

The scour factor associated with a certain β can further be correlated to the Probability of Deceadance (POD). POD is defined as the probability that the predicted scour depth will be less than the measured scour depth, estimated from the Benedict and Caldwell (2014) database. To quantify POD, initially, the frequency distribution of χ_{POD} , which is the ratio of the predicted to the measured scour depth was developed. Using Kernel density estimation, the population probability density function for χ_{POD} was generated, followed by integration of the density function to obtain the cumulative density function. Finally, the POD is obtained by subtracting the

cumulative density value from one. The relationship between the reliability index or the associated probability of deceedance and scour factor is presented in Figure 9.

For example, in Figure 9, if the target reliability index, β_T is 2.0, the corresponding scour factor is 1.70. Therefore, for the pier M1 of the Woodrow Wilson bridge, the scour depth corresponding to $\beta_T=2.0$ is 105.9 ft (32.3 m). Figure 9 further suggests that the use of a $\beta_T > 0$ causes the probability of deceedance (defined as the probability of having a predicted scour magnitude being less than the value occurring in the field) to decrease.

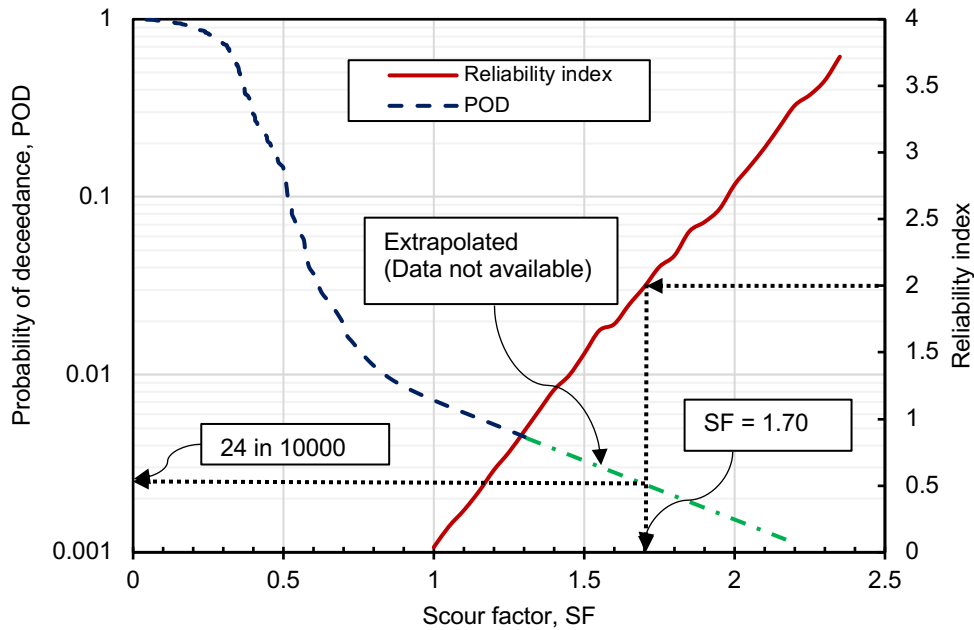


Figure 9. Relationship among probability of deceedance, reliability index and scour factor. (Note: The POD chart has been developed based on HEC 18 model applied to live bed laboratory data)

Probability of Exceedance over the Design Life of Structure

A flood event with a recurrence interval of T years has a $1/T$ probability of being exceeded in any given year. The 100-year flood is generally recommended in HEC 18 for hydraulic analyses. It has a probability of exceedance of $1/100$ in any year and this probability increases as the design life increases. If the design life of a bridge is N years, the probability of exceedance in N years, $P_{cumulative}$, can be represented as a function of annual probability of exceedance, P_N , as expressed in Equation (9).

$$P_{cumulative} = 1 - (1 - P_N)^N \quad (9)$$

A 100-year flood has a 63.4% chance of being exceeded in a design period of 100 years. For a specific bridge, a chart relating the scour depth and the probability of exceedance in N years can be developed, allowing the engineer to select a scour depth corresponding to a target probability of exceedance in N years. Referring to Figure 9, the scour factors are corresponding to a certain annual probability of deceedance, which depending on the design life of the bridge, will provide the probability of exceedance in N years (Equation 9). The scour depth corresponding to a scour factor can be obtained by multiplying the HEC 18-predicted scour depth with the scour factor. Figure 10 shows the relationship between the probability of exceedance in N years and scour depth for different design life. For the pier M1 of Woodrow Wilson bridge, the HEC 18 (2012) suggested scour depth is 62.3 ft (19 m), which in turn has a 40%, 50%, and 76% probability of exceedance over a design life of 75, 100 and 200 years respectively. However, if the reliability index-based scour depth is considered with $\beta = 2$, the scour depth is 105.9 ft (32.3 m) and it has a 17%, 22%, and 38% probability of exceedance over a design life of 75, 100 and 200 years respectively. Therefore, it appears that the β based approach reduces the probability of exceedance by more than 23% over the design life investigated (75-200 years).

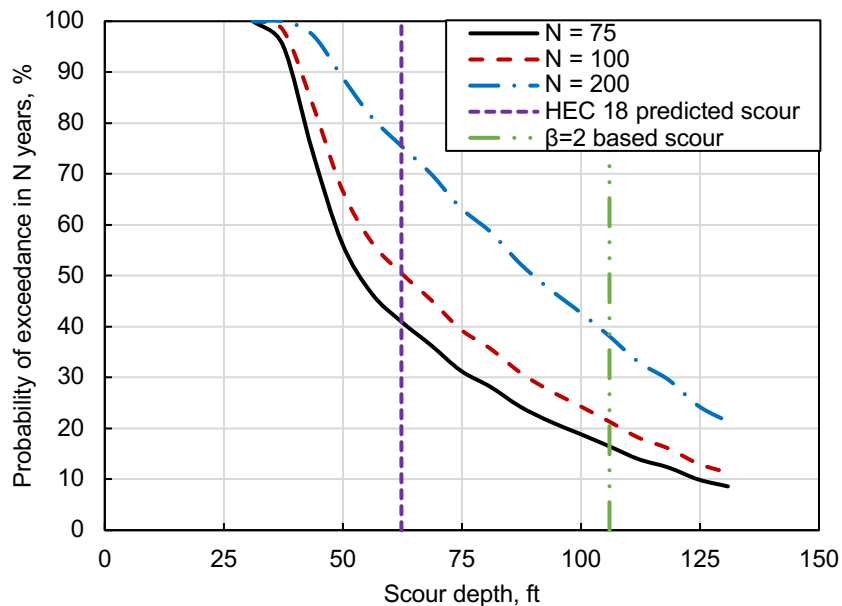


Figure 10. Relationship between probability of exceedance and scour depth for different design life of the bridge when HEC 18 model is used. (Scour depths are for pier M1 of the Woodrow Wilson bridge)

FB-MultiPier Modeling

The details of the FB-MultiPier modeling, AASHTO load cases, and modeling results are presented in Appendix E. The parametric analysis is presented in the following section.

Parametric Analysis

FB-MultiPier analyses were performed to explore the mitigation measures of the increased scour magnitude with the use of the scour factor approach. Subsequently, the effect of variation of pile length and pile diameter on the transverse, longitudinal, and axial displacement of the pile was investigated. While performing the parametric analyses, the center-to-center distance between the piles was kept same as the base case.

Effect of pile length variation

The variation of transverse displacement, longitudinal displacement, axial displacement, and DCR with the changes in pile length is presented in Figure 11. The pile length of the base case model is 210 ft (64 m). The pile length was increased from 210 ft (64 m) to 250 ft (76.2 m) (19%). It appears that an increase of pile length by 40 ft (12.2 m) decreased the transverse and longitudinal displacement by 4.4% and 6.2% respectively, while the axial displacement was reduced by 41.4%. Nevertheless, if the pile length is increased to 220 ft (67.1 m) (increasing length by 4.8%), the axial displacement can be lowered to an acceptable displacement limit of 1 inch (25 mm). It is also apparent that increase of pile length is effective in reducing the axial displacement of the pile.

Effect of pile diameter variation

Figure 11 further shows the variation of pile displacement components with the changes in pile diameter. The pile diameter of the base case model is 70 inches (1778 mm). The pile diameter was increased from 70 inch (1778 mm) to 75 inch (1905 mm). As shown in Figure 11, and for an increase in pile diameter from 70 inches (1778 mm) to 74 inches (1880 mm), the transverse and longitudinal displacement was reduced by 13.2% and 14.4% respectively, while for axial displacement, the reduction was 7.8%. However, as the pile diameter was increased further to 75 inches (1880), the displacement tends to increase. This could be due to the center to center spacing between the piles that was kept same as the base case, which resulted in a reduction of the effective volume surrounding the pile to mobilize the complete foundation resistance. However, it is evident that increase in pile diameter is effective in reducing transverse and longitudinal displacement of the pile.

Scour Risk

Annual risk, R is defined as the product of the annual probability of failure, POF , times the cost of the consequences, C , as expressed in Equation (10) (Baecher and Christian 2003).

$$R = POF \times C \quad (10)$$

In respect to bridge scour study, the probability of exceedance is the probability that a certain scour depth will be exceeded in any future time. Any such event will be considered as a failure event, although failure in this case does not imply a true “collapse” of the foundation system.

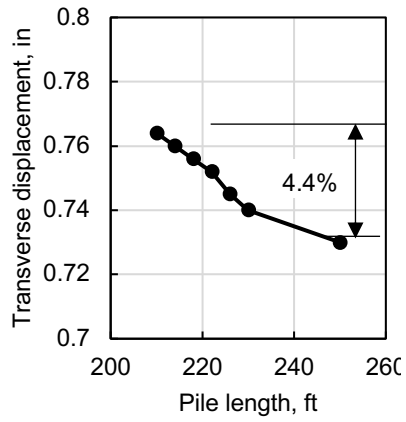
Briaud et al. (2014) described that the target risk level for the civil engineering structures in the United States is 1000 dollars/year and 0.001 fatalities/year. Referring to Figure 9, the HEC 18 (2012) model, without the application of any scour factor, is associated with an exceedance probability of 0.007. Therefore, in the typical frequency-severity chart suggested by Baecher and Christian (2003), the accepted associated cost of consequence will be \$142,900 (1000/0.007). With the target reliability index, β_T of 2.0, the scour factor will be 1.70, and the associated exceedance probability will be 0.0024. For the same cost of consequence = \$142,900, the target risk level will be approximately reduced by a factor of 2/3 and be 343 dollars/year (142,900×0.0024).

Statistics presented in HEC 18 (2012) suggest that in the United States, 493,473 bridges are built over waterways. In a given year, if HEC 18 (2012) suggested approach is used to estimate scour depth, there is a possibility that the scour depth will be exceeded in 3,454 bridges. Whereas, if the scour factor corresponding to the β_T of 2.0 is used, annually, the scour depth would be exceeded in 1,184 bridges, reducing the affected number of bridges by 2,270.

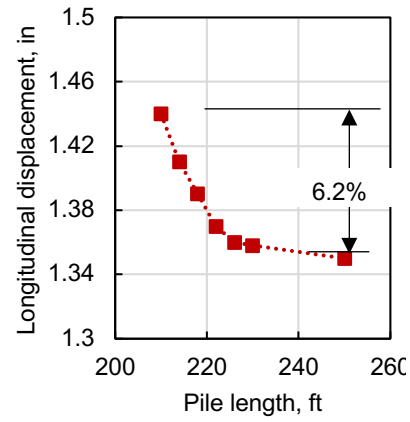
We present herein an example to illustrate the advantage of the proposed approach. Briaud et al. (2014) reported that if the economic loss entails the bridge repair cost, detour cost, and time cost, then the economic loss for one bridge failure can be estimated at \$13,180,158 US Dollars. However, based on the repair cost data reported in California DOT (2011), Briaud et al. (2014) estimated that the average repair cost of one bridge is 560,100 Dollars. For the 2,270 bridges, the economic loss considering only the bridge repair would be 1.27 billion Dollars. Therefore, adopting the scour depth corresponding to the β_T of 2.0 will help to preventing a loss of 1.27 billion Dollars annually. Nevertheless, as presented in the *parametric analyses* section, consideration of β based scour depth might cause the transverse, longitudinal, or axial displacements of the pile to exceed the allowable limit, thereby, requiring a need to optimize pile diameter, pile length, or pile spacing, which might increase the construction cost.

Abutment scour analyses

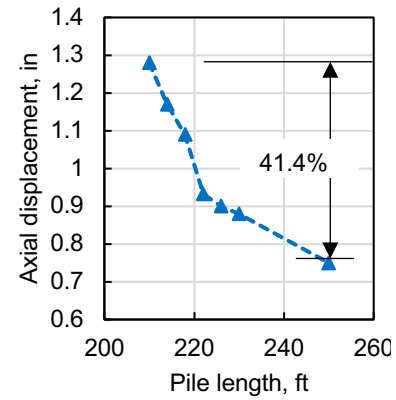
Using the database reported in Sturm (2004), a comparison between the predicted and the measured scour depth is presented. In addition to the SC envelope curve model, three abutment scour prediction models suggested by Hydraulic Engineering Circular No. 18 (HEC 18 2012), namely Froehlich (1989) model, Highway in the River Environment (HIRE) (FHWA 2001) model, and National Cooperative Highway Research Program (NCHRP 2010) model are considered. Results suggest that in general for long abutments, Froehlich (1989) model provides a more conservative estimate of scour depth compared to HIRE (2001) model. Results further indicate that the geometric contraction ratio based scour depth estimation model over-predicts the scour depth by 2.5 times the measured scour depth. A detailed report on the analysis is presented in Appendix F.



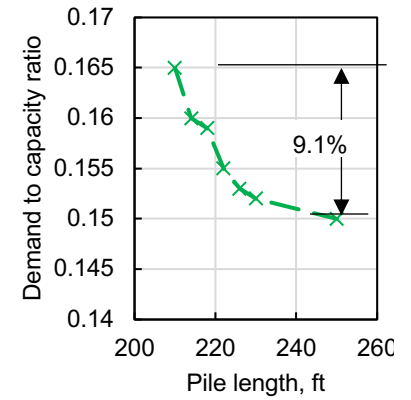
(a)



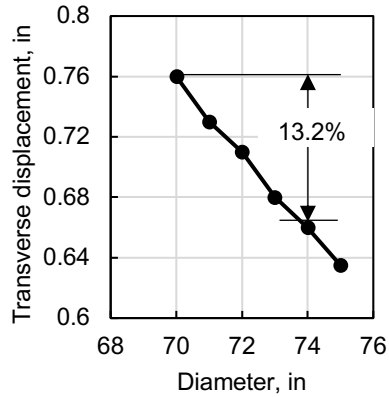
(b)



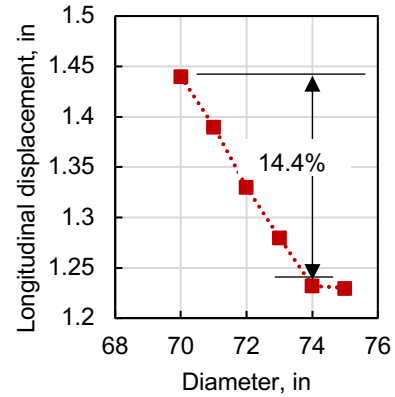
(c)



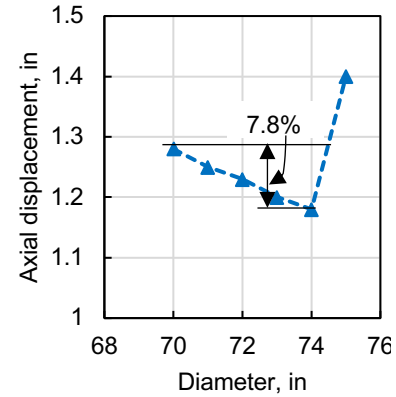
(d)



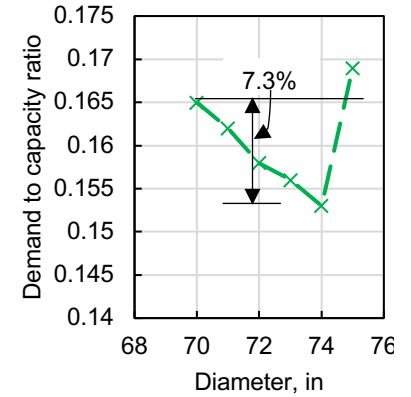
(e)



(f)



(g)



(h)

Figure 11. Variation of (a) transverse displacement, (b) longitudinal displacement, (c) axial displacement, (d) demand to capacity ratio with pile length, and (e) transverse displacement, (f) longitudinal displacement, (g) axial displacement, (h) demand to capacity ratio with pile diameter.

5. Site Selection and Monitored Data

We monitored the seasonal variation in sediment transport at four bridge sites to assess the field-scale scour behavior compared to the modeling results. We developed a list of potential bridge sites all containing a nearby USGS gage. These potential bridges include 16 in the mountain region, 18 in the piedmont region, and 12 in the coastal plain; our preliminary list is included in Appendix G. As discussed with NCDOT and in collaboration with the Research Team for RP 2020-03, six bridge sites in each geologic region of North Carolina were selected as initial options (e.g., ~2 bridge sites in the coastal plain, ~2 bridge sites in the piedmont, and ~2 bridges in the blue ridge mountains).

After the feedback from NCDOT about highlighting any bridges that are of interest and/or proposing alternative sites, we collected the data for the bridges of interest from NCDOT’s database(s) related to bridge inspections (e.g., Unknown Foundations Programs). We also used other resources such as USGS gauges, National Bridge Inventory database, Google Earth, and our own site visits. We assessed the locations for the water level and asked for NCDOT help to deploy our measurement equipment where the water level is deep for field work.

Finally, the bridge sites at Ellerbe Creek, Tar River, Fishing Creek, and Roanoke River were chosen to obtain a variety of characteristics, such as flow, contraction, channel size, and sediment grain size within piedmont and coastal geographic regions of NC (Table 2). After subsequent site visits and assessment of accessibility for field work, Fishing Creek was replaced with Middle Creek due to accessibility issues at Fishing Creek. Both creeks have almost the same size and hydrodynamic condition and the USGS gage number adjacent to the Middle Creek bridge is number 2088000.

Table 2. Field work sites

Site	Bridge Number
Ellerbe Creek	310034
Tar River	340033
Fishing Creek/Middle Creek	320023/ 500092
Roanoke River	410023



Figure 12. Field work sites overlaid on Google Earth satellite image

Field work – October 2020

Ellerbe Creek

In October 2020, we deployed and retrieved our ADCP (acoustic Doppler current profiler) at Ellerbe Creek for detailed measurements of velocity with depth. The ADCP was placed 20m downstream of the bridge (Figure 13) and was programmed to collect data every 10 minutes for 2-minute bursts at 8 Hz (Figure 13, see blue & black colored dot). The ADCP data provide on-site 3D flow and turbulence measurements to be used as both data input and validation in our numerical modeling. We retrieved the device after one month of deployment (from 10-05-2020 to 11-07-2020), however, the measured data analysis showed that it was affected by the flooding on 10-11-2020 (likely due to precipitation from Hurricane Delta) and became buried under deposited sand. Fortunately, 7 days of measured flow velocity and discharge were recorded for model calibration (Figure 14). We also took several transects both upstream and downstream of the bridge to measure bathymetry (Figure 13, 15, & 16), collected sediment samples, and measure velocity using an Acoustic Doppler Velocimeter (Figure 15). All these measurements allow us to refine and increase the accuracy of our computer models.

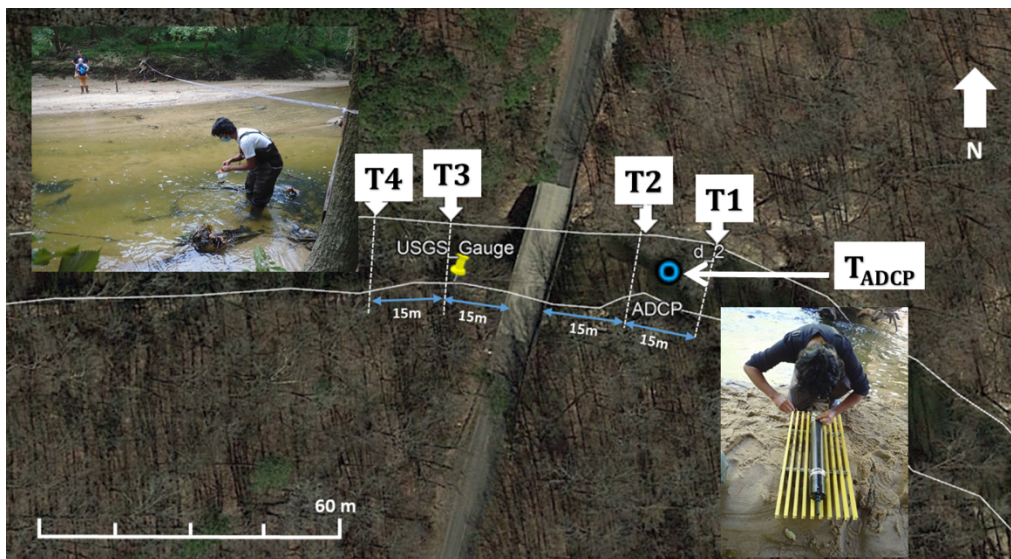


Figure 13. Ellerbe Creek around bridge number 310034 in Google Earth, white dotted lines are the transects where bathymetry profile and sediment samples are taken, blue dot is where ADCP deployed for the month of October 2020

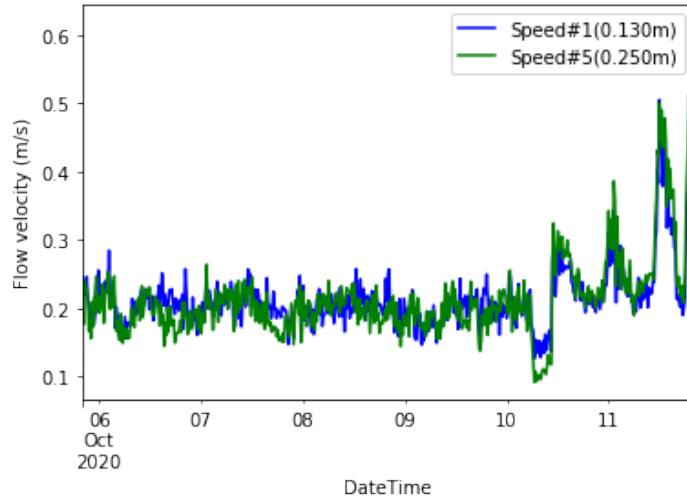


Figure 14. Measured velocity at Ellerbe Creek at 13cm (blue) and 25cm (green) above the riverbed from 10-05-2020 to 10-11-2020

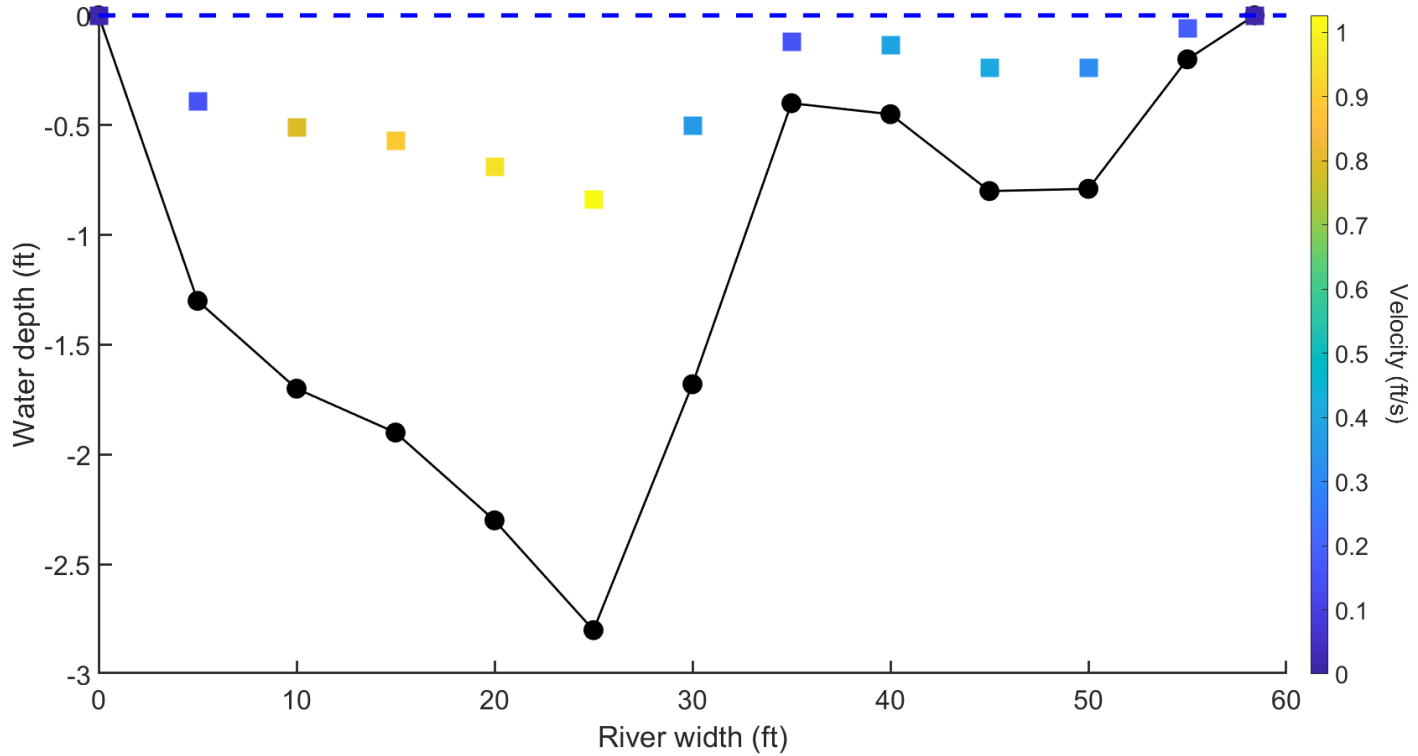


Figure 15. Measured velocity and bathymetry transect at Ellerbe Creek at the location of ADCP.

Cross-sections of Ellerbe Creek

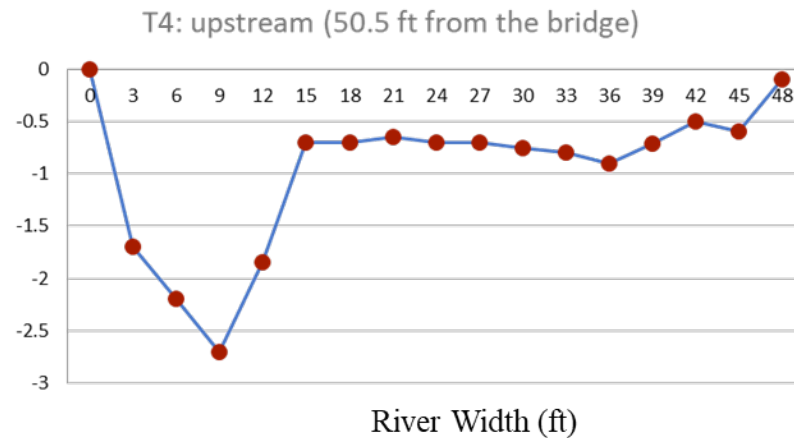
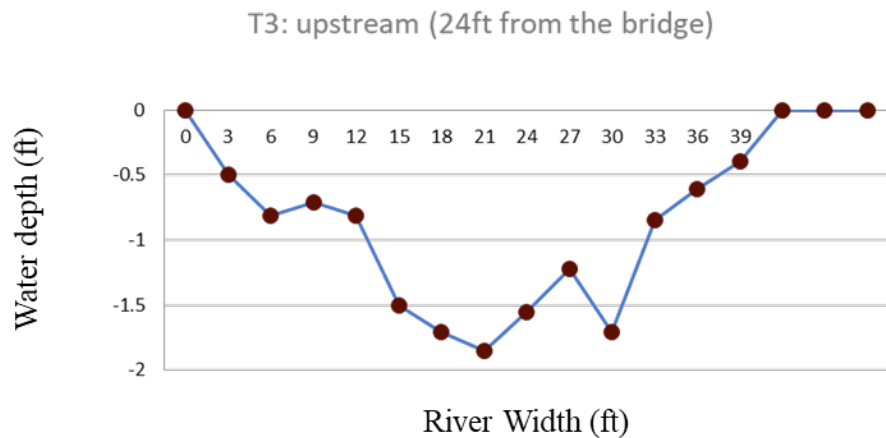
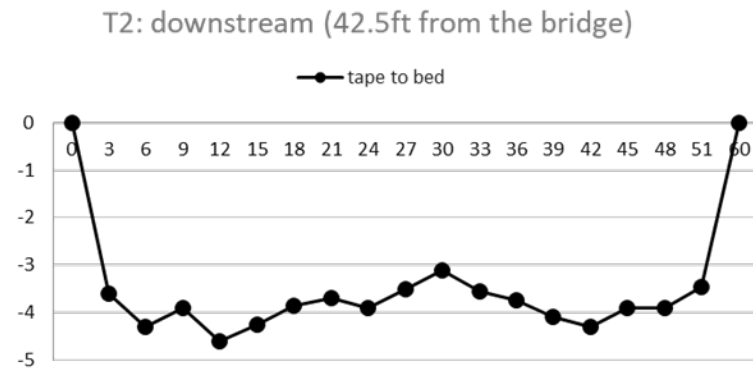
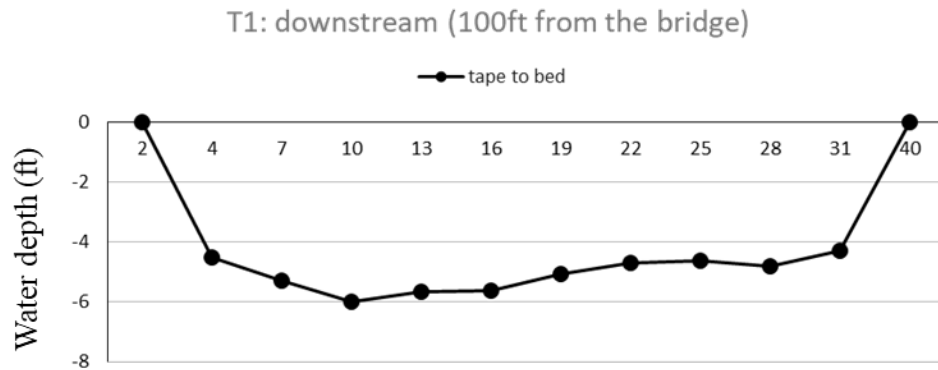


Figure 16. Measured transects at Ellerbe Creek at upstream and downstream of the bridge number 310034, see Figure 10 for locations of transects.

Field work – June 2021

We performed detailed field collection at three selected sites (Tar River, Middle Creek, and Roanoke River) on June 7th, 9th, and 10th 2021 to gather geometric, flow, and sediment data (Table 3). We used a range of instruments for field monitoring: the Nortek Acoustic Doppler Current profiler (ADCP), the River Ray ADCP (from Dr. Castro-Bolinaga’s team), three Tilt Current Meters (TCM), and a Fish Deeper buoy collecting bathymetry via CHIRP.

Table 3. Field work sites and the collected data

	Tar River (2021-07-06)	Middle Creek (2021-09-06)	Roanoke River (2021-10-06)
Flow Velocity	Nortek ADCP River Ray Tilt Current Meter	River Ray Tilt Current Meter	River Ray Tilt Current Meter
Bathymetry	River Ray Fish Deeper	River Ray Fish Deeper	River Ray Fish Deeper
Sediment Samples	✓	✓	✓
Site Geometry	Bridge Report Manual Geometry	Range Finder	Range Finder

We deployed the River Ray ADCP and TCMs at the three bridge sites. The TCMs yielded the flow velocity time-series at a single point about 20-50 cm above the riverbed. We deployed and retrieved the Nortek ADCP in Tar River, however due to device malfunctions and difficulty with deployment methods, it was not used at the Middle Creek and Roanoke River sites. For bathymetry, we attached the River Ray ADCP and Fish Deeper sonar/CHIRP buoy to a kayak or boat for riverbed scanning. We acknowledge herein NCDOT help and supervision, including the extra help by DOT interns for Tar River field work and having boat access while performing Roanoke River data collection. The analysis of the collected data is presented herein. The data are also incorporated into our numerical simulations of the field sites.

Tar River

We deployed and retrieved our ADCP on June 7th, 2021 for 2.5 hours from 11:00 am to 1:30 pm just on the upstream side of the bridge, 25 and 30 ft from the east-side and west-side piers respectively (Figure 17). The device was attached to a cinder block with a height of 15 cm for stability (Figure 18). The ADCP data measured on-site 3D flow and turbulence measurements for calibration and validation in our numerical modeling. The flow velocity measurements start at 42 cm above the riverbed (125 cm total water depth) and it is recorded in 88 different water levels. The measurements were analyzed using Python. Averaging over each burst time (5 minutes) the depth-averaged and time-averaged velocity were calculated and are presented in Figure 19 and Figure 20.

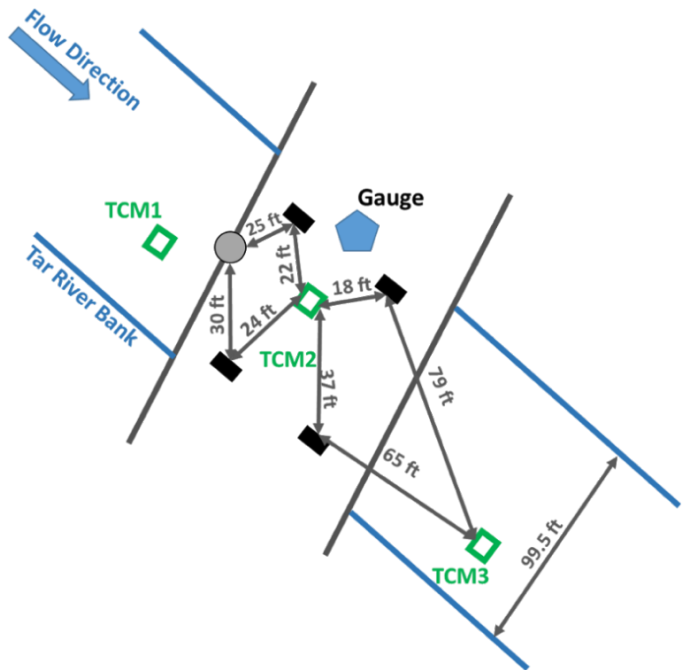


Figure 17. The location of the ADCP, Tilt Current Meters (TCM), USGS Gauge, and bridge piers (black rectangles) in Tar River

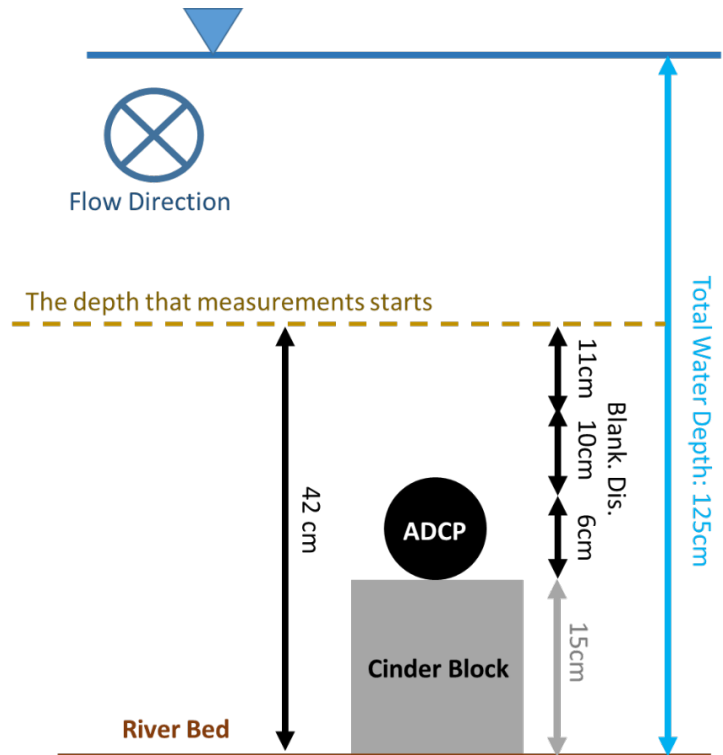


Figure 18. ADCP deployment in Tar River on June 7th, 2021

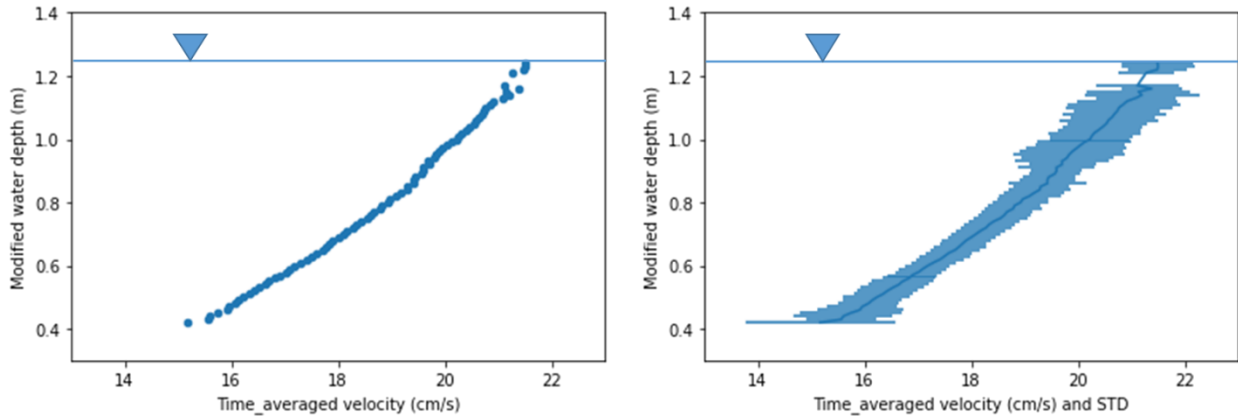


Figure 19. Time-averaged velocity profile (left) from ADCP flow data and its Standard Deviation (right)

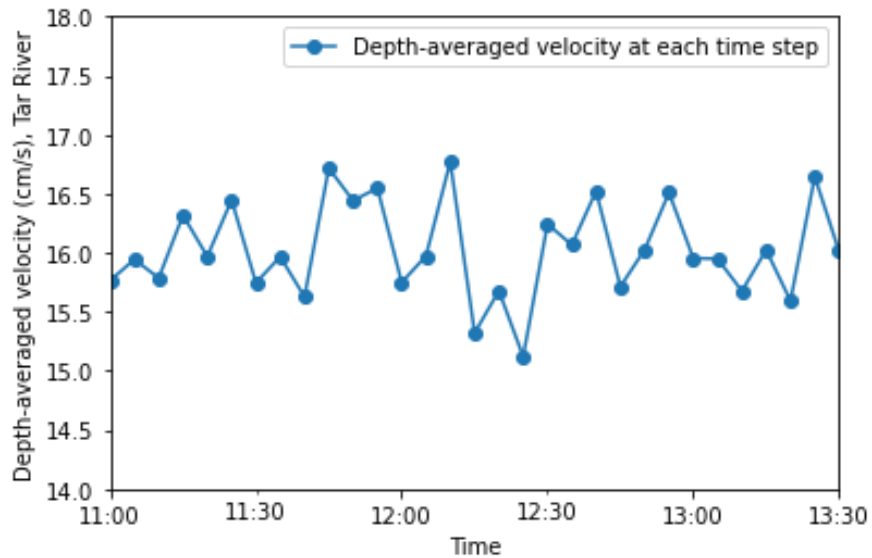


Figure 20. Tar River depth-averaged velocity at each time step from ADCP

The depth-averaged velocity was recorded in a range of 15.1 to 16.8 cm/s on the upstream edge of the bridge where ADCP was deployed. The water depth at this location was recorded to be 125 cm which is slightly lower than the USGS gauge record (160 cm). By having the river cross section (from River Ray-Dr. Castro-Bolinaga’s team), the total discharge can be computed and compared to what USGS Gauge is reporting for June 7th 2021, 11:30 am ($\sim 4.36 \text{ m}^3/\text{s}$).

Three TCMs (TCM 1, 2, and 3) were deployed on the upstream, in the middle, and on the downstream of the bridge piers. These devices collected flow velocity at a single point, 50 cm above the riverbed. We analyzed and averaged the three sets of data and compared them to Nortek ADCP measurements at the same water depth (Figure 21). The shaded area in Figure 19 shows the standard deviation of the averaged data. The TCM3, which is located further downstream of the piers, shows the largest recorded velocity (20 m downstream). At such a location it seems that the effect of the piers on the flow is insignificant. The ADCP data were expected to be higher,

however, due to the wooden debris right upstream of the ADCP, the slightly lower recorded velocity can be explained. Also, a part of the error in the measurements is related to the averaging process and the device measurements' precision.

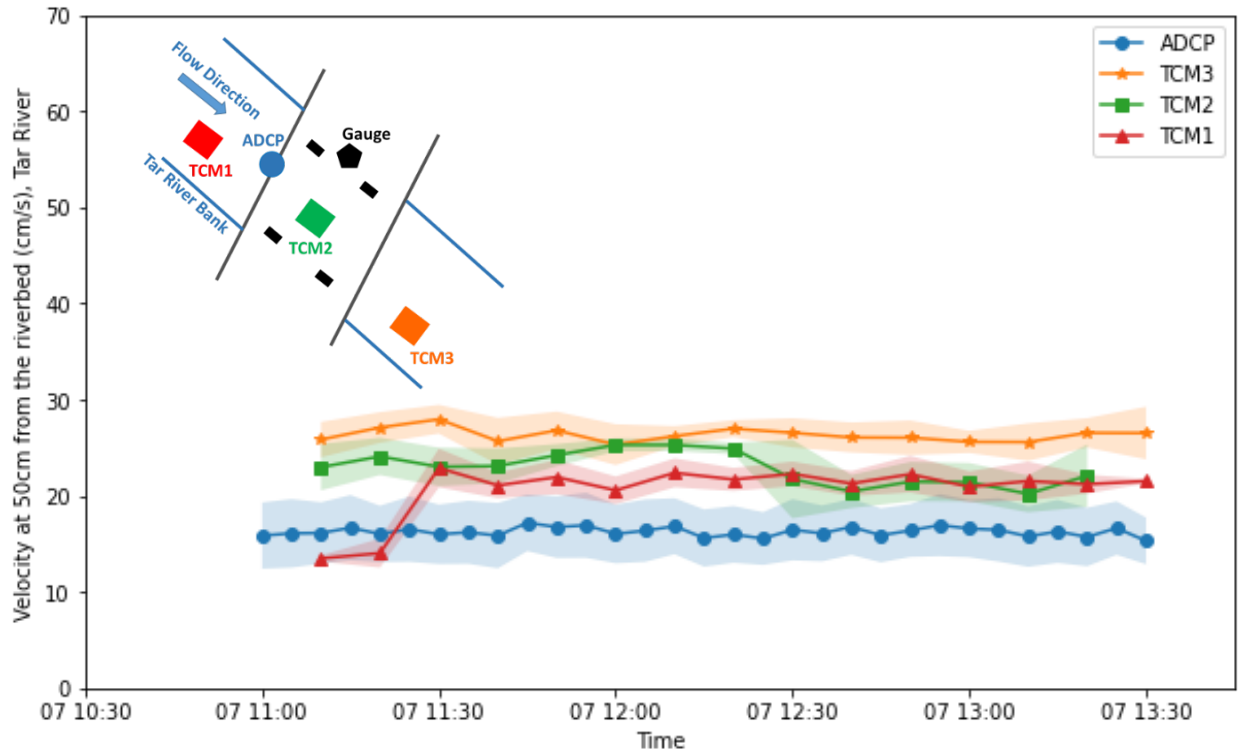


Figure 21. Tar River TCMs and ADCP data, flow velocity at 50 cm above the riverbed

Middle Creek and Roanoke River

We deployed the TCMs in Middle Creek and Roanoke River on June 9th and 10th 2021, respectively. The location of the TCMs with regards to the bridge piers are shown in Figure 22 and Figure 23. The measured velocity at 50 cm water depth is analyzed, averaged, and plotted, as shown in Figure 24. The TCM2 in Roanoke River is located on the upstream of the piers and it recorded the lowest velocity compared to TCM3 (in the middle of the piers) and TCM1 (further downstream of the piers). In Middle Creek, the lowest measured velocity is for the TCM3 located downstream of the piers and the highest measurements are from TCMs located further upstream.

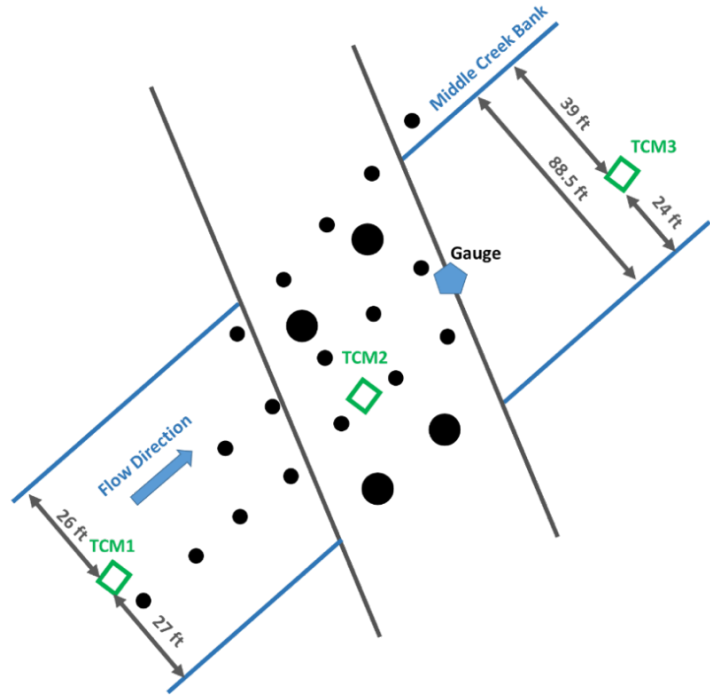


Figure 22. The location of the Tilt Current Meters (TCM), USGS Gauge, bridge piers (large black circles), and subaqueous wooden piers (small black circles) at Middle Creek.

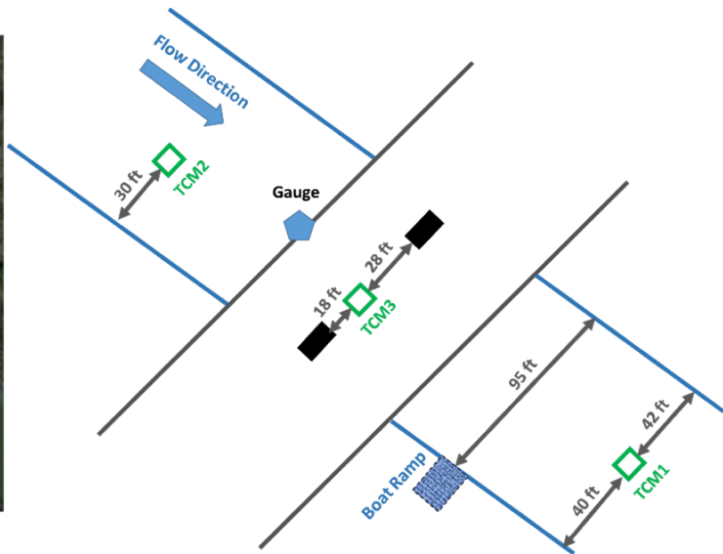


Figure 23. The location of the Tilt Current Meters (TCM), the USGS Gauge, and bridge piers (black rectangles) at Roanoke River.

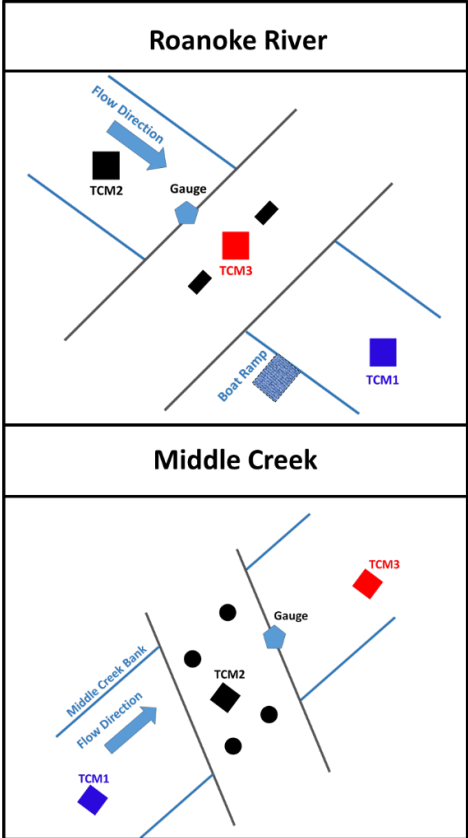
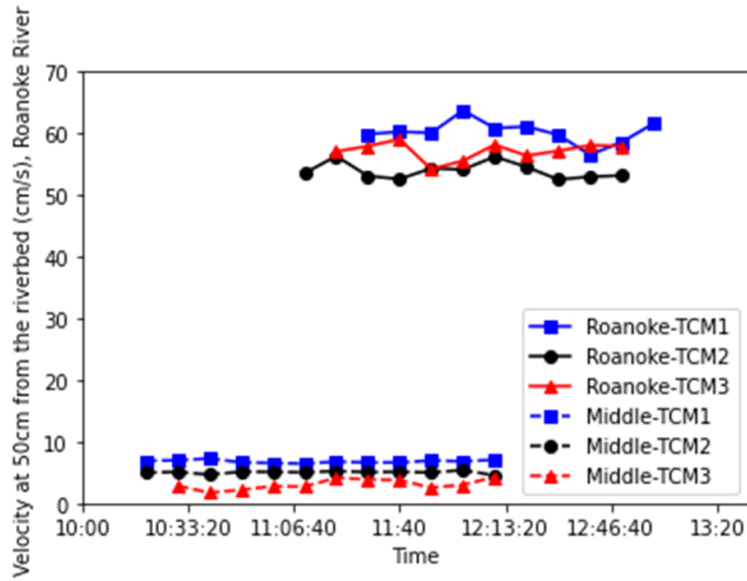


Figure 24. Roanoke River and Middle Creek TCMs data, flow velocity at 50 cm above the riverbed.

6. Numerical Modeling

Delft3D Flexible Mesh, a finite volume hydrodynamic and morphodynamic model, was used to simulate the hydrodynamic condition and scour depth around bridge piers for the Roanoke River bridge site. Overall, the Delft3D morphodynamic modeling of scour is computationally intensive (most runs take several days to complete on a High-Performance Computers, in parallel, or a week on a high-end workstation. The creation of the model mesh, in particular, is a slow process and often failure of the model to converge occurs if the cells in the mesh transition rapidly in size.

During the numerical modeling task, and while technically Delft3D could be used for simulating the response of smaller creeks (i.e. Middle Creek or Ellerbe), we consistently had significant model failures and issues with unrealistic flooding in these smaller domains. Delft3D is optimized to cover larger spatial areas at lower resolution (for example, 10 kmx1 km spatial domain with 100mx100m grid cells (ie a total of 1000 cells) versus, smaller size domains with cell sizes varying from 2mx2m to 24mx24m (where number of cells will be on the order of tens of thousands) In particular, the shallower our river or creek (as occurs with Ellerbe and Middle Creek) the more sensitive the model is to the initial bathymetry and the more likely the model does not converge during a simulation. We had very limited bathymetry data and based on our extended field deployment at Ellerbe Creek, we observed the bathymetry to change very rapidly (such as burying our ADCP under a meter of sand) over a short period of time. Overall, the lack of accurate and representative initial bathymetry and the shallow depth of water hindered our ability to accurately model these smaller systems. Therefore, we focused the numerical modeling of scour on the Roanoke River bridge site. In parallel, hydrodynamic modeling and predicted discharge, flow depth, and flow velocity at the bridge piers for the Tar River and Ellerbe Creek are presented in Appendix H..

The computed scour depth and hydrodynamic characteristics for 25-, 50-, 100-, and 200-year flood conditions for the Roanoke River bridge site are compared to results from FHWA HEC-18 procedure, the SC scour envelope curves, and three other simple models reported in literature. The results obtained from numerical simulations of the other three sites (Ellerbe Creek, Middle Creek, and Tar River) are included in Appendix H.

Roanoke River: Numerical Simulation

Herein we summarize the steps taken to model the hydrodynamic conditions and maximum average scour depth around the bridge piers (Roanoke River, bridge #410023). First, the USGS gages adjacent to the bridge were located and their historic flow elevation and flow discharge data were analyzed to obtain the 25-, 50-, 100-, and 200-year flood characteristics. The only discharge measurements available were from the years 1912 to 2020 at the upstream gage, USGS gage #02080500 “Roanoke River at Roanoke Rapids”. After investigating the yearly peak flow at this location, we realized the presence of a significant drop in the value of the annual peak discharge after 1955; the year in which the Roanoke Rapids dam was built (Figure 25). Therefore, in our Extreme Value analysis we include the recorded data only from 1955 to 2020 (Figure 26) and we found a flow rate of 1,599 m³/s to represent the 100-year flood. On the other hand, the use of the

USGS StreamStats application, including all the annual peak floods in the analysis (1912 to present), yielded a much larger 100-yr flood discharge at 5,097 m³/s. Table 4 shows the computed flood conditions vs USGS StreamStats application. As suggested by the NCDOT Steering Committee, we include StreamStats application 100-yr flood in our modeling to be able to calculate the scour depth in such hydrodynamic condition as well.

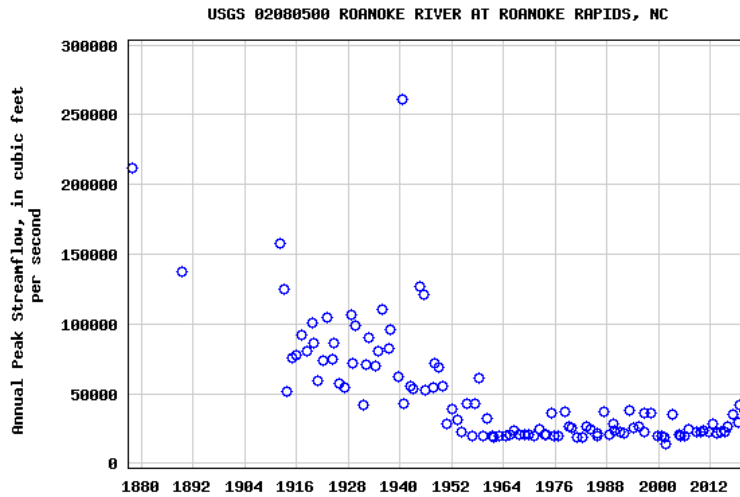


Figure 25. Annual peak discharge at the USGS gage #02080500 Roanoke River at Roanoke Rapids.

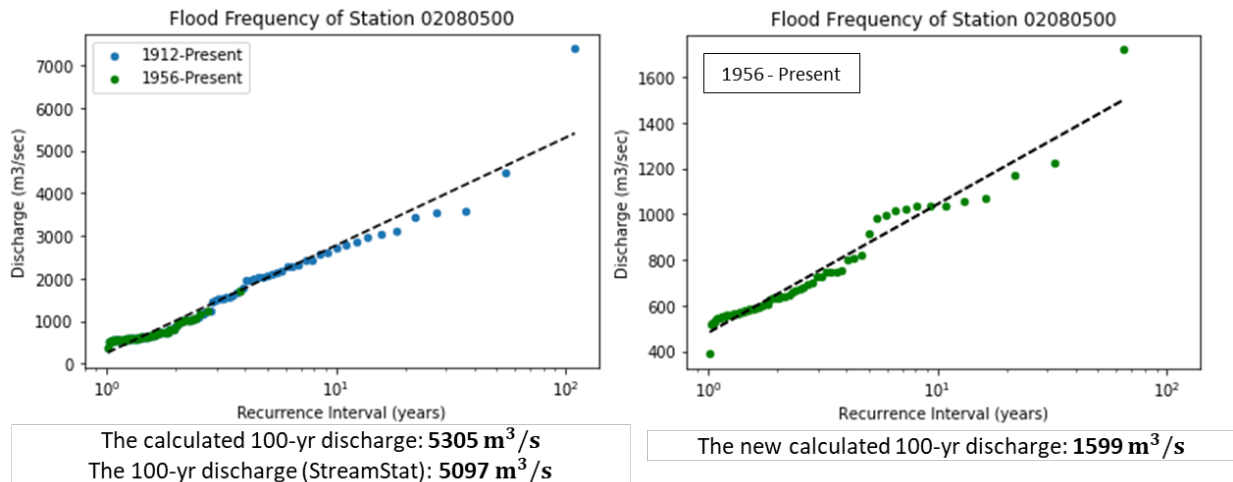


Figure 26. Extreme Value analysis applied to USGS gage #02080500 records from 1956 to 2020 (green dots)

Table 4. Computed flood conditions vs. USGS StreamStats application

Roanoke River/Gage 02080500	years of data	mean Discharge (m ³ /s)	10-yr flood (m ³ /s)	25-yr flood (m ³ /s)	50-yr flood (m ³ /s)	100-yr flood (m ³ /s)	200-yr flood (m ³ /s)
StreamStats application	110 (1912 - present)	216	3427	4078	4588	5098	5664
Research Team Analysis	64 (1956 - 2020)	348	1040	1262	1431	1599	1768

Roanoke River – Model Calibration

We created a curvilinear high-resolution mesh (cell sizes from 2 m² to 200 m²) for Roanoke River, bridge #410023. The spatial domain consists of 33,927 elements and covers an area with a size of ~3 km x ~1.5 km. For the initial riverbed level, the equilibrium bathymetry was obtained by applying the averaged monthly flow data. For the floodplain topography, the NC Risk Management most recent LiDAR data, with 1 m resolution, are used (Figure 27). The process of integrating NC state collected LiDAR topography with measured bathymetric transects into a seamless starting DEM is described in our appended [video](#). The bridge piers are simulated in the bathymetry as non-erodible lumps and the model is run in hydrodynamic mode covering 5 days including the day during which we have performed fieldwork (June 10th). We use the USGS gage 02081000 at the bridge site (Roanoke River) to drive the upstream discharge boundary condition of the model and use the measured water levels at this gage as the downstream water level boundary condition. As shown in Figure 28, the resulting modeled water depth reasonably matches the USGS 02081000 gage recorded water depth at Roanoke River bridge (Figure 28).

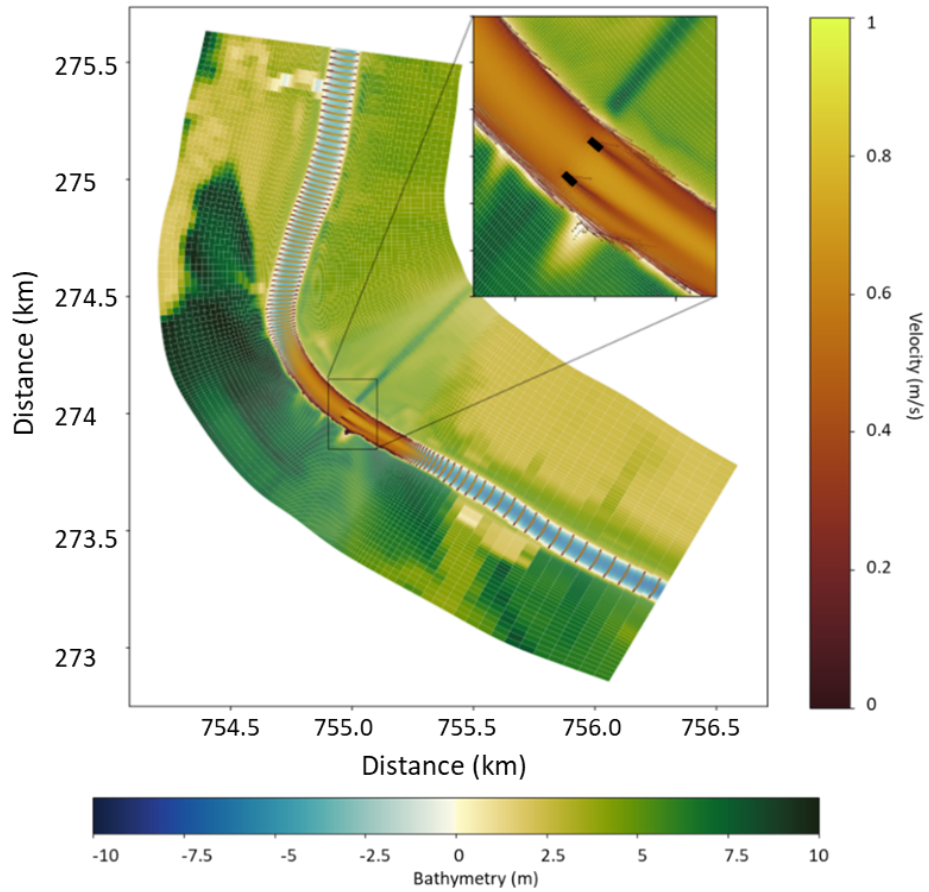


Figure 27. Delft FM Roanoke River spatial domain, mesh, and equilibrium bathymetry overlain by flow velocity; the black rectangles show the bridge piers locations in the model

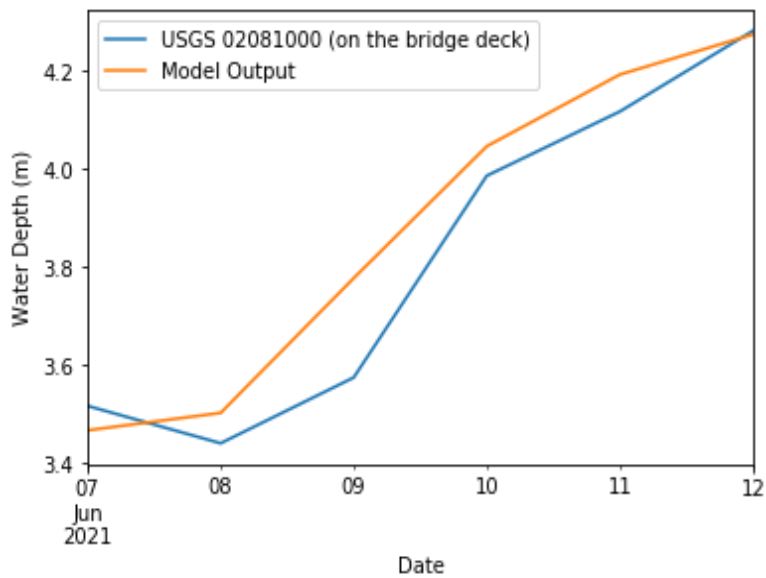


Figure 28. Time series of water depth measured by USGS gage 2081000, located at the bridge (blue line) and modeled water levels (orange line)

Roanoke River – Model Results

Having a calibrated model for our region of interest, we applied the computed flood conditions (Table 4) and analyzed the flow and sedimentation results. Figure 29 shows the flow velocity and the extent of flooding in the whole domain. We have zoomed in on the area near the bridge piers under six different flood conditions. By extracting the approach mean flow velocity and water depth for each flood return period (Table 5) and by knowing the characteristics of the river and the piers, the scour depth is also computed using simpler analytical models (e.g., HEC-18) and the SC approach, for comparison.

Table 5. The modeled approach velocity and approach flow depth for flood condition in Roanoke River

Roanoke River	Discharge (m ³ /s)	Approach mean flow velocity (m/s)	Approach flow depth (m)
10-yr flood	1040	1.6	7.5
25-yr flood	1262	1.8	8.1
50-yr flood	1431	2.1	9
100-yr flood	1599	2.3	9.4
200-yr flood	1768	2.4	10.2
100-yr flood (StreamStats)	5098	3	13.4

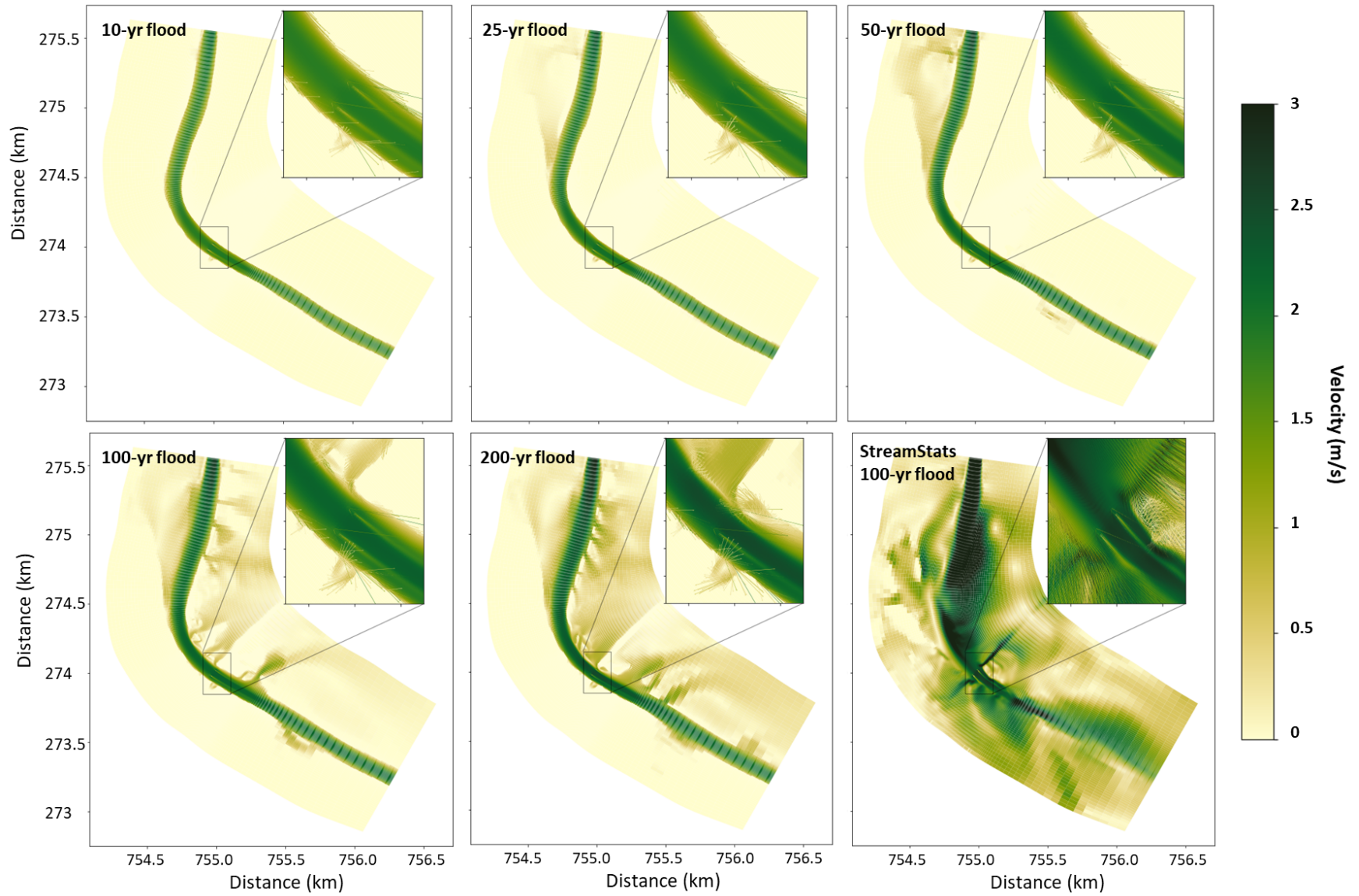


Figure 29. Quiver plot of predicted flow velocity at Roanoke River in flood conditions where color and length of the arrows indicates velocity magnitude.

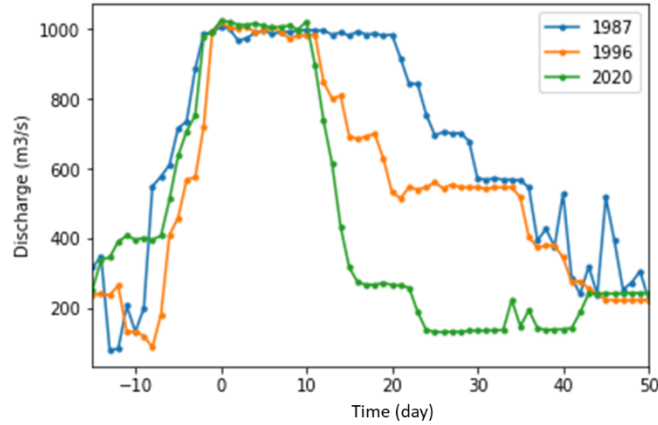


Figure 30. Roanoke River three largest floods (since 1955) hydrograph, recorded by USGS gage number 020280500

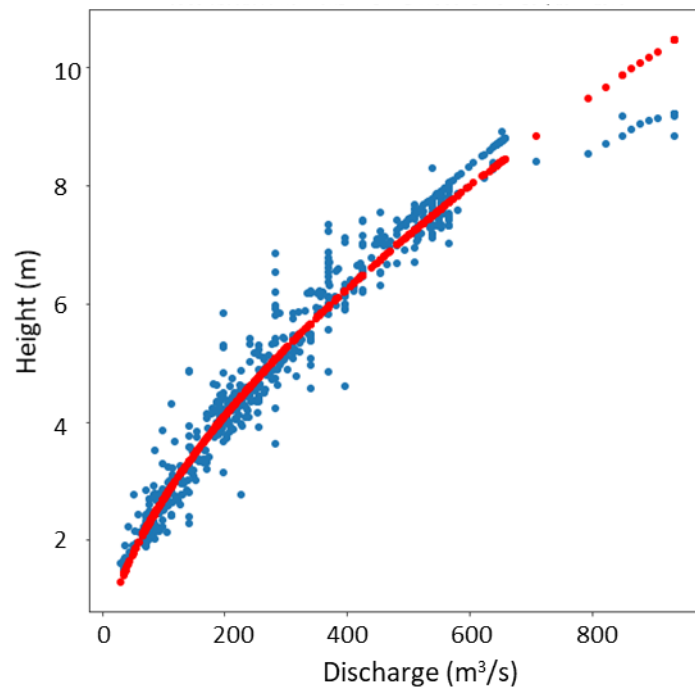


Figure 31. Stage-Discharge rating curve for the USGS gage number 020281000, 1974-1979

By extracting three largest Roanoke River flood events hydrographs (Figure 30) and using the magnitude of 100-yr flood discharge (Table 4), we developed a 100-yr flood hydrograph as the upstream boundary condition in the model. In addition, we generated the stage-discharge rating curve for the USGS gage # 02081000 (the gage on the bridge, Roanoke River Near Scotland Neck) to estimate the associated stage for any given discharge as downstream boundary condition in the model (Figure 31).

The 100-year flood model duration is 30 days (the 100-yr flood discharge is assumed to be occurring for ~10 days; the whole flood event starting from mean discharge to 100-yr discharge, and again back to mean discharge is occurring for 30 days.). This leads to the flood event lasting 10 days) starting and ending with Roanoke River mean annual discharge ($348 \text{ m}^3/\text{s}$).

We investigated the erosion and deposition at distances of 1D, 2D, and 4D around the bridge piers (where D is the width of the pier). Figure 32 indicates the bed level at the end of the flood event for areas around the pier, which are located on the outside of the river bend at our bridge.

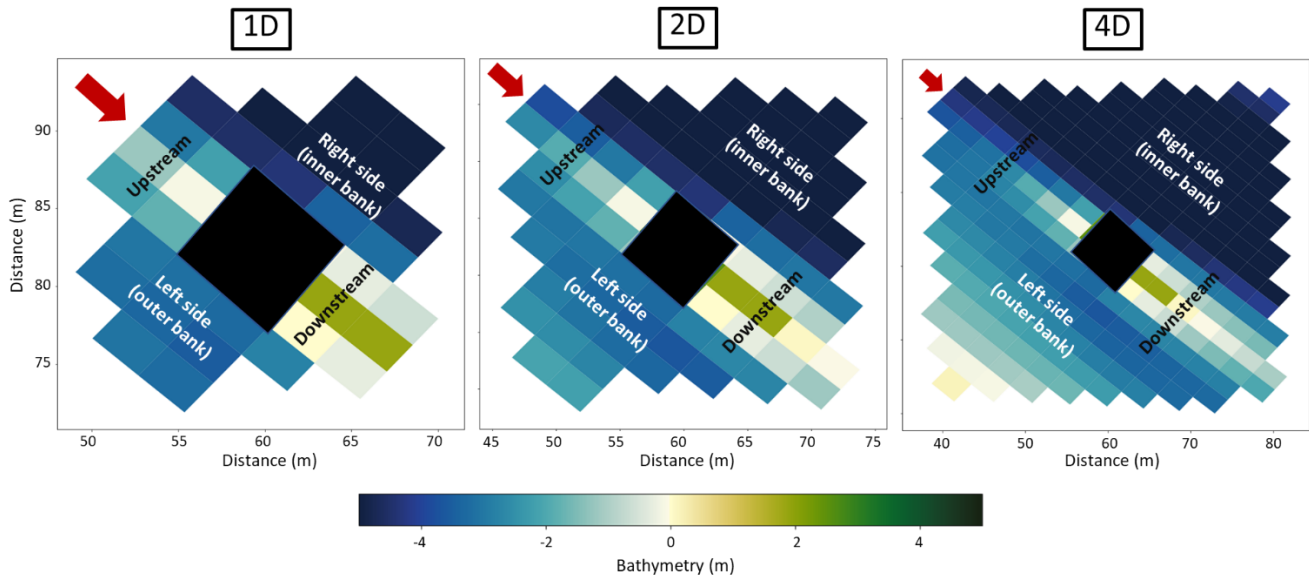


Figure 32. Bed level at the end of the 100-yr flood event for 1D, 2D, and 4D distances around the pier closer to the outside bend of the river; the black rectangles represent the pier, red arrow indicates the flow direction

To compute the maximum scour on the upstream, downstream, right side, and left side of the piers in 1D, 2D, and 4D distances around the piers, we plotted the bed level change per area from the model results (Figure 33). Then, by finding the maximum difference between the extreme points, the maximum average scour depth per meter square, per flood event, was computed (Table 6).

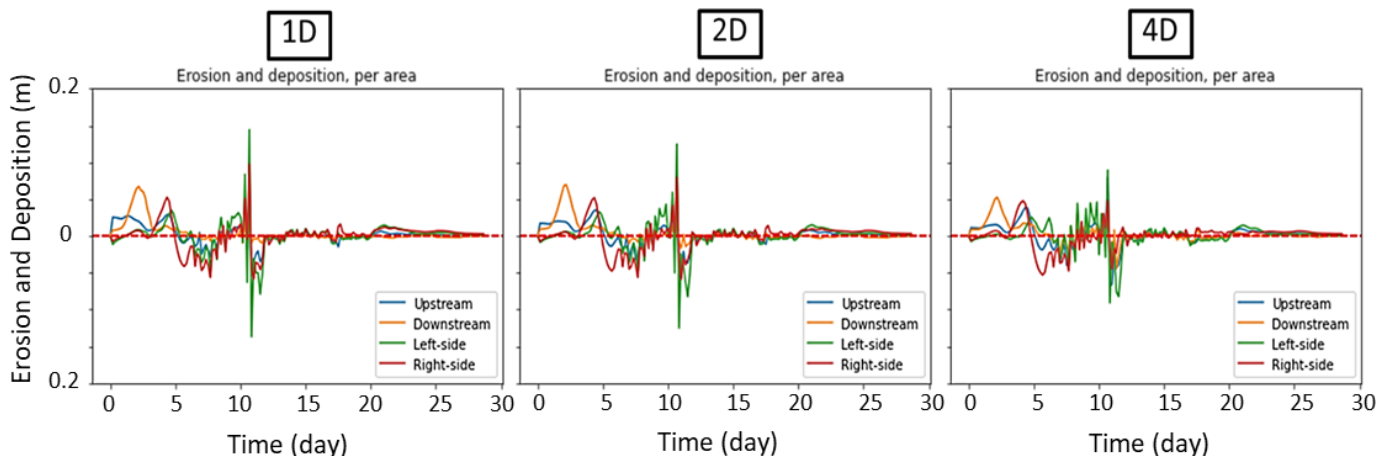


Figure 33. Bed level changes during the 100-yr flood at 1D, 2D, and 4D around the pier closer to the outside bend of the river

Table 6. The computed maximum scour depth during the **100-yr flood** at 1D, 2D, and 4D around the bridge piers on the outside and inside bend of the river

The pier closer to the outside bend of the				The pier closer to the inside bend of the river			
Max scour depth (cm)	1D	2D	4D	Max scour depth (cm)	1D	2D	4D
Upstream	12.3	12.6	14.7	Upstream	9.0	12.2	14.9
Downstream	5.9	6.0	6.9	Downstream	5.6	6.4	11.4
Right side (inner bank)	15.6	13.8	10.0	Right side (outer bank)	19.6	15.7	10.7
Left side (outer bank)	28.1	25.0	18.0	Left side (inner bank)	28.1	22.3	17.4

Due to the model computational efficiency, we simulated the rest of the flood conditions as a constant discharge over one day. Then, we computed max scour depths under 10-, 25-, 50-, 100-, and 200- year flood conditions (Table 7). More detailed tables of max scour depths at 1D, 2D, and 4D distance from the pier, under these flood conditions, are presented in appendix I.

Table 7. The computed maximum scour depth during the 10-, 25-, 50-, 100-, and 200- year flood conditions around the bridge piers on the outside and inside bend of the river

Max Scour Depth (cm/m²)		
10-yr flood	The pier closer to the outside bend	The pier closer to the inside bend
Upstream	2.2±0.9	2.5±1.4
Downstream	9.9±4.4	11.2±6.2
Inner Bank	0.1±0.1	0.2±0.3
Outer Bank	0.3±0.4	0.4±0.2
25-yr flood		
Upstream	2.4±1	2.7±1.5
Downstream	12±5.2	13.9±7.7
Inner Bank	0.2±0.2	0.1±0.1
Outer Bank	0.4±0.4	0.2±0.3
50-yr flood		
Upstream	2.8±1.2	3.3±1.9
Downstream	14.8±6.2	17.6±9.5
Inner Bank	0.3±0.2	0.6±0.7
Outer Bank	0.1±0.2	0.3±0.4
100-yr flood		
Upstream	2.2±1	3.5±1.7
Downstream	14±5.7	19±9.1
Inner Bank	0.5±0.4	0.5±0.5
Outer Bank	0.2±0.1	0.2±0.2
200-yr flood		
Upstream	3±1.1	3.2±1.6
Downstream	17.6±8.5	18.2±8.6
Inner Bank	0.6±0.9	0.9±0.7
Outer Bank	0.7±0.6	0.8±0.5

Based on the analyses results, the magnitudes of maximum scour depth are higher at the left side of the piers (facing upstream). Moreover, the scour depths are smaller immediately downstream of the piers, due to decreased velocities allowing for deposition behind the piers. This response becomes smaller as we include larger areas around the piers (4D vs 1D) and go further away from the piers. Moreover, we see increasing trend of computed maximum scour for increasing flood magnitude (Table 7).

It is however important to note that there is decreased maximum scour for the 100-year flood if run under constant discharge (Table 7, 14-19 cm/m²) compared to a temporal 100-year flood, (Table 6, 25-28 cm/m²). Based on our analysis, increasing the duration of constant discharge for the 100 year flood beyond one day does not increase the total maximum scour occurring.

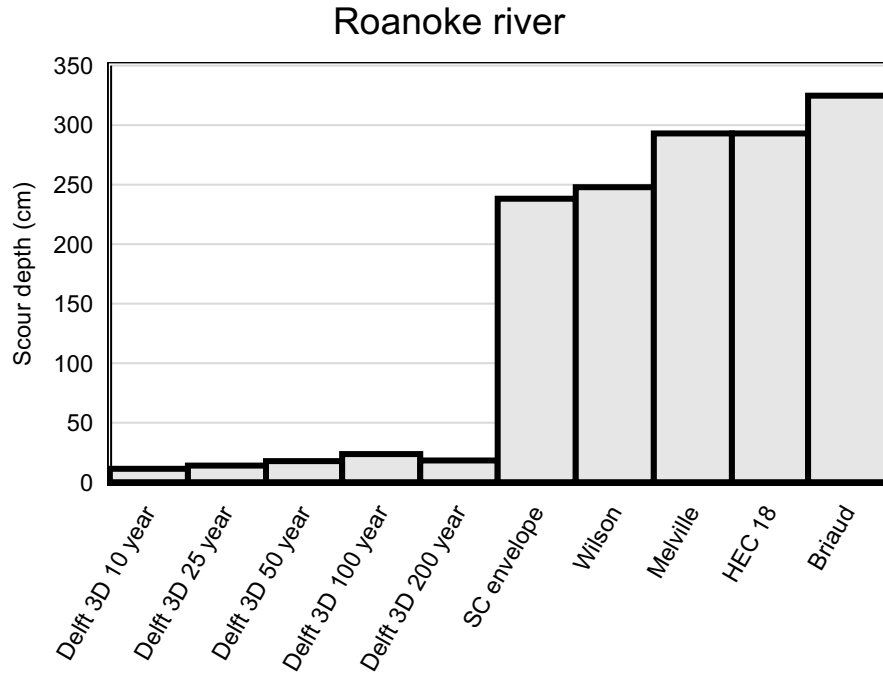
Tutorial Video

https://drive.google.com/file/d/113mw8_hSw9DiX0LmQufEyBFiK07kG_co/view?usp=sharing

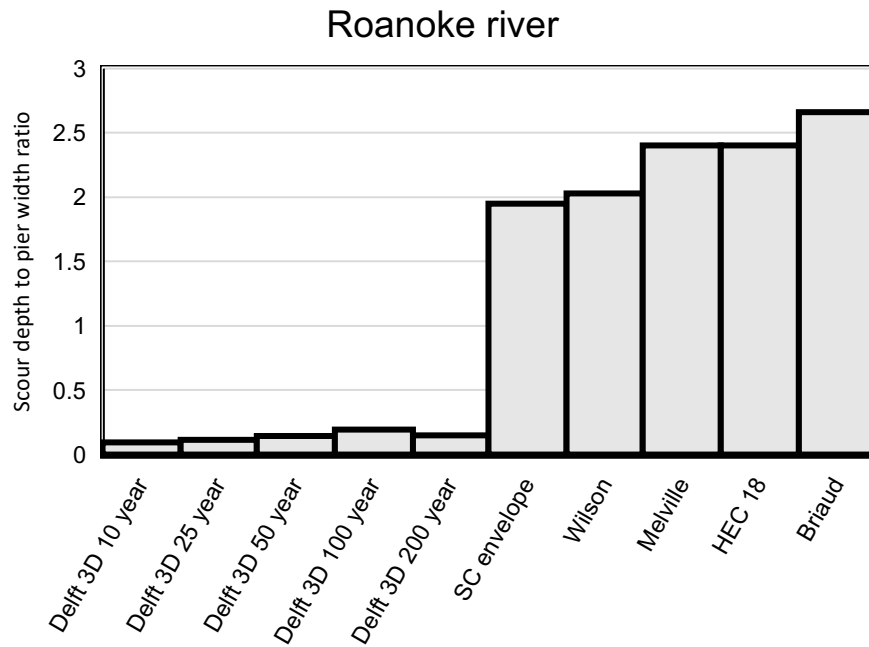
7. Comparative assessment of various scour estimation approaches

The scour magnitudes computed from Delft3D were compared to data from the scour estimation approaches suggested by South Carolina envelope (2018) model, Wilson (1995) model, Melville (1997) model, HEC 18 (2012) model and Briaud (2014) model. Based on the comparative data in Figure 34, the scour prediction from the deterministic approaches provides a scour depth of 2.37 m to 3.24 m; these values are one order of magnitude higher than the scour estimated from the numerical approach. However, these model equations provide pier scour at equilibrium, and the scour was computed based in input parameters associated with 100-year flood water depth and velocities. These conditions are assumed in the analytical model equations to be occurring throughout the lifetime of the bridge. In comparison, the numerical results from Delft 3D proceeded by first establishing equilibrium morphology then inducing the 100-year flood transient flow rate to assess the change in morphology and assess the scour magnitude.

The pier width considered for scour estimation in the deterministic models is 4 ft, and the median grain size considered was 0.23 mm. Figure 34 (b) reveals that the scour depth- to- pier width ratio for the deterministic models ranges from 1.95 to 2.66, as shown in Figure 34 (b).. Both the Melville (1997) model and the HEC 18 (2012) model suggest that for conditions where the Froude number is less than 0.8, the maximum scour depth could be 2.4 times the pier width. As both Melville model and HEC 18 model equations suggest a normalized scour depth of more than 2.4, the normalized scour depth was assessed at 2.4 based on their recommendations.



(a)



(b)

Figure 34: Comparison of scour estimated using different models for Roanoke river (a) in terms of scour magnitude, and (b) in terms of normalized scour.

Example Application

The following example problems illustrates a general overview of the steps needed to be followed to apply the scour factor approach suggested herein.

Example 1: Application of Scour Factors

Site description:

The following two example problems illustrate a general overview of the steps needed to apply the scour factors approach proposed herein.

Example 1

Site description:

The site has a circular pier with a diameter = 2 ft, and a flow skew angle of 0 degree. The stream bed has a median grain size of 0.7 mm.

Step 1: Based on hydraulic and hydrologic studies, determine upstream flow depth and upstream mean flow velocity using the design return period, as suggested by Arneson et al. (2012) (commonly referred to as HEC 18 (2012) manual). HEC 18 (2012) suggests use of U.S. Army Corps of Engineers (USACE) Hydrologic Engineering Center's River Analysis System (HEC-RAS) for this task. For the sake of this example, hydraulic and hydrologic modeling using a return period of 100 years indicated the upstream mean flow velocity and flow depth are 2 ft/sec and 6 ft respectively.

Step 2: Estimate the mean upstream flow velocity at the critical condition, referred to as critical velocity, using the expression suggested by Henderson (1966) and Melville and Sutherland (1988). Compare the critical velocity to the upstream mean flow velocity estimated in step 1 to assess the prevailing flow condition of clear water versus live bed upstream condition.

$$V_c = 5.75u_c^* \log \left(5.53 \frac{y}{d_{50}} \right) \quad (11)$$

and

$$u_c^* = K_u(0.0377 + 0.041d_{50}^{1.4}) \quad \text{For } 0.1 \text{ mm} < d_{50} < 1 \text{ mm} \quad (12)$$

$$u_c^* = K_u(0.01d_{50}^{0.5} - 0.0213/d_{50}) \quad \text{For } 1 \text{ mm} < d_{50} < 100 \text{ mm} \quad (13)$$

Where:

u_c^* is the critical shear velocity in m/s, $K_u = 0.3048$, d_{50} is the median particle size in mm, y is the flow depth directly upstream of the pier, and V_c is the mean approach velocity at the threshold

condition (parameters need to be in consistent units in Equation 11). The critical velocity, V_c is estimated to be 1.50 ft/sec; therefore, live bed upstream condition exists.

Step 3: Compute the equilibrium scour depth using any of the four deterministic models (e.g., Wilson 1995, Melville 1997, HEC 18 2012, Briaud 2014; refer to Equations 1-4 of Appendix B). For example, consider HEC 18 (2012) model.

$$\frac{y_s}{b} = 2K_1K_2K_3\left(\frac{y}{b}\right)^{0.35}F^{0.43} \quad (14)$$

Where,

K_1 = pier nose shape factor = 1.0 (Refer to Table 7.1 of HEC 18 manual)

K_2 = pier alignment factor = 1.0 (Refer to Table 7.1 of HEC 18 manual)

K_3 = bed condition factor = 1.1

y = Mean flow depth directly upstream of the pier = 6 ft

$F = \frac{v}{\sqrt{gy}}$ Froude number directly upstream of the pier = 0.143

v = Mean flow velocity directly upstream of the pier = 2 ft/sec

b = pier diameter = 2 ft

Inputting the numerical values in Equation 14 yields a normalized (with respect to pier diameter) scour depth of 1.40.

Step 4: Specify the reliability index to be achieved. Use the appropriate chart from Figure 5 of Appendix D to estimate the scour factor based on: upstream flow depth to pier width ratio, the specific analytical model used to compute scour, and the upstream flow condition. Multiply the scour factor by the scour depth computed in step 3 to obtain the design scour depth corresponding to the target reliability index.

The upstream flow depth to pier width ratio is 3, indicating narrow pier condition. If the target reliability index is 2.0, then the corresponding scour factor from Figure 35 is obtained as 1.7. Therefore, the design normalized scour depth will be ~2.38 (scour depth will be ~4.76 ft).

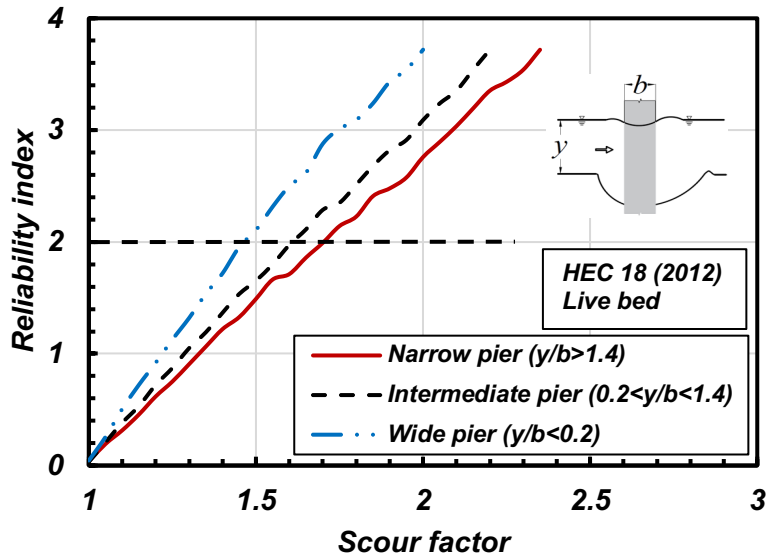


Figure 35: Relationship between reliability index and scour factor for HEC 18 (2012) live bed conditions

Example 2: Scour Factors and Risk Discussion

Site description:

Example 2 illustrates the scour estimation for parameters from the old Woodrow Wilson bridge pier. Furthermore, a discussion is provided to illustrate the application of such approach to risk assessment. The details of the bridge pier cross section and soil properties are provided in Figure 7.

Step 1: Appropriate hydraulic and hydrologic modeling of a stream in HEC-RAS using a return period of 100 years indicated that the upstream mean flow velocity and flow depth are 9.2 ft/sec and 44.6 ft respectively.

Step 2: Estimate the mean upstream flow velocity at the critical condition, referred to as critical velocity, using the expression suggested by Henderson (1966) and Melville and Sutherland (1988). A similar equation set as in Example 1 was adopted, and the critical velocity was observed to be <9.2 ft/sec, as such, live bed condition was considered.

Step 3: The bridge pier consists of three complex geometrical shapes of columns resting on a pile cap, supported by the pile groups. HEC 18 (2012) classifies such pier as complex pier and provides guidance on the calculation of scour depth. Jones and Sheppard (2000) suggested that a superposition of the scour depth component from the pier stem (y_{s-pier}), pile cap

($y_{s-pile\ cap}$) and the pile group ($y_{s-pile\ group}$) is necessary to estimate the total local scour depth, y_s (Equation 15).

$$y_s = y_{s-pier} + y_{s-pile\ cap} + y_{s-pile\ group} \quad (15)$$

Where,

$$\frac{y_{s-pier}}{y_1} = K_{hpier} \left[2K_1K_2K_3 \left(\frac{b}{y_1} \right)^{0.65} \left(\frac{v_1}{\sqrt{gy_1}} \right)^{0.43} \right]$$

$$\frac{y_{s-pile\ cap}}{y_2} = \left[2K_1K_2K_3 \left(\frac{b^*}{y_2} \right)^{0.65} \left(\frac{v_2}{\sqrt{gy_2}} \right)^{0.43} \right]$$

$$\frac{y_{s-pile\ group}}{y_3} = K_{hpg} \left[2K_1K_3 \left(\frac{b^*pg}{y_3} \right)^{0.65} \left(\frac{v_3}{\sqrt{gy_3}} \right)^{0.43} \right]$$

Based on the bridge pier cross section and soil properties presented in Figure 7, the following input parameters were estimated.

K_{hpier} = coefficient to account for height of pier stem above bed and shielding effect by pile cap overhang, to be read from Figure 7.6 of HEC 18 manual = 0.15

K_{hpg} = pile group height factor to be read from Figure 7.13 of HEC 18 manual = 0.75

K_1 = pier nose shape factor = 1.1 (Refer to Table 7.1 of HEC 18 manual)

K_2 = pier alignment factor = 1.0 (Refer to Table 7.2 of HEC 18 manual)

K_3 = bed condition factor = 1.3 (Refer to Table 7.3 of HEC 18 manual)

f = distance between front edge of pile cap and pier = 24.5 ft

h_0 = height of the pile cap above bed at the beginning of computation = 19.35 ft

$h_1 = h_0 + T = 31.5$ ft

T = thickness of the pile cap

$h_2 = h_1 + y_{s-pier}/2 = 24.2$ ft

$h_3 = h_2 + y_{s-pier}/2 + y_{s-pile\ cap}/2 = 33.3$ ft

y_1 = Approach mean flow depth at the beginning of computation = 44.6 ft

$y_2 = y_1 + y_{s-pier}/2 = 49.4$ ft

$$y_3 = y_2 + y_{s-pier}/2 + y_{s-pile\ cap}/2 = 58.5 \text{ ft}$$

v_1 = Approach mean flow velocity at the beginning of computation = 9.18 ft/sec

$$v_2 = v_1(y_1/y_2) = 8.3 \text{ ft/sec}$$

$$v_3 = v_1(y_1/y_3) = 7.0 \text{ ft/sec}$$

b^* = equivalent pier width as estimated using Figure 7.7 of HEC 18 manual = 5.92 ft

b^*_{pg} = effective width of an equivalent full depth pier = 21.7 ft (to be read from Figure 7.9-7.12 of HEC 18 manual)

Inputting the aforementioned numerical values in Equation (15) will yield a scour depth of 60 ft.

Step 4: Specify the reliability index to be achieved. Use the appropriate chart from Figure 5 of Appendix D to estimate the scour factor based on: upstream flow depth to pier width ratio, the model used to compute scour, and the upstream flow condition. Multiply the scour factor by the scour depth computed in step 3 to obtain the design scour depth corresponding to the target reliability index.

The upstream flow depth to pier width ratio >1.4 , indicating narrow pier condition. If the target reliability index is 2.0, then the corresponding scour factor from Figure 35 is obtained as 1.7. Therefore, the design scour depth will be 102 ft.

Briaud et al. (2014) specified the target risk level for the civil engineering structures in the United States is 1000 dollars/year and 0.001 fatalities/year. It was demonstrated in “Scour risk” section that the HEC 18 (2012) model, without the application of any scour factor, is associated with an exceedance probability of 0.007. The accepted associated cost of consequence will be \$142,900. With the target reliability index, β_T of 2.0, the scour factor will be 1.70, and the associated exceedance probability will be 0.0024. For the same cost of consequence = \$142,900, the target risk level will be approximately reduced by a factor of 2/3 and be 343 dollars/year.

In a given year, if HEC 18 (2012) suggested approach is used to estimate scour depth, there is a possibility that the scour depth will be exceeded in 3,454 bridges. Whereas, if the scour factor corresponding to the β_T of 2.0 is used, annually, the scour depth would be exceeded in 1,184 bridges, reducing the affected number of bridges by 2,270.

Briaud et al. (2014) reported that if the economic loss entails the bridge repair cost, detour cost, and time cost, then the economic loss for one bridge failure can be estimated at \$13,180,158 US Dollars. However, based on the repair cost data reported in California DOT (2011), Briaud et al. (2014) estimated that the average repair cost of one bridge is 560,100 Dollars. For the 2,270 bridges, the economic loss considering only the bridge repair would be 1.27 billion Dollars.

Therefore, adopting the scour depth corresponding to the β_T of 2.0 will help to preventing a loss of 1.27 billion Dollars annually.

8. Findings and Recommendations

At present, there are more than twenty pier-scour analytical models available in literature. These models are developed in most cases from extensive laboratory testing data or based on limited field data. In parallel, representative approaches for estimating first order scour magnitude can be used for comparative classification of “scour- critical” hydraulic structures and for providing an upper bound of scour depth. The South Carolina (SC) Bridge-Scour Envelope criteria were developed for such first order estimate of scour. A review of aspects related to scour and soil erodibility has been presented covering details on erodibility parameters and analyses models. The review also included common factors influencing pier scour and demonstrated performance and error statistics of four pier scour analytical models. The research work then aimed at assessing the accuracy of the scour predictions using the SC Scour Envelope comparatively in view of existing scour assessment approaches. We estimate bridge scour using three different approaches: the SC Scour Envelope Curves, four analytical models in literature including HEC-18, and the use of advance numerical model (Delft3D). In addition to the SC Envelope, the Wilson (1995) model, Melville (1997) model, Hydraulic Engineering Circular No. 18 (HEC-18) (2012) model, and Briaud (2014) model are assessed in terms of two statistical parameters, termed Mean Absolute Percentage Error (MAPE,) as a measure of accuracy of the prediction, and “level of conservatism” as a measure of percent of cases where scour estimates from a given approach exceeded measured values.

In addition, field work performed at four bridge sites provided measurements of flow, bathymetry, and bridge geometry data for calibration of the numerical modeling. We then synthesize the results from the various models and provide comparative data demonstrating the applicability of the various approaches. As AASHTO (2007) bridge design specification suggests different target reliability index for the load factors and resistance factors, based on the redundancy and non-redundancy of a structure, a relationship between reliability index and scour factors is introduced herein. Although in the common literature HEC-18 scour prediction model, for example, is considered conservative, the level of reliability or probability of the mode yielding values less than those occurring in the field is unknow. Hence, the use of a reliability-based approach in design should be considered in practice. The “scour factors” developed herein are proposed for application to the deterministic predictions to account for input parameter uncertainty and inherent model bias and are applicable for local scour assessment in riverine flow under clear water and live bed conditions. Based on analyses and data presented herein, the following conclusions are made:

- i. Analyses performed using clear water data collected by Benedict and Caldwell (2014) indicated values of MAPE ranged from 238% to 336%, whereas conservatism ranged from 77% to 97.8%. Briaud (2014) model presented the least error (238%), and SC Envelope (2018) model presented the highest error (336%). The use of the SC Envelope (2018)

- model provided the most conservative scour depth (97.8%), whereas Briaud (2014) model presented the least conservatism (77%).
- ii. In parallel when the live bed laboratory data collected in Benedict and Caldwell (2014), were used, values of MAPE ranged from 23.5% to 1218% with the SC envelope approach yielding the higher end of the MAPE, whereas, conservatism ranged from 28.4% to 100%.
 - iii. Utilizing live bed field data, MAPE ranged from 205.6% to 322% for the five models considered herein. In this case, the SC envelope model also provided the most conservative estimate (97.5%), while HEC 18 (2012) model provided the least conservative scour depth estimate (93.3%).
 - iv. When the limitation of SC envelope curve approach of nominal pier width ≤ 6 ft is imposed, the level of conservatism does not differ significantly (less than 1%) and the MAPE for the SC approach slightly increased from 322% to 349%.
 - v. The accuracy and level of conservatism of a specific model can be adjusted by multiplying the computed scour depth computed per a given deterministic model by proposed modification factors. The proposed modification factors necessary to attain certain accuracy and conservatism level are developed for each model on the basis of laboratory data.
 - vi. A reliability-based pier scour estimation methodology was developed accounting for input parameter uncertainty and inherent model bias. The methodology is applicable for local scour calculation in riverine flow under clear water and live bed condition using four deterministic scour prediction models: Wilson (1995) model, Melville (1997) model, HEC-18 (2012) model, and Briaud (2014) model.
 - vii. As AASHTO (2007) bridge design specification suggests different target reliability index for the load factors and resistance factors, a relationship between reliability index and scour factors is introduced herein. These “scour factors” are proposed for application to the deterministic predictions to account for input parameter uncertainty and inherent model bias and are applicable for local scour assessment in riverine flow under clear water and live bed conditions. These factors are dependent on the pier type (e.g., narrow pier, intermediate pier, and wide pier), upstream sediment transport condition (e.g., clear water and live bed), and the deterministic model being used (e.g., Wilson (1995) model, Melville (1997) model, HEC-18 (2012) model, and Briaud (2014) model).
 - viii. The fieldwork at the four sites highlighted the importance of accessibility for accurate measurements of flow, bathymetry, and bridge geometry. The River Ray ADCP was integral to collecting bathymetry; however the Tilt Current Meters were the easiest to deploy and quickly measure flow velocities and directions. These data were useful in validating our numerical model simulations.
 - ix. Utilizing data from the Roanoke River bridge site, the pier scour magnitude estimated from Delft3D was one order of magnitude lower than the scour estimated from the analytical approaches; i.e. South Carolina envelope (2018), Wilson (1995) model, Melville (1997) model, HEC 18 (2012) model and Briaud (2014) model. This is due to the fact that the pier scour estimates from the numerical model proceeded by first establishing equilibrium morphology under mean flood flow, then inducing the temporal hydrograph of 100-year flood event (where the water depth and velocities varied over a period of 30 days) to assess the change in morphology and discern the pier scour magnitude. In comparison, the

estimates from the simple analytical model equations provide pier scour at equilibrium assuming water depth and velocities corresponding to the 100-year flood.

- x. Utilizing the Roanoke River morphology and flood parameters with 100-year return period yield pier scour magnitude slightly higher than the case in which 200-year flood flow rate was used. This is due to overland flow and the less channelized flow toward the pier.
- xi. Results from the Delft3D numerical approach are insightful, and field spatial morphology can be reasonably represented. However the use of such advanced numerical analyses is best utilized when simulating larger river systems as such modeling is time intensive both in the creation of the discretized global mesh and the running of various scenarios including simulating a realistic flood event with temporally changing upstream discharge conditions.
- xii. In the United States, 493,473 highway bridges are built over waterways. Based on the repair cost data reported in California DOT (2011) and the estimated average repair cost of one bridge by Briaud et al. (2014), it is shown that the use of reliability index-based scour depth in foundation design will help to prevent risking a loss of 1.27 billion Dollars annually.

The AASHTO (2007) bridge design specification suggests different target reliability index, β_T , based on the redundancy and non-redundancy of the structure. The use of a relationship between reliability index and scour factor enables engineers to decide the level of reliability index desired per the importance of the structure. The proposed scour factors herein contribute to mitigating the inconsistency posed by adopting a β -based approach for the design of various superstructure bridge components, while still utilizing the deterministic approach for assessing the scour magnitude. Such approach of having a uniform level in the reliability of the bridge components is needed to facilitate the development of integral risk-based design approach for bridge structures.

Recommendations

The use of SC envelope (2018) model is recommended for first order estimate of scour with the understanding of the inherent bias and level of conservatism. The use deterministic models, e.g., Wilson (1995) model, Melville (1997) model, HEC 18 (2012) model, Briaud (2014) model is predicated upon having sufficient data to develop the required input parameters. The results from these deterministic approaches can be adjusted using the proposed modification factors in order to obtain a the desired “level of conservatism” with a known Mean absolute percentage error. For an approach that is consistent with the LRFD, the use of the introduced reliability-based scour factors is recommended in order to achieve a level of reliability of the scour magnitude estimates that is consistent with the reliability index of the bridge super-and sub-structure components. This is necessary for the development of integral risk-based design approach for bridge structures. The use of numerical models which consider river morphology, morphodynamic evolution, impact of hydrological parameters, site specific issues such as, for example, a dam built on the upstream of the waterways etc. might be helpful in specialized large-scale projects. . While these advanced numerical models are expensive to run in terms of manpower and resources, their results provide an understanding of the impact of various flow scenarios and complex geometrical and morphological conditions not only on the degradation but also on the aggradation changes related to the streambed, with time, at the bridge site.

9. References

- AASHTO (2007). "AASHTO LRFD Bridge Design Specifications: Customary U.S. Units," 4th Edition, American Association of State Highway and Transportation Officials, Washington, D.C.
- ACI 318-05 (2005). "Building Code Requirements for Structural Concrete and Commentary," American Concrete Institute, Farmington Hills, MI.
- AISC 325-05 (2005). "Steel Construction Manual," Thirteenth Edition, American Institute of Steel Construction, Chicago, IL.
- American Petroleum Institute (API) (2003). "Recommended Practice for Field Testing Water-Based Drilling Fluids," API RP 13B-1/ISO 10414-1, 3rd Ed., American Petroleum Institute, Washington, D.C., 1-82.
- ASCE (2010). "Minimum Design Loads for Buildings and Other Structures," ASCE 7-10, American Society of Civil Engineers, Reston, VA.
- Arneson LA, Zevenbergen LW, Lagasse PF, and Clopper PE. (2012). "Evaluating scour at bridges." Hydraulic Engineering Circular No. 18, 5th edition, 1-340.
- Baecher, G. B., and Christian, J. T. (2003). Reliability and statistics in geotechnical engineering, Wiley, New York.
- Benedict, S. T., Feaster, T .D., Caldwell, A. W. (2018) "The South Carolina Bridge-Scour Envelope Curves." U.S. Geological Survey Scientific Investigations Report 2016-5121. U.S. Department of the Interior, 2016 (revised 2018). <https://doi.org/10.3133/sir20165121>.
- Benedict ST, and Caldwell AW. (2014). "A pier-scour database—2,427 field and laboratory measurements of pier scour." U.S. Geological Survey Data Series 845, 1-22.
- Briaud J-L. (2008) Case histories in soil and rock erosion: Woodrow Wilson Bridge, Brazos River Meander, Normandy Cliffs, and New Orleans Levees, *Journal of Geotechnical and Geoenvironmental Engineering, ASCE*; 134(10): 1425-1447.
- Briaud JL. (2014). "Scour depth at bridges: Method including soil properties. I: Maximum scour depth prediction." *Journal of Geotechnical and Geoenvironmental Engineering*; 141(2): 04014104.
- Briaud J-L, Gardoni P, and Yao C. (2014). "Statistical, risk, and reliability analyses of bridge scour." *Journal of Geotechnical and Geoenvironmental Engineering*; 140(2): 04013011.

- California DOT. (2011). "Construction statistics." http://www.dot.ca.gov/hq/esc/estimates/Construction_Stats_2011.pdf (May 1, 2012).
- Deng L., Wang W., and Yu, Y. (2007). "State-of-the-Art Review on the Causes and Mechanisms of Bridge Collapse." *Journal of Performance of Constructed Facilities*; 10.1061/(ASCE)CF.1943-5509.0000731, 04015005.
- Estes A. C., and Frangopol, D. M. (2001). "Bridge lifetime system reliability under multiple limit states." *Journal of Bridge Engineering*, 10.1061/(ASCE)1084-0702(2001)6: 6(523), 523–528
- Ettema R, Constantinescu G, and Melville BW. (2017). "Flow-field complexity and design estimation of pier-scour depth: Sixty years since Laursen and Toch." *Journal of Hydraulic Engineering*; 143(9), 03117006.
- FB-MultiPier Version 5.9 [Computer software]. Bridge Software Institute, Gainesville, FL.
- FB-MultiPier Version 5.9 [Help Manual], (2021). Bridge Software Institute, Gainesville, FL.
- Hydrologic Engineering Center (1986). "Accuracy of Computed Water Surface Profiles," U.S. Army Corps of Engineers, Davis, CA.
- Johnson PA. (1992). "Reliability-based pier scour engineering." *Journal of Hydraulic Engineering*; 118(10), 1344-1358.
- Johnson P.A. (1996). "Uncertainty of Hydraulic Parameters," *Journal of Hydraulic Engineering*; 122(2), 112-115.
- Johnson PA, Clopper PE, Zevenbergen LW and Lagasse PF. (2015). "Quantifying uncertainty and reliability in bridge scour estimations." *Journal of Hydraulic Engineering*; 141(7), 04015013.
- Jones, J.S. (2000). "Hydraulic testing of Wilson bridge designs" Public Roads, March/April, U.S. Department of Transportation, FHWA, Washington, DC, USA, 40-44.
- Jones, J.S. and D.M. Sheppard, (2000). "Local Scour at Complex Pier Geometries," Proceedings of the ASCE 2000 Joint Conference on Water Resources Engineering and Water Resources Planning and Management, July 30 - August 2, Minneapolis, MN.
- Jones JS, and Davis SR. (2007) "Evaluating Scour for the Piers on the New Woodrow Wilson Bridge." World Environmental and Water Resources Congress 2007, 1-10.
- Kim, K. J., M. S. Rahman, M. A. Gabr, R. Z. Sarica, and M. S. Hossain. (2005). "Reliability Based Calibration of Resistance Factors for Axial Capacity of Driven Piles." In *Advances in Deep Foundations*, Geotechnical Special Publication 113, 1–12. Austin, TX: ASCE
- Kulicki J.M., Mertz D.R., and Nowak A.S. (2007). "Updating the Calibration Report for AASHTO LRFD Code," NCHRP Project 20-7/186, Transportation Research Board, National Academies of Science, Washington, D.C.
- Kwak K. (2000). "Prediction of scour depth versus time for bridge piers in cohesive soils in the case of multi-flood and soil systems." Ph.D. dissertation, Department of Civil Engineering, Texas A&M University, College Station, Texas.
- Kwak KS, and Briaud JL (2002). "Case Study: An Analysis of Pier Scour Using the SRICOS Method." *KSCCE Journal of Civil Engineering*, 6(3), 243-253.

- Lagasse P. F., Ghosn M., Johnson P. A., Zevenbergen L.W., and Clopper P. E. (2013). "Risk-based approach for bridge scour prediction." Final Rep., NCHRP Project 24-34, Transportation Research Board, National Academies of Science, Washington, DC.
- Laursen, E.M., (1960). "Scour at Bridge Crossings," *Journal Hydraulic Division, ASCE*, 86 (HY 2).
- LeBeau K. H., and Wadia-Fascetti S. J. (2007). "Fault tree analysis of Schoharie Creek Bridge collapse." *Journal of Performance of Constructed Facilities*;10.1061/(ASCE)0887-3828(2007)21:4(320), 320–326.
- Liang FY, Zhang H, and Huang MS. (2015). "Extreme scour effects on the buckling of bridge piles considering the stress history of soft clay." *Natural Hazards*; 77, 1143–1159.
- Lin, C., J. Han, C. Bennett, and R. L. Parsons. (2014). "Analysis of laterally loaded piles in sand considering scour hole dimensions." *Journal of Geotechnical and Geoenvironmental Engineering*; 140 (6): 04014024.
- Lin, C., Bennett, J. Han, C. and R. L. Parsons. (2015). "Effect of Soil Stress History on Scour Evaluation of Pile-Supported Bridges." *Journal of Performance of Constructed Facilities*; 04014178.
- Link et al. (2019) "Physical scale modelling of scour around bridge piers". *Journal of Hydraulic Research*, 57(2), 227-237.
- LPILE V5.0 [Computer software]. Austin, TX, Ensoft.
- Matlock, H. (1970). "Correlation for Design of Laterally Loaded Piles in Soft Clay," in Proceedings, Second Offshore Technology Conference, Dallas, Texas, pp. 577 - 594.
- Melville BW. and Coleman SE. (2000). "Bridge scour." Highlands Ranch, USA: Water Resources Publications.
- Nowak A. (1999). "Calibration of LRFD bridge design code." NCHRP Rep. 368, Transportation Research Board, Washington, DC.
- Nowak A.S. and Collins K.R. (2000). "Reliability of Structures," McGraw-Hill, New York, NY.
- Paikowsky SG. (2004). "Load and resistance factor design (LRFD) for deep foundations." NCHRP Rep. 507, Transportation Research Board, Washington, DC.
- Parkes J, Castelli R, Zelenko B, O'Conner R, Montesi M, and Godfrey E (2018). "Design, Analysis, and Testing of Laterally Loaded Deep Foundations that Support Transportation Facilities." FHWA-HIF-18-031, 1-296.
- Qi M, Li J, and Chen Q. (2016). "Comparison of existing equations for local scour at bridge piers: parameter influence and validation." *Natural Hazards*; 82(3), 2089-2105.
- Reese, Lymon C., Cox, William R., and Francis D. Koop. (1974) "Analysis of Laterally Loaded Piles in Sand." Paper presented at the Offshore Technology Conference, Houston, Texas.
- Richardson EV, and Davis SR. (2001). Hydraulic Engineering Circular No. 18, Fourth Edition, FHWA NHI 01-001, Federal Highway Administration, Washington, D.C.

- Robinson B, Suarez V, Gabr M, and Kowalsky M (2012). "Configuration Optimization of Drilled Shafts Supporting Bridge Structures: Three Case Studies." *Practice Periodical on Structural Design and Construction*; 17(3), 93-101.
- Robinson, B., Suarez, V., Robalino, P., Kowalsky, M., and Gabr, M. (2006). "Pile bent design criteria." NCDOT Research Project 2005-19, North Carolina Department of Transportation, Raleigh, NC.
- Shahriar AR, Ortiz AC, Montoya BM, and Gabr MA (2021a). "Bridge Pier Scour: An overview of factors affecting the phenomenon and comparative evaluation of selected models," *Transportation Geotechnics*, 28(2021), 100549. DOI: 10.1016/j.trgeo.2021.100549.
- Shahriar AR, Montoya BM, Ortiz AC and Gabr MA (2021b). "Quantifying probability of deceedance estimates of clear water local scour around bridge piers," *Journal of Hydrology*; 597(2021):126177.
- Sheppard, D.M., Odeh, M., and Glasser, T., (2004), Large scale clear-water local pier scour experiments: *Journal of Hydraulic Engineering*; 130(10), 957–963.
- Sheppard, D.M., Jones JS, Odeh, M., and Glasser, T., (2004). "Local Sediment Scour Model Tests for the Woodrow Wilson Bridge Piers" Joint Conference on Water Resource Engineering and Water Resources Planning and Management 2000, 1-9.
- Yao C. (2013). "LRFD calibration of bridge foundations subjected to scour and risk analysis." Ph.D. dissertation, Department of Civil Engineering, Texas A&M University, College Station, Texas.
- Wardhana K, Hadipriono FC. (2003). "Analysis of recent bridge failures in the United States." *Journal of Performance of Constructed Facilities*; 17(3), 144-150.

Appendix A: Literature review

Bridge Pier Scour: An overview of factors involved in the phenomenon and evaluation of selected models

1. Introduction

Scour of foundation systems is the primary cause of bridge collapse in the United States (Melville and Coleman, 2000; Briaud et al. 2001, 2005). Scour leads to damage of the bridge foundation and abutment, causing major operational disruption and financial losses (Shirole and Holt, 1991; Briaud et al. 1999). Murillo (1987), based on the investigation of bridge failures between 1961-1974, observed that among 86 bridge failures, 46 can be attributed to scour. Lagasse et al. (1997) indicated the average cost for flood damage repair of highways in the United States was estimated at \$50 million per year. This cost only considers the damage to infrastructures; however, the additional cost to the afflicted population could be as much as five times the repair costs (Rhodes and Trent, 1993). Mueller (2000) and Fisher et al. (2013) reported that more than 2500 bridges were damaged due to flooding-related scour during the period 1980 to 1990 in the Northeastern and Midwestern USA. Wardhana and Hadipriono (2003), based on their investigation of five hundred bridge failures between 1989 and 2000 across the United States, described that 53% of the recorded failures was due to flooding and scour related complications. Lin et al. (2006) reported that during the period of 1996 to 2001, 68 bridge failures in the United States were related to scour. Hunt (2009) noted that up until 2009, there were 20,904 scour-critical bridges in the United States and additional 80,000 bridges were scour susceptible. During a single flood event in the upstream and downstream Missouri river basins, which occurred in 1993, at least 22 of the 28 bridges on the waterway experienced some form of distress due to scour (Prendergast and Gavin, 2014). The associated repair costs were more than \$8 million as reported in Kamojjala et al. (1994). With extreme weather events becoming frequent (McKenna et al. 2020), the potential economic, financial, and human life loss due to scour-induced failures signify the importance of identifying the principal causes of scour and taking necessary mitigation actions prior to damage being incurred.

Many empirical models have been developed to estimate the equilibrium scour depth at bridge piers. The development for these equations incorporate data from laboratory tests, field tests, or both. Also, pier scour is a complex process being affected by many factors including, for example, flow depth to pier width ratio, pier face shape, pier aspect ratio, and skew angle of pier. Not all these factors are considered while developing the empirical models. In addition, the model equations are commonly based on simplified assumptions, while many practical factors such as pier proximity to abutment, debris accumulation, and flood plain vegetation further complicate the

assessment of scour. Subsequently, under identical hydraulic and geometric conditions, different models yield vastly different scour estimates; these can be conservative or unconservative. Accordingly, the conclusion about the scour criticality of a given bridge pier is dependent on the model being used in the analysis. In the design stage, the use of a model yielding unconservative results may lead to bridge failure, whereas selection of a highly conservative model will result in an adverse economic outcome. Therefore, understanding and documentation of the pier scour estimation models in relation to the factors influencing and complicating pier scour estimation are necessary.

Developments in the understanding of scour mechanism have been made in hydraulic and geotechnical engineering. The hydraulic, geotechnical, and structural impact of scour has been studied in their respective fields. Attempts have been made to relate ‘erodibility magnitude and rate’ to the properties of soil (plasticity index, liquidity index, water content, median grain size, etc.). The review presented herein is focused on summarizing the current state of knowledge on erodibility, geotechnical aspects of erodibility, factors influencing and complicating estimation of pier scour, and databases available on erodibility and pier scour measurements. A summary of the deterministic pier scour models developed since 1990, and the extent to which such models consider factors affecting pier scour, are presented. In addition, developments in probabilistic pier scour analyses, and observation-based models are summarized. Four fundamentally different and widely used pier scour models, namely Wilson (1995) model, Melville (1997) model, Hydraulic Engineering Circular (HEC) No. 18 (Arneson et al. 2012) model, and Briaud et al (2014a) model are chosen for comparative analyses. These four models were developed each relying on a different method of collecting data. The laboratory live bed and clear water data, as summarized by Benedict and Caldwell (2014), were used in the analyses herein. Error statistics were computed and included in the discussion on accuracy, precision, and probabilistic distribution of predictions from these four models. Conclusions were drawn based on the synthesis of literature and critical analyses presented.

2. Scour

2.1 Macro perspective

Scour can be defined as the removal of materials from bed and banks of streams, around the piers and abutment of waterway bridges or other hydraulic structures. Bed materials may consist of granular or cohesive deposits or a combination of the two. Under similar hydraulic conditions, loose granular soil will scour at a rate different from cohesive deposits. Information in the literature suggests that the detachment of particles from the bed can be related to the flow velocity and scour can be classified as occurring under clear-water or live-bed conditions. If the flow velocity is such that there is no transport of bed material from upstream of the bridge crossing, the condition is

considered *clear water*. In contrast, if the transport of bed material occurs from the upstream area, the condition is *live bed*.

It is important to note that there are three main sources of scour, which contributes to the total scour estimate. These are, i) Long-term aggradation and degradation, ii) Contraction scour, and iii) Local scour. Long-term aggradation involves the deposition of material eroded from the upstream of the bridge, whereas degradation is a type of scour that occurs due to a deficit in sediment supply from upstream over relatively long reaches as occurring in clear-water conditions (Arneson et al. 2012). Contraction scour occurs due to the geometric contraction of flow resulting in increased flow velocities, turbulence, and therefore bed shear stress driving removal of materials from the bed. The difference between long-term degradation and contraction scour is the latter is associated with any constriction of flow. Local scour takes place when the flow is obstructed by a structure such as pier, abutment, spurs, or embankment. Arneson et al. (2012) considered local scour as the combined effect of flow acceleration and the vortices induced by the obstruction. Three principle flow features were described in this case: i) down flow at the face of pier, ii) the horseshoe vortex at the base of the pier, and iii) the wake vortices formed at the downstream direction of pier (Arneson et al. 2012, Melville and Coleman 2000). The down flow at the pier face erodes the bed material, which are then transported past the pier by the horseshoe vortex and wake vortices thereafter. The mechanism is presented schematically in Figure 1. Deng and Cai (2010) reported that the strength of the horseshoe vortex is reduced as the depth of scour increases. Thereby, with time, reducing the transport rate of bed material past the bridge pier. For uniform sediments, under clear water conditions, the scour progresses asymptotically towards an equilibrium depth, while, for live bed conditions, the attainment of peak scour depth is relatively faster followed by a fluctuation of bed form (Raudkivi and Ettema 1983; Chiew 1984; Ettema et al. 2011). Chee (1982), Chiew (1984), Melville (1984), Melville and Sutherland (1988) suggest that for uniform sediments, the scour depth prediction under live bed condition depends significantly on the size and steepness of the bed features at a certain flow velocity. If the bed form is higher, then the observed scour depth is lower. Ettema et al. (2011), Oliveto and Hager (2014) illustrated that sediment deposition bar (dune) at the pier tail water alters the flow field, thereby affecting the scour hole development. They also observed that the time required for the dune-crest to attain its maximum height is nearly constant (slightly dependent on sediment uniformity); while the magnitude of maximum dune-crest height is on average 0.25 times the downstream flow depth. As the scouring processes cease, a new-equilibrium is established between bed material inflow and outflow.

2.2 Meso to micro perspective

Soil erodes if the applied hydraulic shear stress exceeds the critical shear stress. The key forces acting on a soil particle are: weight of the particles, electrical forces between the particles, forces at contact points of the particles, and water pressure around the particles. Hofland et al.

(2005), through an experimental investigation on granular beds, showed that the forces exerted on a soil particle due to turbulent stress fluctuation at the bed level is sufficient to dislodge it. The turbulent stress fluctuations acting on the soil particles surrounding an obstruction may result in suction pressures, which affect the erosion of the bed material. Briaud (2008) noted that flow of water exerts a pressure around the particles, and the normal pressure imposed at the base of the particle will be higher than that acting at the top of the particle, resulting in a buoyant force. As conventionally, the shear stress acting on the soil-water interface is considered the parameter most influencing erodibility, Briaud (2008) suggested that the constitutive law of the erosion process can be expressed as in Eq. (1).

$$\dot{z} = f(\tau) \quad (1)$$

Where, \dot{z} is erosion rate and τ is hydraulic shear stress at the interface of soil and water when it exceeds the critical shear stress. To normalize Eq. (1), Shafii et al. (2016) proposed Eq. (2), which can be expressed as-

$$\frac{\dot{z}}{v_c} = \alpha' \left(\frac{\tau - \tau_c}{\tau_c} \right)^m \quad (2)$$

Where, α' and m are unitless erosion model parameters depending on soil properties. v_c and τ_c are critical velocity and critical shear stress respectively (below which no erosion occurs). Shafii et al. (2019), through a hydrodynamic analysis to discern the forces acting on the gravel particles, identified that critical normal stress on the soil particle as another important parameter, which influences erosion rate. The developed model is presented in Eq. (3),

$$\frac{\dot{z}}{0.1} = \left(\frac{\tau}{\tau_c} \right)^\alpha \left(\frac{\sigma}{\sigma_c} \right)^\beta \quad (3)$$

Where, \dot{z} is erosion rate (mm/hr), τ_c and σ_c are critical shear stress (Pa) and critical normal stress associated with an erosion rate of 0.1 mm/hr respectively, σ is the normal stress (Pa) acting on the particle at bed level, α and β are unitless erosion model parameters. Briaud et al. (2019) indicated that parameters α and β cannot be determined definitively with the existing state of knowledge, and it would be cumbersome to estimate the parameters on a site-specific basis.

Numerical analyses are also used to understand the interaction between flow and obstacles and the impact on soil erosion. Zhang et al. (2016) conducted a Molecular Dynamics (MD) simulation, a tool to comprehend physical mechanisms at the molecular scale, to explain the interaction occurring at soil-water interface. Joseph and Hunt (2004), Kloss et al. (2012), Ni et al. (2015), Huang et al. (2014), Chang et al. (2016), Kawano et al. (2017), Tao and Tao (2017) introduced the approach of coupled Computational Fluid-Dynamics-Discrete Element Modeling (CFD-DEM) to investigate various hydro-mechanical problems associated with granular media. CFD was used to model the interstitial fluid flow and DEM was used to simulate the particles assembly. Their introduction of the CFD-DEM technique led researchers, including Guo and Yu

(2017) and Guo et al. (2018), to incorporate the CFD-DEM approach into investigation soil erosion. Although soil erosion was modeled in those studies, none have focused on erosion rate. Consequently, there is a need to better understand the progressive development of scour considering the coupled action of shear stress and the turbulent layer generated when the flow experiences obstructions.

2.3 Critical shear stress and critical velocity

Critical shear stress and critical velocity are two parameters with paramount importance in scour studies. Several attempts have been made to relate erodibility to geotechnical properties. Smerdon and Beasley (1959) developed a relation between critical shear stress with soil plasticity index and the dispersion ratio (Table 1). Grissinger (1966) noted the influence of type and amount of clay minerals, mineral orientation, bulk density, temperature, and antecedent water on erodibility. Parchure and Mehta (1986) observed a log-linear relationship between erosion rate and shear stress in excess of bed shear strength. Their study was focused on erosion rate models for kaolinite and lake mud composed of montmorillonite, illite, kaolinite and quartz. Hanson and Simon (2001) developed a relationship between critical shear stress and “linear slope” of erosion rate versus shear stress for soils with 50-80% silt size materials and relatively low dry unit weight (ranging from 11-15 kN/m³). Julian and Torres (2006) suggested a model to estimate the critical shear stress based on the percent silt and clay content in the material. The minimum critical shear stress was considered 0.1 Pa, based on Shields (1936). It was also noted that the presence of vegetation increases the critical shear stress, and a multiplication factor based on the type of vegetation was introduced. Thoman and Niezgodna (2008) proposed a multilinear regression equation relating soil activity, dispersion ratio, specific weight, pH of the eroding fluid and moisture content to estimate the critical shear stress (τ_c). Their reported critical shear stress ranged between 0.11-15.35 Pa. Both Shields (1936) and Briaud (2008) concluded that τ_c for coarse grained soils depends on median grain size, d_{50} ; for fine grained soil ($d_{50} < 0.075 \text{ mm}$) however, the relationship between τ_c and d_{50} is significantly scattered. Briaud (2008) suggested an expression for critical shear stress for soils with $d_{50} > 0.1 \text{ mm}$, which is listed in Table 1.

Shafii et al. (2016) suggested a set of equations to predict the critical shear stress of coarse-grained soils based on d_{50} , moisture content, and percent of fines. In the case of fine-grained soil, plasticity index, undrained shear strength, d_{50} , and moisture content are considered as primary variables affecting critical shear stress. Briaud et al. (2017) performed a multilinear regression analyses of the testing data obtained from Erosion Function Apparatus (EFA) and proposed a set of equations to predict critical shear stress and velocity. Table 1 presents a summary of the predictive equations and number of tests considered to develop the equations for both coarse grained and fine-grained soil. Briaud et al. (2019) documented the parameters that affect the erodibility of soil and classified these into two categories: viz-a-viz more typically obtained parameters and less typically obtained parameters. A set of equations was suggested to estimate

the critical shear stress obtained from EFA (Table 1). For fine grained soils, the independent variables are unit weight, activity, moisture content, percent fines, d_{50} , and undrained shear strength. For coarse grained soils, coefficient of uniformity, unit weight and d_{50} are the independent variables. Briaud et al. (2019) also provided equations to estimate critical shear stress obtained from Jet Erosion Test (JET) and Hole Erosion Test (HET). Nevertheless, as the equations in Table 1 for assessing the critical stress were developed based on different data sets, there is a need to demonstrate the magnitude of the critical stress estimated using these different methods for a same dataset.

Briaud et al. (2008) developed a chart for different geomaterials, relating erodibility with the soil classification (according to the Unified Soil Classification System). A geomaterial can be classified into one of six categories as presented in Figure 2. It is important to note that a soil class falls across two different categories. As previously discussed, erodibility may not just be a function of the shear stress exerted on the soil particles, as the stress fluctuations due to turbulent boundary layer might also contribute to soil erodibility. Future consideration of this effect might lead to narrowing the bandwidth for a given soil class shown in Figure 2.

Similar to the case of critical shear stress, there are a number of equations available to estimate the critical velocity, which is defined as the flow velocity at, or above which particles dislodge. This critical velocity also determines the live bed or clear water conditions. Therefore, its inaccurate estimation will result in mischaracterization of the state of upstream sediment transport condition and in turn, the scour assessment. Collection of equations to predict critical velocity can be found in Henderson (1966), Melville and Sutherland (1988), Briaud et al. (2019).

3. Pier Scour

Ettema et al. (2011) classified factors influencing pier scour into two broad categories, a) primary factors and b) secondary factors. It was suggested that primary factors are those parameters defining the structure and geometric scale of the pier flow field, thus, influencing the maximum scour depth. Parameters included in the primary factors' category are flow depth to pier width ratio, pier width to d_{50} ratio, pier face shape, pier aspect ratio, and skew angle of pier. In contrast, secondary factors are those which influence the computed scour depth sensitivity within a specific geometric scale limit. These include Flow intensity, Euler number or Reynolds number, sediment non-uniformity, and the temporal rate of scour. Ettema et al. (2011) suggested that consideration of secondary factors will lead to a scour depth estimation less than the potential maximum scour obtained from only considering the primary parameters, thus reducing the conservativeness of the estimate. Figure 3 presents a conceptual sketch of the primary and secondary factors influencing pier scour magnitude.

3.1 Primary factors

Melville and Coleman (2000) and Sheppard and Melville (2011) identified the water depth to pier width ratio (y/b), also termed as the geometric scale of the pier flow field, as one of the most important parameters driving the maximum scour depth. Based on experimental and numerical studies, Melville and Coleman (2000) classified the pier scour flow field into three categories. Table 2 shows such classification based on y/b and summarizes the type of turbulent structures developed due to the presence of obstacles for the three categories of piers.

Sheppard et al. (2004) and Sheppard and Miller (2006) observed that scour depth is dependent on the ratio of pier width to sediment size, b/d_{50} . Lee and Sturm (2009) experimentally observed that smaller values of b/d_{50} can impede the scour progression and subsequently confine the scour depth. They further suggested that scour depth to pier width ratio increases logarithmically in the range $b/d_{50} \leq 25$, while it decreases for $b/d_{50} > 25$, and eventually remains constant if b/d_{50} exceeds 400. Ettema et al. (2011) suggested that if $b/d_{50} \leq 8$, individual particles are large relative to the groove excavated by the down flow and erosion is impeded because the rough and porous bed dissipates some of the down flow energy.

In general, piers are constructed in a variety of shapes that include cylindrical, oblong or rectangular configurations. As pier shape influences the flow field surrounding a pier, the magnitude of scour is also affected in the process. The deterministic pier scour models by Melville (1997), HEC 18 (2012), and Briaud (2014a) adopt a multiplication factor to consider pier shape varieties. From an experimental investigation, Mostafa (1994) observed a variation of scour depth as a function of the magnitude of the aspect ratios; such variation was attributed to the change in formation and spacing of turbulence structures at different aspect ratios. Pier skewness to flow leads to altering the effective pier width and influencing the flow field, and consequently the scour depth. Yang et al. (2017) observed that when skewness exceeds 30° , irrespective of the undisturbed bed level, the bottom of the equilibrium scour hole reaches the same depth below the pile cap in clear water conditions. Nevertheless, it is a common practice to combine the effects of pier skewness, shape, and pier width in terms of expressing an effective pier width (Mostafa 1994, Ettema et al. 1998, and Arneson et al. 2012).

3.2 Secondary factors

Sediment's non-uniformity, presented in Eq. (4) is one of the secondary factors influencing bridge pier scour.

$$\sigma_g = \sqrt{\frac{d_{84}}{d_{16}}} \quad (4)$$

Where, d_{84} and d_{16} are the particle diameters corresponding to 84% and 16% finer. Until recently, the effect of sediment non-uniformity was omitted or not considered. For example, in the Pier Scour Database, PSDb (Benedict and Caldwell, 2014), only in 30% of the cases was the

sediment non-uniformity reported. However, in most of the cases (96%), the median particle size was reported. For clear water condition, the scour depth decreases with the increase in sediment non-uniformity (Ettema 1980; Melville 1997; Raikar and Dey 2005). In case of non-uniform sediments ($\sigma_g > 1.3$), it is possible to form an armor layer surrounding the pier. The armor layer resists the subsequent development of the scour depth due to the progressively increasing critical shear stress with the presence of the larger grain sizes.

The energy associated with turbulence structures is determined in terms of the pier Euler number ($\frac{v^2}{gb}$; where v is the upstream flow velocity, g is the gravitational acceleration, and b is the pier width) and pier Reynolds number ($\frac{\rho V b}{\mu}$; where ρ and μ are the density and viscosity of water respectively). Ettema et al. (1998) and Ettema et al. (2006) observed that scour depth increases significantly as the pier Euler number increases, suggesting the consideration of a correction factor accounting for Euler number impacts. It is interesting to note that most of the scour prediction equations (Wilson 1995; Melville 1997; HEC 18 2012) available in the literature do not consider the effect of the power of turbulence structures.

Pier scour is also affected by the flow intensity, expressed as a ratio of upstream flow velocity, v to the sediment critical velocity, v_c . The effect of uniformity of sediments, size and steepness of bed features in relation to v/v_c has been studied extensively in the literature (Chee 1982; Chiew 1984; Melville 1984; Melville and Sutherland 1988). Temporal evolution of scour has been studied by Shen et al. (1969), Ettema (1980), Melville and Chiew (1999), Oliveto and Hager (2002, 2005), Miller (2003), and Kothyari et al. (2007). However, Ettema et al. (2010) pointed out that data on the time development of local scour at wide piers or piers with complex geometry is scarce; therefore, the validity of the temporal evolution theory when applied to wide piers or long skewed piers is questionable.

4. Databases

The review of databases is classified into two categories, i) system-level scour observations, and ii) material-level erodibility observations.

4.1 System-level scour observations

Benedict and Caldwell (2014) performed an extensive literature review to identify the potential sources of pier scour data and collected 2,427 laboratory and field scour datasets. The data encompass a wide range of laboratory and field conditions. Of the 2427 data, 1858 are field measurements, and the rest are laboratory measurements. The field data were collected from 23 states within the United States and 6 other countries. The collected data include a wide range of stream gradients, drainage areas, sediment sizes, flow depth, flow velocity, and pier sizes. On the other hand, the laboratory data encompasses 569 measurements under a wide range of conditions.

The data were initially compiled by Sheppard et al. (2011) from 17 former investigations. While the laboratory data in the database were classified into clear-water and live-bed categories, the field data were not. Nevertheless, the database is the largest collection of pier scour data available in the United States, with a complete set of parameters to allow for comparative analysis of models that require different input parameters.

4.2 Material-level erodibility observations

Over the past 25 years, various testing approaches for assessing the erodibility of soil have been reported in literature. Some of these tests have laboratory applicability, whereas, some have field applicability. Table 3 presents a summary of erosion evaluation tests. For all testing approaches listed in Table 3, factors considered to influence erosion were critical velocity, critical shear stress, slope of erosion rate versus velocity curve and initial slope of erosion rate versus shear stress curve (Briaud et al. 2019). Review of Table 3 suggests that erosion tests, for which “undisturbed samples” can be retrieved for laboratory testing, were mostly focused on clays and silts; testing approaches for coarser particles are still lacking due to the need to mainly perform testing in-situ.

Briaud et al. (2019) conducted an extensive numerical, and laboratory testing using data from EFA, JET, and HET to observe the differences among the results from different tests. CHEN4D coding (Chen et al. 1990) was used to perform CFD simulations to obtain the hydraulic shear stress on the soil bed prior to erosion. The shear stress at the interface was determined with Moody charts (Moody 1944) as well. The Moody chart is the basis for a critical shear stress estimation using EFA test. It was observed that Moody charts generally overestimated critical shear stress compared to the numerical simulation. The maximum discrepancy was reported for a coarse sand, where the critical shear stress was 25 Pa (from numerical simulation), and using Moody chart the critical shear stress was found to be 50 Pa. Briaud et al. (2019) also mentioned that such discrepancy is more pronounced at higher shear stresses. Comparing with the site-specific cases, the JET test has more applicability when agricultural erosion or levee erosion due to overtopping is of interest. The HET test is suggested to have more suitability in assessing suffusion, or internal erosion of earth embankments. However, for other erosion tests, no explicit comments were made by Briaud et al. (2019) regarding applicability. A database of 950 erosion tests performed all over the world was compiled by Briaud et al. (2019). Geotechnical properties of soil and the erosion test response were reported in the database. This is one of the first attempts to compile comparative data on from various erosion tests to assist in understanding the applicability of different testing approaches.

5. Scour Prediction Models

The available scour prediction studies can be broadly classified into three different categories. These are, i) Deterministic, ii) Probabilistic, and iii) Observation-based.

5.1 Deterministic models

Ettema et al. (2011) and Sheppard et al. (2011) compiled the pier-scour prediction models developed since 1949. At present, there are more than 20 pier-scour models available in the literature. These models are developed in most cases based on either extensive laboratory testing data, from field data, or from both. However, as a part of the review herein the scour prediction models developed since 1990 are presented in Table 4, albeit this list is not exhaustive. Gao et al. (1990) model was developed from local scour data collected in China and consisting of 137 live bed and 115 clear water data points. Wilson (1995) model is based on field data collected from 22 bridges in Mississippi. Melville (1997) model is based on extensive laboratory and field data collected over a period of 25 years. Sheppard and Miller (2006) model was developed primarily based on laboratory data and few field observations. Oliveto and Hager (2002, 2005), Kothyari et al. (2007) model is based on experiments performed on pier width ranging from 0.02-0.50 m, d_{50} ranging from 0.55-5.3 mm. The latest update of HEC-18 model by Arneson et al. (2012) is the most widely used pier-scour prediction model. It is developed based on data from laboratory testing on sediments with median grain size, d_{50} ranging from 0.24-0.52 mm. Briaud (2014a) model is based on data from large scale laboratory flume testing (d_{50} ranged from 0.10-0.60 mm).

To provide a comparative assessment of the influencing parameters on computing scour magnitude, Table 5 is provided, listing the parameters considered in each of the models in Table 4. Sheppard et al. (2011) considered 23 different scour prediction models and investigated the performance of the models when compared to 928 field and 569 laboratory data. Their conclusion suggested that results from Sheppard and Miller (2006) and Melville (1997) models provided reasonable values when compared with field data. Careful observation of Table 5 suggests that these two models incorporated all the primary variables, in contrast to the remaining listed models in Table 5. Sheppard et al. (2011, 2014) melded and empirically modified Sheppard and Miller (2006) and Melville (1997) models to obtain a refined estimate of scour for wide piers, as the existing deterministic models cannot predict the scour depth for wide piers with accuracy (compared to narrow, and intermediate piers).

5.2 Probabilistic approach

Although there seems to be a significant number of studies that were focused on developing deterministic pier scour equations, focus on probabilistic approaches is limited. To the authors' knowledge, the first probability-based pier scour model was introduced by Johnson (1992). The Johnson (1992) study was focused on the relationship between probability of bridge failure and safety factors. Johnson and Dock (1998), using a Monte-Carlo simulation technique, developed probabilistic bridge scour depth estimates, considering hydraulic and geometrical parameter uncertainty. Probabilistic framework was also developed for assessing the likelihood of achieving a specific scour depth, probability of exceedance, as well as adequate pile depth. Briaud et al.

(2007) developed a probabilistic bridge scour model that considered the uncertainty of hydrologic conditions; however, uncertainties associated with input parameters (geometry of obstacle, soil erodibility) were not considered. Bolduc et al. (2008) introduced a probabilistic model based on the bias and scatter around the mean. Bias was defined as the ratio between the mean-measured value to the mean-predicted value. Johnson et al. (2014) examined the overall uncertainty in local pier or abutment scour in combination with contraction scour. As a part of the study, reliability-based scour design factors were suggested. Briaud et al. (2014) developed a reliability-based pier scour model focusing on the risk associated with failure of shallow and deep foundations subjected to scour. It was demonstrated that the scour depth prediction from HEC-18 should be multiplied by the factor 2.05 to ensure a probability of exceedance of 0.001 for shallow foundations in sand subjected to scour. While the HEC-18 scour prediction model is considered to be highly conservative, yet per Briaud et al. (2014), the scour predictions from HEC-18 did not correspond to sufficiently low probability of failure.

5.3 Observation-based approach

The designation of a bridge pier as “*scour critical*” highly depends on the method used to estimate the scour. Most scour prediction models do not take into account the key physical and engineering parameters of soils being eroded, such as plasticity, density and shear strength. Although scour prediction models such as Briaud et al. (2008) and Briaud (2014b) are based on using erodibility parameters, the use of such models necessitates performing site-specific erosion testing. To address this issue, Govindasamy et al. (2013) developed a model that is referred to as the Observation Method for Scour (OMS). One point of subjectivity in the OMS technique is if one soil classification falls into two different categories, the same structure can be classified as scour-critical or non-critical based on the erosion category that was assigned to the soil. Nevertheless, Govindasamy (2009) demonstrated successful application of OMS to 16 Texas bridges. Results however revealed that some of the scour-critical bridges are not scour critical based on the OMS analyses. The OMS technique has been automated for the state of Texas and is used for first order approximation of scour criticality (Govindasamy et al., 2013).

6. Factors Complicating Pier Scour Estimation

The descriptions herein focus on the effect of several factors that have the tendency to complicate scour estimation for bridge piers. Some of the factors affect the flow field surrounding piers, whereas others affect the erodibility of the sediment around the foundation.

6.1 Pier proximity to abutment

Comparatively short first deck span is not uncommon in bridge design due to the construction economy advantages in having the pier close to the abutment (Sturm et al., 2011). However, such placement highly influences the flow field around the abutment. Consequently,

pier scour occurs in the zone of the abutment flow field. Ettema et al. (2011) suggested that scour depth at the pier in such cases is dominated by abutment scour. Nevertheless, the potential severity of pier placement near the abutment toe has received less attention. Hong et al. (2005) observed that the location of deepest scour changes due to the placement of pier near the abutment toe. However, no scour depth prediction model was suggested by Hong et al. (2005). Croad (1989) suggested that if a pier falls in abutment scour region, the scour depth at the pier can be estimated as equal to 0.9 times the abutment scour. Ettema et al. (2011) inferred that the conventional equations for pier scour estimation are not applicable if the pier is located in the abutment scour region.

6.2 Debris accumulation

Waterborne debris, composed primarily of tree trunks and limbs, often accumulates at bridges during high flow events (Lagasse et al. 2010), leading to obstruction or constriction of flow. This might cause damage to the bridge foundation and/or increased scour. The size of debris may vary from a small cluster of tree branches to a near complete blockage of flow by large tree trunks or other debris. The impact of debris accumulation on scour estimation has been studied by Chang and Shen (1979), Diehl (1997), and Parola et al. (2010). None of the studies has however resulted in a complete analysis for debris-loaded pier. Dongol (1989) and Melville and Dongol (1992), based on 17 laboratory investigation in clear water conditions, provided an expression for assessing effective pier width, with the impact of the floating debris.

Lagasse et al. (2010) reported that the photographic archive of debris at bridges across the United States suggests that the geometry of the debris accumulated at the bridges can be classified into a finite number of common shapes. Based on their findings on mobility and transport mechanism of debris, geometry of the debris, Lagasse et al. (2010) suggested a methodology to estimate the effective pier width when debris accumulation is expected, and such width can be used in Richardson and Davis (2001) equation to estimate the magnitude of scour.

The effect of the geomorphic characteristics of rivers, physiographic regions, and types of vegetation present are some of the factors that contribute to quantifying the extent of debris surrounding bridges. Based on the measurements of spring-dominated streams, Manga and Kirchner (2000) showed that although Large Woody Debris (LWD) cover less than 2% of the surface area of the stream, the debris existence contributes to half of the total flow resistance. It was reported that addition of LWD to a stream increases the total shear stress, but reduces the shear stress borne by streambed. Buffington and Montgomery (1999) have also reached the same conclusion. Pagliara and Carnacina (2011) identified that cylindrical shapes can be one of the debris shape, and the effect of downstream extension of debris accumulation is also an important parameter influencing flow features. Panici and de Almeida (2018) concluded that for a given debris length, accumulation pattern varies with the flow velocity. At low flow velocity,

accumulations are wide and shallow, whereas with increased flow velocity, accumulations tend to be narrow and deep. Schalko et al. (2018) reported the backwater rise due to large debris accumulations leads to flood hazard, which can intensify scour critically. Nevertheless, such effects, to the authors' knowledge are yet to be formulated into a comprehensive model for analyses of pier scour loaded with debris. Lagasse et al. (2010) noted that the paucity of data on debris accumulation is a primary factor constraining the development of such a model.

6.3 Vegetation within the floodplain

The flood plain vegetation affects the flow field surrounding the abutment, which influences the scour magnitude (Sturm et al. 2011). Vegetated surface may extend the clear water-scour beyond the critical entrainment condition for the foundation soil or sediment beneath (Ettema et al. 2011). Vegetation in the stream-bed exerts additional drag which eventually reduces the mean flow within vegetated regions (Shi et al. 1995). This reduced velocity promotes sediment accumulation as near-bed stresses are reduced (Leonard and Luther 1995). Guardo and Tomasello (1995) used a modified Manning's equation to model the induced drag. Nepf (1999) noted that modified Manning's model cannot accurately represent the regions of emergent vegetation. Subsequently, Nepf (1999) developed a model describing drag, turbulence, and diffusion for flow through emergent vegetation. Jordanova and James (2003), and Kothyari et al. (2009) suggested that sediment transport rates in vegetated channels are related to the bed shear stress in a way similar to bare channel flows. However, Nepf (2012a), Nepf (2012b), Tanino and Nepf (2008), Biron et al. (2004), Nepf and Vivoni (2000) noted that the typical methods to estimate the bed shear stress are not appropriate in vegetated channels for several reasons including that vegetation-induced turbulence can inhibit sediment deposition (Yang and Nepf, 2018). To predict the bed shear stress in emergent vegetation, Rowinski and Kubrak (2002) developed a one-dimensional model, which is based on modified mixing length concept. An idealized case with equidistant arrangement of vegetation in longitudinal and transverse direction was assumed; transverse momentum transport was not considered in the model. Yang et al. (2015) developed a model to estimate the bed shear stress in vegetated channel within a viscous sub-layer at the bed. Yang et al. (2015) model considers emergent vegetation and channels with smooth and impermeable bed. Yang and Nepf (2018) based on laboratory experiments with model vegetation showed that existing sediment transport models underestimate the sediment transported by an order of magnitude, as the models do not account for the effect of vegetation. A Turbulent Kinetic Energy (TKE) based model was proposed by Yang and Nepf (2018) to estimate bed-load transport rate that is applicable for both bare and vegetated channels. While, possible effects of vegetation on the bed shear stress is studied in relation to sediment transport under wide ranging flow conditions, integration of this understanding in bridge pier scour estimation models remains to be developed.

6.4 Layered sediments

The subsurface soil profile surrounding a pier foundation may consist of multiple subsurface layers with varying level of resistance to scour. If the upper bed soil layer is sufficiently deep to accommodate the maximum scour depth, then the conventional approaches available for uniform deposits can be used. In contrast, if scour reaches an underlying layer with different soil type once a top layer is eroded, then scour rate and magnitude will vary. Ettema et al. (1980), Breusers and Raudkivi (1991), and Melville and Coleman (2000) identified that the scour depth in the latter case depends on the disintegration of the layer in upstream direction, downstream direction, or both. Lagasse et al. (2007) and Mashahir et al. (2010) identified the necessity of sediment layering considerations in riprap protection of piers. In addition to several available laboratory testing techniques, the in-situ erosion evaluation probe introduced by Gabr et al. (2013), and Kayser and Gabr (2013) provides the means for assessing the erodibility parameters with depth in the field. The Federal Highway Administration recently developed an in-situ scour and erosion testing device (ISTD) (Bergendahl and Kerényi, 2016), which measures the scour potential of the sediment based on the reduction in erosion rate due to water flow with the depth. Briaud et al. (2019) noted that ISTD is applicable for soils that have a maximum SPT N-value of 30. In addition, the applicability is limited to soils that are below the groundwater table.

6.5 Vertical contraction of flow

When the bridge deck is submerged, as in the case of severe flood storms for example, an additional scour-inducing process, namely vertical contraction of flow is introduced. This process can result in a significantly larger scour depth, exceeding the estimates from the conventional scour prediction models. Deck submergence is studied by Richardson and Davis (1995), Arneson and Abt (1998), Lyn (2008), and Guo et al. (2009). However, in most cases clear water situations were considered. Guo et al. (2009) developed an expression for maximum scour depth in pressure flow situations under clear water conditions, assuming a rectangular girder, uniform bed material, and no pier present to simplify the analyses. A model assessing scour with the presence of a pier in live bed conditions, or with non-rectangular girders, or non-uniform bed materials with the vertical contraction of flow is lacking in literature.

7. Applicability of Four Models

7.1 Data for analyses

Database reported in Benedict and Caldwell (2014), also referred to as PSDb (2014), were used herein. The database encompasses 569 measurements with a wide range of laboratory conditions. The dataset was initially classified into two categories: clear-water and live-bed. It is noted that laboratory live-bed tests are mostly conducted using uniform sediments. Similarly, only 27 out of 340 reported clear water laboratory tests were performed on non-uniform sediments.

In most cases, the deterministic pier-scour models do not differentiate their application in terms of clear-water versus live-bed conditions. However, the performance of a model may vary depending on comparing its output using the clear-water versus live-bed scour data. Under this assumption, the ranges of selected variables for live-bed and clear water conditions are presented in Table 6 and Table 7, respectively. It is important to note that the minimum, median, and maximum values reported in Tables 6 and 7 reflect the range for a particular variable but do not correspond to the minimum and maximum values in the other column (i.e. data across rows are not from the same test). Accordingly, the data in Tables 6 and 7 are not correlated to each other across each row. A total of 229 live-bed scour measurements were compiled in Benedict and Caldwell (2014), with the rest being clear water measurements.

7.2 Analyses

The focus herein was on four pier-scour prediction models, namely: Wilson (1995) model, Melville (1997) model, HEC-18 (2012), and Briaud (2014a) model. These four models are chosen due to the differences in the groups of data upon which these models were developed. Details on the group of data for each of the models are presented in the *Deterministic models'* section. The model equations are provided in Table 4. Error in models' estimation was considered as the metric describing the performance of a model. Error is defined as the difference between the predicted and measured scour depth, expressed as a percentage of measured scour depth, as shown in Eq. (5):

$$Error, \% = \frac{y_s(\text{predicted}) - y_s(\text{measured})}{y_s(\text{measured})} \times 100\% \quad (5)$$

Where, $y_s(\text{predicted})$ and $y_s(\text{measured})$ are the predicted and measured scour depths respectively. A positive error magnitude indicates that the pier-scour model is over-predicting the "measured" value and conversely, a negative error is indicative of under-prediction.

7.2.1 Error-scour depth relation

Error-normalized scour depth relation for the four models, using live bed and clear water datasets, are presented in Figures 4 and 5, respectively. Analyses of the data in Figure 4 show that the four predictive models have large error margins (-61% to 467%). For Melville (1997) and HEC 18 (2012) models, the scatter in data seems to be reduced as the magnitude of the normalized scour depth (y_s/b) is increased. The error in the Melville (1997) model decreases as y_s/b increases from 1.0-2.5. In the case of HEC 18 (2012) model, the error consistently reduces as y_s/b increases from 1.5-2.5. The error in the scour estimates from Briaud (2014) model did not yield a discernable trend. In the live-bed dataset of PSDb (2014), there are only five data points corresponding to the wide pier category (Table 2). These five data points provide y_s/b values that are < 1 . At $\frac{y_s}{b} < 1$, and in a number of occasions, error exceeding 100% (Eq. 5) was observed. Measurements'

inaccuracy might be partially contributing to such high error (>100%) at the $\frac{y_s}{b} < 1$. The lack of achievement of scour depth equilibrium during testing can also be an issue contributing to the estimated error, as the flow duration was not reported in 15 out of 18 occasions in which $\frac{y_s}{b} < 1$ was observed. Data analyses also suggest sediment non-uniformity (σ_g) might contribute to the error when $\frac{y_s}{b} < 1.3$. However, it is evident that there is a lack of experimental data with large σ_g and $\frac{y_s}{b} < 1.3$. As mentioned earlier, Melville (1997) suggested that in case of non-uniform sediments, it is possible that fine particles are transported away, and an armor layer of the remaining coarse material is formed at the pier.

Data in Figure 5 suggest that the error associated with clear water condition varies in the range of minus 69.5% to plus 2240%, which is significantly higher than the range utilizing the live bed dataset. For all the four models, and at $y_s/b < 1$ the error tended to exceed 500%. The error scatter from HEC 18 (2012) and Melville (1997) models seems to be less dispersed as compared to the results from the other two models. The laboratory test corresponding to the maximum error in all four models was performed for 200 minutes, thereby raising the concern of whether the results are representing the full evolution of scour depth.

7.2.2 Error-sediment size relation

Figures 6 and 7 show the relation between the % error and b/d_{50} . Data in Figure 6 suggest that the error in Briaud (2014a) model decreases as the b/d_{50} is increased. Briaud (2014a) model was developed based on flume testing results on clays ($d_{50} < 0.075 \text{ mm}$) and sands ($d_{50} = 0.1 - 0.6 \text{ mm}$). The model does not explicitly consider the effect of b/d_{50} as noted in Table 5. Although Lee and Sturm (2009) suggested that at $b/d_{50} \leq 25$, the scour progression is impeded, implying the predicted scour depth should exceed the measured scour depth, such a trend cannot be discerned from Figures 6 and 7. However, in the range of $b/d_{50} = 40-80$, and for all four models' predictions for live bed data, six measurements are noted to provide anomalous error compared to the response obtained utilizing the rest of the dataset (refer to Figure 6). The parameters associated with these six measurements are presented in Table 8. All these measurements are associated with narrow pier category (Table 2), and the sediments are coarse grained ($d_{50} > 0.6 \text{ mm}$). The concern seems to be the sediment non-uniformity (reported to be 2.8 and 5.5,) being quite high compared to the demarcation value of 1.3 (Melville 1997). As previously noted, high σ_g is suggestive of potential armor layer formation, which can effectively reduce the progression of scour depth. For live bed conditions b/d_{50} was observed to vary from 10-1989; whereas, for clear water conditions the range is 3.67-4160, indicating a wider range of laboratory test data coverage for clear water conditions.

7.2.3 Error distribution and statistics

The relationship between the predicted and measured normalized scour depth is presented in Figures 8 and 9. It appears that on average, Melville (1997), HEC-18 (2012), and Briaud (2014) models provide a conservative estimate of scour under live bed conditions. However, strong correlation between predicted and measured y_s/b (as indicated by R^2 value) was not obtained for the four models considered herein. The degree of conservatism of Melville (1997) and HEC-18 (2012) models tends to be of similar magnitude (42%). Results show that use of Wilson (1995) model would require increasing the predicted normalized scour depth by a magnitude of 2 standard deviations (0.82 in this study) to ensure a conservative estimate.

For clear water conditions, and as presented in Figure 9, the four models provide conservative estimates. The degree of conservativeness being highest (34%) for the Wilson (1995) and Melville (1997) models. Predicted and measured normalized scour depths are not strongly correlated in the four models, as indicated by the R^2 . Melville (1997) model can be considered as the most conservative model among the four models as Melville (1997) model underpredicted measured data in least number of occasions ($n = 11$ out of 340 total cases).

The distributions of error, in terms of the cumulative density function, for the four models used herein are presented in Figure 10. The error distributions for live bed and clear water conditions in all four models are normally distributed with a positive skew. Figure 10(a) shows that the probability to obtain an underprediction using Wilson (1995) model is 72%, whereas, for Briaud (2014a) model, the probability is 23%. While using Melville (1997) and HEC 18 (2012) models, the probability of obtaining an underprediction is 4%, and 9% respectively.

The probability, for example, to obtain an error $<150\%$ is 98%, 96%, 98%, and 95% for Wilson (1995), Melville (1997), HEC 18 (2012), and Briaud (2014a) models, respectively. The probability of obtaining an error for a given range of underestimating or overestimating scour magnitude is summarized in Table 9. Analyses of data in Figure 10(b) suggest that the probability of an unconservative estimate from Wilson (1995), Melville (1997), HEC 18 (2012), and Briaud (2014a) models are 43%, 11%, 18%, and 42% respectively. These values are higher compared to the probability corresponding to the estimates for live bed condition. Although the error-normalized scour depth relation for clear water case in Figure 5 showed occurrences of error exceeding 500%, data in Figure 10(b) suggests that for all the four models, the probability to obtain an error $>500\%$ is $\leq 4\%$. Evaluation of probabilities corresponding to live bed and clear water conditions in Table 9 indicates that for Melville (1997), HEC 18 (2012) and Briaud (2014a) models, the probability of obtaining an unconservative estimate of scour is higher (by 7%, 10%, and 19% respectively) for clear water conditions. It also seems that obtaining an error $>150\%$ is more probable for clear water conditions compared to the live bed conditions.

However, the choice of a model should not only depend on the conservativeness of the predictions, but also on the consistency of estimation, i.e. its precision and spread of error. The

statistical parameters computed based on the results of the four models and including average error, standard deviation, and variance are shown in Tables 10 and 11. Although the average error from Melville (1997), HEC-18 (2012), and Briaud (2014) models ranges from 43-60% for live bed conditions, the standard deviation and variance of Briaud (2014a) model are 0.64 and 0.42 respectively, which is relatively higher compared to the standard deviation and variance of the other two models. For clear water condition, maximum standard deviation and variance for Wilson (1995) model are 1.13 and 1.27, respectively, whereas, the minimums were obtained for Melville (1997) model (which are 0.41 and 0.17, respectively).

8. Summary and Conclusions

A review of aspects related to scour and soil erodibility has been presented covering details on erodibility parameters and analyses models. The review also included common factors influencing pier scour and demonstrated performance and error statistics of four pier scour models. Based on the review and analyses presented herein, the following conclusions are made:

1. Data in literature indicate that the stress fluctuations due to turbulent boundary layer contribute to soil erodibility. Future consideration of this effect can lead to narrowing the current erodibility criteria for a given soil class and thereby reducing the possibility to classify a soil across two different erodibility categories.
2. Similar to the observation of Melville and Coleman (2000), Ettema et al. (2017), laboratory data on wide pier studies are scarce. There is a need for research to develop the reliability of pier scour estimates for wide piers. Sheppard et al. (2011, 2014) provided the only complete analysis for wide piers focusing on a parametric response.
3. Until recently the effect of sediment non-uniformity was not considered in the soil erosion analyses. Laboratory studies, as reported in PSDb (2014), were mainly focused on flume testing with uniform deposits, whereas non-uniform deposits may lead to an armor layer formation at the pier. Such formation can progressively reduce the boundary layer velocity, leading to reduction in the scour magnitude. Further laboratory studies on non-uniform sediments are needed to discern such phenomenon for both live bed and clear water conditions.
4. Although a significant number of studies were focused on developing deterministic pier scour equations, the focus on probabilistic approach is limited. A probabilistic approach can also have different connotation; it may account for uncertainties in hydraulic loading, geometrical site conditions including flood plain, sediments spatial and depth variabilities, or failure mechanism assumed for the bridge elements. Studies suggest that although in the common literature HEC-18 scour prediction model is considered to be highly conservative, it is yet not sufficient to

ensure a low probability of failure. Hence, the use of a reliability-based approach in design should be considered in practice.

5. To mitigate the cost concerns associated with site-specific erosion testing, Observation Method for Scour (OMS) was developed by Govindasamy et al. (2013). This approach can be used for first order scour criticality assessment although sufficient level of site data is needed with subjectivity of the approach embedded in the a priori assumption of the type of bed material and erosion category.
6. A rigorous study is required to develop a clear demarcation between abutment scour region and contraction scour region and possible relationship to scour depth formulae. Further studies are also needed to systematically integrate the effect of vegetation on bridge pier scour onto estimation models. In view of the frequent occurrence of hurricanes and severe rainstorms, studies are required for pressure flow situations in live-bed conditions with non-rectangular girders, and non-uniform bed materials to complete the research gap.
7. For both live bed and clear water conditions, and at a normalized scour depth $y_s/b < 1$, the four pier scour prediction models considered herein yielded significant error (for live bed conditions, $>100\%$; for clear water conditions, $>500\%$) when comparison with measured data was made. Measurement inaccuracy, sediment non-uniformity, non-equilibrium scour depth during measurements, and/or pier category difference might be the reasons for such error level.
8. On average, for live bed condition, Melville (1997), HEC-18 (2012), and Briaud (2014) models provide a conservative estimate of pier scour. Both Melville (1997) and HEC-18 (2012) models are conservative to a similar extent (42%). In comparison, for clear water condition, all the four models provide a conservative estimate, with the degree of conservatism being highest (34%) for Wilson (1995) and Melville (1997) models. However, the “average” measure of error needs to be presented in the context of the precision of prediction (i.e. being consistently conservative for example).
9. For live bed condition, Briaud (2014a) model yielded the highest standard deviation and variance; whereas, for clear water condition, Wilson (1995) model yielded the highest standard deviation and variance. For live bed condition, the probability to obtain an underprediction of scour magnitude using in Wilson (1995) model is 72%, whereas, for Melville (1997) model, such probability is 4%. For clear water condition, the probability to obtain an underprediction using Wilson (1995) model is 43%; whereas, for Melville (1997) model, such probability is 11%.

In general, the shear stress acting at the soil-water interface layer is considered as a key parameter influencing erodibility. Briaud et al. (2019) observed that Moody charts generally overestimated

critical shear stress compared to the CFD modeling, with the discrepancy more pronounced at higher shear stress magnitudes. With the advancement of numerical analysis techniques, such as coupled CFD-DEM or coupled CFD-MD, understanding of the initiation and progression of particles mobility and transport, and considering the coupled action of shear stress and the turbulent interface layer, is needed especially in cases when flow experiencing obstructions.

Acknowledgements

Funding from North Carolina Department of Transportation (NCDOT) is gratefully appreciated. Any conclusions, findings, opinions, and recommendations expressed in this article are those of the authors and do not necessarily reflect the views of NCDOT.

Data Availability

Datasets for this research is available in the in-text data citation reference: Benedict and Caldwell (2014).

References

- Arneson L, Abt S. Vertical contraction scour at bridges with water flowing under pressure conditions, Transportation Research Record 1647, TRB, National Research Council, Washington, D.C, 1998; 1-17.
- Arneson LA, Zevenbergen LW, Lagasse PF, Clopper PE. Evaluating scour at bridges. Hydraulic Engineering Circular No. 18, 2012; 5th ed. 1-340.
- Benedict ST, Caldwell AW. A pier-scour database—2,427 field and laboratory measurements of pier scour. U.S. Geological Survey Data Series 845, 2014, 1-22.
- Bergendahl BS, Kerenyi K. 2016. In-situ Scour Testing Device. United States Patent, Patent No. US 9,322,142 B2.
- Biron PM, Robson C., Lapointe MF, Gaskin SJ. Comparing different methods of bed shear stress estimates in simple and complex flow fields, *Earth Surface Processes and Landforms*, 2004; 29(11), 1403–1415.
- Bloomquist D, Sheppard DM, Schofield S, Crowley RW. The Rotating Erosion Testing Apparatus (RETA): A laboratory device for measuring erosion rates versus shear stresses of rock and cohesive materials. *Geotechnical Testing Journal*, 2012; 35(4), 641-648.
- Bolduc LC, Gardoni P, Briaud J-L. Probability of exceedance estimates for scour depth around bridge piers. *Journal of Geotechnical and Geoenvironmental Engineering*, ASCE, 2008; 10.1061/(ASCE)1090-0241(2008)134:2(175), 175–184.
- Breusers HNC, Raudkivi AJ. Scouring, *Hydraulic Structures Design Manual*, 1991; No. 2, I.A.H.R., Balkema, Rotterdam, Netherlands.
- Briaud J-L. Case histories in soil and rock erosion: Woodrow Wilson Bridge, Brazos River Meander, Normandy Cliffs, and New Orleans Levees, *Journal of Geotechnical and Geoenvironmental Engineering*, ASCE, 2008; 134(10): 1425-1447.
- Briaud J-L. *Geotechnical Engineering: Unsaturated and Saturated Soils*, John Wiley and Sons, Inc., Hoboken, New Jersey, 1st Edition, 823-857, 2013.
- Briaud JL. Scour depth at bridges: Method including soil properties. I: Maximum scour depth prediction. *Journal of Geotechnical and Geoenvironmental Engineering*, ASCE, 2014a; 141(2): 04014104.
- Briaud JL. Scour depth at bridges: Method including soil properties. II: Time rate of scour prediction. *Journal of Geotechnical and Geoenvironmental Engineering*, ASCE, 2014b; 141(2): 04014105.
- Briaud J-L, Brandimarte L, Wang J, D’Odorico P. Probability of scour depth exceedance due to hydrologic uncertainty. *Georisk: Assess. Manage. Risk Eng. Syst. Geohazards*, 2007; 1(2), 77–88.

- Briaud JL, Chedid M, Chen H-C, Shidlovskaya A. Borehole erosion test. *Journal of Geotechnical and Geoenvironmental Engineering*, ASCE, 2017; 143(8), S. 04017037-1–04017072-12.
- Briaud JL, Chen HLY, Nurtjahyo P, Wang J. SRICOS-EFA method for contraction scour in fine-grained soils. *Journal of Geotechnical and Geoenvironmental Engineering*, ASCE, 2005; 131(10):1283-1294.
- Briaud J-L, Gardoni P, Yao C. Statistical, risk, and reliability analyses of bridge scour. *Journal of Geotechnical and Geoenvironmental Engineering*, ASCE, 2014; 140(2): 04013011.
- Briaud JL, Govindasamy AV, Shafii I. Erosion Charts for Selected Geomaterials. *Journal of Geotechnical and Geoenvironmental Engineering*, ASCE, 2017; 143(10), S. 04017072-1–04017072-13.
- Briaud JL, Shafii I, Chen H-C, Cetina Z-M. Relationship between erodibility and properties of soil. Transportation Research Board of the National Academies, National Cooperative Highway Research Program Web Document 915 (Project 24–43), 2019; 1-328.
- Briaud JL, Ting F, Chen HC, Cao Y, Han SW, Kwak K. Erosion function apparatus for scour rate predictions. *Journal of Geotechnical and Geoenvironmental Engineering*, ASCE, 2001; 127(2):105-113.
- Briaud JL, Ting F, Chen HC, Gudavalli R, Perugu S, Wei G. SRICOS: Prediction of scour rate in cohesive soils at bridge piers. *Journal of Geotechnical and Geoenvironmental Engineering*, ASCE, 1999; 125(4):237-246.
- Buffington JM, Montgomery DR. Effects of hydraulic roughness on surface textures of gravel-bed rivers, *Water Resources Research*, 1999; 35, 3507-3521.
- Chabert J, Engeldinger P. 1956. Etude des affouillements autour des Piles des ponts (Study on scour around bridge piers): Chatou, France, Laboratoire National d'Hydraulique, as cited in Sheppard et al. (2011).
- Chang LY, Chen Q Ye FM. Particle flow simulation for contact erosion between uniform particles. *Chinese Journal of Geotechnical Engineering*, 2016; 38 (S2): 312–317.
- Chee RKW. Live-bed scour at bridge piers, Report No. 290, School of Engineering, The University of Auckland, Auckland, New Zealand, 1982.
- Chen HC, Patel VC, Ju S. Solutions of Reynolds-averaged Navier–Stokes equations for three-dimensional incompressible flows. *Journal of Computational Physics*, 1990; 88(2), 305–336.
- Chiew YM. Local scour at bridge piers. Report No 355, Department of Civil Engineering, University of Auckland, New Zealand, 1984.
- Croad RN. Investigation of the pre-excavation of the abutment scour hole at bridge abutments, Report 89-A9303, Central Laboratories, Works and Development Services Corporation (NZ) Ltd., Lower Hutt, New Zealand, 1989.

- Deng L, Cai CS. Bridge scour: Prediction, modeling, monitoring, and countermeasures-Review. *Practice Periodical on Structural Design and Construction*, 2010; 15(2), 125–134.
- Diehl TH. Potential drift accumulations at bridges, Report RD-97-28, Federal Highway Administration, U.S. Dept of Transportation, McLean, VA, 1997.
- Dongol MS. Effect of debris rafting on local scour at bridge piers, Report No. 473, School of Engineering, University of Auckland, Auckland, New Zealand, 1989.
- Ettema R. Scour at bridge piers, Report No. 216, School of Engineering, The University of Auckland, Auckland, New Zealand, 1980.
- Ettema R, Mostafa EA, Melville BW, Yassin AA. On local scour at skewed piers, *Journal of Hydraulic Engineering*, ASCE, 1998; 124 (7), 756-760.
- Ettema R, Kirkil G, Muste M. Similitude of large-scale turbulence in experiments on local scour at cylinders. *Journal of Hydraulic Engineering*, ASCE, 2006; 132(1), 33-40.
- Ettema R, Constantinescu G, Melville BW. Evaluation of bridge scour research—Pier scour processes and predictions: Transportation Research Board of the National Academies, National Cooperative Highway Research Program Web Document 175 (Project 24–27(01)), 2011; 1-181.
- Ettema R, Constantinescu G, Melville BW. Flow-field complexity and design estimation of pier-scour depth: Sixty years since Laursen and Toch. *Journal of Hydraulic Engineering*, ASCE, 2017; 143(9), 03117006.
- Fisher M, Chowdhury MN, Khan AA, Atamturkur S. An evaluation of scour measurement devices. *Flow Measurement and Instrumentation*, 2013; 33(2013), 55-67.
- Gabr M, Caruso C, Key A, Kayser M. Assessment of in situ scour profile in sand using a jet probe. *Geotechnical Testing Journal*, 2013; 36(2), 264–274.
- Gao D, Posada GL, Nordin CF. Pier scour equations used in the Peoples Republic of China - Review and Summary. National Hydraulics Conference, ASCE, San Francisco, CA, 1993; 1031-1036.
- Govindasamy AV. Simplified method for estimating future scour depth at existing bridges, Ph.D. Dissertation, Texas A&M University, College Station, Texas, 2009.
- Govindasamy AV, Briaud J-L, Kim D, Olivera F, Gardoni P, Delphia J. Observation method for estimating future scour depth at existing bridges. *Journal of Geotechnical and Geoenvironmental Engineering*, ASCE, 2013; 139(7):1165-1175.
- Grissinger EH. Resistance of selected clay systems to erosion by water. *Water Resources Research*, 1966; 2(1), 131–138.
- Guardo M, Tomasello R. Hydrodynamic simulations of a constructed wetlands in south Florida, *Journal of the American Water Resources Association*, 1995; 31(4), 687-701.

- Guo J, Kerenyi K, Pagan-Ortiz J. Bridge Pressure Flow Scour for Clear Water Conditions, Report FHWA-HRT-09-041, Federal Highway Administration, McClean, VA, 2009.
- Guo Y, Yu X. Comparison of the implementation of three common types of coupled CFD-DEM model for simulating soil surface erosion. *International Journal of Multiphysics Flow*, 2017; 91 (May): 89–100.
- Guo Y, Yang Y, Yu X. Influence of particle shape on the erodibility of non-cohesive soil: Insights from coupled CFD–DEM simulations. *Particuology*, 2018; 39 (Aug): 12–24.
- Hanson GJ. Surface erodibility of earthen channels at high stresses. Part II: Developing an in situ testing device. *Transactions of the ASAE*, 1990; 33(1), 132–137.
- Hanson GJ, Cook KR. Apparatus, test procedures, and analytical methods to measure soil erodibility: In situ. *Applied Engineering in Agriculture*, 2004; 20(4), 455–462.
- Hanson GJ, Simon A. Erodibility of cohesive streambeds in the loess area of the Midwestern USA. *Hydrologic Processes*, 2001; 15(1), 23–38.
- Henderson FM. (1966). *Open channel flow*. MacMillan Publishing Co. Inc., New York, N.Y.
- Hofland B, Battjes JA, Booij R. Measurement of fluctuating pressures on coarse bed material. *Journal of Hydraulic Engineering*, ASCE, 2005; 131(9), 770–781.
- Hong S. Interaction of bridge contraction scour and pier scour in a laboratory river model, M.S. Thesis, Civil and Environmental Engineering Dept., Georgia Institute of Technology, Atlanta, GA, 2005.
- Hong JH, Chiew YM, Yeh PH, Chan HC. Evolution of local pier-scour depth with dune migration in subcritical flow conditions. *Journal of Hydraulic Engineering*, ASCE, 2017; 143(4), 04016098.
- Huang QF, Zhan ML, Sheng JC, Luo YL. Investigation of fluid flow-induced particle migration in granular filters using a DEM-CFD method. *Journal of Hydrodynamics, Series B*, 2014; 26(3): 406–415.
- Hunt D. Monitoring scour critical bridges. NCHRP synthesis 396. Washington, D.C.: Transportation Research Board, 2009.
- Johnson PA. Reliability-based pier scour engineering. *Journal of Hydraulic Engineering*, ASCE, 1992; 118(10), 1344-1358.
- Johnson PA, Dock DA. Probabilistic bridge scour estimates. *Journal of Hydraulic Engineering*, ASCE, 1998; 124(7), 750–754.
- Johnson PA, Clopper PE, Zevenbergen LW, Lagasse PF. Quantifying uncertainty and reliability in bridge scour estimations. *Journal of Hydraulic Engineering*, ASCE, 2014; 141(7), 04015013.

- Jordanova AA, James C. Experimental study of bed load transport through emergent vegetation, *Journal of Hydraulic Engineering*, ASCE, 2003; 129(6), 474–478.
- Joseph GG, Hunt ML. Oblique particle wall collisions in a liquid. *Journal of Fluid Mechanics*, 2004; 510 (2004): 71–93.
- Julian JP, Torres R. Hydraulic erosion of cohesive riverbanks, *Geomorphology*, 2006; 76 (1-2): 193-206.
- Kamojjala S, Gattu NP, Parola AC, Hagerty DJ. Analysis of 1993 Upper Mississippi flood highway infrastructure damage. Proceedings of the 1st international conference of water resource engineering. New York: American Society of Civil Engineers; 1994; 1061-1165.
- Kawano K, Shire T, O’Sullivan C. Coupled DEM-CFD analysis of the initiation of internal instability in a gap-graded granular embankment filter. In Vol. 140 of Proc., EPJ Web of Conf., 10005. Les Ulis, France: EDP Sciences, 2017.
- Kayser M, Gabr MA. Assessment of scour on bridge foundations by means of in situ erosion evaluation probe. *Transportation Research Record*. 2013; 2335(1):72-78.
- Kloss C, Goniva C, Hager A, Amberger S, Pirker S. Models, algorithms and validation for open source DEM and CFD-DEM. *Progress in Computational Fluid Dynamics*, 2012 12(2/3): 140–152.
- Kothyari UC, Hager WH, Oliveto G. Generalized approach for clearwater scour at bridge foundation elements, *Journal of Hydraulic Engineering*, ASCE, 2007; 133(11), 1229-1240.
- Kothyari UC, Hashimoto H, Hayashi K. Effect of tall vegetation on sediment transport by channel flows, *Journal of Hydraulic Research*, 2009; 47(6), 700–710.
- Lagasse PF, Richardson EV, Schall JD, Price GR. NCHRP report 396: Instrumentation for measuring scour at bridge piers and abutments. TRB, National Research Council, Washington D.C., 1997.
- Lagasse PF, Clopper PE, Zevenbergen LW, Girard LG. Countermeasures to protect bridge piers from scour, NCHRP Report 593, Transportation Research Board of the National Academies, Washington, D.C., 2007.
- Lagasse PF, Clopper PE, Zevenbergen LW, Spitz WJ, Girard LG. Effects of debris on bridge pier scour, NCHRP Report 653, Transportation Research Board of the National Academies, Washington, D.C., 2010.
- Lee SO, Sturm TW. Effect of sediment size scaling on physical modeling of bridge pier scour. *Journal of Hydraulic Engineering*, ASCE, 2009; 135(10), 793–802.
- Lefebvre G, Rohan K, Douville S. Erosivity of natural intact structured clay: evaluation. *Canadian Geotechnical Journal*, 1985; 22, 508–517.
- Leonard L, Luther M. Flow hydrodynamics in tidal marsh canopies, *Limnology and Oceanography*, 1995; 40(8), 1474-1484.

- Lin YB, Lai JS, Chang KC, Li LS. Flood scour monitoring system using fiber Bragg grating sensors. *Smart Materials and Structures*, 2006; 15(6), 1950-1959.
- Lyn DA. Pressure-flow scour: a re-examination of the HEC-18 equation, *Journal of Hydraulic Engineering*, ASCE, 2008; 134(7), 1015-1020.
- Manga M, Kirchner JW. Stress partitioning in streams by large woody debris, *Water Resources Research*, 2010; 36(8), 2373-2379.
- Mashahir M, Zarati A, Mokallar E. Application of riprap and collar to prevent scouring around rectangular bridge piers, *Journal of Hydraulic Engineering*, ASCE, 2010; 136(3), 183-187.
- McKenna G, Argyroudis SA, Winter MG, Mitoulis SA. Multiple hazard fragility analysis for granular highway embankments: moisture ingress and scour, *Transportation Geotechnics*, 2020; DOI: 10.1016/j.trgeo.2020.100431
- Melville BW. Live-bed scour at bridge sites, *Journal of Hydraulic Engineering*, ASCE, 1984; 110(9), 1234-1247.
- Melville BW. Pier and abutment scour: Integrated approach. *Journal of Hydraulic Engineering*, ASCE, 1997; 123(2), 125–136.
- Melville BW, Coleman SE. *Bridge scour*. Highlands Ranch, USA: Water Resources Publications, 2000.
- Melville BW, Chiew YM. Time scale for local scour at bridge piers, *Journal of Hydraulic Engineering*, ASCE, 1999; 125(1), 59-65.
- Melville BW, Dongol DM. Bridge pier scour with debris accumulation, *Journal of Hydraulic Engineering*, ASCE, 1992; 118(9), 1306–1310.
- Melville BW, Sutherland AJ. Design method for local scour at bridge piers, *Journal of Hydraulic Engineering*, ASCE, 1988; 114(10), 1210-1226.
- Miller W. Model for the time rate of local sediment scour at a cylindrical structure. Ph.D. dissertation, University of Florida, Gainesville, FL, 2003.
- Moody LF. Friction factors for pipe flow. *Transactions of the American Society of Civil Engineers*, 1944; 66.
- Moore WL, Masch FD Jr. Experiments on the scour resistance of cohesive sediments. *Journal of Geophysical Research*, 1962; 67(4), 1437–1449.
- Mostafa EA. Scour around skewed bridge piers, Ph.D. thesis, Dept. of Civil Engineering, Alexandria University, Alexandria, Egypt, 1994.
- Mueller DS. *National bridge scour program-measuring scour of the streambed at highway bridges*. Reston, VA: U.S. Geological Survey, 2000.
- Murillo JA. The scour of scour. *Civil Engineering*, ASCE, 1987; 66–69.

- Nepf H. Drag, turbulence, and diffusion in flow through emergent vegetation, *Water Resources Research*, 1999; 35(2), 479–489.
- Nepf H, Vivoni E. Flow structure in depth-limited, vegetated flow, *Journal of Geophysical Research*, 2000; 105(C12), 28, 547–28,557.
- Nepf HM. Flow and transport in regions with aquatic vegetation, *Annual Review of Fluid Mechanics*, 2012a; 44, 123–142.
- Nepf HM. Hydrodynamics of vegetated channels, *Journal of Hydraulic Research*, 2012b; 50(3), 262–279.
- Ni XD, Zhu CM, Wang Y. Hydro-mechanical analysis of hydraulic fracturing based on an improved DEM-CFD coupling model at micro-level. *Journal of Computational and Theoretical Nanoscience*, 2015; 12(9): 2691–2700.
- Oliveto G, Hager WH. Temporal evolution of clear-water pier and abutment scour. *Journal of Hydraulic Engineering*, ASCE, 2002; 128(9), 811–820.
- Oliveto G, Hager WH. Further results to time-dependent local scour at bridge elements. *Journal of Hydraulic Engineering*, ASCE, 2005; 131(2), 97–105.
- Oliveto G, Hager WH. Morphological evolution of dune-like bed forms generated by bridge scour. *Journal of Hydraulic Engineering*, ASCE, 2014; 140(5), 06014009.
- Pagliara S, Carnacina I. Influence of wood debris accumulation on bridge pier scour. *Journal of Hydraulic Engineering*, ASCE, 2014; 137(2), 254-261.
- Panici D, de Almeida GAM. Formation, growth, and failure of debris jams at bridge piers. *Water Resources Research*, 2018; 54, 6226–6241.
- Parchure TM, Mehta AJ. Erosion of soft cohesive sediment deposits. *Journal of Hydraulic Engineering*, ASCE, 1986; 111(10), 1308–1326.
- Parola AC, Hagerty DJ, Kamojjala S. Highway Infrastructure Damage caused by the 1993 Upper Mississippi River Basin Flooding, NCHRP Report 417, TRB, National Research Council, Washington, D.C., 1998.
- Prendergast LJ, Gavin K. A review of bridge scour monitoring techniques. *Journal of Rock Mechanics and Geotechnical Engineering*, 2014; 6(2014), 138-149.
- Raikar RV, Dey S. Clear-water scour at bridge piers in fine and medium gravel beds, *Canadian Journal of Civil Engineering*, 2005; 32(4), 775-781.
- Raudkivi AJ, Ettema R. Clear-water scour at cylindrical piers, *Journal of Hydraulic Engineering*, ASCE, 1983; 109(3), 339-350.
- Rhodes J, Trent R. Economics of floods, scour and bridge failures. In: Shen HW, Su ST, Wen F, editors. *Proceedings of 1993 ASCE conference hydraulic engineering '93*. San Francisco, CA, 1993.

- Richardson EV, Davis SR. Evaluating scour at bridges, Report No. FHWA-IP-90-017, Hydraulic Engineering Circular No. 18 (HEC-18), Third Edition, Office of Technology Applications, HTA-22, Federal Highway Administration, U.S. Department of Transportation, Washington, D.C., 1995.
- Rowinski PM, Kubrak J. A mixing-length model for predicting vertical velocity distribution in flows through emergent vegetation, *Hydrological Sciences Journal*, 2002; 47(6), 893–904.
- Schalko I, Schmocker L, Weitbrecht V, Boes RM. Backwater rise due to large wood accumulations. *Journal of Hydraulic Engineering*, ASCE, 2018; 144(9), 04018056.
- Shafii I, Briaud J. and Chen H. Shidlovskaya A. Relationship between soil erodibility and engineering properties. In: ICSE 2016 (8th International Conference on Scour and Erosion), 12-15 September 2016, Oxford, UK.
- Shafii I, Zhang Z, Briaud JL. Measurement of hydrodynamic forces on gravel particles in the erosion function apparatus. In *Scour and Erosion IX: Proceedings of the 9th International Conference on Scour and Erosion* (Y. Keh-Chia, ed.), Taylor and Francis Group, London, 2019, 519–542.
- Shen HW, Schneider VR, Karaki SS. Local scour around bridge piers. *Journal of the Hydraulics Division*, 1969; 95(HY6), 1919–1940.
- Sheppard DM, Melville B, Demir H. Evaluation of existing equations for local scour at bridge piers. *Journal of Hydraulic Engineering*, ASCE, 2014; 140(1), 14–23.
- Sheppard DM, Demir H, Melville B. Scour at wide piers and long skewed piers Washington, D.C., Transportation Research Board, NCHRP Report 682, 2011.
- Sheppard DM, Miller Jr. W. Live-bed local pier scour experiments. *Journal of Hydraulic Engineering*, ASCE, 2006; 132(7), 635–642.
- Sheppard DM, Odeh M, Glasser T. Large scale clearwater local pier scour experiments. *Journal of Hydraulic Engineering*, ASCE, 2004; 130(10), 957–963.
- Sherard JL, Dunnigan LP, Decker RS. Identification and nature of dispersive soils. *Journal of the Geotechnical Engineering Division*, 1976; 102, 298–312.
- Shi Z, Pethick J, Pye K. Flow structure in and above the various heights of a saltmarsh canopy: A laboratory flume study, *Journal of Coastal Research*, 1995; 11, 1204-1209.
- Shields IA. (1936). Application of similarity principles and turbulence research to bed-load movement. In: Ott, W.P., van Uchelen, J.C. (Eds.), (Translators), *Hydrodynamics Laboratory Publication*, vol. 167. California Institute of Technology, Pasadena.
- Shirole AM, Holt RC. Planning for a comprehensive bridge safety assurance program. *Transportation Research Record*. Washington DC: Transport Research Board; 1991; 137-142.

- Smerdon DB, Beasley ML. The tractive force theory applied to stability of open channels in cohesive soils, Research Bulletin, University of Missouri, Columbia, MO, 1959.
- Sturm TW, Ettema RW, Melville BM. Evaluation of bridge scour research-Abutment and contraction scour processes and prediction, Transportation Research Board of the National Academies, National Cooperative Highway Research Program Web Document 175 (Project 24–27(02)), 2011; 1-93.
- Tanino Y, Nepf HM. Laboratory investigation of mean drag in a random array of rigid, emergent cylinders, *Journal of Hydraulic Engineering*, ASCE, 2008; 134(1), 34–41.
- Tao H, Tao J. Quantitative analysis of piping erosion micro-mechanisms with coupled CFD and DEM method. *Acta Geotechnica*, 2017;12(3), 573–592.
- Thoman RW, Niezgoda SL. Determining erodibility, critical shear stress, and allowable discharge estimates for cohesive channels: Case study in the Powder River basin of Wyoming, *Journal of Hydraulic Engineering*, ASCE, 2008; 134(12), 1677-1687.
- Yang Y, Melville BM, Sheppard DM, Shamseldin AY. Clear-water local scour at skewed complex bridge piers, *Journal of Hydraulic Engineering*, ASCE, 2017; 144(6), 04018019.
- Yang JQ, Nepf HM. A turbulence-based bed-load transport model for bare and vegetated channels. *Geophysical Research Letters*, 2018; 45, 428-10, 436.
- Yang JQ, Kerger F, Nepf HM. Estimation of the bed shear stress in vegetated and bare channels with smooth beds, *Water Resources Research*, 2015; 51, 3647–3663,
- Wan CF, Fell R. Investigation of Internal Erosion and Piping of Soils in Embankment Dams by the Slot Erosion Test and the Hole Erosion Test. UNICIV Report R-412. University of New South Wales, Sydney, Australia, 2002.
- Wardhana K, Hadipriono FC. Analysis of recent bridge failures in the United States. *Journal of Performance of Constructed Facilities*, 2003; 17(3), 144-150.
- Wilson KV Jr. Scour at selected bridge sites in Mississippi. Resources Investigations Report 94–4241, Geological Survey Water, Reston, VA, 1995.
- Zhang C, Liu Z, Deng P. Contact angle of soil minerals: A molecular dynamics study. *Computers and Geotechnics*, 2016; 75(2016), 48-56.

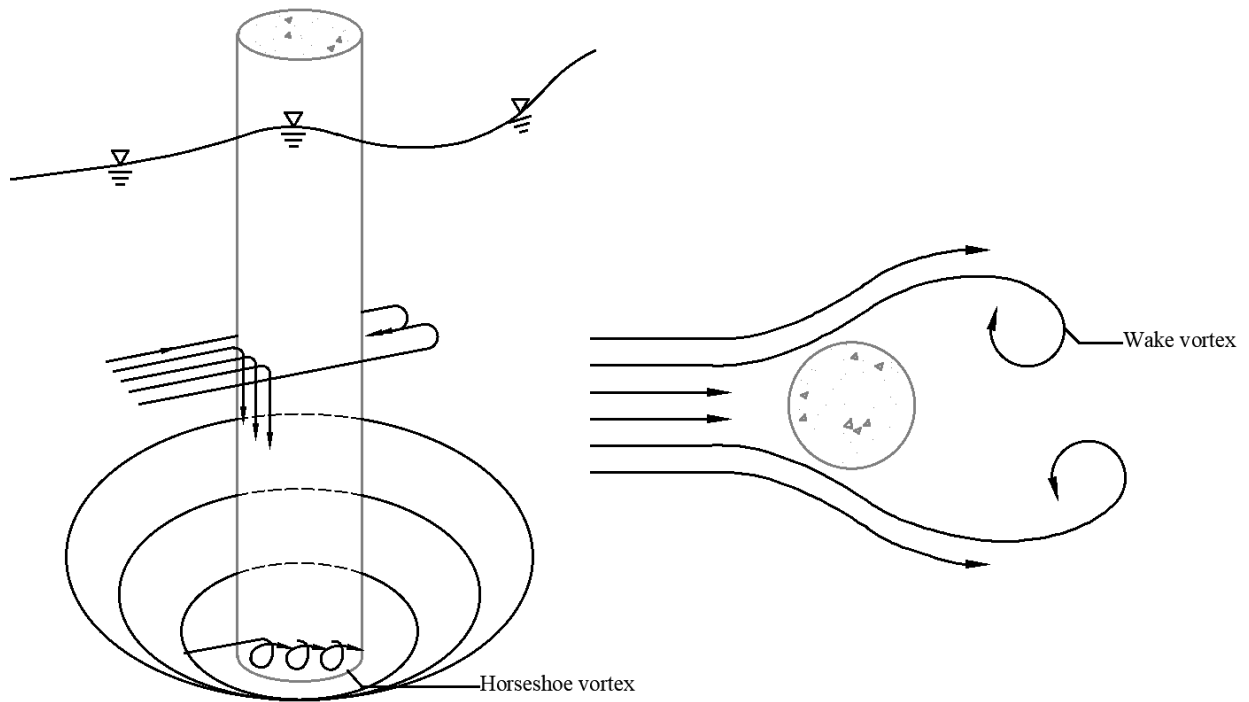


Figure 1. Illustration of the flow around a circular pier in a scour hole (from Arneson et al. 2012)

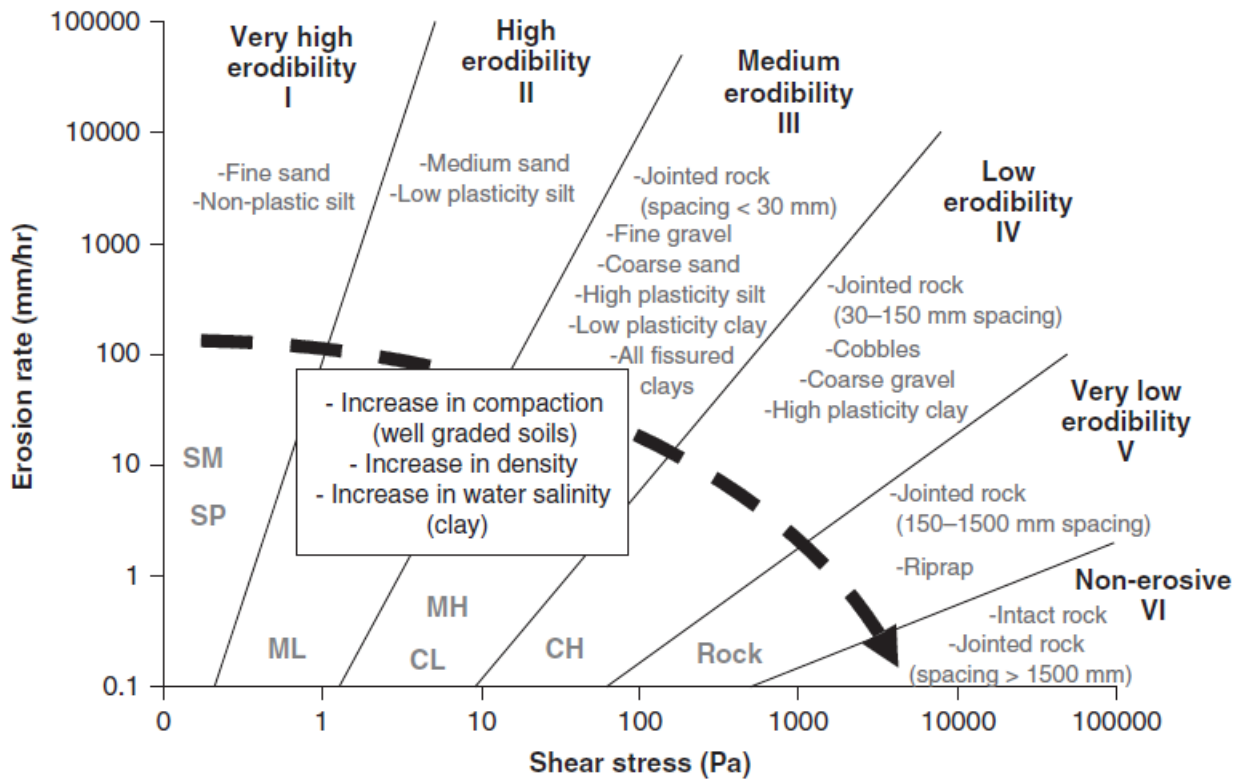


Figure 2. Erosion category chart with USCS symbols (from Briaud 2013)

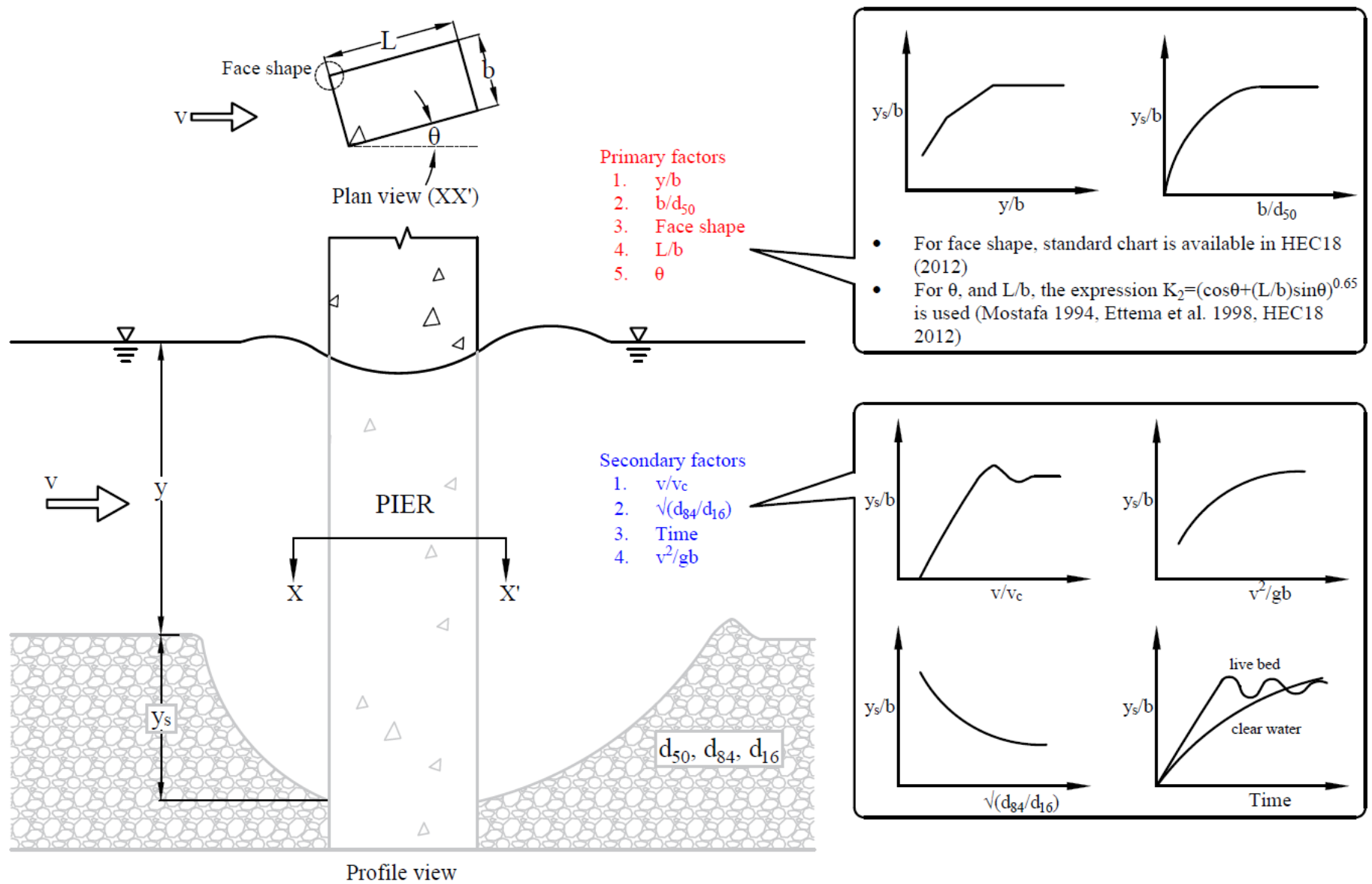


Figure 3. A conceptual sketch showing the primary and secondary factors influencing pier scour

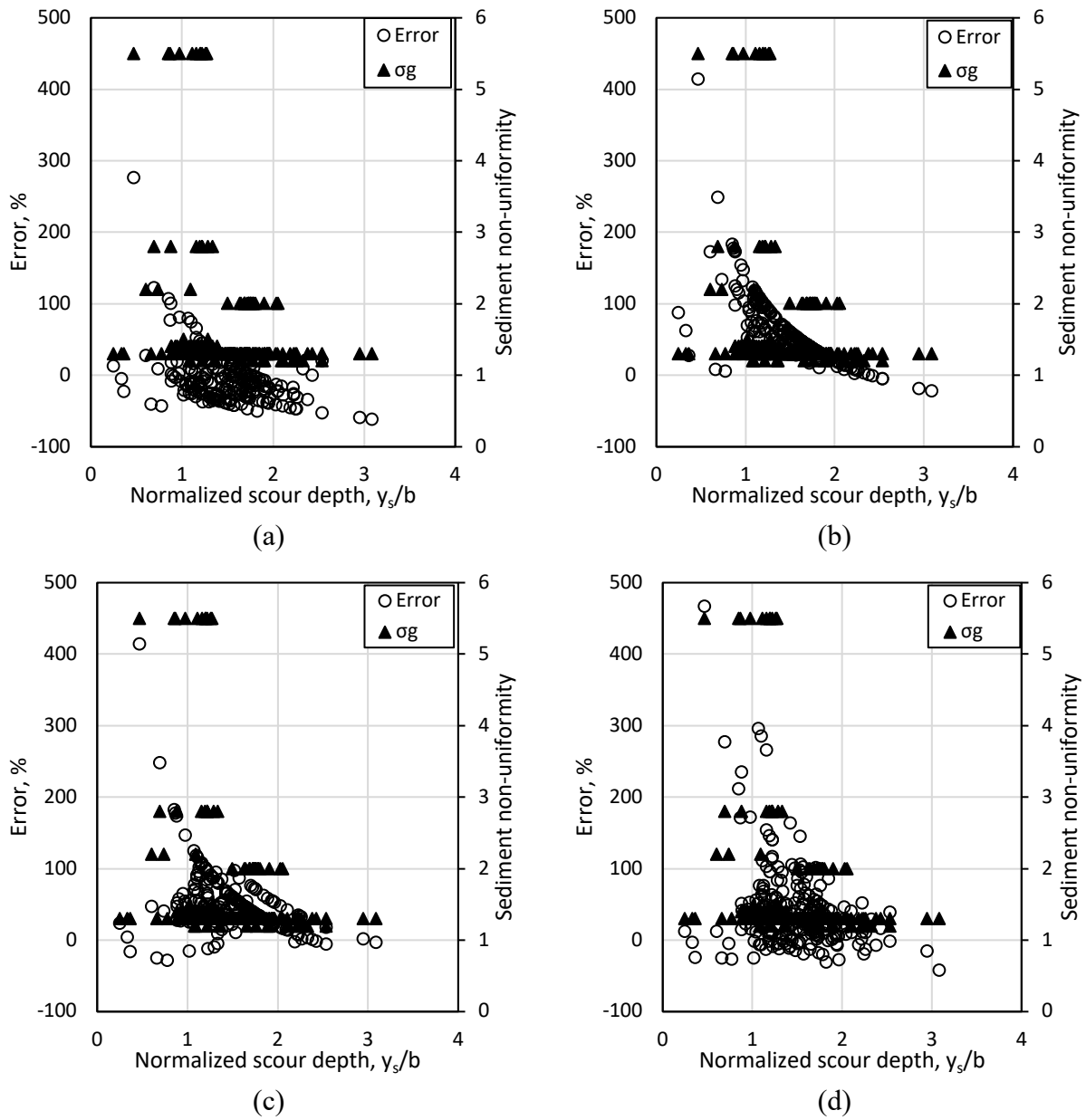


Figure 4. Error- normalized scour depth relation for (a) Wilson (1995) model, (b) Melville (1997) model, (c) HEC-18 (2012) model, and (d) Briaud (2014a) model using live-bed dataset

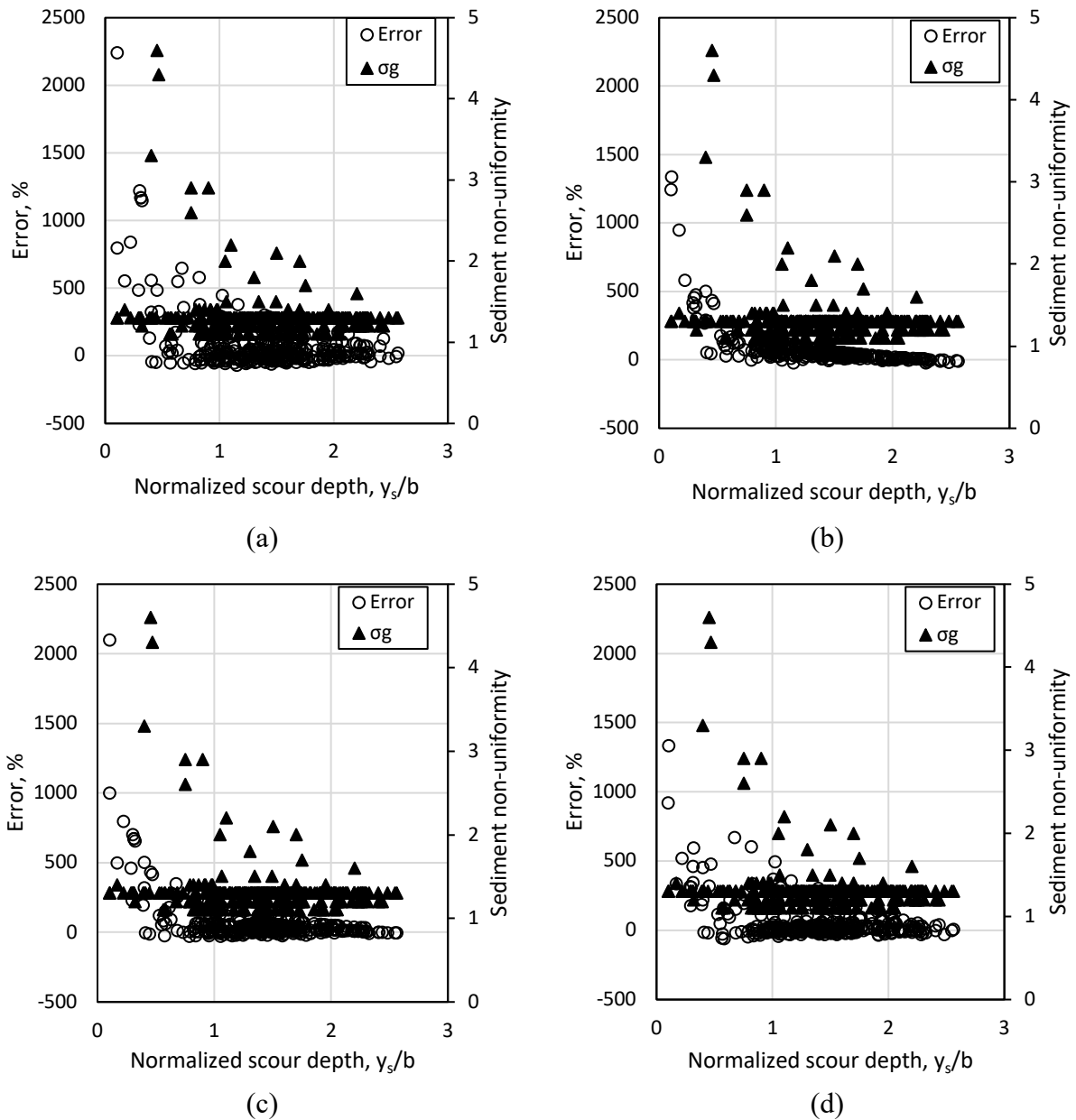


Figure 5. Error- normalized scour depth relation for (a) Wilson (1995) model, (b) Melville (1997) model, (c) HEC-18 (2012) model, and (d) Briaud (2014a) model using clear water dataset

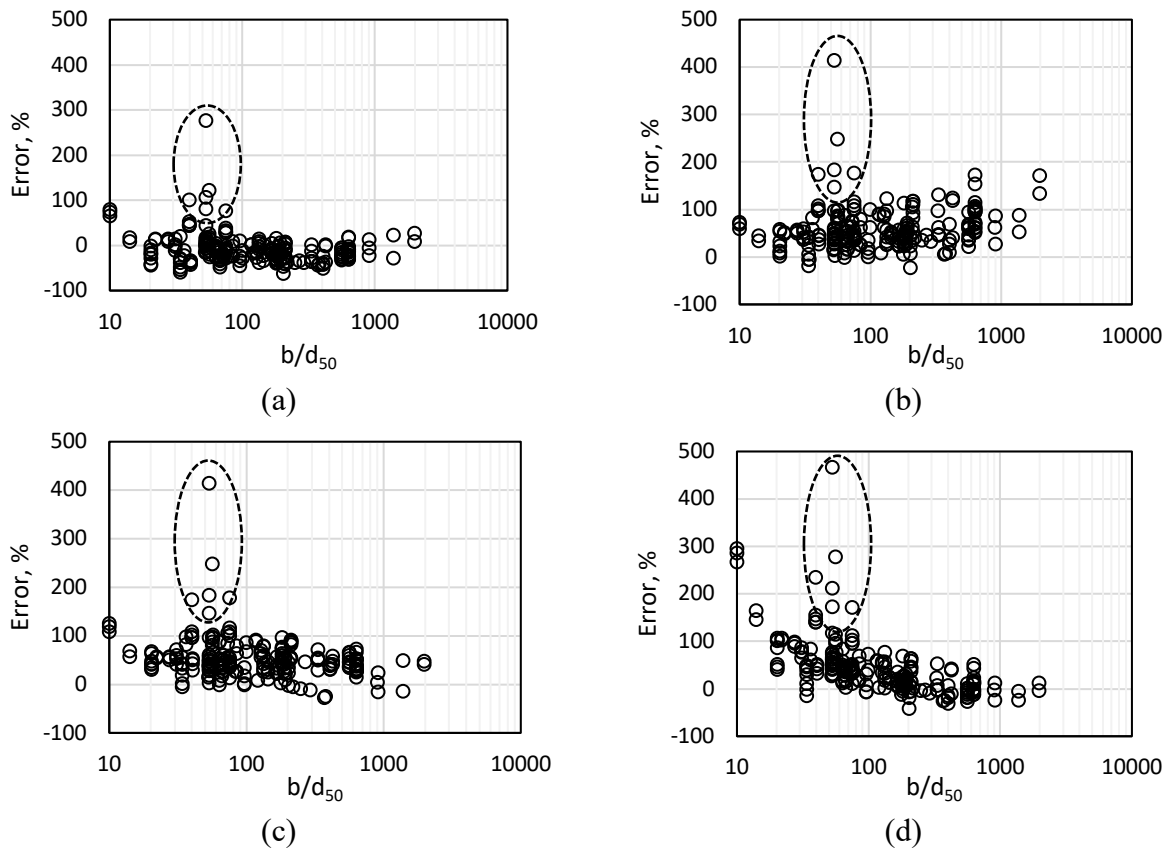


Figure 6. Error- b/d_{50} relation in the range for (a) Wilson (1995) model, (b) Melville (1997) model, (c) HEC-18 (2012) model, and (d) Briaud (2014a) model using live bed dataset. Six measurements that provided anomalous error are identified using a dashed oval boundary.

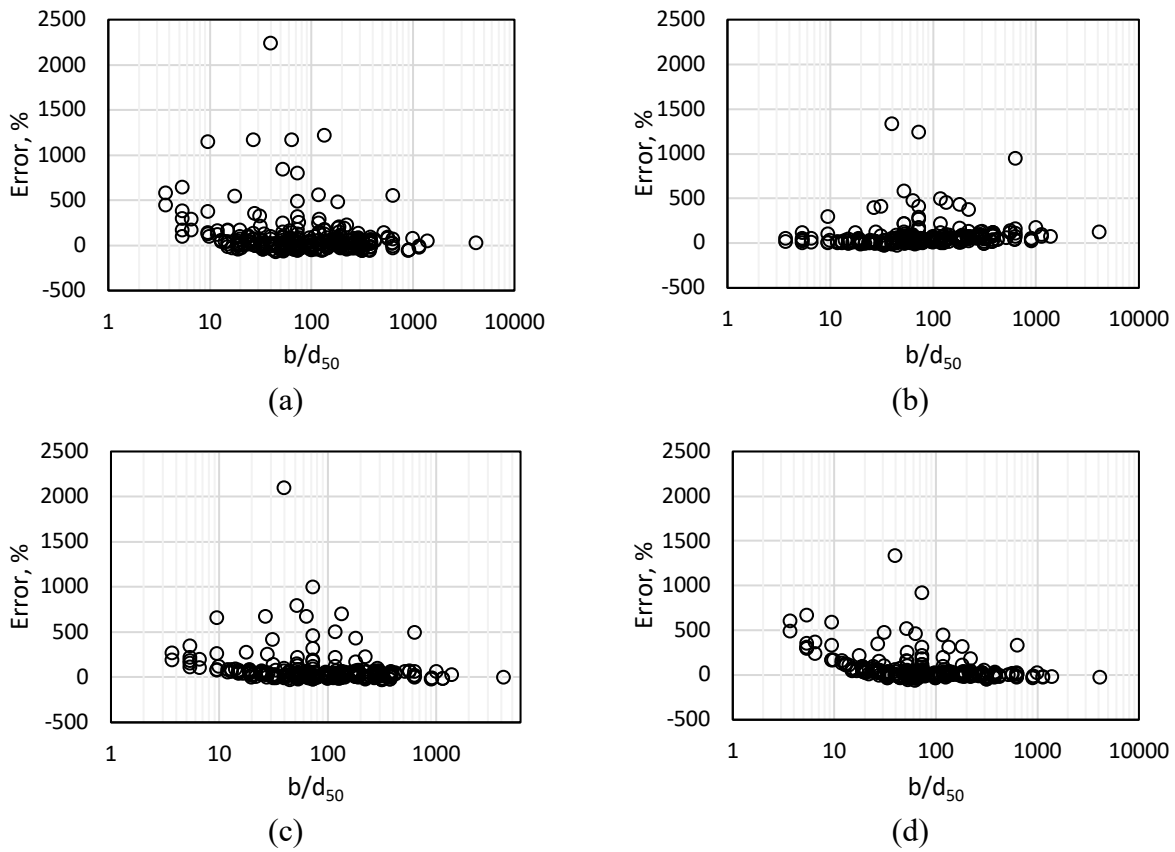
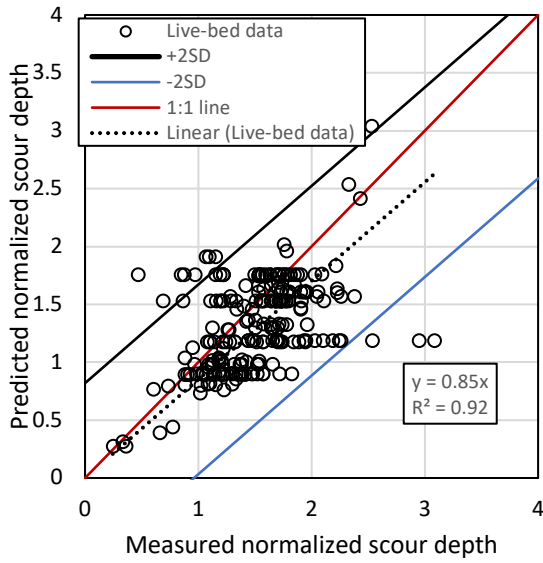
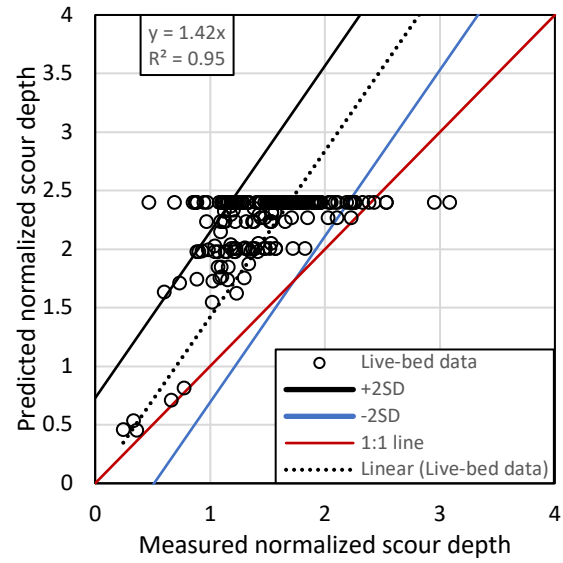


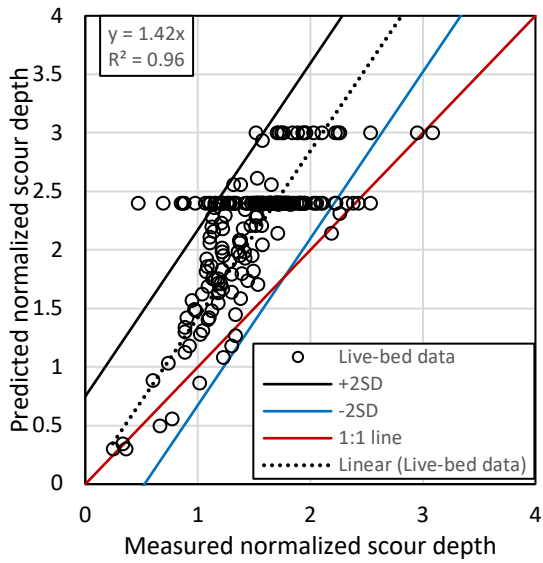
Figure 7. Error- b/d_{50} relation in the range for (a) Wilson (1995) model, (b) Melville (1997) model, (c) HEC-18 (2012) model, and (d) Briaud (2014a) model using clear water dataset.



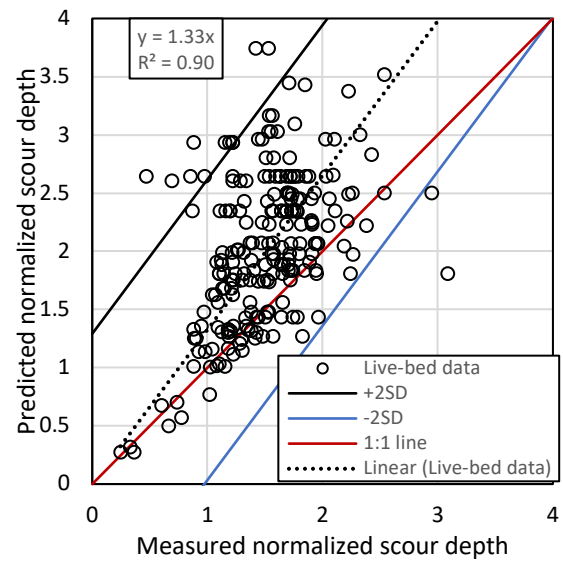
(a)



(b)



(c)



(d)

Figure 8. Predicted-measured normalized scour depth relation for: (a) Wilson (1995) model, (b) Melville (1997) model, (c) HEC-18 (2012) model, and (d) Briaud (2014a) model using live bed dataset.

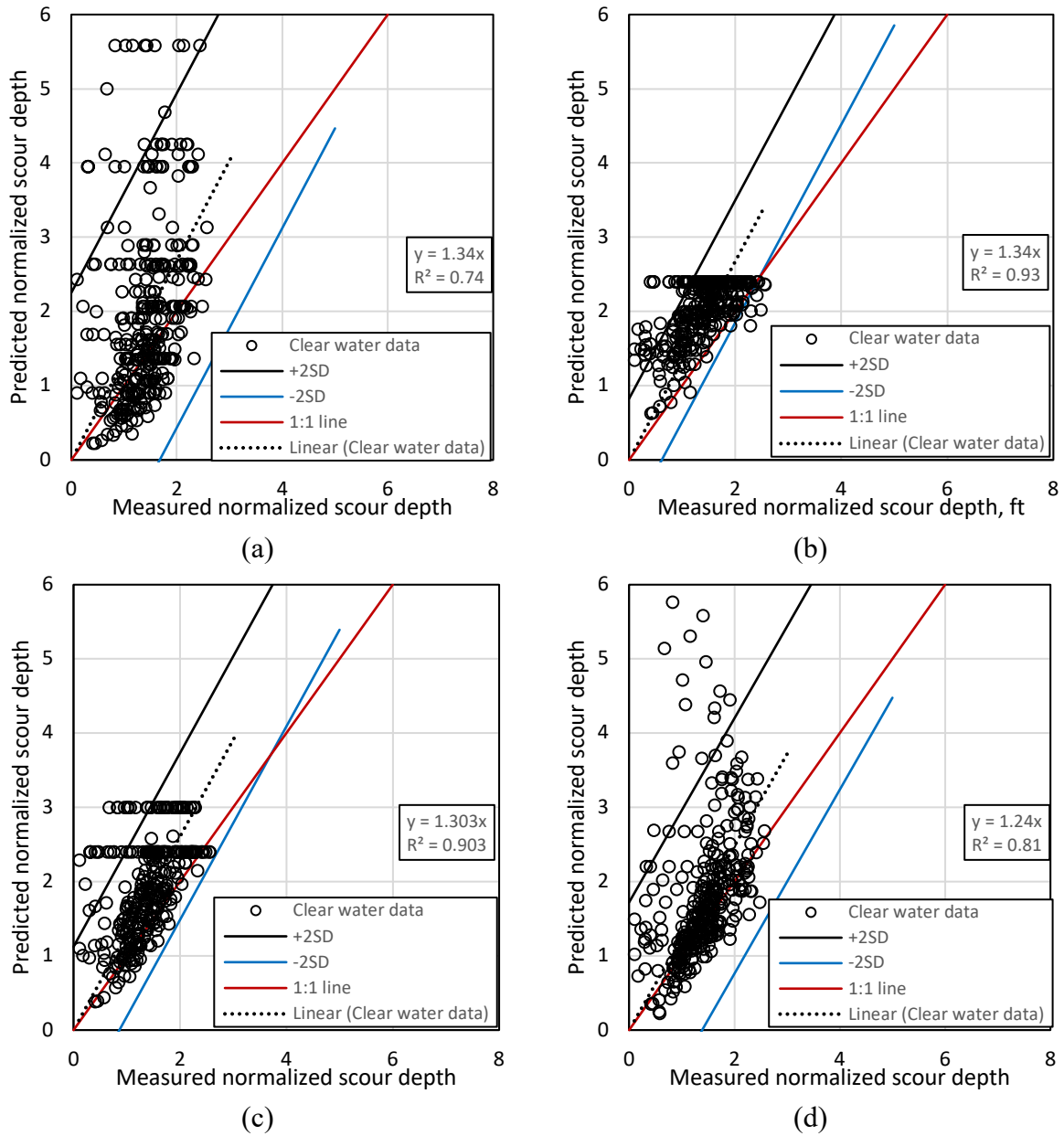
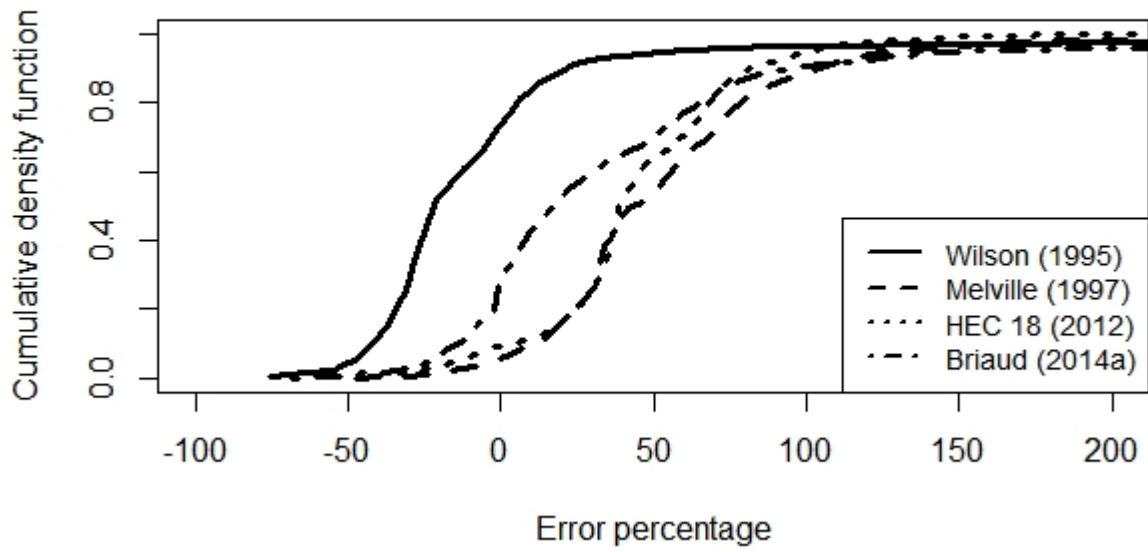
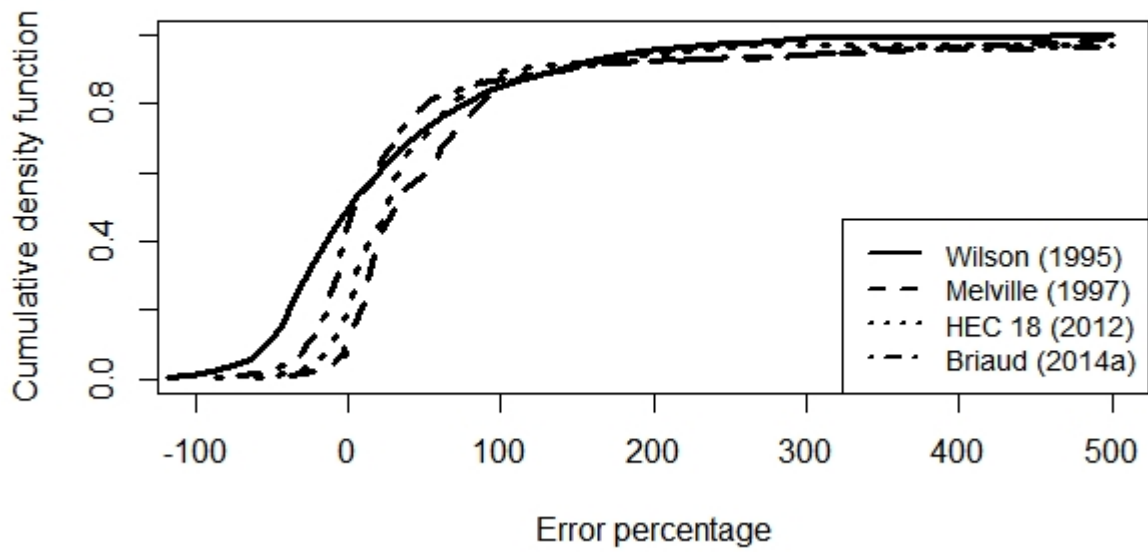


Figure 9. Predicted-measured normalized scour depth relation for: (a) Wilson (1995) model, (b) Melville (1997) model, (c) HEC-18 (2012) model, and (d) Briaud (2014a) model using clear water dataset.



(a)



(b)

Figure 10. For the four models considered in the study cumulative density function for (a) live-bed conditions, and (b) clear water conditions

Table 1. Models to estimate critical shear stress based on geotechnical properties

Reference	Model expression	Number of data	Test type	Soil type	R ²
Shields (1936)	$\tau_c(Pa) = 0.63d_{50}(mm)$	--	--	Coarse	--
Smerdon and Beasley (1959)	$\tau_c(psf) = 0.0034PI(\%)^{0.84}$	11	Flume	Fine	0.80
Smerdon and Beasley (1959)	$\tau_c(psf) = 0.213DR(\%)^{-0.63}$	11	Flume	Fine	0.80
Parchure and Mehta (1986)	$ln \frac{\epsilon}{\epsilon_f} = \alpha(\tau_b - \tau_s)^{1/2}$	47*	Flume	Fine	--
Hanson and Simon (2001)	$\epsilon(m/s) = 0.2\tau_c(Pa)^{-0.5}(\tau_e - \tau_c)(Pa)$	--	JET	Coarse and fine	0.64
Julian and Torres (2006)	$\tau_c(Pa) = 0.1 + 0.1779SC(\%) + 0.0028SC(\%)^2 - 2.34E - 5.0 SC(\%)^3$	16	--	Fine	0.91
Thoman and Niezgoda (2008)	$\tau_c(Pa) = 77.28 + 2.2A + 0.26DR - 13.49SG - 6.4pH + 0.12WC(\%)$	25	JET	Fine	0.72
Briaud (2008)	$\tau_c(Pa) = d_{50}(mm)$	--	EFA	Coarse	--
Shafii et al. (2016)	$\tau_c(Pa) = 0.165 \times d_{50}(mm)^{0.529} \times WC(\%)^{0.788} \times PF(\%)^{-0.23}$	180	EFA	Coarse	0.79
Shafii et al. (2016)	$\tau_c(Pa) = 0.005 \times PI^{0.44} \times S_u(kPa)^{0.83} \times WC(\%)^{1.03} \times d_{50}(mm)^{0.29}$	180	EFA	Fine	0.52
Briaud et al. (2017)	$\tau_c(Pa) = 2.507 \times 10^{-12} \times \gamma(kN/m^3)^{3.931} \times PF(\%)^{4.382}$	13	EFA	Coarse	0.5
Briaud et al. (2017)	$\tau_c(Pa) = 0.978 \times WC(\%)^{-2.306} \times PF(\%)^{1.991}$	13	EFA	Coarse	0.7
Briaud et al. (2017)	$\tau_c(Pa) = 3.347 \times 10^{-10} \times PI(\%)^{-1.855} \times d_{50}(mm)^{-1.05} \times WC(\%)^{6.707}$	17	EFA	Fine	0.72
Briaud et al. (2017)	$\tau_c(Pa) = 2.28 \times 10^{-15} \times PI(\%)^{-1.732} \times WC(\%)^{3.106} \times PF(\%)^{6.412}$	55	EFA	Fine	0.6

Briaud et al. (2017)	$\tau_c(Pa) = 1.354 \times 10^{-7} \times PL(\%)^{0.666} \times d_{50}(mm)^{-0.189} \times WC(\%)^{4.046}$	17	EFA	Fine	0.5
Briaud et al. (2019)	$\tau_c(Pa) = 158.06 \times \gamma^5 \times A^{-0.46} \times WC(\%)^{10.03} \times S_u(kPa)^{1.83} \times PF(\%)^{-18.28} \times d_{50}(mm)^{-4.21}$	44	EFA	Fine	0.94
Briaud et al. (2019)	$\tau_c(Pa) = 1.58 \times C_u^{-0.04} \times \gamma(kN/m^3)^{0.02} \times d_{50}(mm)^{0.77}$	28	EFA	Coarse	0.93
Briaud et al. (2019)	$\tau_c(Pa) = -0.248 \times PC(\%) - 1.23 \times \gamma + 0.21 \times WC(\%) + 0.07 \times S_u(kPa) - 36.89 \times d_{50}(mm) + 31.82$	28	JET	Coarse and fine	0.50
Briaud et al. (2019)	$\tau_c(Pa) = 25.07 \times PI^{0.27} \times S_u(kPa)^{0.55} \times d_{50}(mm)^{0.50}$	21	HET	Coarse and fine	0.64

Note: τ_c = critical shear stress, d_{50} = median grain size, PI = plasticity index, DR = dispersion ratio, ϵ = erosion rate, ϵ_f = floc erosion rate (erosion rate when $\tau_b - \tau_s = 0$), $\alpha = 18.4 m/N^{1/2}$, τ_b = time-mean bed shear stress, τ_s = bed shear strength, ϵ = erosion rate, τ_e = effective bed shear stress, SC = silt content, E = lateral erosion rate, A = activity, SG = specific gravity, WC = water content, S_u = undrained shear strength, PF = percent finer than sieve #200, γ = wet unit weight, PL = plastic limit, C_u = coefficient of uniformity, PC = percent clay

*Counted from the figure presented in Parchure and Mehta (1986)

Table 2. Classification of pier based on y/b (summarized from Melville and Coleman 2000; Ettema et al. 2011)

Pier class	Range of y/b	Remarks*
Narrow pier	$\frac{y}{b} > 1.4$	The vertical component of flow at the pier's leading face causes the deepest scour to occur at the pier face. Flow contraction occurs as the stream passes the pier's sides, leading to scour in the trailing face of pier as well. The deterministic pier scour models can reasonably predict the scour for narrow piers.

Intermediate pier	$0.2 \leq \frac{y}{b} \leq 1.4$	The main flow field feature is similar to narrow pier, however, as the flow depth decreases in relation to pier width, the main flow features become disrupted leading to a reduced capacity of flow to erode bed material. The deterministic pier scour models can reasonably predict the scour for intermediate piers.
Wide pier	$\frac{y}{b} < 0.2$	The down flow development is disrupted owing to the lateral movement of the flow along the pier's leading face and causes the deepest scour to occur at the pier flanks. Laboratory data on wide piers are fairly scarce, a modicum of research is necessary to assess the reliability in pier scour estimates.
*Ettema et al. (2017) presented a comprehensive summary of the complex flow field evolution for the three categories of pier.		

Table 3. Erosion tests available in the literature with the applicable soil types

Reference	Erosion test	Applicable soil type
Moore and Masch (1962)	Rotating Cylinder Test (RCT)	Cohesive
Sherard et al. (1976)	Pinhole Erosion Test (PET)	Cohesive
Lefebvre et al. (1985)	Drill Hole Test (DHT)	Cohesive
Hanson (1990), Hanson and Cook (2004)	Jet Erosion Test (JET)	Cohesive, cohesionless
Briaud et al. (2001)	Erosion Function Apparatus (EFA)	Cohesive, cohesionless
Wan and Fell (2002)	Hole Erosion Test (HET)	Cohesive
Wan and Fell (2002)	Slot Erosion Test (SET)	Cohesive
Bloomquist et al. (2012)	Rotating Erosion Testing Apparatus (RETA)	Stiff clays, hard rock
Gabr et al. (2013)	In Situ Erosion Evaluation Probe (ISEEP)	Cohesionless
Briaud et al. (2017)	Borehole Erosion Test (BET)	Cohesive, cohesionless

Table 4. List of deterministic pier scour models developed since 1990

Reference	Model	Remarks
Gao et al. (1993)	$y_s = 0.46K_\xi b^{0.6} y^{0.15} d_{50}^{-0.07} \left(\frac{v - v_c'}{v_c - v_c'} \right)^n$	y_s = scour depth K_ξ = pier shape factor b = pier width y = flow depth upstream of pier d_{50} = median grain size v = approach flow velocity v_c = sediment critical velocity v_c' = initial velocity of local scour
Wilson (1995)	$\frac{y_s}{b'} = 0.9 \left(\frac{y}{b'} \right)^{0.4}$	b' = projected pier width
Melville (1997)	$y_s = K_{yb} K_I K_d K_s K_\theta K_G$	K_{yb} = pier depth-size factor K_I = flow intensity factor K_d = sediment size factor K_s = pier nose shape factor K_θ = pier alignment factor K_G = channel geometry factor (= 1 for pier)
Sheppard and Miller (2006)	$\frac{y_s}{b'} = 2.5 f_1 \left(\frac{y}{b'} \right) f_2 \left(\frac{b'}{d_{50}} \right) \left[1 - 1.75 \left\{ \ln \left(\frac{v}{v_c} \right) \right\}^2 \right]$ <p>For $0.47 \leq \frac{v}{v_c} \leq 1$</p> $\frac{y_s}{b'} = f_1 \left(\frac{y}{b'} \right) \left[2.2 \left(\frac{\frac{v}{v_c} - 1}{\frac{v_{lp}}{v_c} - 1} \right) + 2.5 f_2 \left(\frac{b'}{d_{50}} \right) \left(\frac{\frac{v_{lp}}{v_c} - \frac{v}{v_c}}{\frac{v_{lp}}{v_c} - 1} \right) \right]$ <p>For $1 \leq \frac{v}{v_c} \leq \frac{v_{lp}}{v_c}$</p> $\frac{y_s}{b'} = 2.2 f_1 \left(\frac{y}{b'} \right)$	v_{lp} = live bed peak scour velocity

For $\frac{v}{v_c} \geq \frac{v_{lp}}{v_c}$

$$f_1\left(\frac{y}{b'}\right) = \tanh\left\{\left(\frac{y}{d_{50}}\right)^{0.4}\right\}$$

$$f_2\left(\frac{b'}{d_{50}}\right) = \frac{\frac{b'}{d_{50}}}{0.4\left(\frac{b'}{d_{50}}\right)^{1.2} + 10.6\left(\frac{b'}{d_{50}}\right)^{-0.13}}$$

Kothyari et al. (2007)
Oliveto and Hager
(2002, 2005)

$$\frac{y_s}{(yD)^{1/3}} = 0.068N\left(\frac{d_{84}}{d_{16}}\right)^{-0.25}F^{1.5}\log\left(\frac{t}{t_R}\right)$$

$$t_R = \frac{(yD)^{1/3}}{\left(\frac{d_{84}}{d_{16}}\right)^{1/3}(gd_{50})^{0.5}}$$

D = pier diameter
 N = shape factor
 F = Froude number
 g = gravitational acceleration
 d_{84} = diameter corresponding to 84% finer
 d_{16} = diameter corresponding to 16% finer

Arneson et al. (2012)

$$\frac{y_s}{b} = 2K_1K_2K_3\left(\frac{y}{b}\right)^{0.35}F^{0.43}$$

K_1 = pier nose shape factor
 K_2 = pier alignment factor
 K_3 = bed condition factor

Briaud (2014a)

$$\frac{y_s}{b'} = 2.2K_{pw}K_{psh}K_{pa}K_{psp}(2.6F_{pier} - F_{c(pier)})^{0.7}$$

K_{pw} = water depth influence factor
 K_{psh} = pier shape influence factor
 K_{pa} = aspect ratio influence factor
 K_{psp} = pier spacing influence factor
 F_{pier} = pier Froude number
 $F_{c(pier)}$ = critical pier Froude number

Table 5. Consideration of pier scour influencing parameters in different models developed since 1990

Reference	y/b	b/d_{50}	Pier face shape	Aspect ratio	Skew angle	v/v_c	Sediment non-uniformity	Euler/Reynolds number	Temporal rate
Gao et al. (1993)	C	C	C	C	C	C	NC	NC	NC
Wilson (1995)	C	NC	NC	NC	NC	NC	NC	NC	NC
Melville (1997)	C	C	C	C	C	C	C	NC	NC
Sheppard and Miller (2006)	C	C	C	C	C	C	NC	NC	NC
Kothyari et al. (2007)	C	NC	NC	NC	NC	C	C	NC	C
Arneson et al. (2012)	C	NC	C	C	C	NC	NC	NC	NC
Briaud (2014a)	C	NC	C	C	C	C	NC	C	C

Note: C means considered in the respective model; NC means not considered in the respective model

Table 6. Range of some selected variables associated with live-bed laboratory data in Benedict and Caldwell (2014)

Parameter	Pier width normal to flow, b' (ft)	Approach flow velocity, v (ft/s)	Approach flow depth, y (ft)	Median grain size, d_{50} (mm)	Measured pier-scour depth, y_s (ft)
Minimum	0.094	0.76	0.164	0.24	0.049
Median	0.164	2.03	0.558	0.6	0.253
Maximum	0.5	5.28	1.969	3.2	0.492

Table 7. Range of some selected variables associated with clear-water laboratory data in Benedict and Caldwell (2014)

Parameter	Pier width normal to flow, b' (ft)	Approach flow velocity, v (ft/s)	Approach flow depth, y (ft)	Median grain size, d_{50} (mm)	Measured pier-scour depth, y_s (ft)
Minimum	0.052	0.49	0.066	0.22	0.013
Median	0.246	0.98	0.656	0.96	0.327
Maximum	3.002	3.96	6.234	7.80	4.626

Table 8. Data associated with high error for live bed condition in the range of $40 \leq b/d_{50} \leq 80$

Data source	Pier width normal to flow, b' (ft)	Median grain size, d_{50} (mm)	Sediment non-uniformity, σ_g	Sediment size scaling factor, b/d_{50}	Flow depth to pier width ratio, y/b	Froude number, F_r	Pier-scour depth, y_s (ft)
Chiew (1984)	0.105	0.6	5.5	53.35	5.31	0.29	0.049
Chiew (1984)	0.105	0.8	2.8	40.02	5.31	0.32	0.092
Chiew (1984)	0.105	0.6	5.5	53.35	5.31	0.39	0.089
Chiew (1984)	0.105	0.6	5.5	53.35	5.31	0.61	0.102
Chiew (1984)	0.148	0.8	2.8	56.40	3.77	0.29	0.102
Chiew (1984)	0.148	0.6	5.5	75.20	3.77	0.37	0.128

Table 9. Probabilistic error analyses using live bed and clear water dataset

Error range	Probability							
	Wilson (1995)		Melville (1997)		HEC 18 (2012)		Briaud (2014a)	
	Live bed	Clear water	Live bed	Clear water	Live bed	Clear water	Live bed	Clear water
<-50%	0.04	0.08	0.00	0.00	0.00	0.01	0.01	0.02
-50%-0%	0.68	0.35	0.04	0.11	0.09	0.18	0.22	0.40
0%-50%	0.23	0.29	0.45	0.46	0.54	0.52	0.45	0.36
50%-100%	0.02	0.11	0.38	0.30	0.30	0.17	0.23	0.08
100%-150%	0.01	0.08	0.09	0.08	0.05	0.04	0.04	0.04
>150%	0.02	0.09	0.04	0.05	0.02	0.08	0.05	0.09

Table 10. Live bed error statistics corresponding to the four models considered in the study

Models	Wilson (1995)	Melville (1997)	HEC 18 (2012)	Briaud (2014a)
Average error (%)	-7.63	59.37	52.10	43.51
Minimum error (%)	-61.44	-22.18	-27.77	-41.39
Maximum error (%)	276.20	414.29	414.29	466.86
Standard deviation	0.41	0.36	0.37	0.65
Variance	0.17	0.13	0.14	0.42

Table 11. Clear water error statistics corresponding to the four models considered in the study

Models	Wilson (1995)	Melville (1997)	HEC 18 (2012)	Briaud (2014a)
Average error (%)	71.75	74.38	67.07	51.15
Minimum error (%)	-69.49	-20.83	-31.32	-61.95
Maximum error (%)	2239.94	1339.04	2099.83	1334.02
Standard deviation	1.13	0.41	0.56	0.86
Variance	1.27	0.17	0.32	0.74

Appendix B: Bridge Pier Scour: Analyses using clear water data

Introduction

Bridge scour is a complex process of interaction among flow, sediments, and structure leading to the mobilization and transport of sediments surrounding the structure. The erosion process initiates if the applied hydraulic shear stress exceeds the sediment mobilization critical stress. The scouring process causes damage to the foundation of the bridge, which may lead to operational disruption and economic losses (Shirole and Holt, 1991; Briaud et al. 1999; Azamatullah et al. 2013). Wardhana and Hadipriono (2003) analyzed 503 failures of bridge structures that occurred in the United States, and concluded that 85% of the bridge failure is related to externally-triggered events, such as flood, collision, overload etc. It was also found that the principal cause (243 cases) of bridge failure is flood-induced scour, while the rest can be related to collision, overload, deterioration, and miscellaneous (like fire, ice etc.). The average annual cost for flood damage and scour repair of highways in the United States is estimated to be \$50 million (Lagasse et al. 1995; 2012). Rhodes and Trent (1993) reported that the additional cost to the afflicted population can be as much as five times the repair cost. Hunt (2009) noted that there are 20,904 scour-critical bridges in the United States and approximately 80,000 bridges that are scour susceptible. With the impact of the climate change and the likely increase in heavy precipitation, severe flooding coupled with scour is poised to be the leading cause of bridge damage (Liang et al. 2015). This demonstrates the importance of properly estimating the scour magnitude beforehand and thoroughly incorporating in design and countermeasure actions.

Pier scour is influenced by multiple factors including flow depth to pier width ratio, pier width to median grain size ratio, pier face shape, pier aspect ratio, skew angle of pier, flow intensity, Euler number or Reynolds number, sediment non-uniformity, and the temporal rate of evolution (Melville and Coleman 2000; Sheppard et al. 2011; Ettema et al. 2017). Table 1 shows the summary of the factors that are included in some of the traditional deterministic pier scour prediction models. Evidently, not all the factors are equally important; thereby, based on the findings, investigators emphasized some of the factors over others. The differences in the choice of which scour influencing factors included in a given deterministic models leads to different scour magnitudes under similar set of hydraulic, structural, and geotechnical parameters. Current practice of pier scour analysis is based on the use of deterministic models. Deterministic scour prediction models do not account for inherent model uncertainties and errors. The use of deterministic models does not yield the inherent model bias (conservativeness/unconservativeness). Without the prior knowledge of the degree of biasness of these deterministic models (each model predicts different scour depths for a similar set of parameters), one cannot discern whether or not these predictions are conservative and the extent of conservatism in view a given model's application to a wider set of site conditions. This raises the importance of further developing the probabilistic models for scour assessment to include the aleatory and epistemic

uncertainties (statistical error, measurement error, human error, model error), albeit a sufficient level of data is needed for such development.

Multiple researchers investigated the probabilistic aspects of bridge pier scour. Briaud et al. (2007) developed a probabilistic bridge scour model that considered the uncertainty of hydrologic conditions; uncertainties associated with input parameters (geometry of obstacle, soil erodibility) were however not considered. Briaud et al. (2014) developed a reliability-based pier scour model focusing on the risk associated with stability of shallow and deep foundations subjected to scour. Johnson et al. (2015) examined the hydraulic and hydrologic uncertainties associated with HEC-18 and FDOT (2011) scour prediction models. Johnson et al. suggested “scour design factors” based on target reliability index. In scour prediction models, uncertainties arise from multiple sources including hydraulic, geotechnical, structural, or predictive model errors (Yao 2013). While the hydraulic, geotechnical, and structural uncertainties can be improved through better-quality field characterization and measurement accuracy, or by accumulating more data, it is often the case that scour prediction is performed with insufficient data set. Moreover, inherit model errors vary across the different models and should be addressed for informed prediction of the complex phenomena of bridge scouring.

The study herein is focused on assessment of five bridge scour prediction models, viz. Wilson (1995) model, Melville (1997) model, HEC-18 (2012) model, Briaud (2014) model, and SC Envelope (2018) model. The assessment includes investigation of Accuracy and conservatism of a given model within the context of comparing the models’ results with measured clear-water field scour-depth data. The database reported in Benedict and Caldwell (2014) is used with the exception of some data points for which insufficient information was reported to be able to apply the predictive models. In order to evaluate and quantify the scatter and uncertainty associated with scour prediction using deterministic models, the performance of several statistical models is assessed and the appropriate models are proposed. Finally, a relationship between probability of exceedance of a given measured scour depth and a modification factor (that is applied onto the deterministic prediction) is devised..

Data for analyses

Benedict and Caldwell (2014) collected scour data from 23 states within the United States, Canada, China, New Zealand, Nigeria, Russia, and Yugoslavia. The database entails a total of 1858 field scour measurements. Data reported in Benedict and Caldwell (2014) can be classified into two categories: clear water and live bed scour. As presented in Table 1, various deterministic models consider different factors that influence pier scour. As such, any missing information related to one or more of the given variables in Table 1 will impair the scour depth calculation using a specific model. Therefore, an initial screening was performed on the collected database, and those sites which lacked any of the parameters necessary to compute scour depth using either of the five models, were not considered further. The initial screening yielded 1320 usable datasets. Among these data points, 469 sites have clear water condition, whereas 850 sites have live bed

condition. The study herein focuses on clear water field data. The range of the selected variables for the clear water field data, including pier width, upstream flow depth, approach flow velocity, median grain size, and measured scour depth are presented in Table 2. The values in Table 2 reflect the minimum, median, and maximum values for a given variable within the database. It is important to note that the data across a single row do not correspond to each other; i.e., the minimum, median, and maximum values across one row are not for a specific site. These values rather indicate the minimum, median, and maximum values of the specified variable within the whole database.

Deterministic models for analyses

Five pier scour prediction models, namely Wilson (1995) model, Melville (1997) model, HEC-18 (2012) model, Briaud (2014) model, and the SC envelope curve approach (2018) are utilized herein. The model equations are provided in Table 2. Wilson (1995) model is based on field data collected from 22 bridges in Mississippi. Melville (1997) model is based on extensive laboratory and field data collected over a period of 25 years. The latest update of HEC-18 model by Arneson et al. (2012) is the most widely used pier-scour prediction model and it was developed based on data from laboratory testing on sediments with median grain size, d_{50} ranging from 0.24-0.52 mm. Briaud (2014) model is based on data from large scale laboratory flume testing (d_{50} ranged from 0.10-0.60 mm). The SC envelope curve (2018) is developed based on pier scour field data collected from piedmont and coastal plains regions of South Carolina. The database for clear water SC envelope curve has a maximum d_{50} of 0.99 mm.

Data screening

While laboratory investigations on pier scour evolution processes are performed under well controlled environment, relatively accurate representation of downscaled parameters including pier width, flow depth, flow velocity, and scour depth, field observations do come with some limitations. The uncertainties associated with field data might include (i) the accuracy of measured scour (depending on the tool used like Ground Penetrating Radar, soundings with fathometers, survey levels etc.), (ii) maturity of scour depth (the measured scour might not reflect the equilibrium scour depth), and, (iii) accuracy of hydraulic properties (depending on the method used to approximate, like based on historical information, based on one-dimensional flow models). However, the collected database parameters might not always contain all the descriptions regarding the associated uncertainties. Sheppard et al. (2014) concluded that identification of outliers in the field data sets might not always be possible owing to whether the measured scour depth represents equilibrium scour depth values for the specified flow, sediment, and structure conditions. Therefore, statistical measures, and when applicable, site-specific observations are necessary to identify outliers.

Error in models' estimation is a parameter that can be considered as a performance measure of the deterministic models. Error is defined as the difference between the predicted and measured scour depth, expressed as a percentage of the measured scour depth, as shown in Equation (6):

$$Error, \% = \frac{y_{sp} - y_{sm}}{y_{sm}} \times 100\% \quad (6)$$

Where, y_{sp} and y_{sm} are the predicted and measured scour depths respectively. A positive error magnitude indicates that the deterministic model is over-predicting the “measured” value and conversely, a negative error is indicative of under-prediction. Figure 1 shows the distribution of Error for the five deterministic models considered herein. It is apparent that the error varied within a wide range (-100% to 8023%) for all the five models. Another observation is that the pattern of over-prediction is very similar in some regions, as highlighted on Figure 1. Although for developing the five deterministic models, researchers considered different parameters (refer to Table 1), the over-prediction trend is similar. This might be an indication that the measured scour depth values in the database were not the equilibrium scour depths. The high peaks of the error magnitude increase the average error for the deterministic model, which might not be a representative performance of a given model. Subsequently, a statistical outlier identification technique was adopted. Figure 2 presents the error box-plot for the five models considered herein. As evident from the figure, all the models have positive outliers. Wilson (1995), Melville (1997), HEC 18 (2012), Briaud (2014), and SC Envelope (2018) models have 44, 45, 41, 34, and 42 outliers respectively. These outliers were considered unreasonable data, and were eliminated from the database.

The next criterion applied to identify the unreasonable data was the magnitude of the measured scour depth being equal to the accuracy tolerance of the measurement instrument. Through these screening processes, the number of data count was reduced to 405, which will be considered for further analyses. Figure 3 shows the error distribution from the five deterministic models considering the screened clear water field data. Evidently, the error distribution does not suggest presence of outliers. Important to note that the analyses to be performed are dependent on the “field measurements” being at equilibrium level. The data screening process, while does not assure that all field scour data represent equilibrium, is used to eliminate values most likely not to represent equilibrium condition.

Accuracy and conservatism analyses

A perfectly accurate scour prediction model would be the one that yields a predicted scour depth that is exactly equal to the measured scour depth in the field. As the scour processes depend on multiple factors, it is unreasonable to expect that a deterministic model would exactly predict the measured scour depth for varying hydraulic, structural, and geotechnical conditions.

A perfectly reliable scour prediction model would be the one that never yield a predicted scour depth that is less than the measured scour depth in the field. Tan and Duncan (1991) adopted similar logic while assessing the performance of the deterministic models to estimate the settlement of footings on sand.

In this study, accuracy will be measured in terms of Mean Absolute Percentage Error (MAPE). For each of the 405 data sets, the absolute percentage error will be calculated, and the

mean value of the error will be reported as the MAPE associated with a specific deterministic model. The “level of conservatism” will be defined as the ratio of the number of cases the calculated scour depth is more than the measured scour depth, expressed as percentage of the total number of data sets (405-screened data).

The results of the MAPE, and conservatism of the five deterministic models are presented in Figure 4. Values of MAPE ranged from 238% to 336%, whereas, conservatism ranged from 77% to 97.8%. Briaud (2014) model provided the least error; however, the model was also least conservative. Briaud (2014) model under-predicted the measured scour depth in 23% occasions. SC Envelope (2018) model provided the most conservative scour depth, under-predicting the measured scour depth in only 2.2% occasions. The associated MAPE for SC Envelope (2018) model is 336%. Melville (1997) model provided an error of 330%, however presented a conservatism of 94.3%, which is more than the conservatism of HEC 18 (2012), and Briaud (2014) models.

The accuracy and conservatism of a given model can be adjusted by multiplying the calculated scour depth obtained from the deterministic model by a correction factor. Figure 5 demonstrates the relationship between MAPE and conservatism when a correction factor is applied for the five models considered herein. When the correction factor is applied to the predicted scour depth, y_{sp} from any deterministic model, refer to Equation (6), the difference between y_{sp} and y_{sm} increases, while the denominator y_{sm} remains the same, leading to an increase in the MAPE magnitude. However, owing to the application of the correction factor, a deterministic scour prediction, which was unconservative initially (without application of a correction factor), may become conservative, leading to an increase in the conservatism magnitude. For example, HEC 18 (2012) model has a MAPE and conservatism of 265% and 91.9% respectively (refer to Figure 4). If the values of calculated scour depth for all the 405 cases is multiplied by a factor of 1.5, the MAPE increases to 442%, while the conservatism increases to 97.5%. Multipliers ranging from 1 to 2 were applied and corresponding MAPE and conservatism are calculated and presented. It is apparent that there is a tradeoff between MAPE and conservatism. Improvement of conservatism through application of the correction factors involves an increase in the overall MAPE of a model. For Wilson (1995), Melville (1997), and HEC 18 (2012) models, application of a multiplying factor of 1.5, 1.6, and 1.8 respectively to the calculated scour depth leads to a conservatism of 99%. For SC Envelope (2018) model, application of a multiplying factor of 1.6 leads to a conservatism of 100%. However, application of a multiplying factor of 2 to Briaud (2014) model results in a conservatism of 86.4%, which is comparatively less than the rest three models. This is owing to the fact that in Briaud (2014) model, if the upstream mean flow velocity is less than 0.385 times the sediment critical velocity, no scour will occur surrounding the obstruction. There are 33 field data sets where the upstream flow velocity was less than 0.385 times the sediment critical velocity, leading to a zero scour using Briaud’s model. However, in the field some scouring was observed in those 33 sites. As such, application of a multiplication factor to the calculated scour depth did not increase the conservatism substantially.

Statistical model

Figure 6 shows the relationship between the predicted and the measured scour depths using the five models considered in the study. It is apparent that in general, the deterministic models have the tendency to over-predict the measured scour depth. Briaud (2014) model presented the maximum number of under-predicted scour depth cases. The scatter of the data is not uniform, which leads to non-constant variance, statistically known as heteroscedasticity (Stone 1996). Figure 7 presents the residuals versus fitted value plot while applying Wilson (1995) model. Residual, in this case is defined as the difference between measured and predicted values obtained from the best-fit curve, which is a linear expression between the measured and the predicted values. The disproportionate scatter in positive and negative sides of residuals suggest that the datasets have heteroscedasticity. The standardized residuals versus theoretical quantile plot suggest that the dataset is right-skewed; indicating that a linear relationship between the predicted and the measured normalized scour depth is not adequate. Therefore, a statistically robust model needs to be selected that can reduce the heteroscedasticity and non-normal error. Operation of dependent variable include application of transformation functions that include Box-Cox (Box and Cox 1964) transformation, logarithmic transformation, exponential transformation, inverse transformation, square root transformation, inverse square root transformation, cubic transformation, and inverse cubic transformation. Based on the analyses of residual diagnostics, the appropriate model was selected. The general form of the statistical model can be presented as in Equation 7a.

$$f\left(\frac{y_{sp}}{b}, \lambda\right) = m \frac{y_{sm}}{b} + k + \xi \quad (7a)$$

For Wilson (1995) model,

$$f\left(\frac{y_{sp}}{b}, \lambda\right) = \left(\frac{y_{sp}}{b}\right)^{\frac{1}{3}} \quad (7b)$$

For Melville (1997), and HEC 18 (2012) models,

$$f\left(\frac{y_{sp}}{b}, \lambda\right) = y^{(\lambda)} = \frac{(y_{sp}/b)^{\lambda} - 1}{\lambda} \quad (7c)$$

For Briaud (2014) model,

$$f\left(\frac{y_{sp}}{b}, \lambda\right) = \log\left(\frac{y_{sp}}{b}\right) \quad (7e)$$

For SC Envelope (2014) model,

$$f\left(\frac{y_{sp}}{b}, \lambda\right) = \left(\frac{y_{sp}}{b}\right)^3 \quad (7b)$$

Where, b denotes the pier width; m , κ , and λ are constant terms depending on the deterministic model being considered, and ξ is the error term describing the uncertainty of model prediction. The calculated parameters for Wilson (1995) model, Melville (1997) model, HEC-18 (2012) model, Briaud (2014) model, SC Envelope (2018) model are presented in Table 4. The R^2 of the fitted models is low and vary from 0.008 for Briaud (2014) model to 0.28 for Wilson (1995) model. Interpretation of standard error suggest that Wilson (1995) model had the least variance,

while Melville (1997) model presented the maximum variance. Shahriar et al. (2021) observed that Box-Cox transformation provided the best response while fitting models to the clear-water laboratory scour measurements reported in Benedict and Caldwell (2014). When the clear-water field measurements are utilized, Melville (1997), and HEC 18 (2012) models seem to agree with the observations of Shahriar et al. (2021). Application of Box-Cox transformation lead to high standard error (0.53) in Wilson (1995) model, while, for Briaud (2014) and SC Envelope (2018) models, Box-Cox transformation was not capable of reducing the heteroscedasticity, and non-normal error. However, applicability of logarithmic transformation for Briaud (2014) model agrees with the observation of Gardoni et al. (2002), and Bolduc et al. (2008), who observed that a logarithmic transformation best depict the scour measurements reported in Gudavalli database (Gudavalli 1997), Landers-Mueller database (Landers and Mueller 1996), and Kwak database (Kwak 2000).

Figure 8 shows the relationship between the measured normalized scour depth and fitted model using the parameters listed in Table 4. In addition to the selected model, 95% confidence limits and 95% prediction limits are shown on the same plot. The very narrow range of confidence interval, i.e. high confidence of the fitted Wilson model is owing to the fact that the residual error associated with Wilson (1995) model is very small (0.003). SC Envelope (2018) model demonstrated the highest residual error (0.243) among the five models considered in the study.

Figure 9 demonstrates the influence of approach flow depth-to-pier width ratio on the normalized predicted scour depth for the five models considered in the study. Melville and Coleman (2000) developed an envelope curve for the estimated scour depth as a function of the upstream flow depth to pier width ratio (y/b). While developing the envelope, a linear relationship between scour depth and flow velocity was assumed, and the ratio of approach mean flow velocity to critical velocity is assumed equal to one (extreme case for clear-water condition). The envelope curve given by Melville and Coleman (2000) is also presented in Figure 9. Owing to the differences in the flow field generated, pier scour can be classified into three categories depending on y/b (Melville and Coleman 2000). A $y/b > 1.4$ indicates “narrow pier” condition, and $y/b < 0.2$ indicates “wide pier” condition, while for a y/b magnitude ranging from 0.2-1.4, the condition can be considered “intermediate pier.”

It is apparent from Figure 9 that the number of data points in wide-pier category is low, while most datasets fall in narrow pier category. Figure 9a suggests that for a $y/b > 5$, Wilson (1995) model predicts a scour depth that exceeds the envelope curve proposed by Melville and Coleman (2000). While Melville (1997) model and HEC 18 (2012) model satisfy the envelope curve; in several instances, Briaud (2014) model seems to over-predict the scour depth for narrow and intermediate piers. SC Envelope (2018) model frequently over-predicted the scour depth for narrow and wide pier cases. Benedict and Caldwell (2016) reported that the laboratory and field scour data of Benedict and Caldwell (2014) is well enveloped by the Melville and Coleman (2000) limit for clear water. Figure 9 also presents the lower limit of the predicted normalized scour depth, below which the proposed model is not applicable. For Wilson (1995), and Briaud (2014) models,

the proposed statistical model of the present study can be applied to both narrow and intermediate pier category; however, for Melville (1997), and HEC 18 (2012) models, y/b should be greater than 0.5, and 0.35 respectively for the proposed model to be applicable. The dispersion of the data points below the model limit is high compared to the same above the model limit. Melville and Coleman (2000), and Ettema et al. (2011) pointed out the fact that there is a lack of data, insight, and understanding of scour depth formulation for wide pier category, and transition from wide to intermediate pier category, which presented itself through the non-applicability of the model in the region with frequent dispersed data.

Probability of deceedance-modification factor relation

Probability of deceedance (POD) can be defined as the probability that a predicted scour depth will be less than the measured scour depth. Exceedance and deceedance probabilities are a useful way to assess the engineering properties of a deterministic model (NRC 2000). The relationship between probability of deceedance and μ_{POD} , which is the ratio of predicted to the measured scour depth reported in Benedict and Caldwell (2014), is presented in Figure 10. The figure was developed using a non-parametric process, termed as Kernel density estimation. The frequency distribution of μ_{POD} is initially quantified, leading to the generation of probability density function. Thereafter, cumulative density function is obtained through integration of probability density function. Probability of deceedance is calculated by deducting the cumulative density function from one. The expected scour depth corresponding to a POD to the measured scour depth can be related by Equation (8).

$$\frac{y_{se}}{b} |_{POD} = \mu_{POD} \frac{y_{smed}}{b} \quad (8)$$

Where, y_{se} is the expected scour depth corresponding to a certain POD, and y_{smed} is the median scour depth obtained considering $\xi = \text{zero}$ in Equation 7a. Figure 10 suggests that as the POD decreases, the modification factor increases. The rate of increase of modification factor increases significantly at $POD < 0.2$. The use of the deterministic models of Wilson (1995), Melville (1997), HEC-18 (2012), Briaud (2014), and SC Envelope (2018) model will lead to probability of deceedance of 66.9%, 78.6%, 76.4%, 77.8%, and 75% respectively. The modification factors reported herein are comparatively higher than the modification factors proposed by Shahriar et al. (2021), where the clear-water laboratory datasets reported in Benedict and Caldwell (2014) were utilized. The higher modification factor, to some extent, can be attributed to the limitation of the field scour measurements. While the laboratory measurements provide a relatively accurate measurements of downscaled parameter associated scour, field measurements may not represent an equilibrium scour depth. Although, through the screening process, the extreme outliers were eliminated from the dataset, there are still possibility that a non-equilibrium scour measurement remain in the dataset utilized herein, which increased the inherent uncertainty of the model (refer to Figure 3, frequent occurrence of comparatively high errors) and thereby increased the value of the developed modification factor, based on the measured field scour data.

Conclusions

Based on the results obtained so far, the following conclusions are drawn.

1. Five bridge scour prediction models are assessed in terms of two statistical parameters, termed Mean Absolute Percentage Error (MAPE, as a measure of accuracy of the prediction), and “level of conservatism” (as a measure of conservativeness of the model). Values of MAPE ranged from 238% to 336%, whereas, conservatism ranged from 77% to 97.8%.
2. SC Envelope (2018) model estimates provided the highest conservatism factor, whereas Briaud (2014) model presented the least conservatism factor. With regards to MAPE, Briaud (2014) model presented the least error magnitude, and SC Envelope (2018) model presented the highest error.
3. The accuracy and conservatism of a specific model can be adjusted by multiplying the scour depth computed using a given deterministic model by a correction factor. The proposed correction factors necessary to attain certain conservatism level for the five models considered herein are presented.
4. Deterministic models used for bridge pier scour do not account for inherent model uncertainties. The scatter associated with the scour prediction produces heteroscedasticity, and non-normal errors. The performance of several statistical models are assessed to identify the appropriate model addressing such concerns, and subsequently, a model is proposed.
5. A relationship between probability of exceedance of a given measured scour depth and a modification factor (that is applied into the deterministic prediction) is proposed. The modification factor allows for the use of the deterministic models while quantifying the probability of the computed scour depth being less than or more than the most likely value per measurements reported in the utilized database.

The proposed approach allows for the selection of a suitable modification factor to satisfy a target probability of exceedance. Using the framework presented herein, it is possible to extend any deterministic model to assess the probability of exceedance, and to develop associated modification factors for a different set of database. It is important to note that the approach presented herein is developed considering the clear-water field dataset reported in Benedict and Caldwell (2014). This dataset is the largest collection of pier scour data available in the United States, with a complete set of parameters to allow for comparative analysis of models that require different input parameters. It is suggested however that users be cautious while applying the proposed approach to a specific site having a hydraulic, structural, and geotechnical parameters outside the range investigated in the present study.

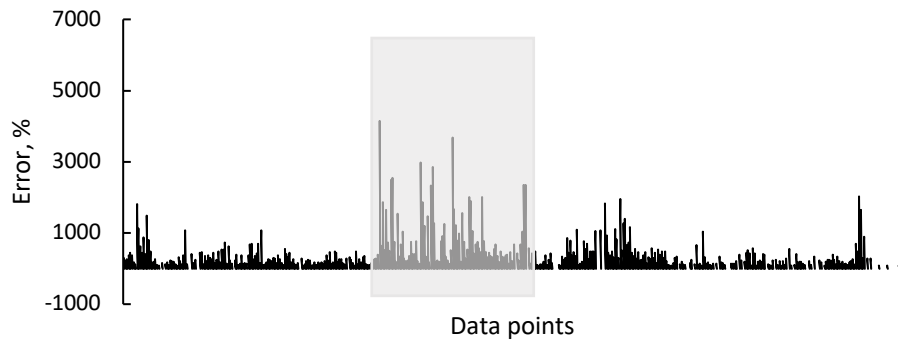
References

Arneson LA, Zevenbergen LW, Lagasse PF, and Clopper PE. (2012). “Evaluating scour at bridges.” Hydraulic Engineering Circular No. 18, 5th edition, 1-340.

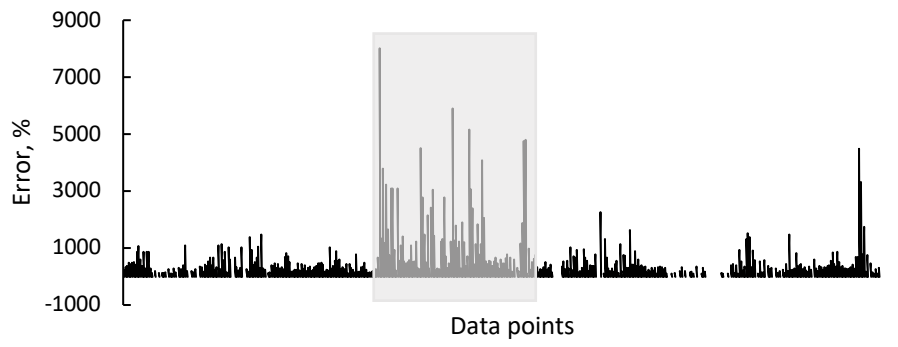
- Azamatullah HM, Yusoff MAM, and Hasan ZA (2014). “Scour below submerged skewed pipeline.” *Journal of Hydrology*, 509(2014): 615-620.
- Benedict ST, and Caldwell AW. (2014). “A pier-scour database—2,427 field and laboratory measurements of pier scour.” U.S. Geological Survey Data Series 845, 1-22.
- Benedict ST, and Caldwell AW. (2016). “Upper Bound of Pier Scour in Laboratory and Field Data.” *Transportation Research Record*, 2588(1), 145–153.
- Benedict ST, Feaster TD, and Caldwell AW. (2018). The South Carolina bridge-scour envelope curves (ver. 1.1, January 2018): U.S. Geological Survey Scientific Investigations Report 2016– 5121, 1-96.
- Box GEP, and Cox DR. (1964). “An analysis of transformations,” *Journal of the Royal Statistical Society*, Series B; 26, 211-252.
- Briaud JL. (2014). “Scour depth at bridges: Method including soil properties. I: Maximum scour depth prediction.” *Journal of Geotechnical and Geoenvironmental Engineering*; 141(2): 04014104.
- Briaud J-L, Gardoni P, and Yao C. (2014). “Statistical, risk, and reliability analyses of bridge scour.” *Journal of Geotechnical and Geoenvironmental Engineering*; 140(2): 04013011.
- Briaud JL, Ting F, Chen HC, Gudavalli R, Perugu S, and Wei G. (1999). “SRICOS: Prediction of scour rate in cohesive soils at bridge piers.” *Journal of Geotechnical and Geoenvironmental Engineering*; 125(4):237-246.
- Briaud J-L, Brandimarte L, Wang J, and D’Odorico P. (2007). “Probability of scour depth exceedance due to hydrologic uncertainty.” *Georisk: Assessment and Management of Risk for Engineered Systems and Geohazards*; 1(2), 77–88.
- Ettema R, Constantinescu G, and Melville BW. (2017). “Flow-field complexity and design estimation of pier-scour depth: Sixty years since Laursen and Toch.” *Journal of Hydraulic Engineering*; 143(9), 03117006.
- Florida Department of Transportation (FDOT) (2011). "Bridge Scour Manual," Tallahassee, FL.
- Gudavalli SR. (1997). “Prediction model for scour rate around bridge piers in cohesive soil on the basis of flume tests.” Ph.D. dissertation, Department of Civil Engineering, Texas A&M University, College Station, Texas.
- Hunt D. (2009). “Monitoring scour critical bridges.” NCHRP synthesis 396. Washington, D.C.: Transportation Research Board.
- Johnson PA, Clopper PE, Zevenbergen LW and Lagasse PF. (2015). “Quantifying uncertainty and reliability in bridge scour estimations.” *Journal of Hydraulic Engineering*; 141(7), 04015013.
- Kwak K. (2000). “Prediction of scour depth versus time for bridge piers in cohesive soils in the case of multi-flood and soil systems.” Ph.D. dissertation, Department of Civil Engineering, Texas A&M University, College Station, Texas.

- Lagasse PF, Schall JD, Johnson F, Richardson EV, Chang F. (1995). "Stream stability at highway structures." Washington DC.
- Lagasse PF, Zevenbergen LW, Spitz WJ, and Arneson LA. (2012). "Stream stability at highway structures." Hydraulic Engineering Circular No. 18, 4th edition, 1-328.
- Landers MN, and Mueller DS. (1996). "Channel scour at bridges in the United States." *Report No. FHWA-RD-95-184*, Federal Highway Administration, Washington, D.C.
- Liang FY, Zhang H, and Huang MS. (2015). "Extreme scour effects on the buckling of bridge piles considering the stress history of soft clay." *Natural Hazards*; 77, 1143–1159.
- Melville BW. (1992). "Local scour at bridge abutments." *Journal of Hydraulic Engineering*; 118(4), 615-630.
- Melville BW. (1997). "Pier and abutment scour: Integrated approach." *Journal of Hydraulic Engineering*; 123(2), 125–136.
- Melville BW. and Coleman SE. (2000). "Bridge scour." Highlands Ranch, USA: Water Resources Publications.
- National Research Council. (2000). *Risk Analysis and Uncertainty in Flood Damage Reduction Studies*. Washington, DC: The National Academies Press.
- Rhodes J, and Trent R. (1993). "Economics of floods, scour and bridge failures." In: Shen HW, Su ST, Wen F, editors. Proceedings of 1993 ASCE conference hydraulic engineering '93. San Francisco, CA.
- Richardson EV, and Davis SR. (1995). "Evaluating scour at bridges," Report No. FHWA-IP-90-017, Hydraulic Engineering Circular No. 18 (HEC-18), 3rd Edition, Office of Technology Applications, HTA-22, Federal Highway Administration, U.S. Department of Transportation, Washington, D.C.
- Shahriar AR, Montoya BM, Ortiz AC and Gabr MA (2021). "Quantifying probability of deceedance estimates of clear water local scour around bridge piers," *Journal of Hydrology*, Under Review.
- Shen HW, Schneider VR, and Karaki SS. (1966). "Mechanics of local scour." *Report*, U.S. Dept. of Commerce, National Bureau of Standards, Inst. for Appl. Technol., Washington, D.C.
- Sheppard M, Demir H, and Melville BW. (2011). "Scour at wide piers and long skewed piers," NCHRP Report 682, Transportation Research Board of the National Academies, Washington D.C.
- Sheppard M, Melville B, and Demir H. (2014). "Evaluation of existing equations for local scour at bridge piers." *Journal of Hydraulic Engineering*; 140(1), 14–23.
- Shirole AM, and Holt RC. (1991). "Planning for a comprehensive bridge safety assurance program." *Transportation Research Record*, Washington DC: Transport Research Board; 137-142.
- Stone JC. (1996). *A course in probability and statistics*, Duxbury Press, 1st Edition, Belmont, California.

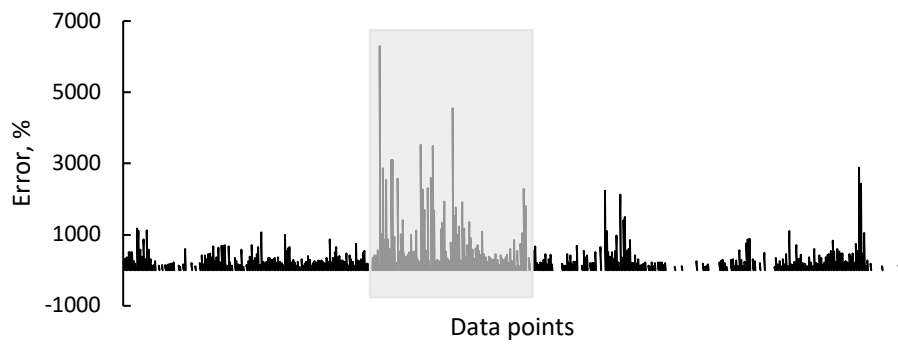
- Tan, CK. and Duncan JM. (1991). "Settlement of footings on sands- Accuracy and reliability," in Proceedings of the Geotechnical Engineering Congress, Jun 10-12 1991, Boulder, USA, Published by ASCE, NY, USA, p. 446-455.
- Yao C. (2013). "LRFD calibration of bridge foundations subjected to scour and risk analysis." Ph.D. dissertation, Department of Civil Engineering, Texas A&M University, College Station, Texas.
- Wardhana K, Hadipriono FC. (2003). "Analysis of recent bridge failures in the United States." *Journal of Performance of Constructed Facilities*; 17(3), 144-150.
- Wilson KV Jr. (1995). "Scour at selected bridge sites in Mississippi." *Resources Investigations Report 94-4241*, Geological Survey Water, Reston, Virginia.



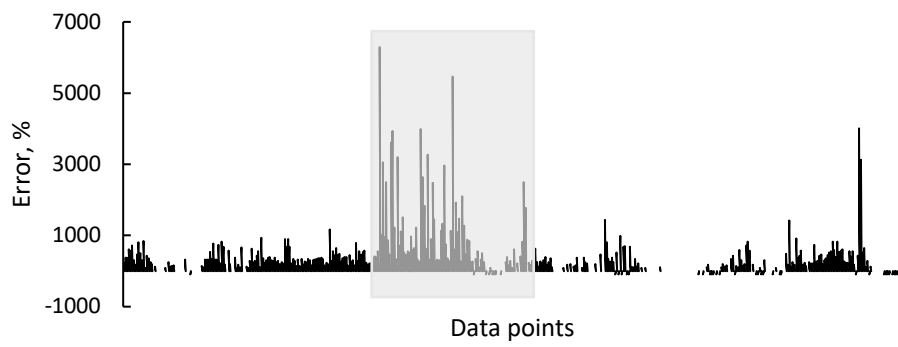
(a)



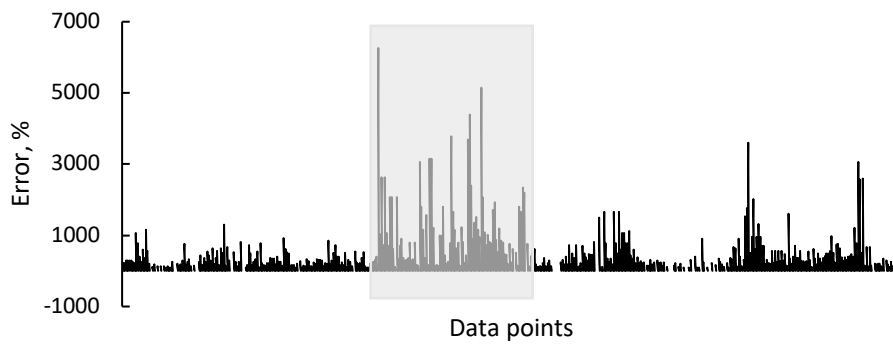
(b)



(c)



(d)



(e)

Figure 1: Error distribution considering clear water field datasets (Data count: 469) for (a) Wilson 1995, (b) Melville 1997, (c) HEC 18 2012, (d) Briaud 2014, and (e) SC Envelope 2018 models

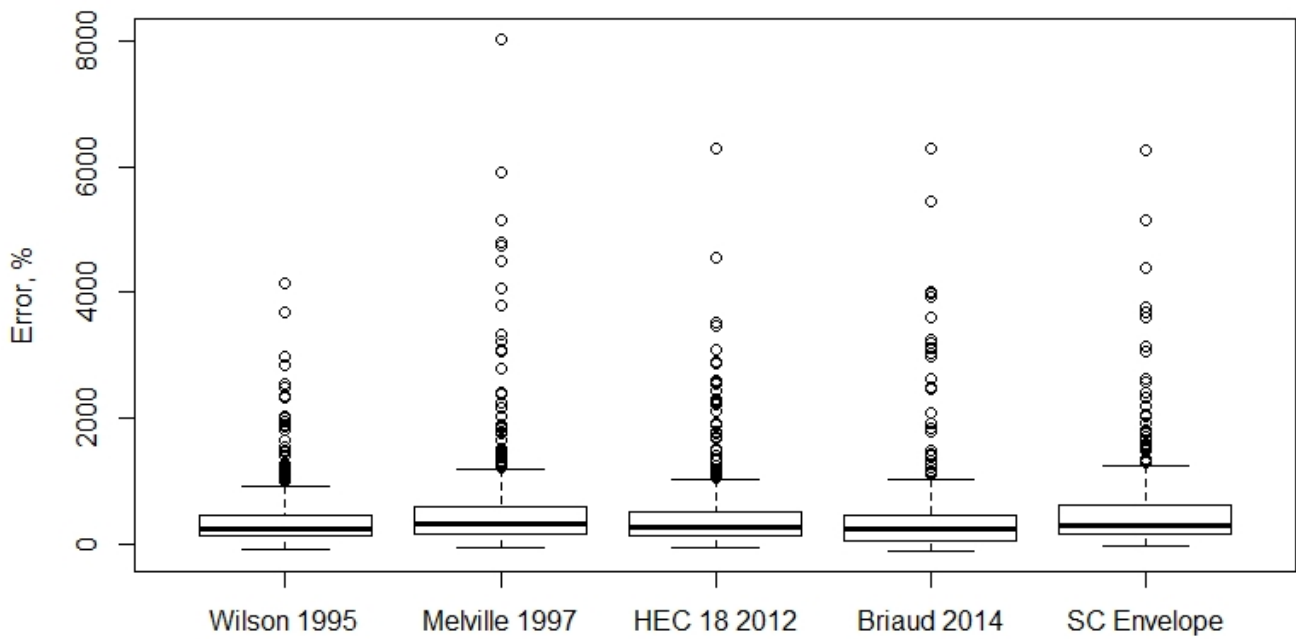
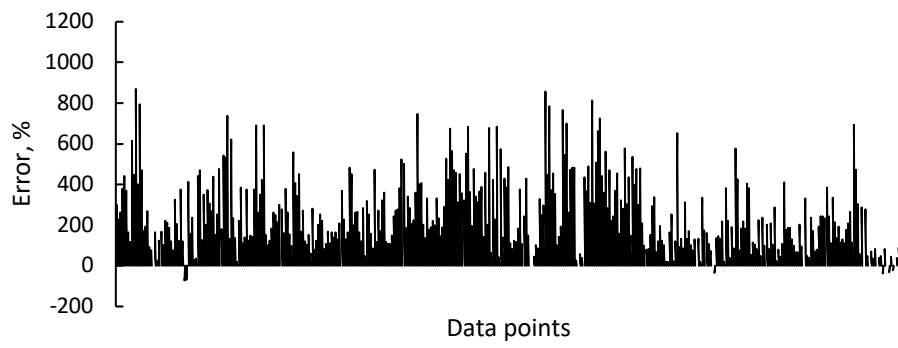
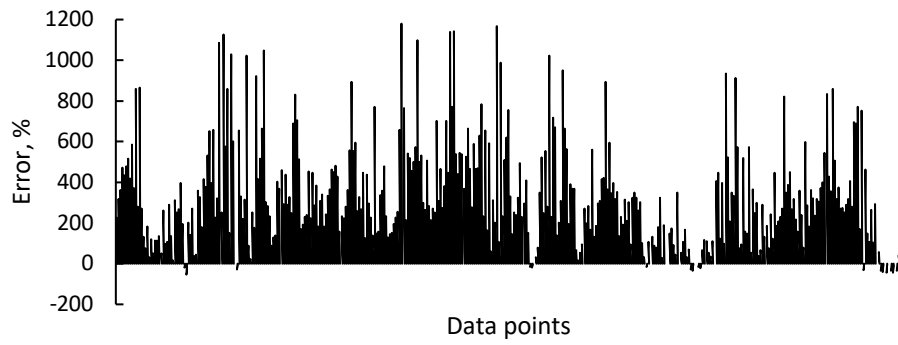


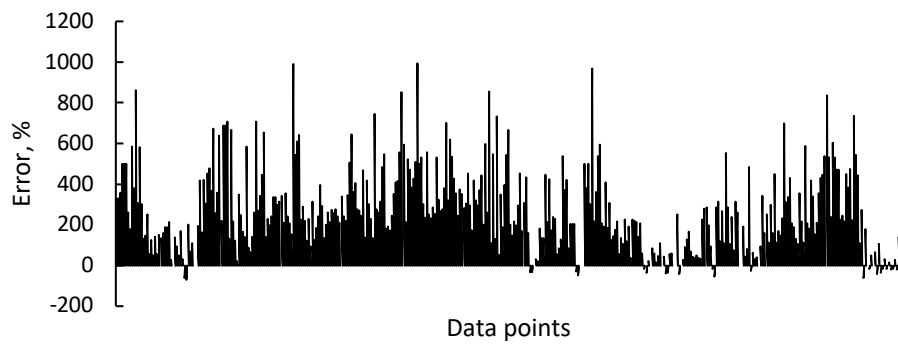
Figure 2: Error box-plot for the five deterministic models considered in the study



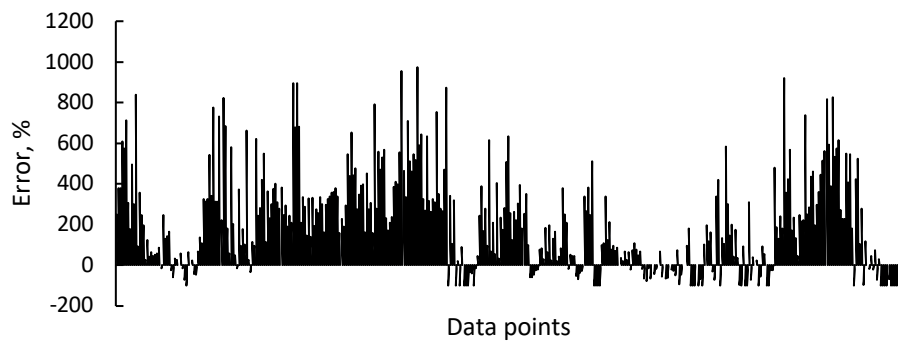
(a)



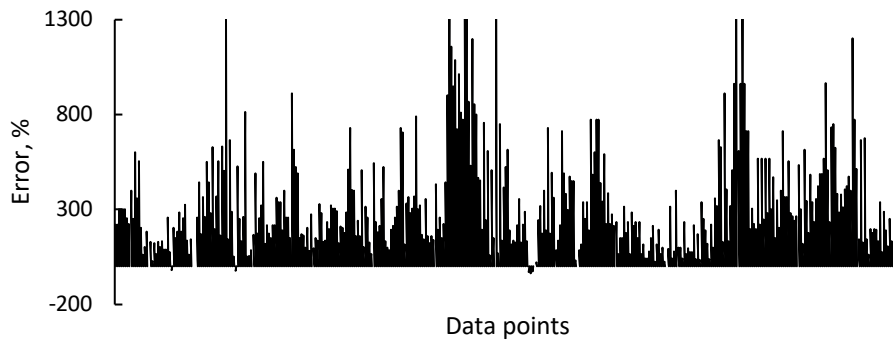
(b)



(c)



(d)



(e)

Figure 3: Error distribution considering the screened clear water field datasets (Data count: 405) for (a) Wilson 1995, (b) Melville 1997, (c) HEC 18 2012, (d) Briaud 2014, and (e) SC Envelope 2018 models

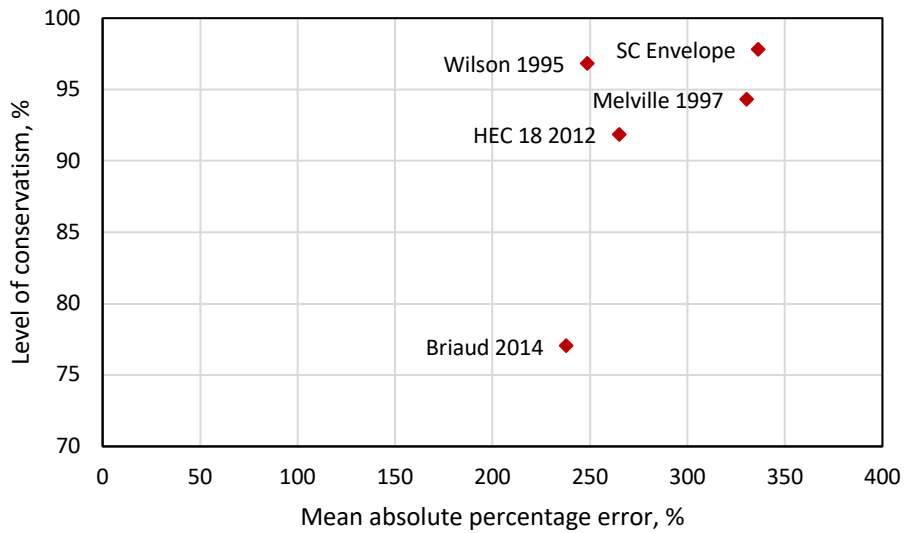
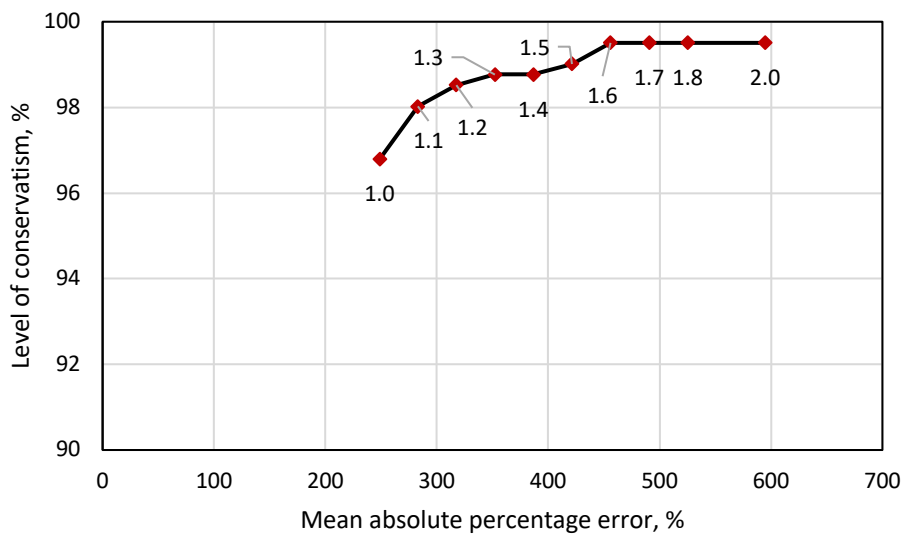
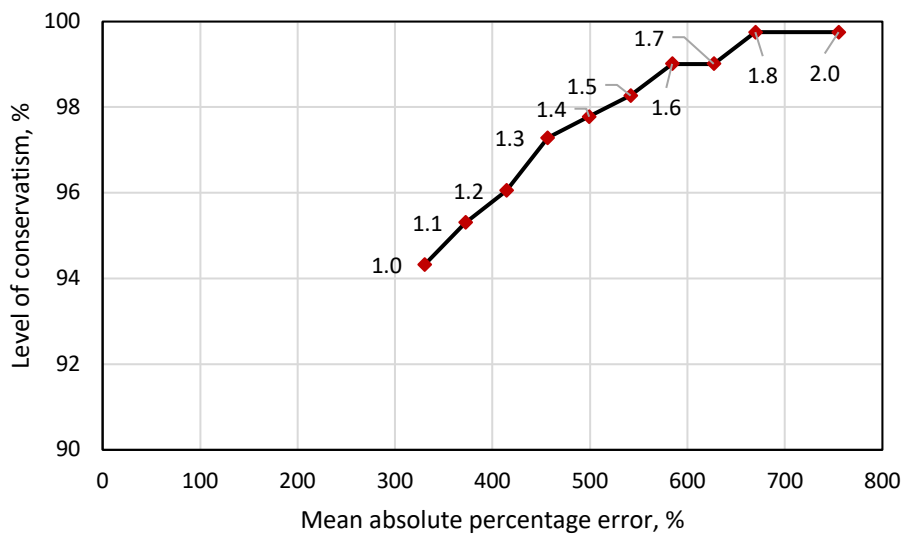


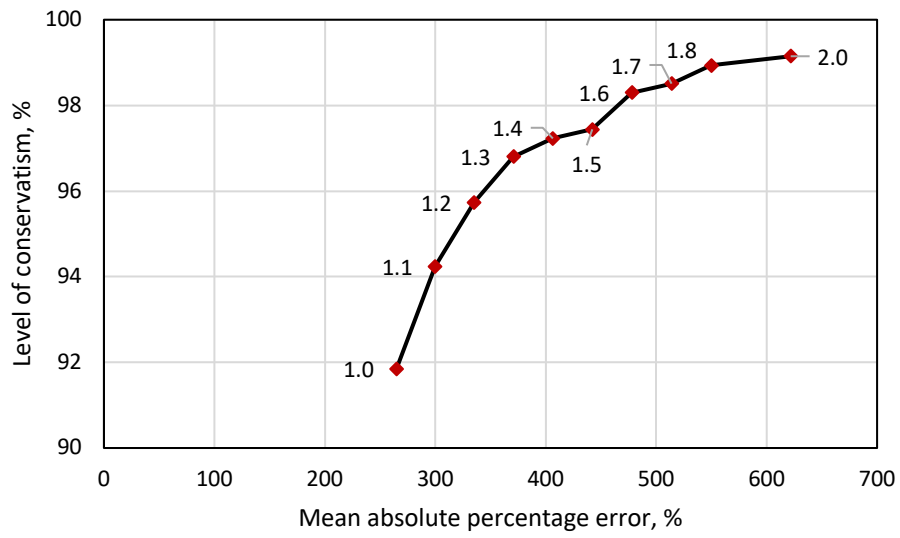
Figure 4: Relationship between conservatism and mean absolute percentage error for the five models considered in the study



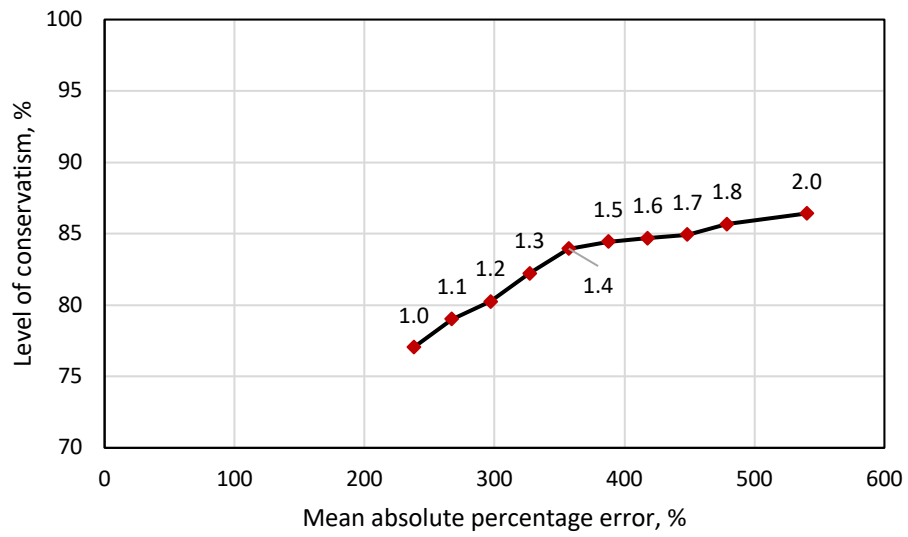
(a)



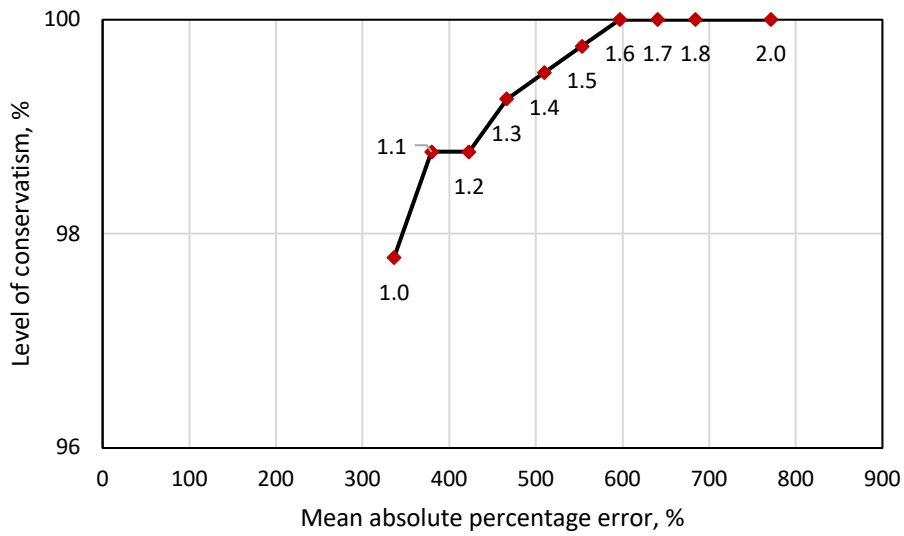
(b)



(c)

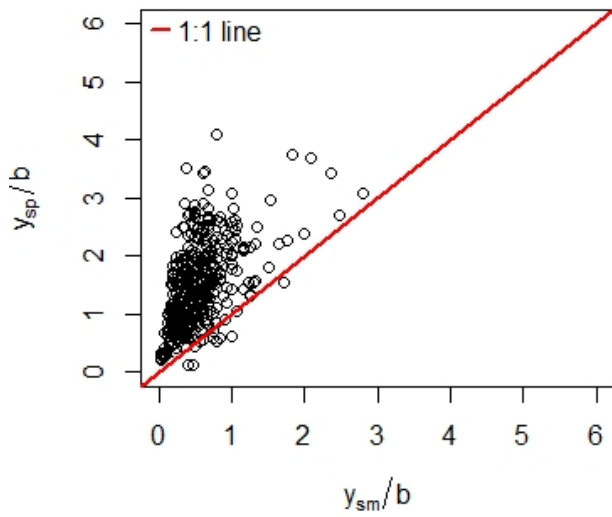


(d)

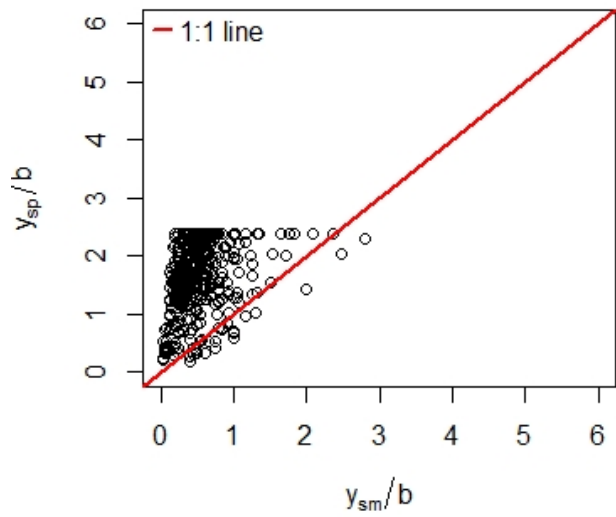


(e)

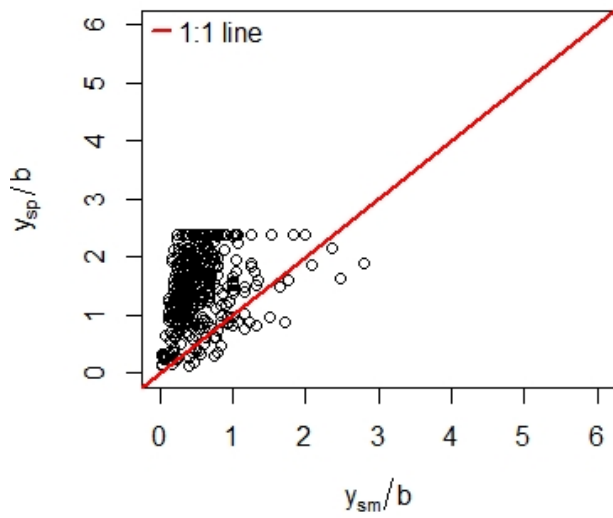
Figure 5: Effect of adjustment factor on the conservatism and mean absolute percentage error for (a) Wilson 1995, (b) Melville 1997, (c) HEC 18 2012, (d) Briaud 2014, and (e) SC Envelope 2018 models



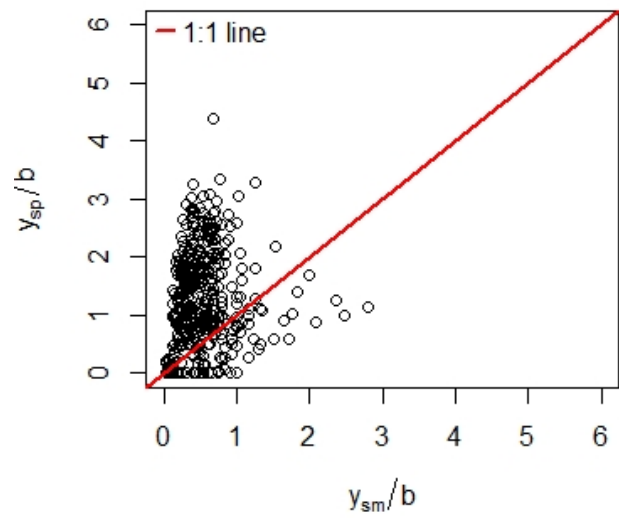
(a)



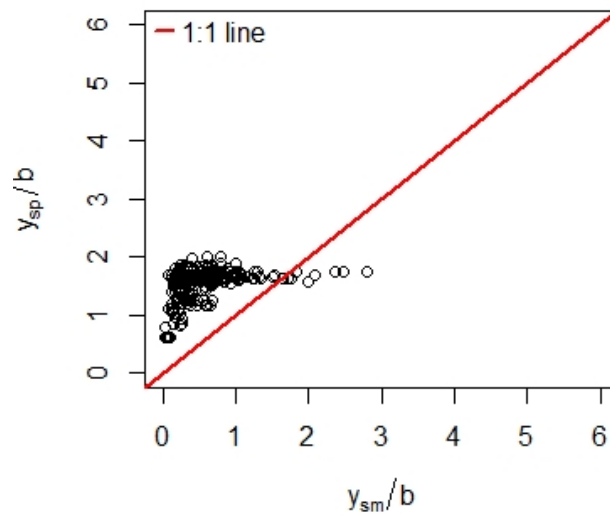
(b)



(c)



(d)



(e)

Figure 6: Predicted-measured normalized scour depth relation for: (a) Wilson (1995) model, (b) Melville (1997) model, (c) HEC-18 (2012) model, (d) Briaud 2014 model, and (e) SC Envelope 2018 model using screened clear water field dataset. b denotes the pier width, and y_{sp} , y_{sm} indicate the predicted and the measured scour depth respectively.

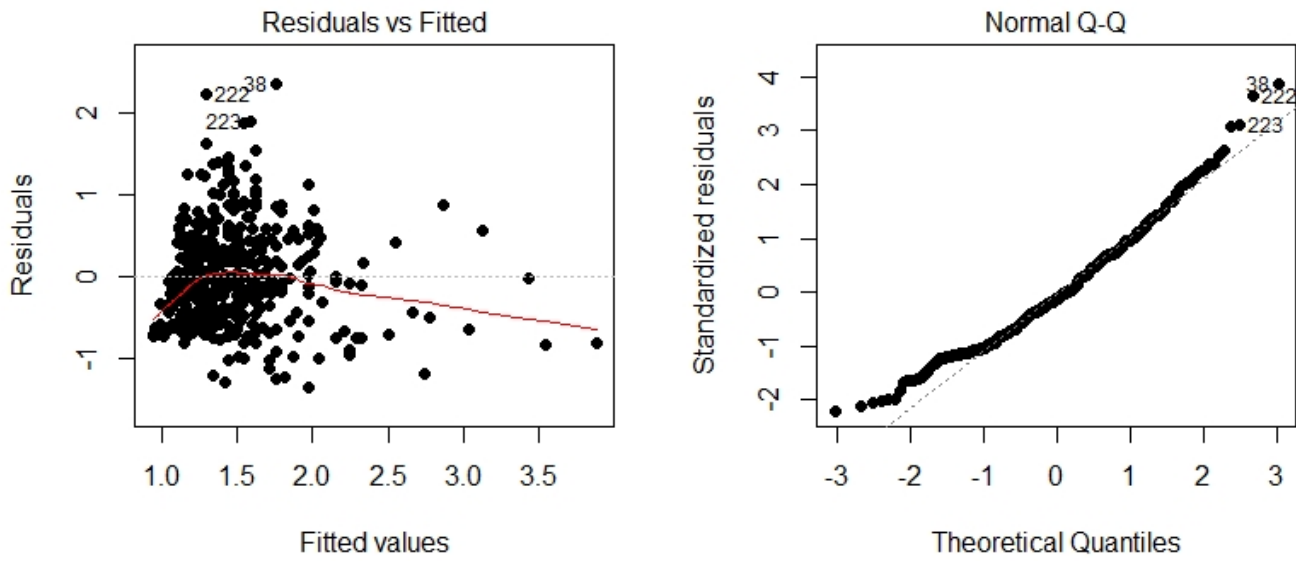
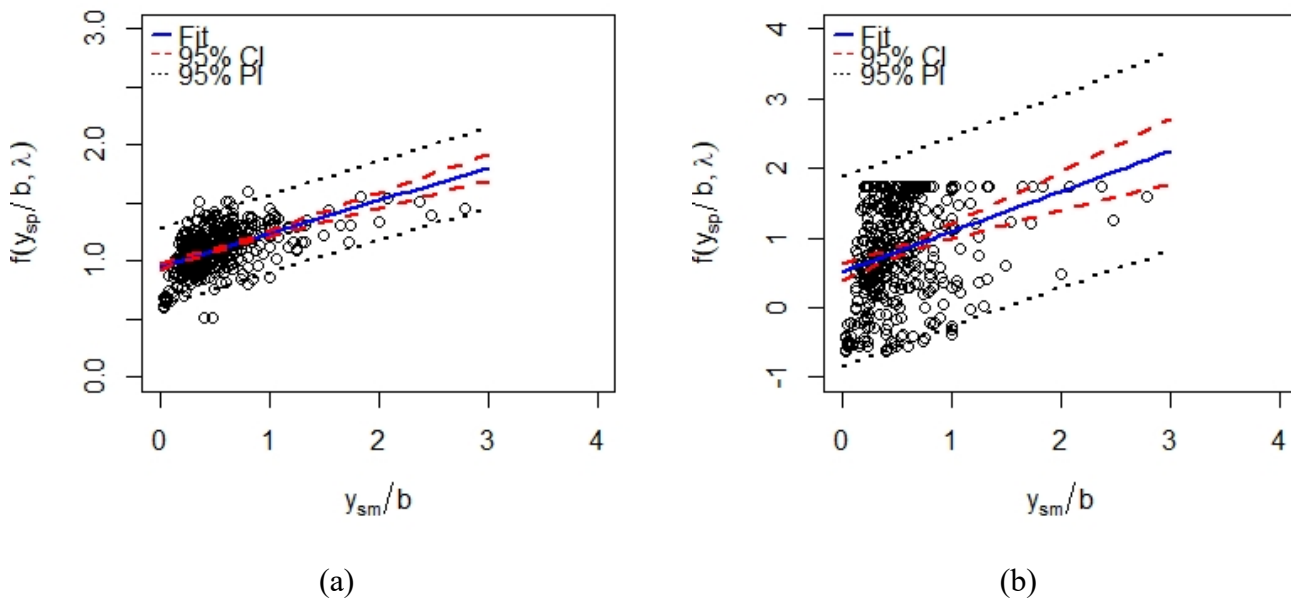
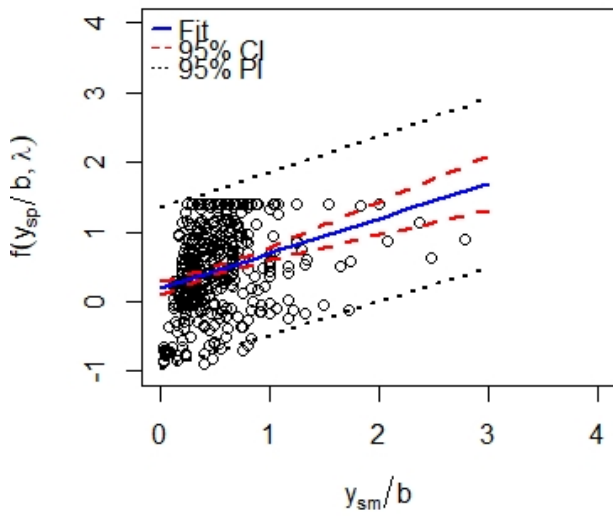
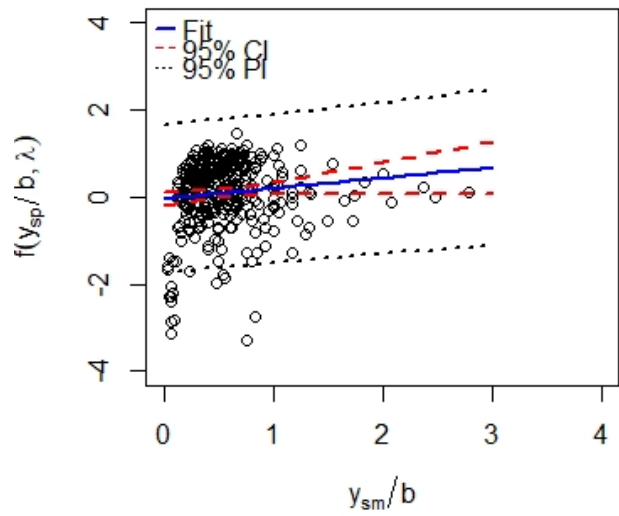


Figure 7: Demonstration of heteroscedasticity and non-normal errors associated with predicted-measured normalized scour depth relation using Wilson (1995) model

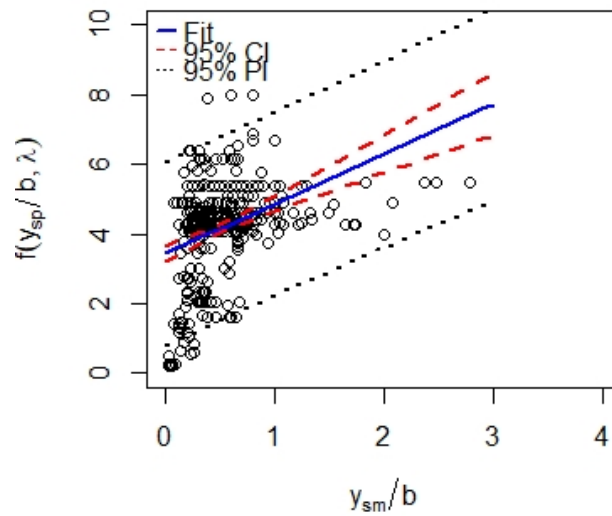




(c)

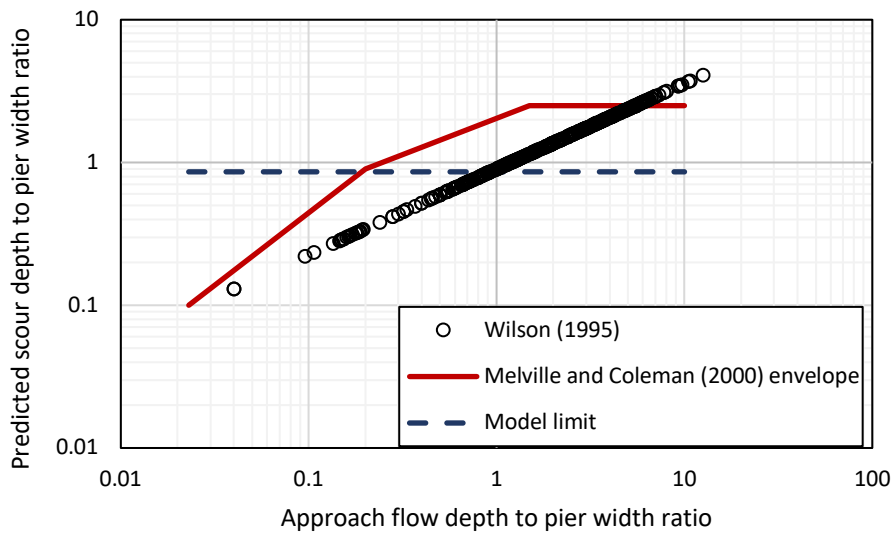


(d)

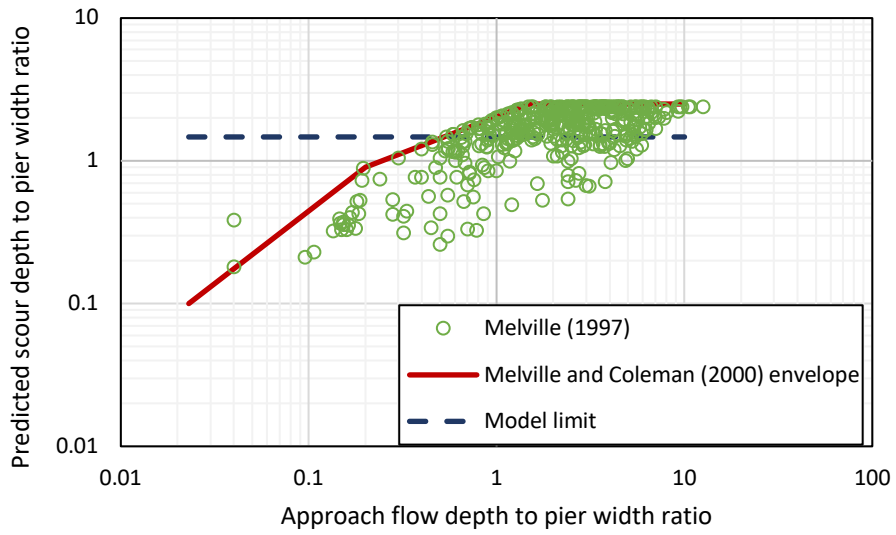


(e)

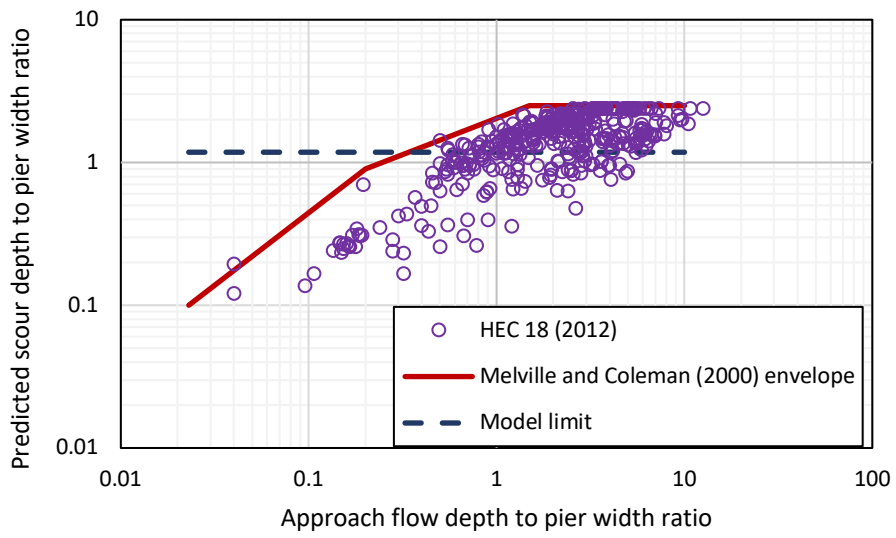
Figure 8: Variation of $f(y_{sp}/b, \lambda)$ with the measured normalized scour depth for: (a) Wilson (1995) model, (b) Melville (1997) model, (c) HEC-18 (2012) model, (d) Briaud (2014) model, and (e) SC Envelope (2018) model using screened clear water field dataset. CI and PI denote Confidence Interval and Prediction Interval respectively.



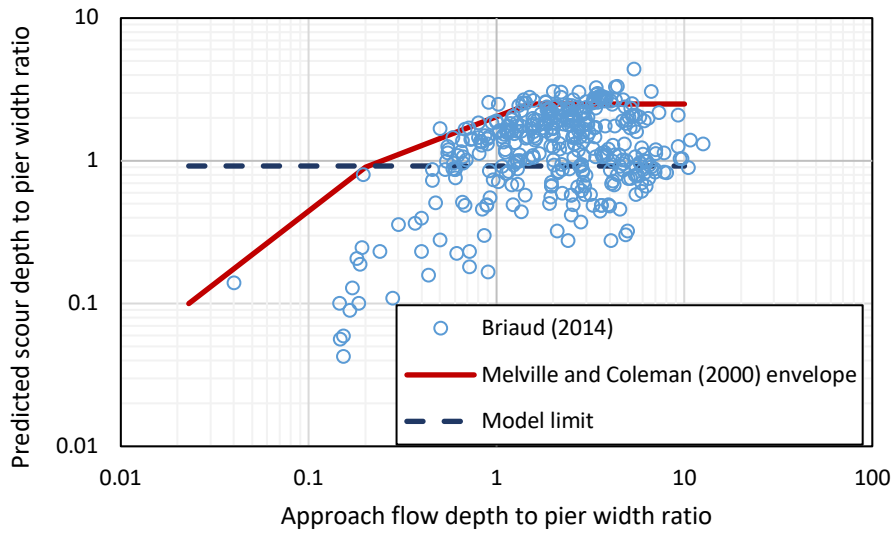
(a)



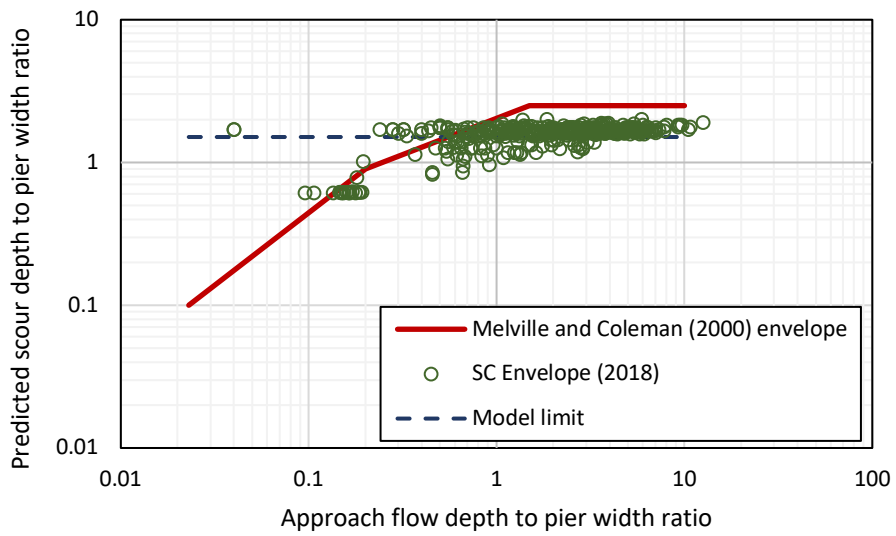
(b)



(c)

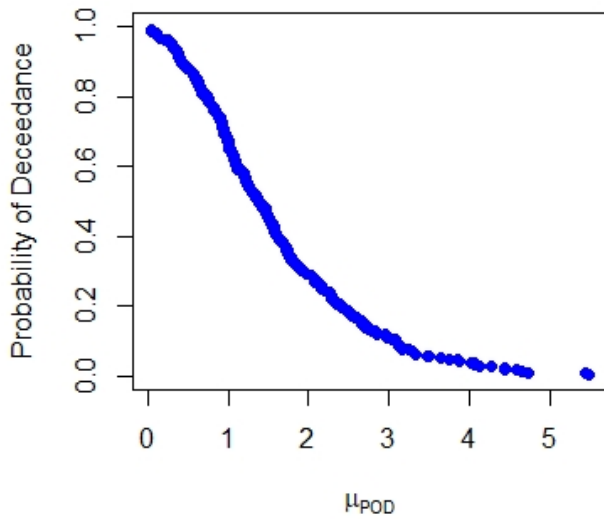


(d)

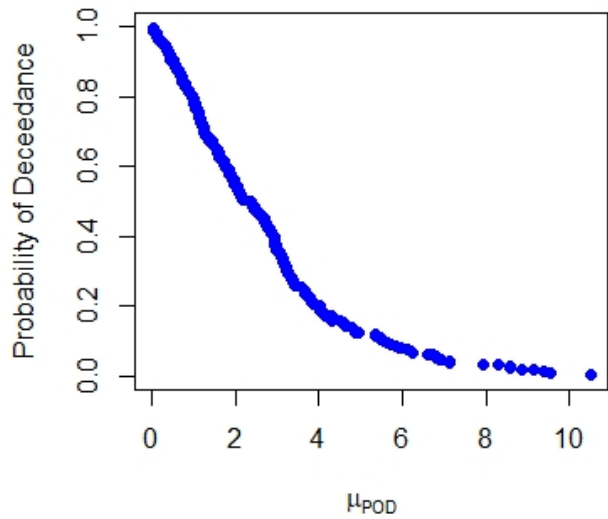


(e)

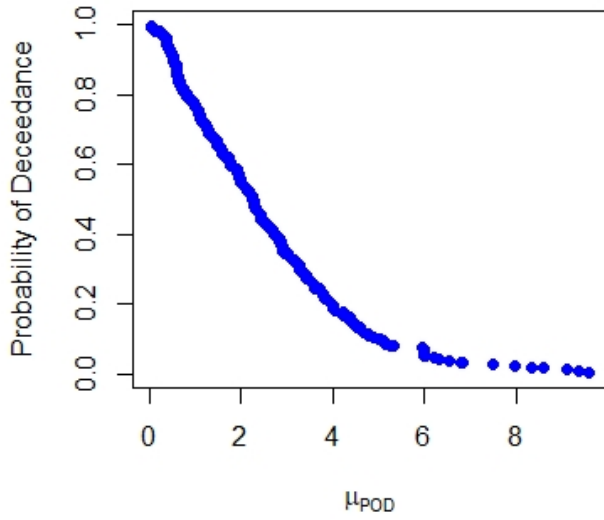
Figure 9: Influence of approach flow depth to pier width ratio on the normalized predicted scour depth for: (a) Wilson (1995) model, (b) Melville (1997) model, (c) HEC-18 (2012) model, (d) Briaud (2014) model, and (e) SC Envelope (2018) model using screened clear water field dataset.



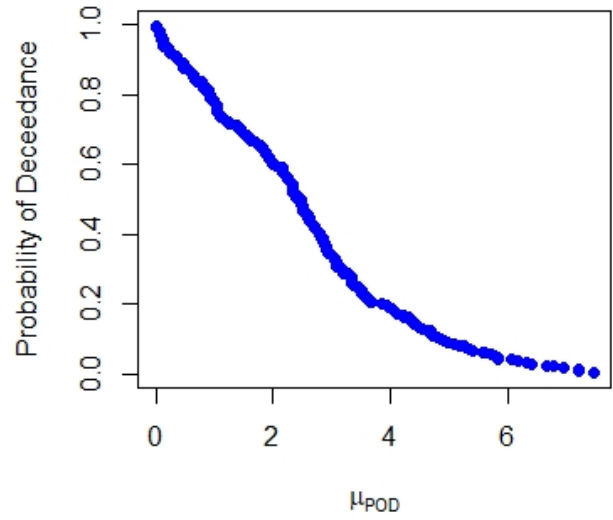
(a)



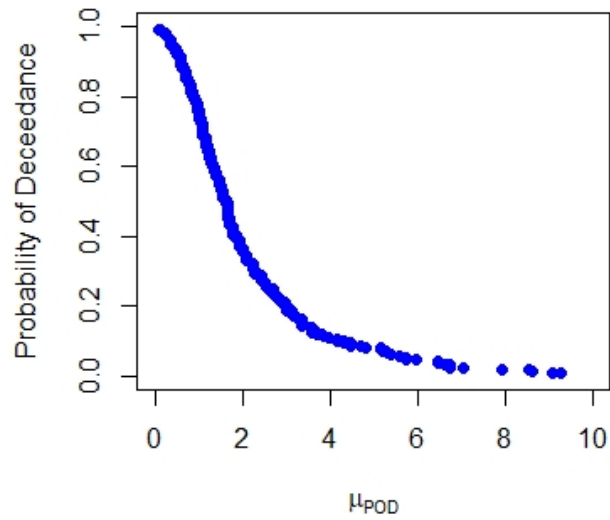
(b)



(c)



(d)



(e)

Figure 10: Probability of deceedance-modification factor relation for: (a) Wilson (1995) model, (b) Melville (1997) model, (c) HEC-18 (2012) model, (d) Briaud (2014) model, and (e) SC Envelope (2018) model using screened clear water field dataset.

Table 1. Consideration of pier scour influencing parameters in selected deterministic models (Shahriar et al. 2021)

Reference	y/b	b/d_{50}	Pier face shape	Aspect ratio	Skew angle	v/V_c	Sediment non-uniformity	Euler/Reynolds number	Temporal rate
Wilson (1995)	C	NC	NC	NC	NC	NC	NC	NC	NC
Melville (1997)	C	C	C	C	C	C	C	NC	NC
Arneson et al. (2012)	C	NC	C	C	C	NC	NC	NC	NC
Briaud (2014)	C	NC	C	C	C	C	NC	C	C

Note: C means considered in the respective model; NC means not considered in the respective model

Table 2. Range of some selected variables associated with clear-water field data in Benedict and Caldwell (2014)

Parameter	Pier width normal to the flow, b' (ft)	Approach flow velocity, v (ft/s)	mean Approach depth, y (ft)	flow Median grain size, d_{50} (mm)	Measured pier-scour depth, y_{sm} (ft)
Minimum	1.00	0.07	0.10	0.01	0.20
Median	3.50	4.12	8.10	29.0	1.50
Maximum	55.33	11.50	41.70	228.5	12.00

Table 3. Deterministic pier scour model equations considered in the present study (modified from Shahriar et al. 2021)

Reference	Model	Equation No.	Remarks
Wilson (1995)	$\frac{y_{sp}}{b'} = 0.9\left(\frac{y}{b'}\right)^{0.4}$	(1)	b' = projected pier width y_{sp} = predicted scour depth

			y = flow depth upstream of pier
Melville (1997)	$y_{sp} = K_{yb}K_IK_dK_sK_\theta K_G \quad (2)$		K_{yb} = pier depth-size factor K_I = flow intensity factor K_d = sediment size factor K_s = pier nose shape factor K_θ = pier alignment factor K_G = channel geometry factor (= 1 for pier)
Arneson et al. (2012)	$\frac{y_{sp}}{b} = 2K_1K_2K_3\left(\frac{y}{b}\right)^{0.35}F^{0.43} \quad (3)$		K_1 = pier nose shape factor K_2 = pier alignment factor K_3 = bed condition factor b = pier width F = Froude number
Briaud (2014)	$\frac{y_{sp}}{b'} = 2.2K_{pw}K_{psh}K_{pa}K_{psp}(2.6F_{pier} - F_{c(pier)})^{0.7} \quad (4)$		K_{pw} = water depth influence factor K_{psh} = pier shape influence factor K_{pa} = aspect ratio influence factor K_{psp} = pier spacing influence factor F_{pier} = pier Froude number $F_{c(pier)}$ = critical pier Froude number
SC envelope curve (Benedict et al. 2018)	$y_{sp} = K_2(1.5b + 0.5) \quad (5)$		

Table 4. Calculated parameters in Equations (7a-e) for the five models considered in the study

Reference	Parameter			Statistics				
	m	k	λ	Significance level	Standard error	Median residual error	F statistic	R^2
Wilson (1995)	0.284	0.953	--	0.01	0.169	0.003	155.2	0.276
Melville (1997)	0.577	0.514	1.4343	0.01	0.689	0.0355	38.45	0.085
Arneson et al. (2012)	0.504	0.185	0.9899	0.01	0.59	0.012	39.86	0.088
Briaud (2014)	0.238	-0.036	--	0.01	0.865	0.187	3.867	0.008
SC Envelope (2018)	1.431	3.432	--	0.01	1.336	0.243	62.9	0.133

Appendix C: Bridge Pier Scour: Analyses using live-bed data

Introduction

Bridge scour is a complex process of interaction among flow, sediments, and structure leading to the mobilization and transport of sediments surrounding the structure. The erosion process initiates if the applied bed shear stress exceeds the sediment mobilization critical stress. The scouring process causes damage to foundation systems supporting bridges and other hydraulic structures, which may lead to operational disruption and economic losses (Shirole and Holt, 1991; Briaud et al. 1999; Azamatullah et al. 2013). Wardhana and Hadipriono (2003) analyzed 503 failures of bridge structures that occurred in the United States, and concluded that 85% of the bridge failure is related to externally-triggered events, such as flood, collision, overload etc. It was also found in 243 cases that the principal cause of failure is flood-induced scour. Hunt (2009) noted that there are 20,904 scour-critical bridges in the United States and approximately 80,000 bridges that are scour susceptible. The cost for flood damage and scour repair of the 1993 flood in the Midwestern US was estimated to be 178 million, while the flood in Georgia in 1994 resulted in a repair cost of 130 million (Mueller 2000). Rhodes and Trent (1993) reported that the additional cost to the afflicted population can be as much as five times the repair cost. With the impact of the climate change and the likely increase in heavy precipitation, severe flow flooding coupled with scour is poised to be the leading cause of bridge damage (Liang et al. 2015). For existing bridges, the base flow assumption used in design decades ago may be no longer valid. For new hydraulic structures, properly estimating the scour magnitude incorporating model uncertainty is critical in developing robust design.

It is well established that pier scour is influenced by multiple factors including flow depth to pier width ratio, pier width to median grain size ratio, pier face shape, pier aspect ratio, skew angle of pier, flow intensity, Euler number or Reynolds number, sediment non-uniformity, and the temporal rate of evolution (e.g. Melville and Coleman 2000; Sheppard et al. 2011; Ettema et al. 2017). Evidently, not all the factors are equally important. The choice of which scour-influencing factors are included in a given deterministic model leads to different scour magnitudes under similar set of hydraulic, structural, and geotechnical parameters (Shahriar et al. 2021a). The deterministic scour prediction models do not account for inherent model uncertainties and errors including model bias. Without prior knowledge of the extent of biasness yielded by a given deterministic model (each model predicts different scour depths for a similar set of parameters), one cannot discern whether these predictions are conservative or unconservative and the extent of conservatism in view a given model's application to a wider set of site conditions.

Multiple researchers investigated the probabilistic aspects of bridge pier scour albeit the considered sources of uncertainty varied. In scour prediction models, uncertainties arise from multiple sources including hydraulic, geotechnical, structural or predictive model errors (Yao

2013). While the hydraulic, geotechnical, and structural uncertainties can be improved through better-quality field characterization and measurement accuracy, or by accumulating more data, it is often the case that scour prediction is performed with insufficient data set. Briaud et al. (2007) developed a probabilistic bridge scour model that considered the uncertainty of hydrologic conditions; uncertainties associated with input parameters (geometry of obstacle, soil erodibility) were however not considered. Briaud et al. (2014) developed a reliability-based pier scour model focusing on the risk associated with stability of shallow and deep foundations subjected to scour; the focus on this case was on the foundation system. Johnson et al. (2015) examined the hydraulic and hydrologic uncertainties associated with HEC-18 (2012) and FDOT (2011) scour prediction models. Johnson et al. suggested “scour design factors” based on target reliability index. More research on inherent predictive model errors is need for informed prediction of the complex phenomena of bridge scouring.

The study herein is focused on assessment of five bridge scour prediction models, viz Wilson (1995) model, Melville (1997) model, HEC-18 (2012) model, Briaud (2014) model, and South Carolina (SC) envelope (2018) model. The assessment includes investigation of *Accuracy* and *Level of conservatism* of a given model within the context of comparing the models’ predicted results with measured live-bed laboratory and field scour-depth data. The database reported in Benedict and Caldwell (2014) is used with the exception of few data points for which insufficient information was reported to be able to apply the predictive models. Statistical analyses are used to evaluate and quantify the scatter and uncertainty associated with scour prediction using the five deterministic models herein. A statistical model is proposed to quantify model prediction bias and required parameters and soundness of the model are presented. Finally, a relationship between probability of exceedance of a given measured scour depth and a modification factor (that is applied onto the deterministic prediction) is devised.

Scour prediction models

Five pier-scour prediction models, namely Wilson (1995) model, Melville (1997) model, HEC-18 (2012) model, Briaud (2014) model, and SC envelope (2018) model are utilized herein. The model equations are provided in Shahriar et al. (2021a) except the SC envelope model, which is available in Benedict et al. (2018). Wilson (1995) model is based on field data collected from 22 bridges in Mississippi during the period 1938-1994. The drainage area of the selected sites ranged from 60.8 to 5,720 square miles. The measured pier scour depth at these sites ranged from 0.6 to 20.4 ft. The corresponding scour depth to pier width ratio was 0.25 and 4.86 respectively. Melville (1997) model is based on extensive laboratory and field data collected over a period of 25 years. The tests were mostly performed in the University of Auckland, New Zealand (Melville and Sutherland 1988; Melville 1992, Dongol 1994). The model includes a number of factors (e.g. flow intensity, sediment size) that influences scour. The values of these factors are determined from the envelope curve fitted to the data (Melville 1997; Sheppard et al. 2011). The latest update of HEC-18 model by Arneson et al. (2012) is the most widely used pier-scour prediction model; the US Federal Highway Administration (FHWA) recommends its use for estimating equilibrium

scour depth. The initial HEC-18 model, known as Richardson et al. (1995) model was developed based on a subset of the data collected by Chabert and Engeldinger (1956) and Shen et al. (1966). The subset database consisted of data from laboratory testing on sediments with median grain size, d_{50} ranging from 0.24-0.52 mm. Thereafter, and based on the studies of Melville and Sutherland (1988) and Jain and Fisher (1979), limits on the maximum scour depth based on Froude number was imposed. Briaud (2014) model is based on data from 94 laboratory flume testing, as well as dimensional analysis. The d_{50} ranged from 0.10-0.60 mm. The critical shear stress of the bed material varied from 0.1 to 0.8 Pa. The SC envelope (2018) model is developed based on 141 field scour measurements taken from piedmont and coastal plains of South Carolina with pier scour ranging from 1.7-16.9 ft. The d_{50} ranged from 0.5-1.7 mm. The drainage area ranged from 17.2-9360 square miles.

Data for analyses

Benedict and Caldwell (2014) collected scour data from 23 states within the United States, Canada, China, New Zealand, Nigeria, Russia, and Yugoslavia. The database includes a total of 569 laboratory, and 1,858 field scour measurements. Data reported in Benedict and Caldwell (2014) can be classified into two categories: dataset from clear water scour and another from live bed scour. The five deterministic models considered in the study emphasize different factors that influence pier scour. As such, any missing information related to one or more of the variables that a deterministic model considers will impair the scour depth calculation using the specific model. Therefore, an initial screening was performed on the database, and those sites that lacked any of the parameters necessary to compute scour depth were not further considered. The initial screening yielded 1,319 usable field scour measurements, while the laboratory database did not have any missing information. Among the 1,319 field scour measurements, data from 469 sites have clear water condition, whereas data from 850 sites have live bed condition. For the 569 laboratory measurements, data from 340 sites have clear water condition, and data from 229 sites have live bed condition. The study herein is focused on the live bed laboratory and field data; while analyses on the clear water datasets have been presented elsewhere in Shahriar et al. 2021b. The ranges of the selected variables for the live bed laboratory and field data, including pier width, upstream flow depth, approach flow velocity, median grain size, and measured scour depth are presented in Tables 1 and 2. The values in Tables 1, and 2 reflect the minimum, median, and maximum values for a given variable within the database. It is important to note that the data across a single row do not correspond to each other; i.e., the minimum, median, and maximum values across one row are not for a specific site. These values rather indicate the minimum, median, and maximum values of the specified variable within the whole database.

Data screening

While laboratory investigations on pier scour evolution processes are performed under well-controlled environment, relatively accurate representation of downscaled parameters including pier width, flow depth, flow velocity, and scour depth, field observations do come with

some limitations. The uncertainties associated with field data might include (i) the accuracy of measured scour (depending on the tool used like Ground Penetrating Radar, soundings with fathometers, survey levels etc.), (ii) maturity of scour depth (the measured scour might not reflect the equilibrium scour depth), and, (iii) accuracy of hydraulic properties (depending on the method used to approximate, like based on historical information, based on one-dimensional flow models). However, the collected database parameters might not contain all the descriptions regarding the associated uncertainties. Sheppard et al. (2014) concluded that identification of outliers in the field data sets might not always be possible owing to the unknown nature of whether the measured scour depth represents equilibrium scour depth values for the specified flow, sediment, and structure conditions. Therefore, statistical measures, and when applicable, site-specific observations are necessary to identify outliers.

Error in models' estimation is a parameter that can be considered to quantify adequacy of a given deterministic model. Error is defined as the difference between the predicted and the measured scour depth, expressed as a percentage of the measured scour depth, as shown in Equation (1):

$$Error, \% = \frac{y_{sp} - y_{sm}}{y_{sm}} \times 100\% \quad (1)$$

Where, y_{sp} and y_{sm} are the predicted and measured scour depths respectively. A positive error magnitude indicates that the deterministic model is over-predicting the “measured” value and conversely, a negative error is indicative of under-prediction. Figure 1 shows the distribution of Error for the five deterministic models (corresponding to the field data) considered herein, on the basis of prediction associate with database parameters. It is apparent that the error varied within a wide range (-100% to 4840%) for all the five models. It is noted that the pattern of over-prediction is very similar in some regions, with the peak errors corresponding to each model are occurring usually at the similar test sites. Although for the five deterministic models different parameters were utilized in their development, the over-prediction trend is similar. This might be an indication that the measured scour depth values in the database were not the equilibrium scour depths. The high peaks of the error magnitude increase the average error for the deterministic model, which might not be a representative performance of a given model. To ascertain possible dependence of high error magnitudes on the pier scour influencing factors, the relationship between error magnitude and four variables, viz. effective pier width, upstream flow depth to pier width ratio, upstream mean flow velocity to critical velocity, and effective pier width to median grain size ratio is investigated. Figure 2 shows the typical relationship for HEC-18 (2012) model. The data points are classified into three segments, with Error<0% (under-prediction from the model), Error= 0-500%, and Error>500%. Figure 2 does not suggest a discernible trend of relationship between error magnitude and the considered parameters throughout the range of error magnitude. In addition, as pointed out before, the measured scour depth may not represent the equilibrium scour depth, thus relating error to the explanatory variables might not provide a representative relation. Subsequently, a statistical outlier identification technique was adopted. Figure 3 presents the error

box-plot for the five models considered herein. As evident from Figure 3, all the five models have positive outliers. Wilson (1995), Melville (1997), HEC 18 (2012), Briaud (2014), and SC envelope (2018) models show 48, 54, 41, 54, and 45 outliers respectively. These outliers were considered unreasonable data and were eliminated from further analyses herein.

The next criterion applied to identify the “unreasonable” data was the magnitude of the measured scour depth being equal to the accuracy tolerance of the measurement instrument. Through these screening processes, the number of field live-bed scour data count was reduced to 758, which was considered for further analyses. Important to note that the analyses to be performed are predicated upon the assumption that the “field measurements” being at equilibrium level. The data screening process described herein, while does not assure that all field scour data represent equilibrium, is used to eliminate values most likely not to represent equilibrium condition.

To ascertain if data points with some specific trend has been excluded or not, the relationship between effective pier width, upstream flow depth to pier width ratio, upstream mean flow velocity to critical velocity, and effective pier width to median grain size ratio with the error magnitude is explored. Figure 4 shows the typical relationship when HEC 18 model is used. The data points entail the 41 data that was screened out through the outlier identification technique. Figure 4(a) suggest that most of the excluded data has an effective pier width < 20 ft. Refer to Figure 2(a-c), 824 data points out of the total 850 data points (97%) had an effective pier width < 20 ft, thereby suggesting that the excluded data points are dispersed within the range of effective pier width investigated. Melville and Coleman (2000) suggested that pier scour flow field can be classified into three categories, i) $y/b < 0.2$, (ii) $0.2 \leq y/b \leq 1.4$, and (iii) $y/b > 1.4$ (y , and b are upstream flow depth and effective pier widths respectively). It is also established that the data points corresponding to wide pier ($y/b < 0.2$) is scarce. In the present study as well, among the 850 field cases, only 10 sites had a wide pier condition. Figure 4(b) suggest that among the 41 data points excluded, only one had a wide pier condition, while the rest 40 sites had $y/b > 0.2$. Figure 4(c) suggest that the excluded data points had a $v/v_c < 6$, while among the 850 live bed data points (refer to Figure 2g-i), 814 data points (96%) had a $v/v_c < 6$. Therefore, any dependence of the excluded data points on v/v_c is not discerned, rather the excluded data points are dispersed within the range of v/v_c investigated. Lee and Sturm (2009) experimentally noticed that smaller value of b/d_{50} can impede the scour progression. Ettema et al. (2017) observed that if the $b/d_{50} < 8$, individual particles are so large relative to the pier that scour occurs due to erosion at pier sides, and yields a reduced scour magnitude. However, the considered database entailed only one site with $b/d_{50} < 8$ (Figure 2k), and the excluded data points had b/d_{50} ranging from 32 to 39200. Therefore, it can be concluded that the excessive over-prediction (based on the screening process) was not related to any site-specific attribute, rather can be related to the fact that the reported scour depths might not be the equilibrium scour magnitudes.

Accuracy and conservatism analyses

A perfectly accurate scour prediction model would be one that yields a predicted scour depth that is equal to the measured scour depth in the field. As the scour processes depend on multiple factors, it is unlikely a deterministic model would exactly predict the measured scour depth for varying hydraulic, structural, and geotechnical conditions.

A perfectly reliable scour prediction model would be the one that never yield a predicted scour depth that is less than the measured scour depth in the field. Tan and Duncan (1991) adopted similar logic while assessing the performance of the deterministic models to estimate the settlement of footings on sand.

In this study, accuracy was measured in terms of Mean Absolute Percentage Error (MAPE). For each of the data sets, the absolute percentage error was calculated, and the mean value of the error was reported as the MAPE associated with a specific deterministic model. Conservatism was defined as the ratio of the number of cases the calculated scour depth is more than the measured scour depth, expressed as percentage of the total number of data sets.

Analyses with laboratory data

The results of the MAPE, and level of conservatism of the five deterministic models are presented in Figure 5(a). Except for SC envelope (2018) model, values of MAPE ranged from 23.5% to 59.8%, whereas, conservatism ranged from 28.4% to 97.8%. SC envelope (2018) model presented a MAPE of 1218%. Wilson (1995) model provided the least error; however, the model was also least reliable (28.4%). Briaud (2014) model under-predicted the measured scour depth in 18.3% of the number of data points. SC envelope (2018) model provided a 100% reliable estimate of the scour depth, while among the rest models, Melville (1997) model provided the most reliable scour depth, under-predicting the measured scour depth in 2.2% occasions. The associated MAPE for Melville (1997) model is 59.8%. HEC 18 (2012) model provided an error of 53.1%, however presented a conservatism of 95.2%, which is more than the conservatism levels of Wilson (1995), and Briaud (2014) models.

The accuracy and conservatism of a given model can be adjusted by multiplying the scour depth computed from the deterministic model by a factor. Figure 6(a) demonstrates the relationship between MAPE and conservatism when a multiplication factor is applied for the five models considered herein. When the factor is applied to the predicted scour depth, y_{sp} from any of the five deterministic model, refer to Equation (1), the difference between y_{sp} and y_{sm} increases, while the denominator y_{sm} remains the same, leading to an increase in the MAPE magnitude. However, at the same time, a deterministic scour prediction which was unconservative initially (without application of a modification factor), may become conservative, leading to an increase in the conservatism of the estimation (in the sense of the scour magnitude estimated during the design phase is not exceeded.) For example, Briaud (2014) model has a MAPE and conservatism of 47.6% and 81.7% respectively (refer to Figure 5a). If the values of calculated scour depth for all the 229 cases is multiplied by a factor of 1.4, the MAPE increases to 101.1%, while the conservatism increases to 99.1%. Multipliers ranging from 1 to 2 were applied and corresponding MAPE and

conservatism are calculated and presented. It is apparent that there is a tradeoff between MAPE and conservatism. Improvement of conservatism through application of the modification factors involves an increase in the overall MAPE of a model. For Melville (1997), HEC 18 (2012) and Briaud (2014) models, application of a multiplying factor of 1.4 to the calculated scour depth leads to a conservatism of >99%. For Wilson (1995) model, application of a multiplying factor of 2.0 leads to a conservatism of 98.3% from 28.4% (with no multiplication factor applied). The MAPE increases from 23.5% to 85.2% in the process. For SC envelope (2018) model, such modification factor cannot be proposed owing to the fact that the model, in the present form provides a 100% reliable estimate when laboratory data is considered. Selection of the multiplier is dependent on the desired level of *Accuracy* and *Level of conservatism*. For example, if it desired to select a model that provides 98% conservatism, then any of the five deterministic models in this study can be selected; albeit, each prediction should be multiplied with different factors. If Wilson (1995), Melville (1997), HEC 18 (2012), or Briaud (2014) model is selected, the prediction from the respective deterministic model should be multiplied by a factor 1.70, 1.0, 1.18, and 1.3 respectively (refer to Figure 6(a), the abscissa corresponding to 98% conservatism ordinate). The corresponding MAPE from these models are 59%, 59%, 75% and 98% respectively (refer to Figure 6(a), the secondary axis ordinates corresponding to the multiplying factors). Now, if it is also desired to select a model that provides the minimum MAPE (with 98% conservatism), then Wilson (1995), and Melville (1997) models are the potential candidate options to be selected.

Analyses with field data

When the field scour measurement data are considered, the conservatism -MAPE relation changes. The variation of conservatism and MAPE is depicted in Figure 5(b). In contrast to the relation using the laboratory measurements, the use of field measurements yields a higher MAPE (except for the SC envelope model), which is understandable in view of the limitations of field measurements not necessarily being at equilibrium. SC model is developed based on enveloping the upper bound of the field measured scour depth considering the effective pier width only, which in turn may not capture the downscaled (in laboratory) pier scour affecting parameters. The use of SC model resulted in a significantly high error (1218%) in laboratory case compared to the field case (322%). Conservatism varied from 93.3% to 97.5%, while MAPE ranged from 205.6% to 322%. SC envelope (2018) model presented the most reliable estimate (97.5%), at the same time provided the highest MAPE, 322%. Melville (1997) model provided a MAPE of 319%; however, the associated conservatism is 95%. Although HEC 18 (2012) model showed the least reliable estimate among the five models being considered, its conservatism is still 93.3%. It is important to note that when the laboratory data were considered, Wilson (1995) model presented a conservatism of only 28.4%, while for field measurement associated conservatism increased to 95.1%. Wilson (1995) model considers the upstream flow depth to effective pier width ratio (y/b) as the only parameter influencing the scour depth measurement. It is congruent with the approach Wilson (1995) followed, who used field measurements from 22 bridges to develop the model.

Therefore, while the use of the y/b ratio captures the field conditions well, it is possible it cannot represent the laboratory hydraulic and geometric conditions properly.

A similar technique, as described in the previous section was adopted to estimate the conservatism and MAPE when the predicted scour depth is multiplied by a factor. The variation of conservatism and MAPE when a multiplying factor is applied is presented in Figure 6(b). For all the five models considered in the study, application of a multiplying factor of 1.6 ensured a conservatism $>99\%$. The associated MAPE for Wilson (1995), Melville (1997), HEC 18 (2012), Briaud (2014), and SC envelope (2018) models are 386%, 567%, 386%, 443%, and 574% respectively.

Benedict et al. (2018) reported that the SC envelope model is applicable for nominal pier widths less than or equal to 6. While Figure 5(b) contains 117 data points that have $b >6$ ft, Figure 5(c) is developed considering the data points that have $b \leq 6$ ft. The conservatism magnitudes in Figure 5(b) and 5(c) differ by only 1%. In regards to MAPE, when the limit on SC envelope model is imposed (Case with 641 data sets), the MAPE increased from 322% to 349% (for SC model).

Statistical model

Figure 7 shows the relationship between the predicted and the measured scour depths when laboratory and field scour measurements are considered using the five models investigated herein. It is apparent in general that the deterministic models have the tendency to over-predict the measured scour depth. The use of Wilson (1995) model yielded the maximum number of under-predicted scour depth cases when laboratory data are considered (Figure 7a), which agrees with the low conservatism shown in Figure 5(a). Observation of Figure 7 reveals that the scatter of the data is not uniform, which leads to non-constant variance, statistically known as heteroscedasticity (Stone 1996). Figure 8 presents the residuals versus fitted value plot for the five models considered herein. Residual in this case is defined as the difference between measured and predicted values obtained from the best-fit curve, which is a linear expression between the measured and the predicted values. The disproportionate scatter in positive and negative sides of residuals suggest that the datasets have heteroscedasticity, with such observation being prominent for field measurements (Figure 8f-j). The standardized residuals versus theoretical quantile plot suggest that the dataset has left-skewness (e.g. Figure 8f, 8g, 8h), and long-tailed distribution (e.g. Figure 8a, 8b, 8c, 8d, 8i); indicating that a linear relationship between the predicted and the measured normalized scour depth is not adequate. Therefore, a statistically robust model needs to be selected that can address the heteroscedasticity and non-normal error. Accordingly, the method suggested by Box and Cox (1964), commonly referred to as Box-Cox method, is adopted for this purpose. The main objective of applying the Box-Cox transformation to the database is, after the transformation, the following is obtained:

- (i) The error variance is constant (homoscedasticity)
- (ii) The observations are normally distributed

- (iii) A model, which is linear in the independent variable, can represent the expected value of the transformed response, i.e. no interaction terms are required.

The probabilistic model, considering the scatter in scour prediction is formulated as in Equation 2a.

$$f\left(\frac{y_{sp}}{b}, \lambda\right) = k \frac{y_{sm}}{b} + \vartheta + \xi \quad (2a)$$

Where, b denotes the effective pier width; κ , ϑ , and λ are constant terms depending on the deterministic model being considered, and ξ is the residual error term. And,

$$f\left(\frac{y_{sp}}{b}, \lambda\right) = y^{(\lambda)} = \frac{(y_{sp}/b)^\lambda - 1}{\lambda} \quad (2b)$$

To estimate the parameter λ , the large-sample maximum likelihood theory (Equation 6c) is adopted.

$$\frac{1}{(2\pi)^{\frac{n}{2}} \sigma^n} \exp \left\{ -\frac{(y^{(\lambda)} - E\{y^{(\lambda)}\})'(y^{(\lambda)} - E\{y^{(\lambda)}\})}{2\sigma^2} \right\} \prod_{i=1}^n \left| \frac{dy_i^{(\lambda)}}{dy_i} \right| \quad (2c)$$

Where, n is the total number of observations, $y^{(\lambda)}$ is the column vector of transformed observations, $E\{y^{(\lambda)}\}$ is the expected value of $y^{(\lambda)}$, $(y^{(\lambda)} - E\{y^{(\lambda)}\})'$ is the transpose of the vector $y^{(\lambda)} - E\{y^{(\lambda)}\}$, and σ^2 is the variance of data.

The computed parameters for Wilson (1995) model, Melville (1997) model, HEC-18 (2012) model, Briaud (2014) model, and SC envelope (2018) model are presented in Tables 3 and 4 for laboratory data and field data, respectively. The R^2 of the fitted models vary from 0.15 for SC envelope (2018) model to 0.46 for HEC 18 (2012) model when laboratory data are considered; while for the field data-based statistics, R^2 vary from 0.12 for Melville (1997) model to 0.32 for Wilson (1995) model. Interpretation of standard error suggest that Wilson (1995) model had the least variance, while SC envelope (2018) model presented the maximum variance when laboratory data are considered. For field scour measurements, SC envelope (2018) model had the least variance, while Melville (1997) model presented the maximum variance. Shahriar et al. (2021) observed that Box-Cox transformation provided the best response while fitting models to the clear-water laboratory scour measurements reported in Benedict and Caldwell (2014). When the live bed laboratory and field measurements are utilized, the trends based on data from the five models considered herein seem to agree with the observation reported in Shahriar et al. (2021b). The distribution of parameter λ is obtained from Figure 9. The 95% confidence limit of the λ parameter is also presented in the same plot. Application of logarithmic transformation for Briaud (2014) model agrees with the observation of Gardoni et al. (2002), and Bolduc et al. (2008), who observed that a logarithmic transformation best depict the scour measurements reported in Gudavalli database (Gudavalli 1997), Landers-Mueller database (Landers and Mueller 1996), and Kwak database (Kwak 2000). However, for the live bed laboratory and field measurements considered herein, application of logarithmic transformation was not effective in reducing heteroscedasticity

and non-normal errors. Referring to Figure 9, if the parameter λ is 0, then the Box-Cox transformation will be converted to the logarithmic transformation form; however, in neither of the cases (laboratory and field), a $\lambda = 0$ was noticed, suggesting logarithmic transformation is not suitable for the large database considered herein. The residual diagnostics of the fitted statistical model are illustrated in Figure 10. It is apparent that the non-normal error has been addressed for most cases except for results from Melville (1997) and HEC 18 (2012) models when applied to the field scour measurement data (Figure 10g and 10h). Although, HEC 18 (2012) model presented a prevalence of short-tailed distribution, the effect of which is minimal in statistical analyses (Devore 1996), the left skewness of Melville (1997) model data could not be reduced significantly. The residuals versus fitted plot of Melville (1997) and HEC 18 (2012) models shows a congregation of data points along a straight line. Melville (1997) suggested a limiting value for the factors being considered in the model, like flow depth-pier size factor, flow intensity factor, sediment size factor. For example, if $b/d_{50} > 25$, then sediment size factor, $K_d = 1$. Similarly, if all the limiting values for each of the factors are reached, the corresponding normalized predicted scour depth converges to 2.4, leading to a congregation of data points, representing the site conditions when the limiting values are reached. HEC 18 (2012) model includes the provision of Froude number $F \leq 0.8$ yields maximum normalized predicted scour depth, $\frac{y_{sp}}{b} = 2.4$; while for $F > 0.8$, the value is 3.0. Therefore, in situations when the HEC 18 (2012) model expression predicted $\frac{y_{sp}}{b} > 2.4$ while $F \leq 0.8$, the predicted normalized scour depth was restricted to be 2.4. A similar explanation is valid for $F > 0.8$, while the HEC 18 (2012) model expression suggests $\frac{y_{sp}}{b} > 3$. These model's limits led to a congregation of data points in the residuals versus fitted plot of HEC 18 (2012) model. The residuals versus leverage plots for the five models suggest that any outliers or influential data points are not prevalent.

Figure 11 shows the relationship between the measured normalized scour depth and fitted model applying the parameters listed in Tables 3 and 4. The data points seem to be well dispersed on either side of the fitted model, although for Melville (1997) and HEC 18 (2012) models, a horizontal congregation of data points are apparent. As described before, this is indicative of sites with conditions that limit the applicability of the respective models. When Melville (1997) model is used, the predicted scour depth is most sensitive to the measured scour depth as indicated by the highest slope, $k = 2.78$ and 1.19 respectively for laboratory and field database respectively.

Bias in the selected models

Figures 12 shows the relationship between probability of occurrence and μ_p for both the laboratory and field database reported scour depth. The μ_p can be defined as the ratio of the reported scour depth in Benedict and Caldwell (2014) to the predicted scour depth from the respective deterministic models (e.g. Wilson model, Melville model, HEC 18 model, Briaud model, SC envelope model). Therefore, if $\mu_p > 1$, the predicted scour depth is less than the reported scour depth in the database, thereby representing an unconservative estimate. In contrast, if $\mu_p < 1$, the predicted scour depth can be considered conservative. A Probability of Deceadance

(POD) is defined as the probability that the predicted scour depth will be less than the measured ones. The POD can be estimated by deducting the probability magnitude corresponding to $\mu_p = 1$ from one. As shown in Figure 12(a), Wilson (1995) model provides the maximum POD (71%), while SC envelope (2018) model provides the minimum POD (0%), which is congruent with the observation from the conservatism-MAPE relation (Figure 5a). However, for field database-related probability estimates, the difference among the PODs for different models studied are not clearly discerned. The PODs corresponding to Wilson, Melville, HEC 18, Briaud, and SC envelope models are 5%, 5%, 7%, 6%, and 2% respectively. The POD values for field database are also reflective of the observation made previously based on conservatism-MAPE response (Figure 5b). Nevertheless, from the probability estimates obtained using laboratory and field data, it is apparent that although in literature the deterministic models are considered overly conservative, at a minimum a 2% POD is associated with any of the deterministic models investigated in the study.

Probability of deceedance-modification factor

Exceedance and deceedance probabilities are a useful way to assess the engineering properties of a deterministic model (NRC 2000). The relationship between probability of deceedance and μ_{POD} , which is the ratio of predicted to the measured scour depth is presented in Figure 13. The figure is developed using a non-parametric process, termed as Kernel density estimation. The frequency distribution of μ_{POD} is initially quantified, leading to the generation of probability density function. Thereafter, cumulative density function is obtained through integration of probability density function. Probability of Deceedance is calculated by deducting the cumulative density function from one. The expected scour depth corresponding to a POD to the measured scour depth can be related by Equation (3).

$$\frac{y_{se}}{b} |_{POD} = \mu_{POD} \frac{y_{smed}}{b} \quad (3)$$

Where, y_{se} is the expected scour depth corresponding to a certain POD, and y_{smed} is the median scour depth obtained considering ξ (residual error term) = zero in Equation 2a.

Figure 13 suggests that as the POD decreases, the modification factor increases. The rate of increase of modification factor increases significantly at $POD < 0.1$ for based on applying the five deterministic models to both laboratory and field data. For comparison, the modification factors proposed in Shahriar et al. (2021b) are also presented in Figure 13. Clear water scour measurements reported in Benedict and Caldwell (2014) was utilized in Shahriar et al. (2021b). Figure 13(a) suggests that the factors proposed for clear water laboratory scour measurements are comparatively higher than the live bed laboratory scour measurements throughout the POD range. The reason can be attributed to the fact that the live bed estimates of the scour depth using the models proposed herein are inherently more conservative than the clear water scour estimates obtained from Shahriar et al. (2021b) model. As a result, to attain a similar POD, the scour estimates from the clear water models need to be multiplied with a higher factor than the one corresponding to the live-bed case. In addition, for the live bed analyses, a μ_{POD} of 1.85 ensure a $POD \leq 0.1$ for all the four models (except SC model), while to ensure $POD \leq 0.1$, a factor ranging

from 2.2-2.6 is required for the clear water analyses based statistics suggested in Shahriar et al. (2021b). A development of POD chart for SC envelope model was not approached owing to the fact that all the scour predictions were conservative while SC model is used (refer to Figure 5a). For rest of the four models corresponding to clear water analyses, the μ_{POD} continued to increase until a $\mu_{POD} = 5$, while for the live bed case, an increase in μ_{POD} beyond a $\mu_{POD} = 3.2$ was not noticed. Interpretation of Figure 13(b) does not suggest a discernible difference between the clear water and live bed μ_{POD} except for HEC 18, Briaud, and SC envelope models in the POD range of 0.10-0.65. The modification factors reported herein for field measurement based statistics are comparatively higher than the modification factors proposed for laboratory measurement based statistics. The higher modification factor, to some extent, can be attributed to the limitation of the field scour measurements. While the laboratory measurements provide a relatively accurate measurements of downscaled parameter associated scour, field measurements may not represent an equilibrium scour depth. Although, through the screening process, the extreme outliers were eliminated from the dataset, there are still possibilities that a non-equilibrium scour measurement remain in the dataset utilized herein, which increased the inherent uncertainty of the model (refer to Figure 1, frequent occurrence of comparatively high errors); thereby increased the value of the developed modification factor, based on the measured field scour data.

Summary and Conclusions

Five bridge scour prediction models are assessed in terms of two statistical parameters, termed Mean Absolute Percentage Error (MAPE, as a measure of accuracy of the prediction), and Level of conservatism (as a measure of conservativeness of the model). Live bed laboratory scour measurements (Data points: 229), and live bed field scour measurements (Data points: 758) are utilized herein. Conservatism is defined as the extent to which prediction from a given model is unlikely to yield a scour depth that is less than the measured scour depth in the field. A statistical model to adjust models' prediction is proposed, the statistical parameters are presented, and applicability of the model is described. Based on the results presented herein, the following conclusions are drawn

1. Except for SC envelope (2018) model, values of MAPE ranged from 23.5% to 59.8% when live bed laboratory data is considered. SC envelope (2018) model presented a MAPE of 1218%. For live bed field data, MAPE ranged from 205.6% to 322% for the five models considered herein.
2. Considering the live bed laboratory data, SC envelope model's estimates provided the highest conservatism factor, whereas Wilson's (1995) model yielded the least conservatism factor. When the live bed field data are considered, SC envelope model provided the most reliable estimate, while HEC 18 (2012) model provided the least reliable scour depth estimate.
3. When the limitation of SC envelope curve approach, which is nominal pier width should be ≤ 6 ft, is imposed, the conservatism values do not differ much (less than 1%). In regards

to MAPE, when the limit on SC envelope model is applied (Case with 641 data sets), the MAPE rather increased from 322% to 349%.

4. The accuracy and conservatism of a specific model are adjusted by multiplying the scour depth computed using a given deterministic model by a modification factor. The proposed modification factors necessary to attain certain conservatism level for the five models considered herein are presented.
5. Deterministic models used for bridge pier scour do not account for inherent model's uncertainties. The scatter associated with the scour prediction produces heteroscedasticity, and non-normal errors. As shown, statistical measures can be developed to reduce the error associated with data distribution.
6. Utilizing both laboratory and field databases, a relationship between probability of exceedance of a given measured scour depth and a modification factor (that is applied into the deterministic prediction) is proposed. The modification factor allows for the use of the deterministic models while quantifying the probability of the computed scour depth being less than or more than the most likely value per measurements reported in the utilized databases.

The proposed approach allows for the selection of a suitable modification factor to satisfy a target probability of exceedance. Using the framework presented herein, it is possible to extend a given deterministic model to assess the probability of exceedance, and to develop associated modification factors for a different set of database. It is important to note that the approach presented herein is developed considering the live-bed laboratory and field datasets reported in Benedict and Caldwell (2014). This dataset is the largest collection of pier scour data available in the United States, with a complete set of parameters to allow for comparative analyses of deterministic models that require different input parameters.

References

- Arneson LA, Zevenbergen LW, Lagasse PF, and Clopper PE. (2012). "Evaluating scour at bridges." Hydraulic Engineering Circular No. 18, 5th edition, 1-340.
- Azamatullah HM, Yusoff MAM, and Hasan ZA (2014). "Scour below submerged skewed pipeline." *Journal of Hydrology*, 509(2014): 615-620.
- Benedict ST, and Caldwell AW. (2014). "A pier-scour database—2,427 field and laboratory measurements of pier scour." U.S. Geological Survey Data Series 845, 1-22.
- Benedict ST, Feaster TD, and Caldwell AW. (2018). "The South Carolina bridge-scour envelope curves (ver. 1.1, January 2018): U.S. Geological Survey Scientific Investigations Report 2016– 5121, 1-96.
- Bolduc LC, Gardoni P. and Briaud J-L. (2008). "Probability of exceedance estimates for scour depth around bridge piers." *Journal of Geotechnical and Geoenvironmental Engineering*; 134:2(175), 175–184.

- Box GEP, and Cox DR. (1964). "An analysis of transformations," *Journal of the Royal Statistical Society*, Series B; 26, 211-252.
- Briaud JL. (2014). "Scour depth at bridges: Method including soil properties. I: Maximum scour depth prediction." *Journal of Geotechnical and Geoenvironmental Engineering*; 141(2): 04014104.
- Briaud J-L, Gardoni P, and Yao C. (2014). "Statistical, risk, and reliability analyses of bridge scour." *Journal of Geotechnical and Geoenvironmental Engineering*; 140(2): 04013011.
- Briaud JL, Ting F, Chen HC, Gudavalli R, Perugu S, and Wei G. (1999). "SRICOS: Prediction of scour rate in cohesive soils at bridge piers." *Journal of Geotechnical and Geoenvironmental Engineering*; 125(4):237-246.
- Briaud J-L, Brandimarte L, Wang J, and D'Odorico P. (2007). "Probability of scour depth exceedance due to hydrologic uncertainty." *Georisk: Assessment and Management of Risk for Engineered Systems and Geohazards*; 1(2), 77–88.
- Chabert J, and Engeldinger P. (1956). "Etude des affouillements autour des piles des ponts." Laboratoire d'Hydraulique, Chatou, France (in French).
- Dongol DMS. (1994). "Local scour at bridge abutments." *Report No. 544*, School of Engineering, The University of Auckland, New Zealand.
- Devore JL. (2012). *Probability and Statistics for Engineering and the Sciences*, 8th Edition, Brooks/Cole Cengage Learning, Boston, MA, USA.
- Ettema R, Constantinescu G, and Melville BW. (2017). "Flow-field complexity and design estimation of pier-scour depth: Sixty years since Laursen and Toch." *Journal of Hydraulic Engineering*; 143(9), 03117006.
- Florida Department of Transportation (FDOT) (2011). "Bridge Scour Manual," Tallahassee, FL.
- Gardoni P, Der Kiureghian A, and Mosalam KM. (2002). "Probabilistic capacity models and fragility estimates for reinforced concrete columns based on experimental observations." *Journal of Engineering Mechanics*; 128(10), 1024–1038.
- Gudavalli SR. (1997). "Prediction model for scour rate around bridge piers in cohesive soil on the basis of flume tests." Ph.D. dissertation, Department of Civil Engineering, Texas A&M University, College Station, Texas.
- Hunt D. (2009). "Monitoring scour critical bridges." NCHRP synthesis 396. Washington, D.C.: Transportation Research Board.
- Jain SC, and Fischer EE. (1979). "Scour around bridge piers at high Froude numbers." *Report No. FH-WA-RD-79-104*, Federal Highway Administration, Washington, D.C.
- Johnson PA, Clopper PE, Zevenbergen LW and Lagasse PF. (2015). "Quantifying uncertainty and reliability in bridge scour estimations." *Journal of Hydraulic Engineering*; 141(7), 04015013.

- Kwak K. (2000). "Prediction of scour depth versus time for bridge piers in cohesive soils in the case of multi-flood and soil systems." Ph.D. dissertation, Department of Civil Engineering, Texas A&M University, College Station, Texas.
- Landers MN, and Mueller DS. (1996). "Channel scour at bridges in the United States." *Report No. FHWA-RD-95-184*, Federal Highway Administration, Washington, D.C.
- Lee SO, Sturm TW. (2009). Effect of sediment size scaling on physical modeling of bridge pier scour. *Journal of Hydraulic Engineering, ASCE*, 135(10), 793–802.
- Liang FY, Zhang H, and Huang MS. (2015). "Extreme scour effects on the buckling of bridge piles considering the stress history of soft clay." *Natural Hazards*; 77, 1143–1159.
- Melville BW. (1992). "Local scour at bridge abutments." *Journal of Hydraulic Engineering*; 118(4), 615-630.
- Melville BW. (1997). "Pier and abutment scour: Integrated approach." *Journal of Hydraulic Engineering*; 123(2), 125–136.
- Melville BW. and Coleman SE. (2000). "Bridge scour." Highlands Ranch, USA: Water Resources Publications.
- Melville BW. and Sutherland AI. (1988). "Design method for local scour at bridge piers." *Journal of Hydraulic Engineering*; 114(10), 1210-1226.
- Mueller DS. (2000) "National bridge scour program-measuring scour of the streambed at highway bridges." Reston, VA: U.S. Geological Survey.
- National Research Council. (2000). *Risk Analysis and Uncertainty in Flood Damage Reduction Studies*. Washington, DC: The National Academies Press.
- Rhodes J, and Trent R. (1993). "Economics of floods, scour and bridge failures." In: Shen HW, Su ST, Wen F, editors. Proceedings of 1993 ASCE conference hydraulic engineering '93. San Francisco, CA.
- Richardson EV, and Davis SR. (1995). "Evaluating scour at bridges," Report No. FHWA-IP-90-017, Hydraulic Engineering Circular No. 18 (HEC-18), 3rd Edition, Office of Technology Applications, HTA-22, Federal Highway Administration, U.S. Department of Transportation, Washington, D.C.
- Shahriar AR, Ortiz AC, Montoya BM, and Gabr MA (2021a). "Bridge Pier Scour: An overview of factors affecting the phenomenon and comparative evaluation of selected models," *Transportation Geotechnics*, doi.org/10.1016/j.trgeo.2021.100549.
- Shahriar AR, Montoya BM, Ortiz AC and Gabr MA (2021b). "Quantifying probability of exceedance estimates of clear water local scour around bridge piers," *Journal of Hydrology*, 597(126177). DOI: doi.org/10.1016/j.jhydrol.2021.126177.
- Shen HW, Schneider VR, and Karaki SS. (1966). "Mechanics of local scour." *Report*, U.S. Dept. of Commerce, National Bureau of Standards, Inst. for Appl. Technol., Washington, D.C.

- Sheppard M, Demir H, and Melville BW. (2011). "Scour at wide piers and long skewed piers," NCHRP Report 682, Transportation Research Board of the National Academies, Washington D.C.
- Sheppard M, Melville B, and Demir H. (2014). "Evaluation of existing equations for local scour at bridge piers." *Journal of Hydraulic Engineering*; 140(1), 14–23.
- Shirole AM, and Holt RC. (1991). "Planning for a comprehensive bridge safety assurance program." *Transportation Research Record*, Washington DC: Transport Research Board; 137-142.
- Stone JC. (1996). *A course in probability and statistics*, Duxbury Press, 1st Edition, Belmont, California.
- Tan, CK. and Duncan JM. (1991). "Settlement of footings on sands- Accuracy and reliability," in Proceedings of the Geotechnical Engineering Congress, Jun 10-12 1991, Boulder, USA, Published by ASCE, NY, USA, p. 446-455.
- Yao C. (2013). "LRFD calibration of bridge foundations subjected to scour and risk analysis." Ph.D. dissertation, Department of Civil Engineering, Texas A&M University, College Station, Texas.
- Wardhana K, Hadipriono FC. (2003). "Analysis of recent bridge failures in the United States." *Journal of Performance of Constructed Facilities*; 17(3), 144-150.
- Wilson KV Jr. (1995). "Scour at selected bridge sites in Mississippi." *Resources Investigations Report 94-4241*, Geological Survey Water, Reston, Virginia.

Table 1. Range of some selected variables associated with live bed laboratory data in Benedict and Caldwell (2014)

Parameter	Pier width normal to the flow, b (ft)	Approach flow velocity, v (ft/s)	mean Approach depth, y (ft)	flow Median grain size, d_{50} (mm)	Measured pier-scour depth, y_{sm} (ft)
Minimum	0.094	0.76	0.131	0.22	0.049
Median	0.167	2.03	0.558	0.6	0.292
Maximum	3.001	7.08	4.003	3.2	2.2

Table 2. Range of some selected variables associated with live bed field data in Benedict and Caldwell (2014)

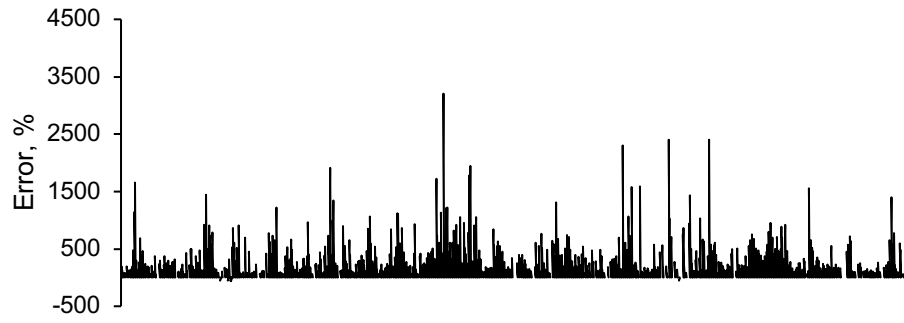
Parameter	Pier width normal to the flow, b (ft)	Approach flow velocity, v (ft/s)	mean Approach depth, y (ft)	flow Median grain size, d_{50} (mm)	Measured pier-scour depth, y_{sm} (ft)
Minimum	0.80	1.20	0.50	0.001	0.10
Median	4.28	4.10	13.05	0.49	2.50
Maximum	94.17	15.00	73.90	73.00	34.10

Table 3. Calculated parameters in Equations (2a-b) for the five models considered in the study (Laboratory data)

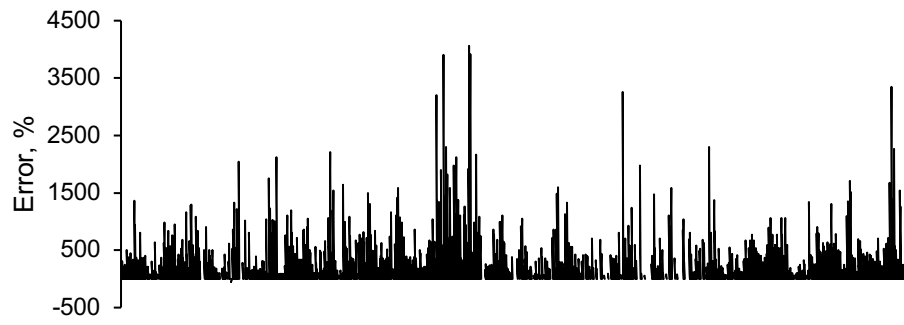
Reference	Parameter			Statistics				
	λ	k	ϑ	Significance level	Standard error	Median residual error	F statistic	R^2
Wilson (1995)	0.67	0.432	-0.358	0.01	0.31	-0.02	78.42	0.26
Melville (1997)	4.0	2.78	2.52	0.01	1.86	0.57	90.7	0.28
Arneson et al. (2012)	2.12	1.69	-0.32	0.01	0.77	-0.038	194.3	0.46
Briaud (2014)	0.61	0.58	0	0.01	0.48	-0.047	58.25	0.20
SC envelope (2018)	0.55	2.36	3.49	0.01	2.35	-0.0038	40.83	0.15

Table 4. Calculated parameters in Equations (2a-b) for the five models considered in the study (Field data)

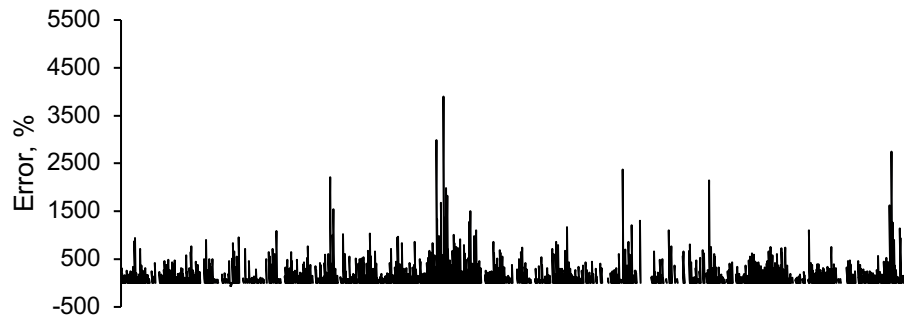
Reference	Parameter			Statistics				
	λ	k	ϑ	Significance level	Standard error	Median residual error	F statistic	R^2
Wilson (1995)	0.48	0.574	0.20	0.01	0.61	0.015	365.4	0.32
Melville (1997)	4.0	1.19	5.77	0.01	2.39	1.08	101.6	0.12
Arneson et al. (2012)	1.64	0.55	0.59	0.01	0.68	-0.001	265.7	0.26
Briaud (2014)	0.42	0.37	0.42	0.01	0.53	0.011	201.7	0.21
SC envelope (2018)	-0.48	0.135	0.48	0.01	0.26	-0.021	114.8	0.13



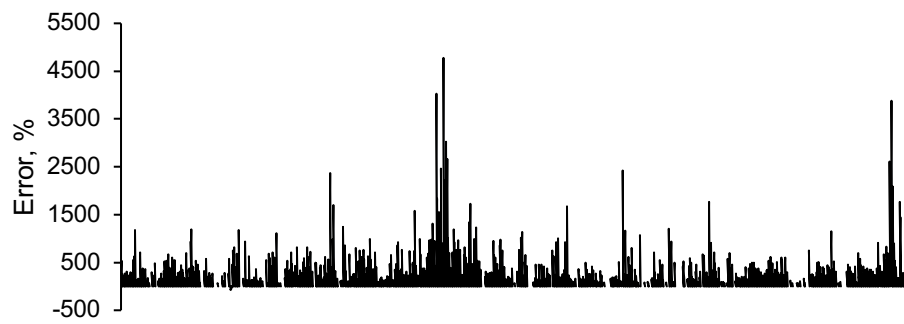
(a)



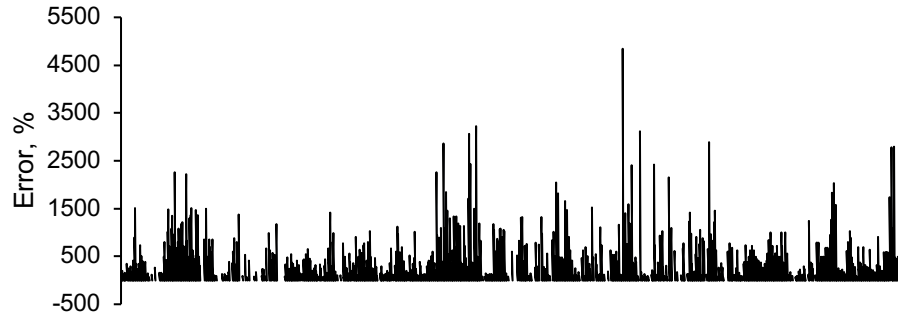
(b)



(c)

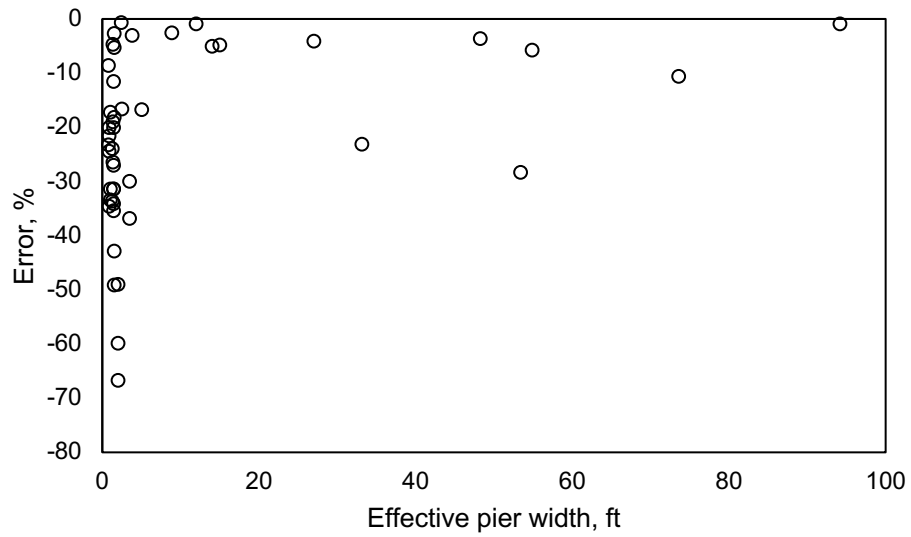


(d)

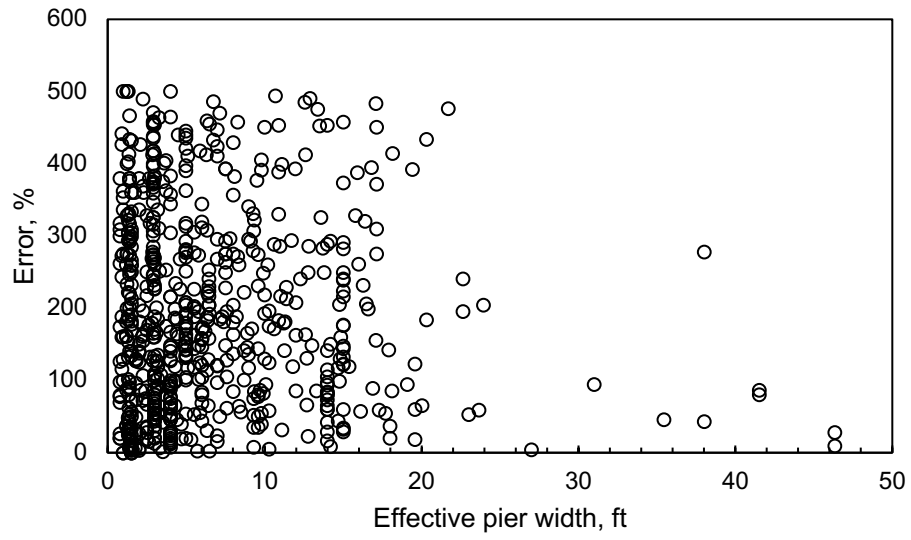


(e)

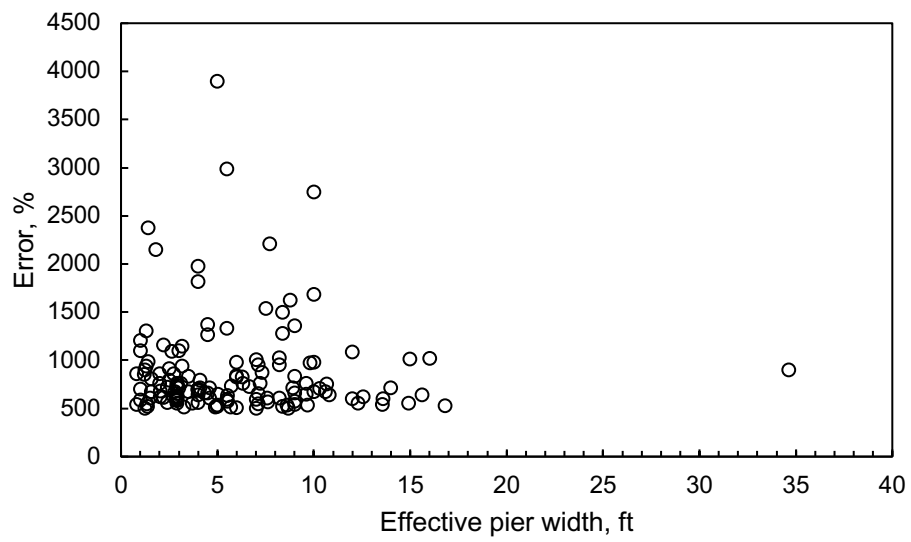
Figure 1: Error distribution considering live bed field datasets (Data count: 850) for (a) Wilson 1995, (b) Melville 1997, (c) HEC 18 2012, (d) Briaud 2014, (e) SC Envelope (2018) models



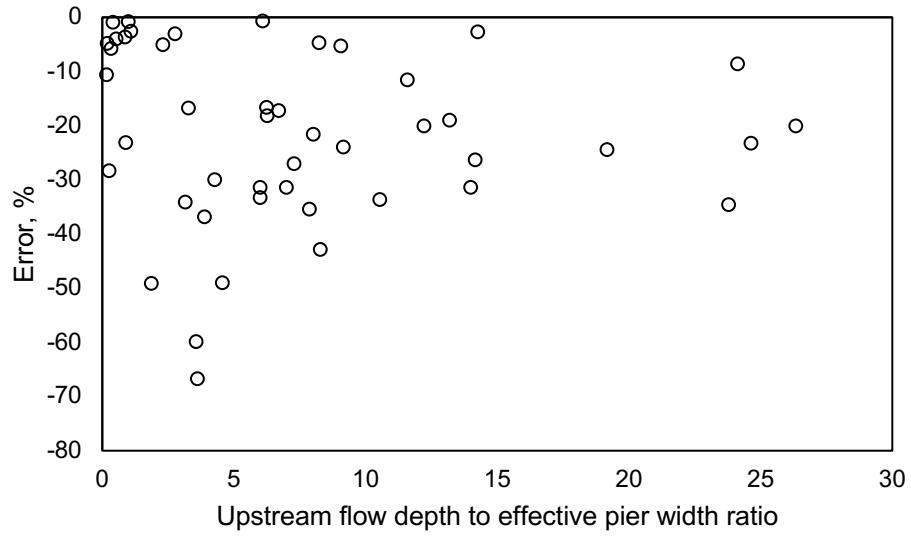
(a)



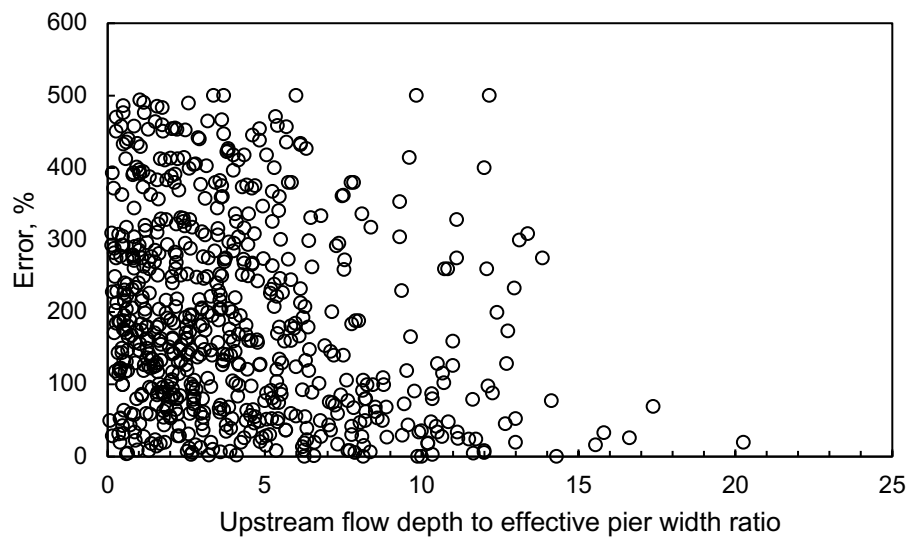
(b)



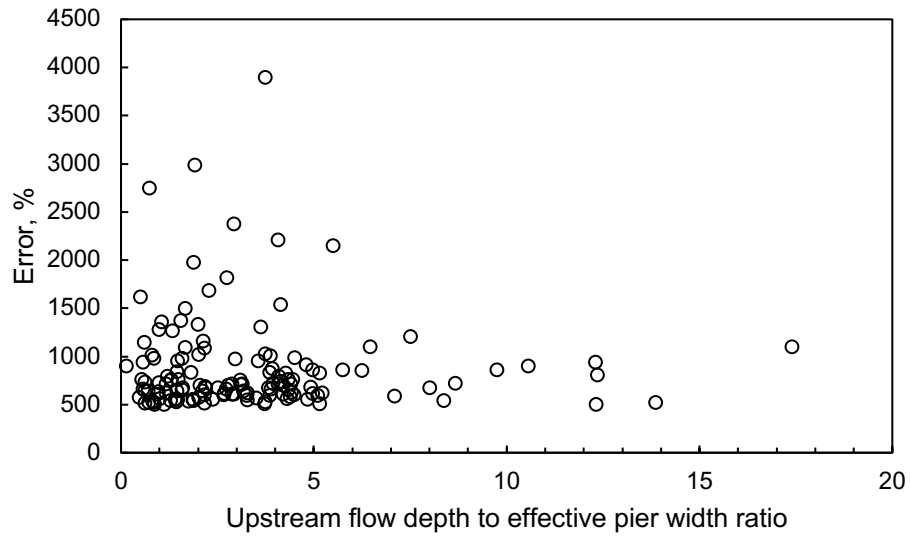
(c)



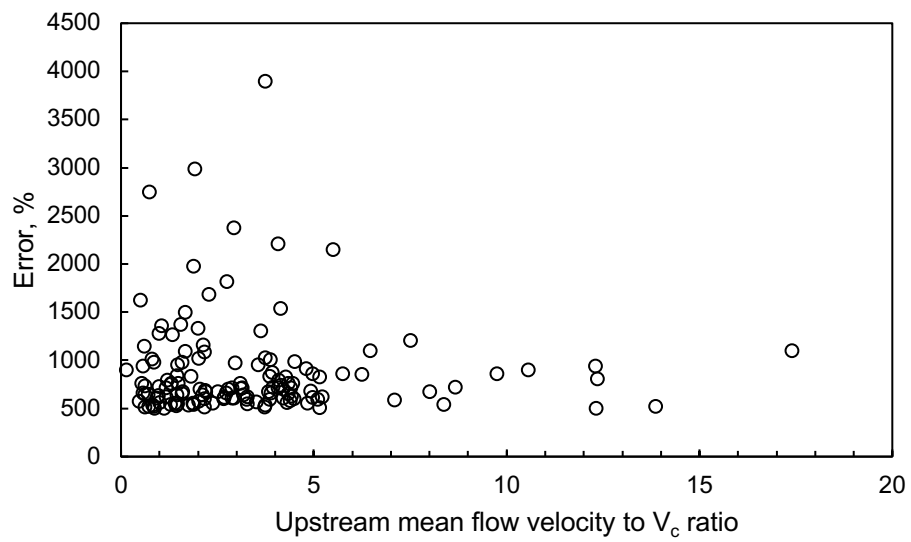
(d)



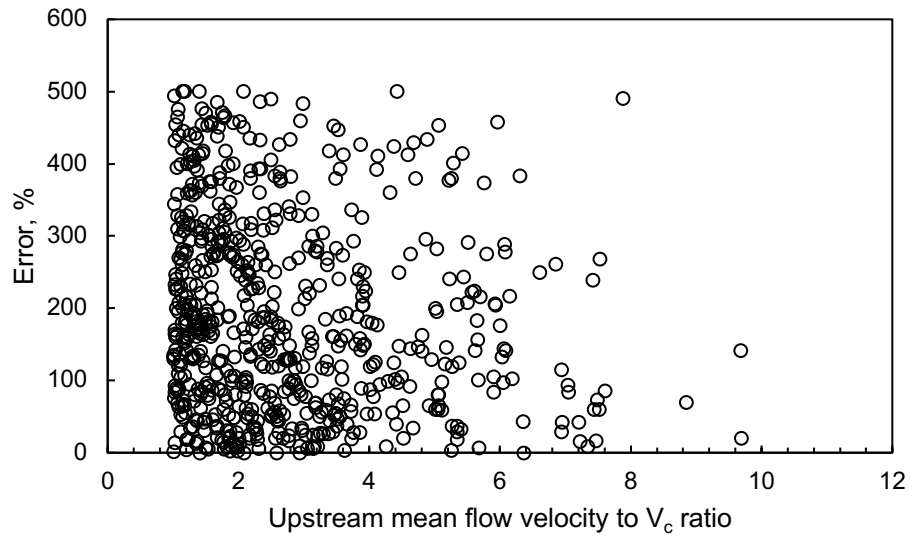
(e)



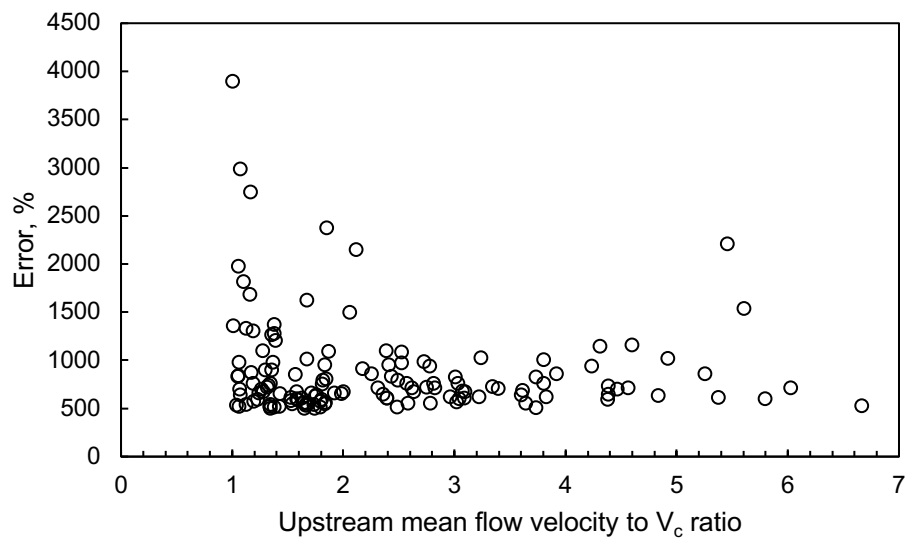
(f)



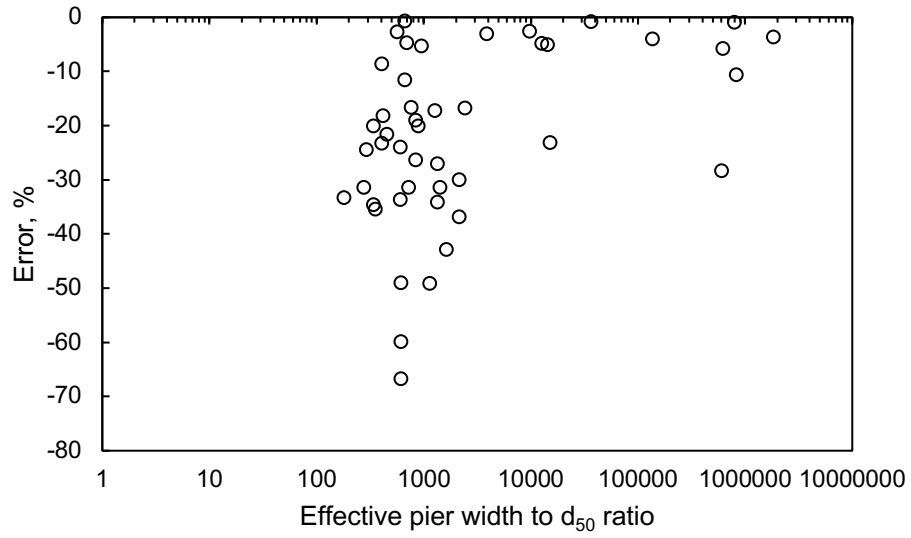
(g)



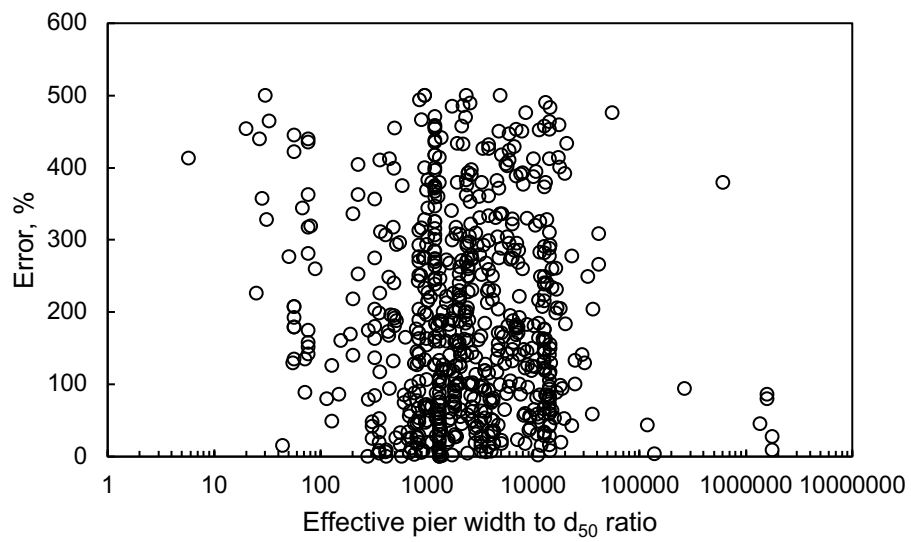
(h)



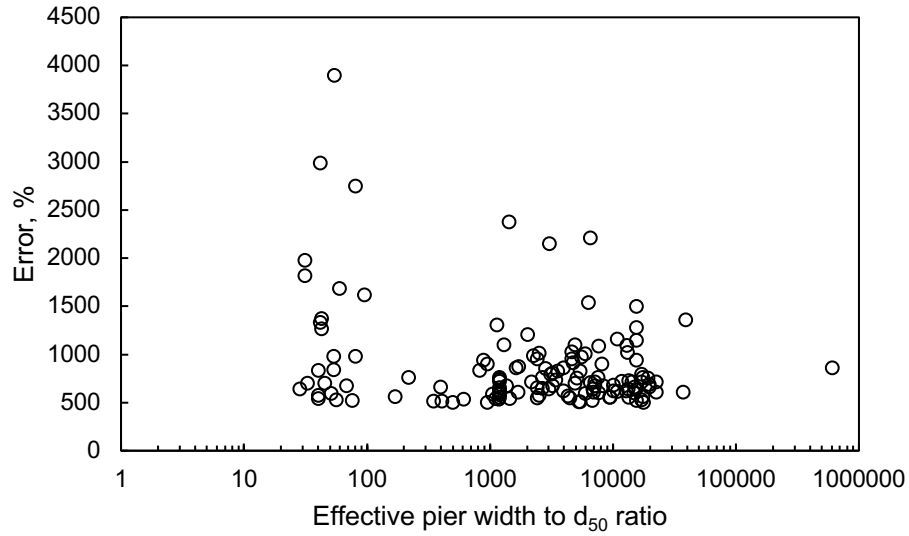
(i)



(j)



(k)



(l)

Figure 2: Relationship between error magnitude and (a-c) Effective pier width, (d-f) Upstream flow depth to pier width ratio, (g-i) Upstream mean flow velocity to the critical velocity, and (j-l) Effective pier width to median grain size ratio when HEC-18 (2012) model is used

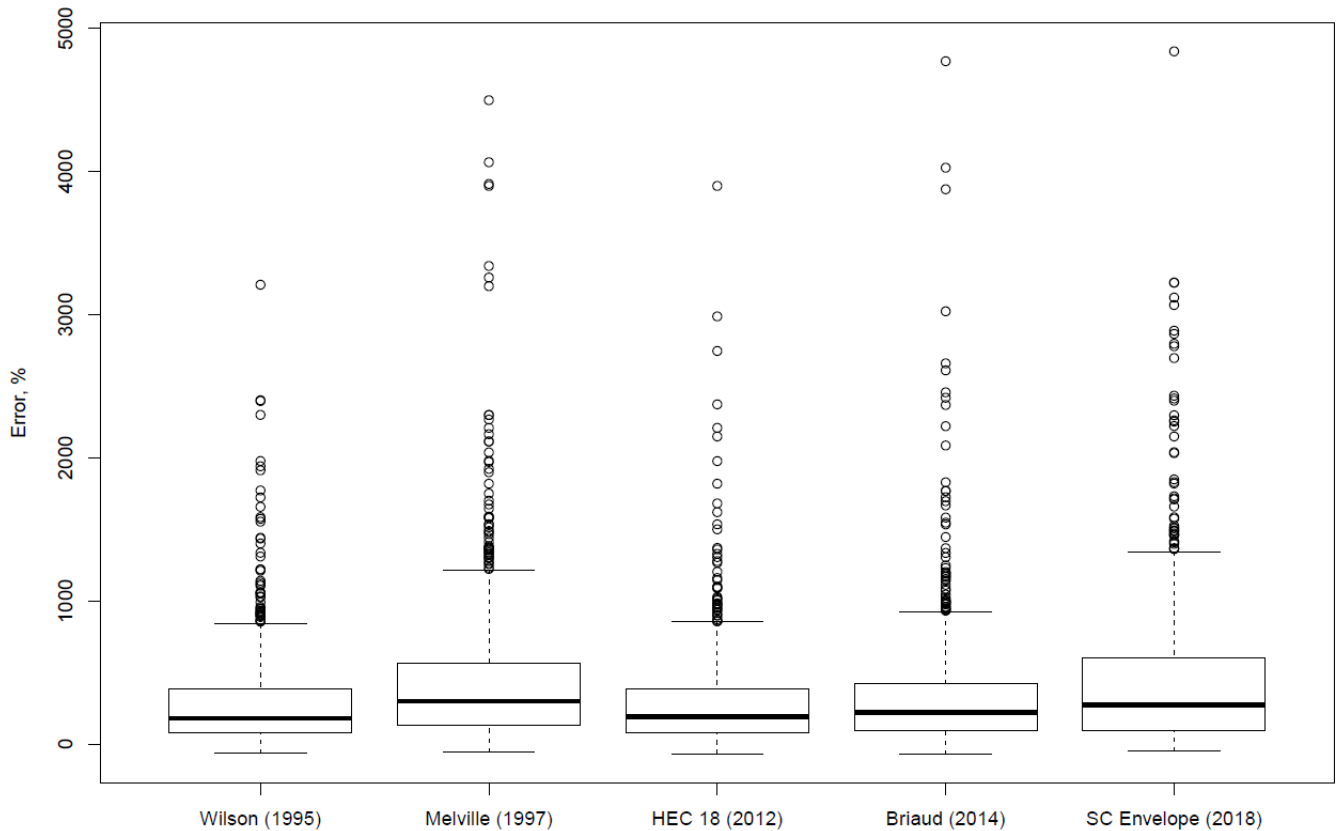
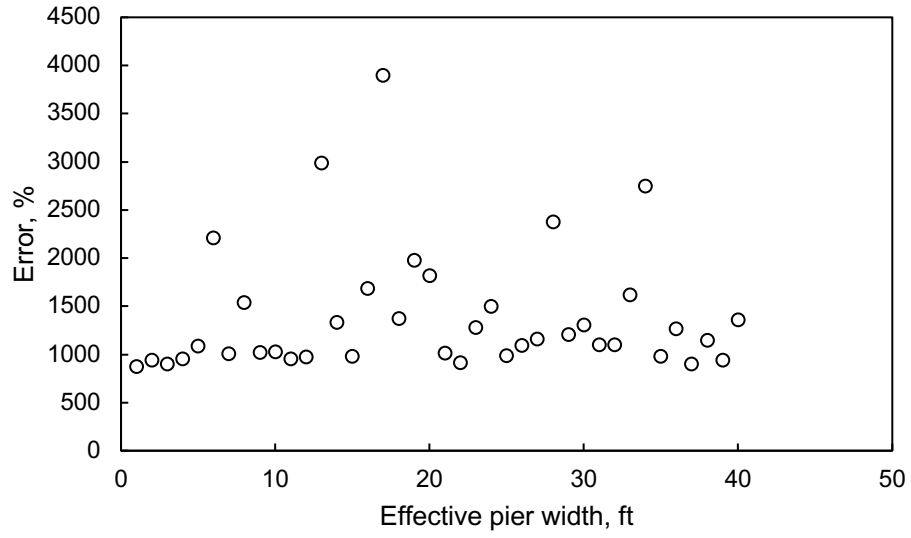
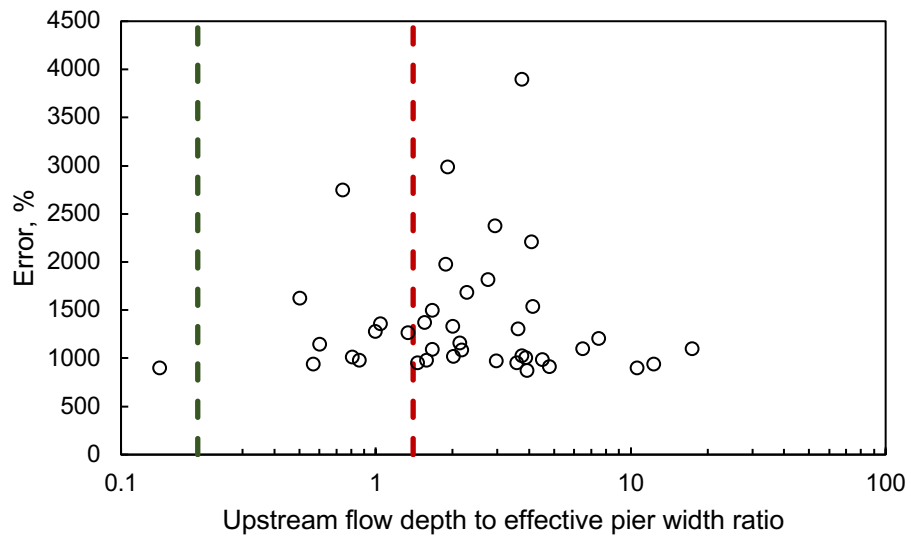


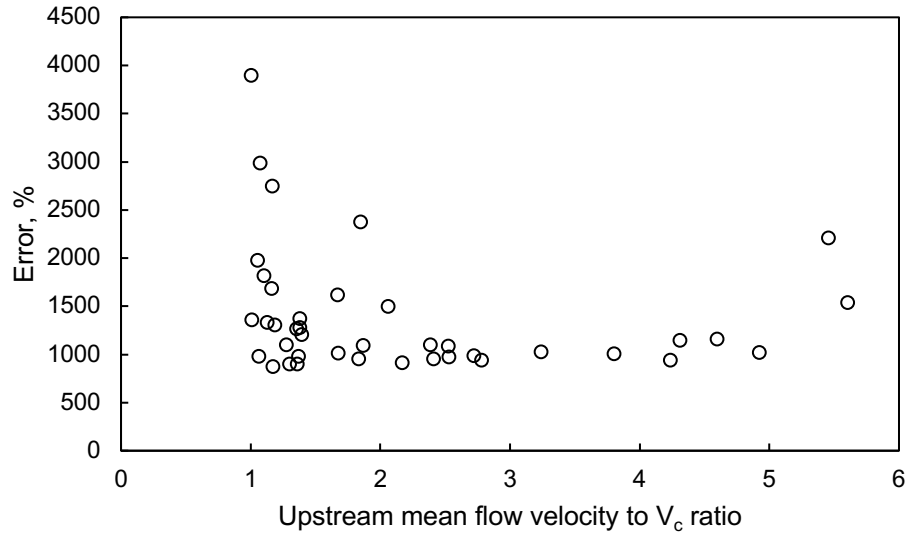
Figure 3: Error box-plot for the five deterministic models considered (Dataset: Live bed field, Data count: 850)



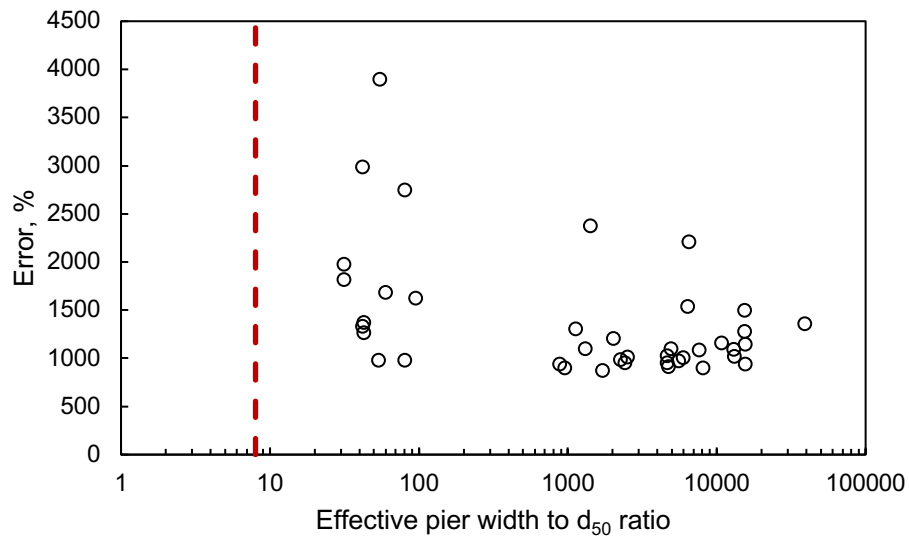
(a)



(b)

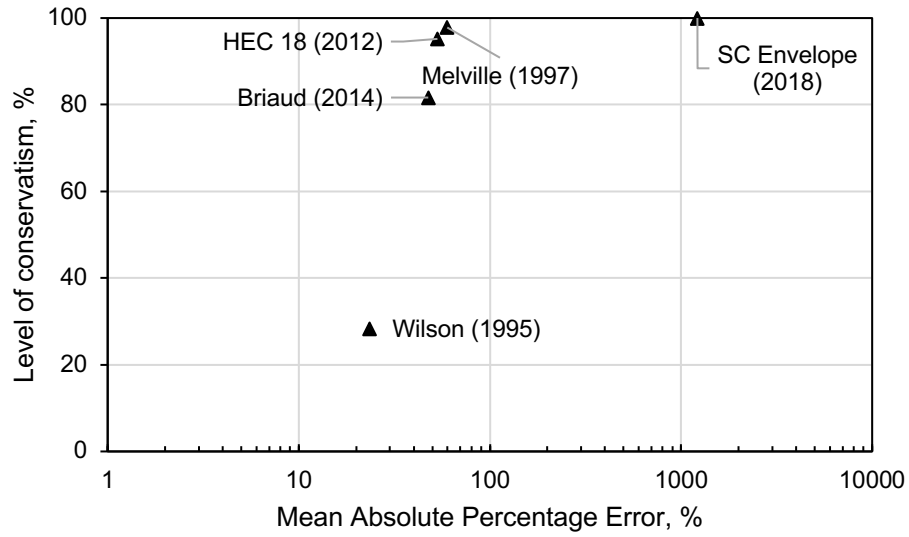


(c)

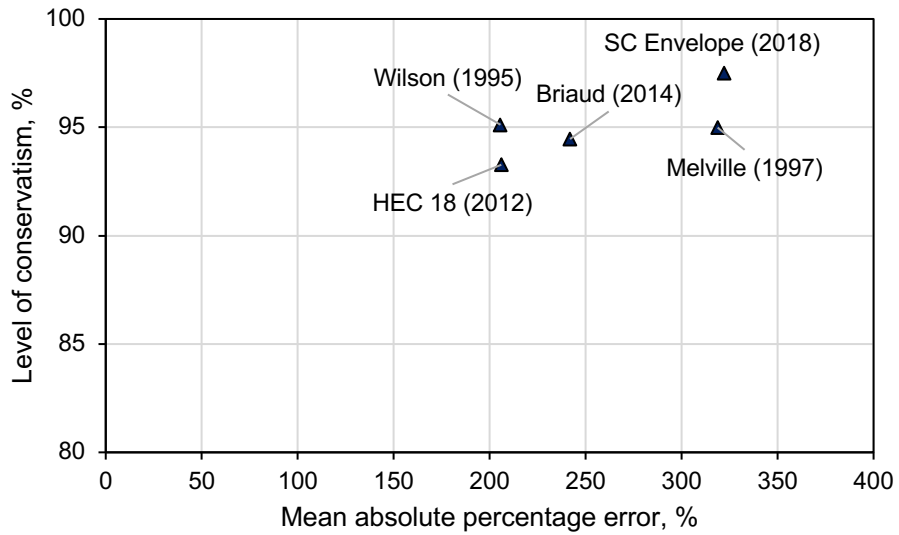


(d)

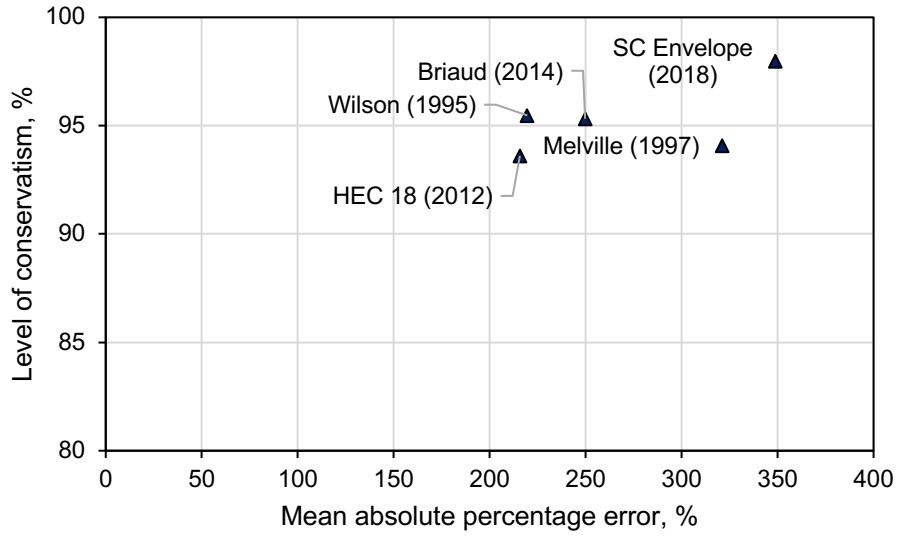
Figure 4: For the excluded data points, relationship between error magnitude and (a) Effective pier width, (b) Upstream flow depth to pier width ratio, (c) Upstream mean flow velocity to the critical velocity, and (d) Effective pier width to median grain size ratio when HEC-18 (2012) model is used (Data count: 41)



(a)

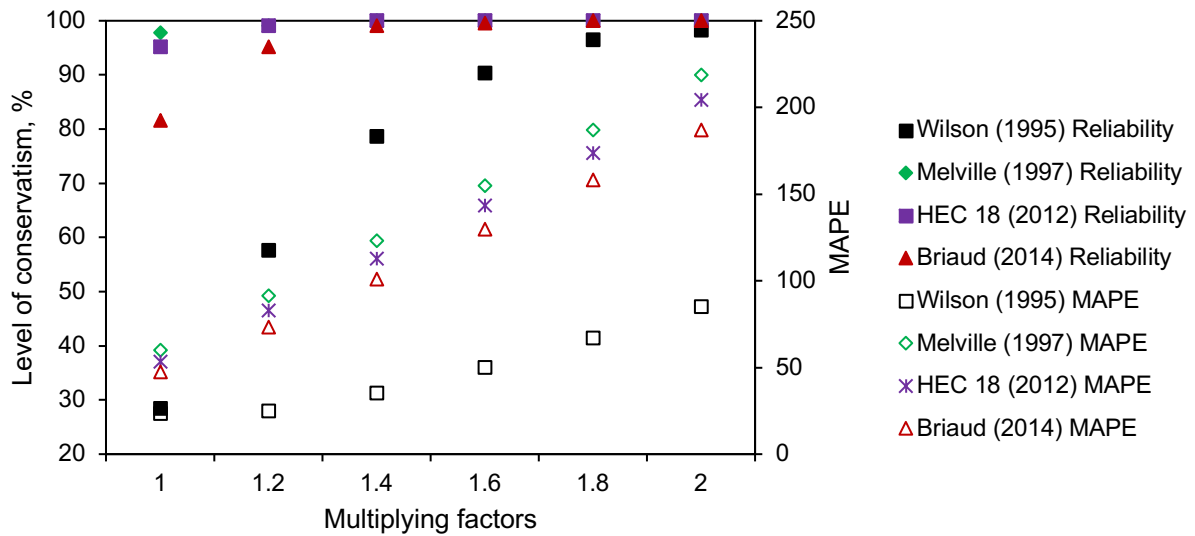


(b)

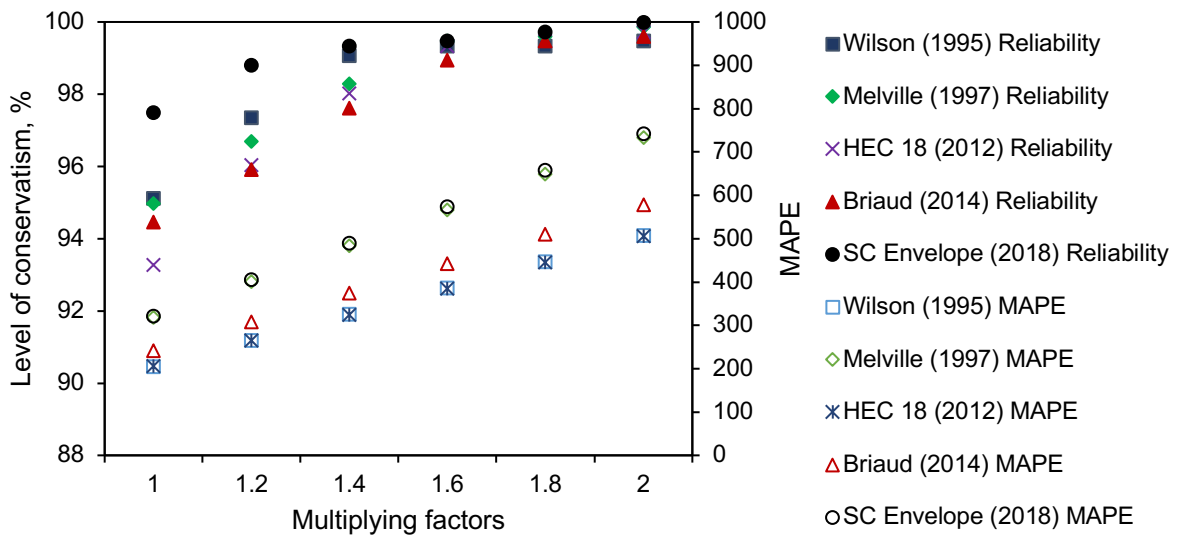


(c)

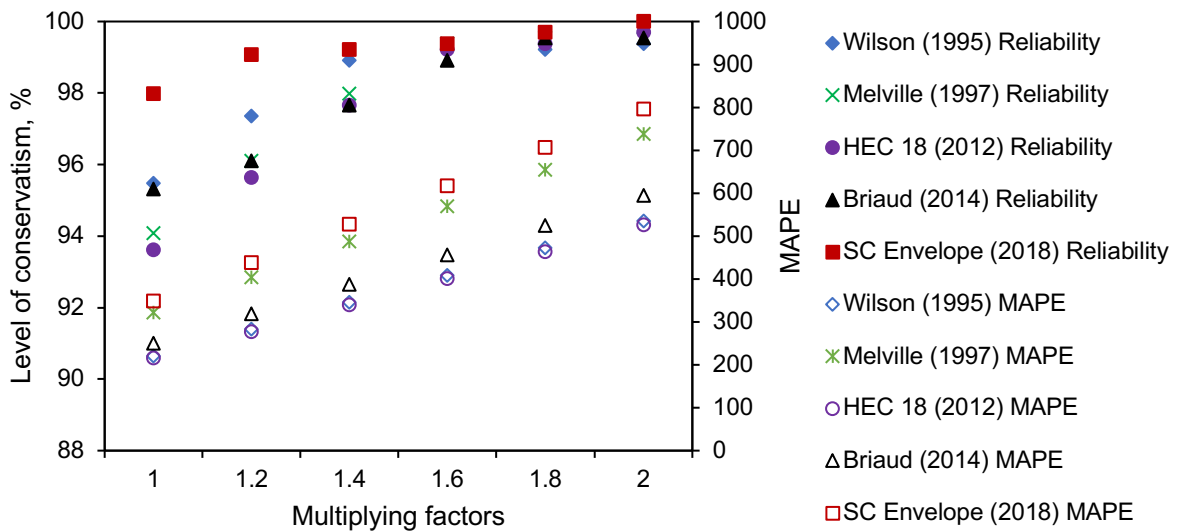
Figure 5: Relationship between conservatism and mean absolute percentage error for the models considered (a) Dataset: live bed laboratory data (Data count: 229), (b) Dataset: live bed field data (Data count: 758), (c) Dataset: live bed field data with nominal pier width <6 ft (Data count: 641)



(a)

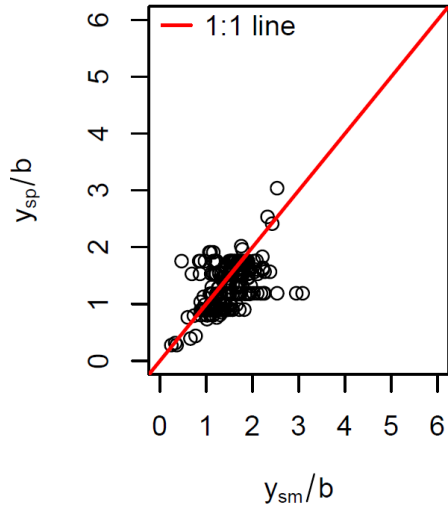


(b)

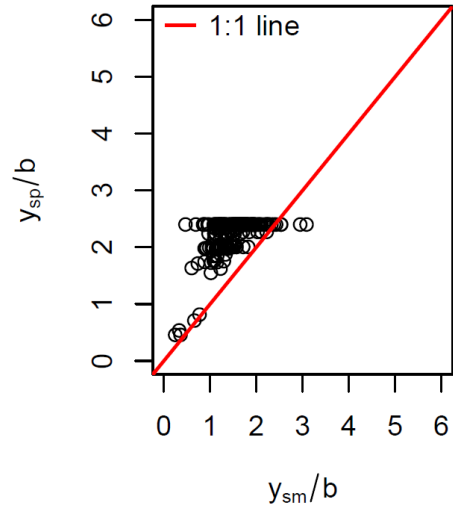


(c)

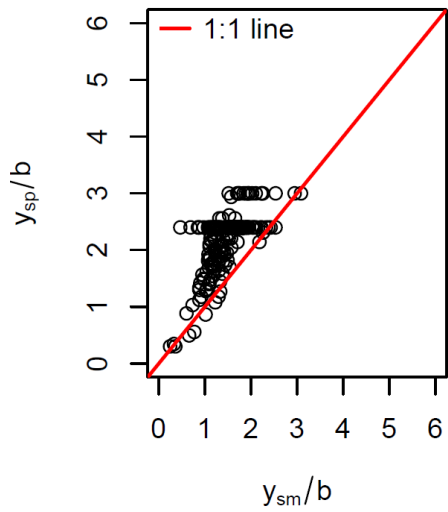
Figure 6: Effect of the multiplication factor on the conservatism and mean absolute percentage error for the deterministic models considered (a) Dataset: live bed laboratory data (Data count: 229), (b) Dataset: live bed field data (Data count: 758), (c) Dataset: live bed field data with nominal pier width <6 ft (Data count: 641)



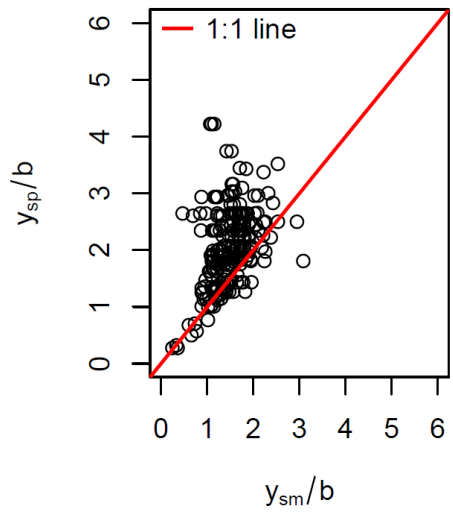
(a)



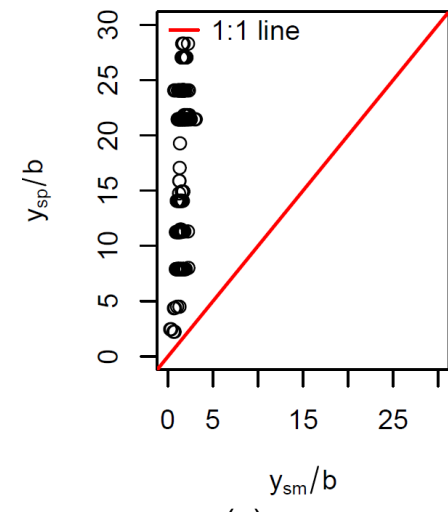
(b)



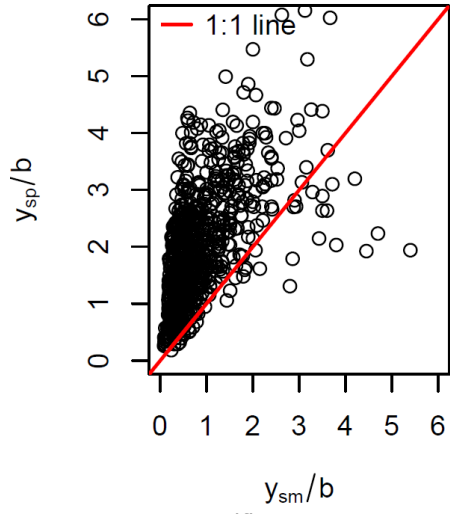
(c)



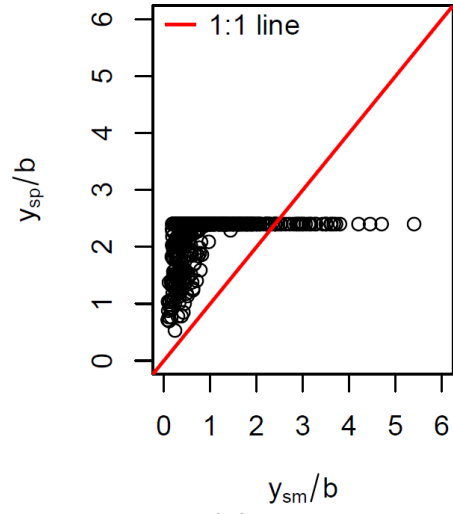
(d)



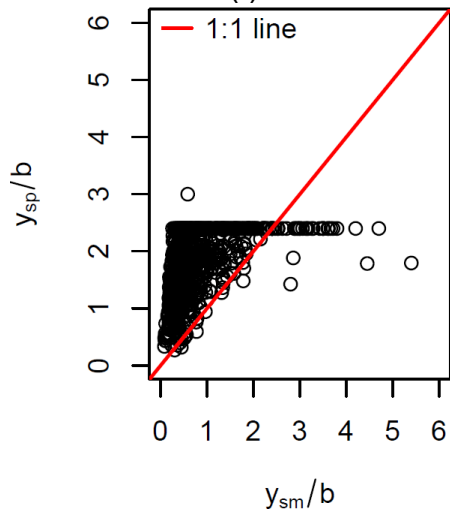
(e)



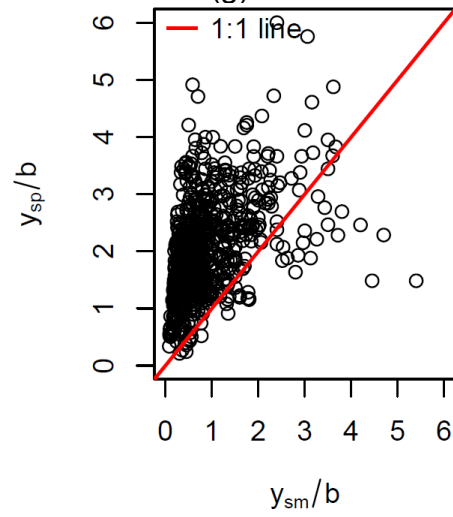
(f)



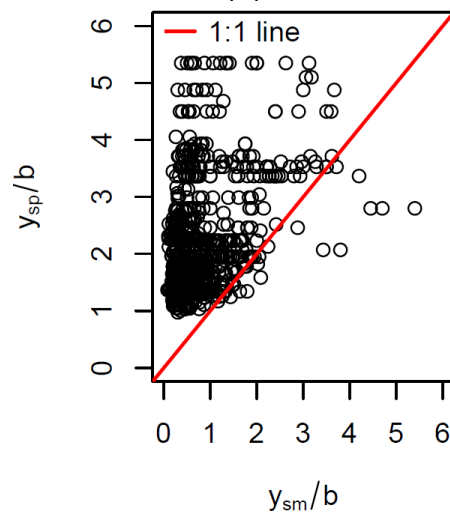
(g)



(h)

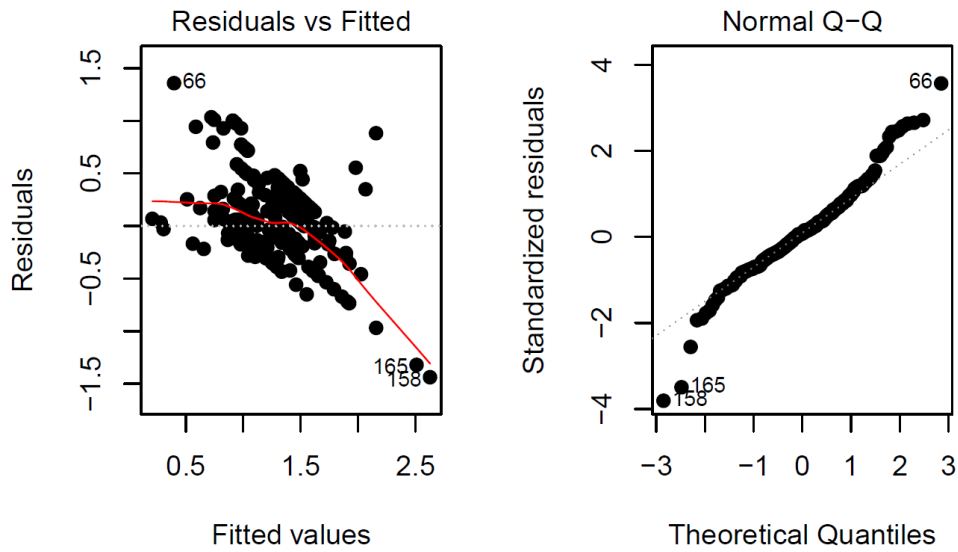


(i)

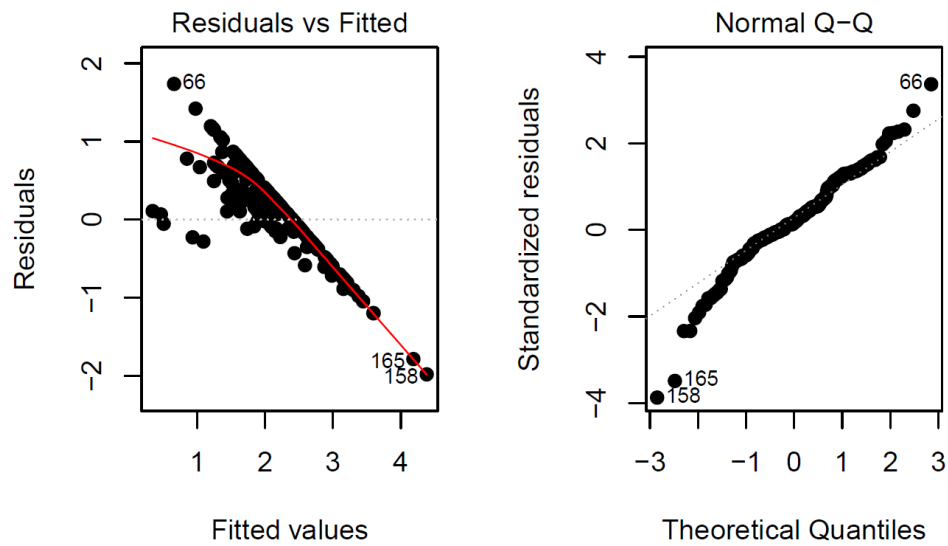


(j)

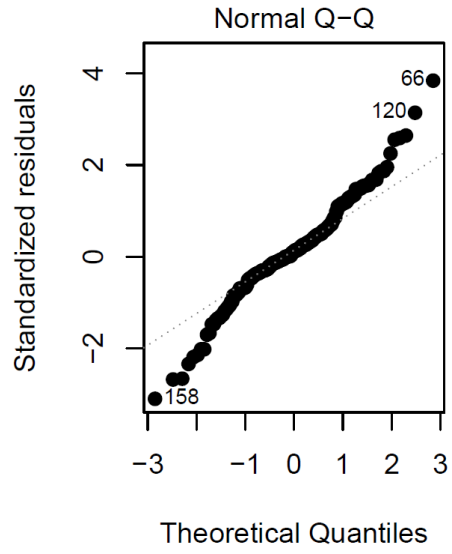
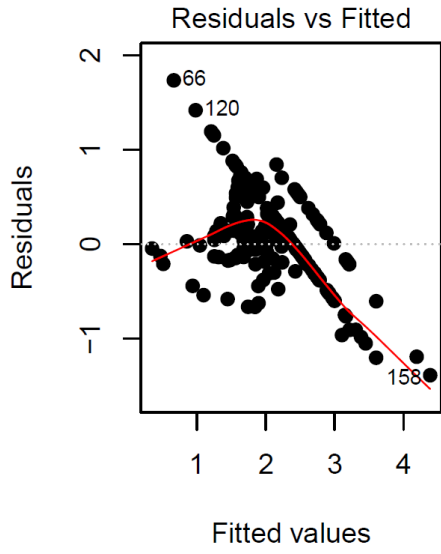
Figure 7: Predicted-measured normalized scour depth relation for: a) Wilson (1995) model, (b) Melville (1997) model, (c) HEC-18 (2012) model, (d) Briaud (2014) model, and (e) SC envelope (2018) model using laboratory live bed dataset (Data count: 229), (f) Wilson (1995) model, (g) Melville (1997) model, (h) HEC-18 (2012) model, and (i) Briaud (2014) model, and (j) SC envelope (2018) model using field live bed dataset (Data count: 758). b denotes the effective pier width, and y_{sp} , y_{sm} indicate the predicted and the measured scour depth respectively.



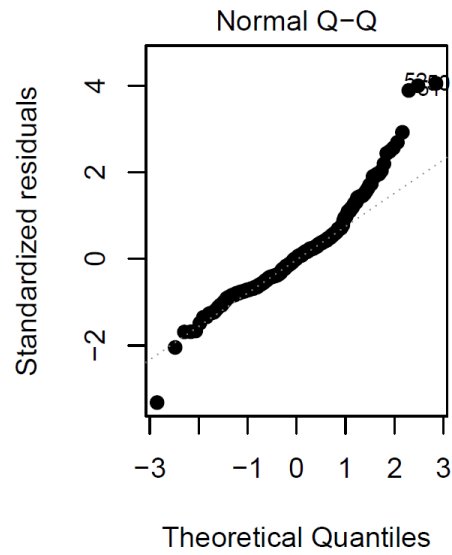
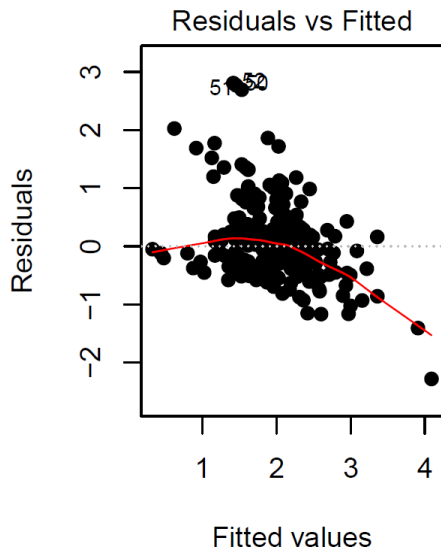
(a)



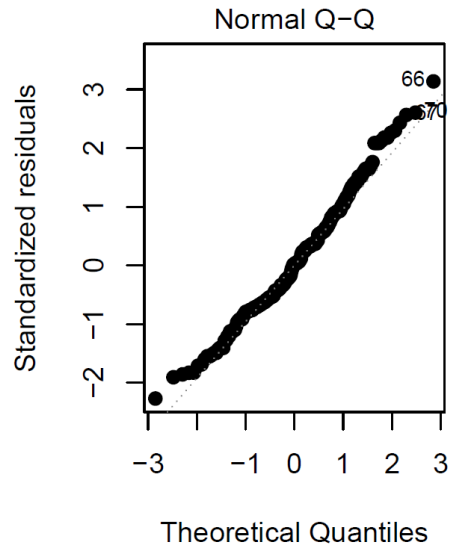
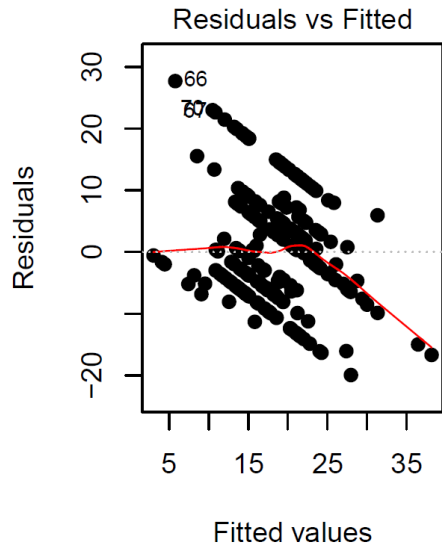
(b)



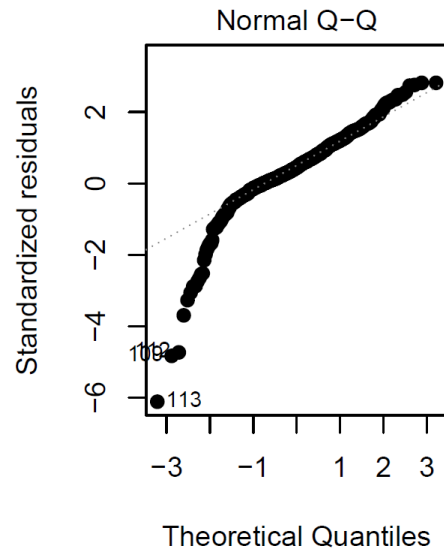
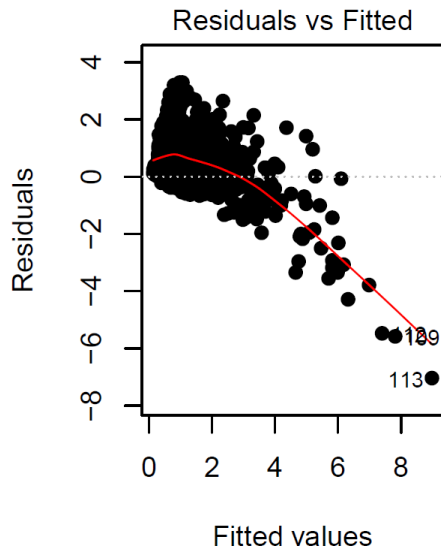
(c)



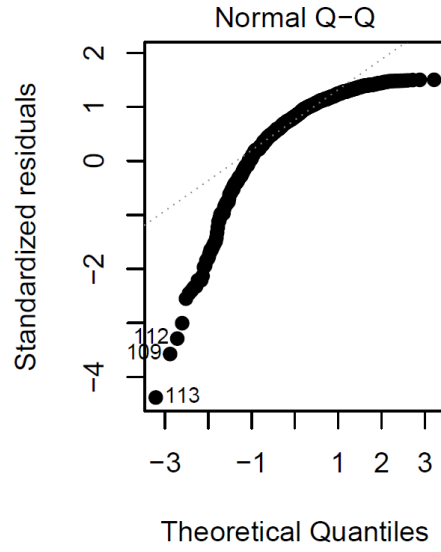
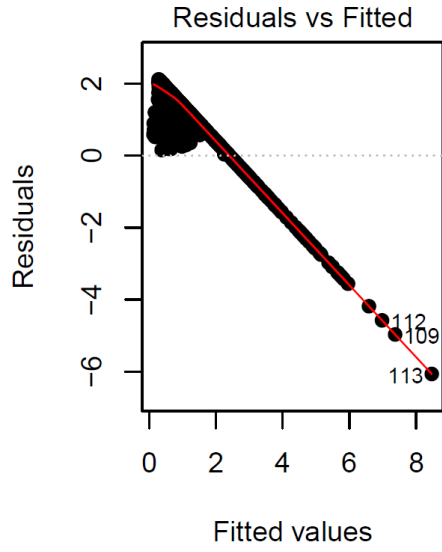
(d)



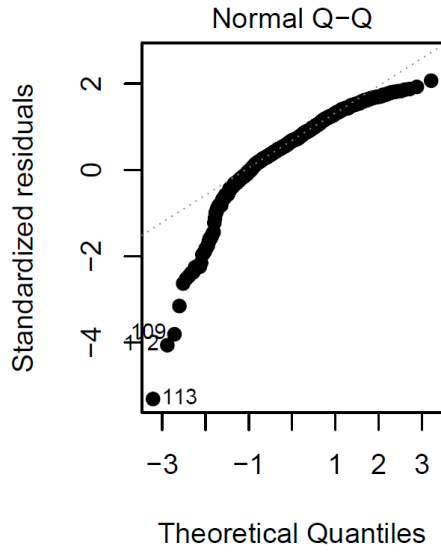
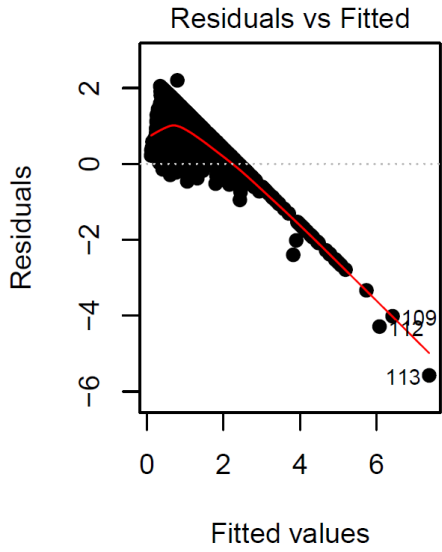
(e)



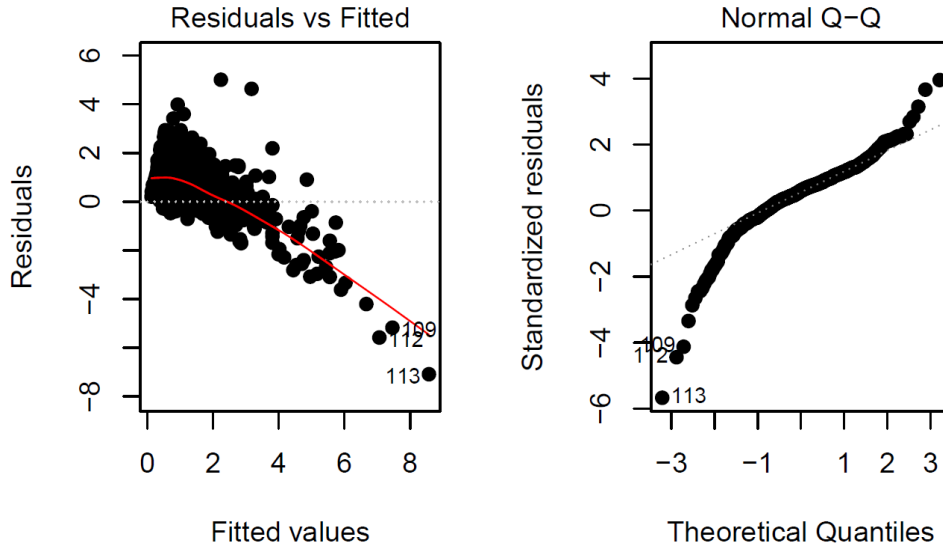
(f)



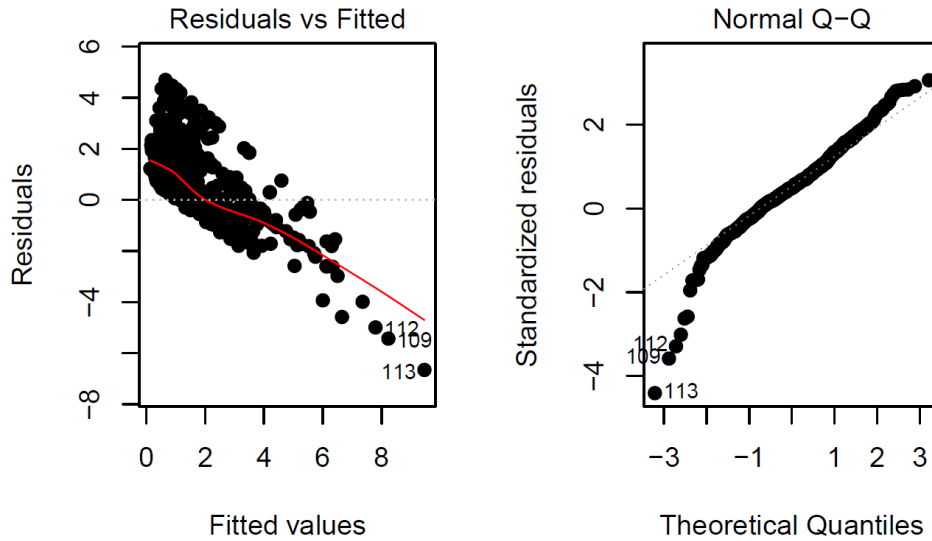
(g)



(h)

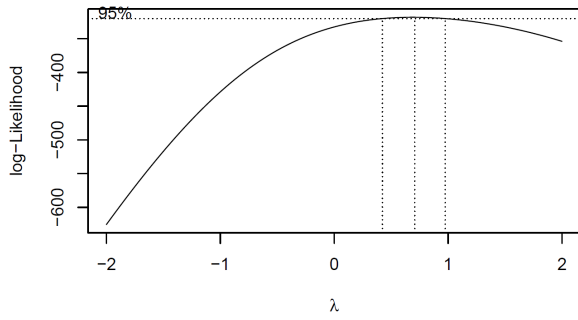


(i)

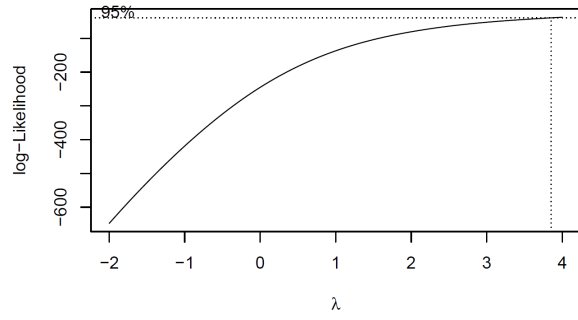


(j)

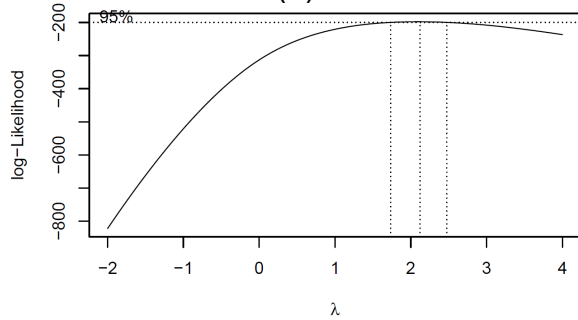
Figure 8: Demonstration of heteroscedasticity and non-normal errors associated with predicted-measured normalized scour depth relation for: a) Wilson (1995) model, (b) Melville (1997) model, (c) HEC-18 (2012) model, (d) Briaud (2014) model, (e) SC envelope (2018) model using laboratory live bed dataset (Data count: 229), (f) Wilson (1995) model, (g) Melville (1997) model, (h) HEC-18 (2012) model, (i) Briaud (2014) model, and (j) SC envelope (2018) model using field live bed dataset (Data count: 758).



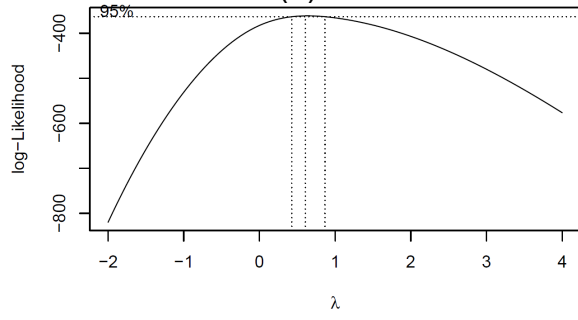
(a)



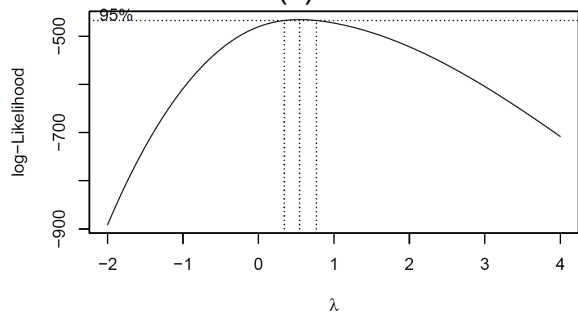
(b)



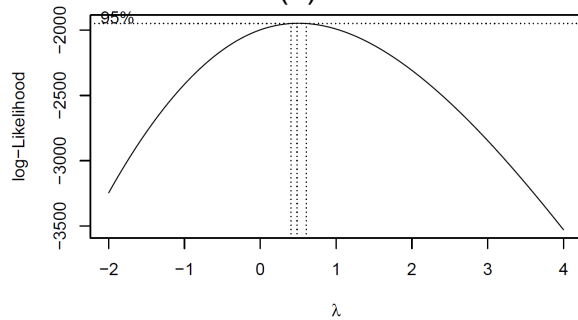
(c)



(d)



(e)



(f)

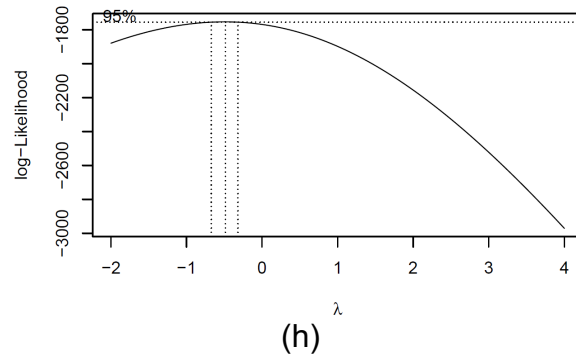
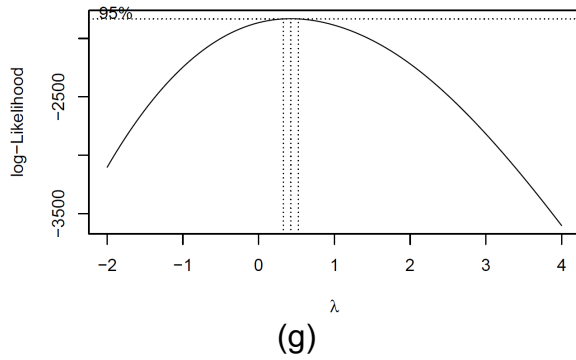
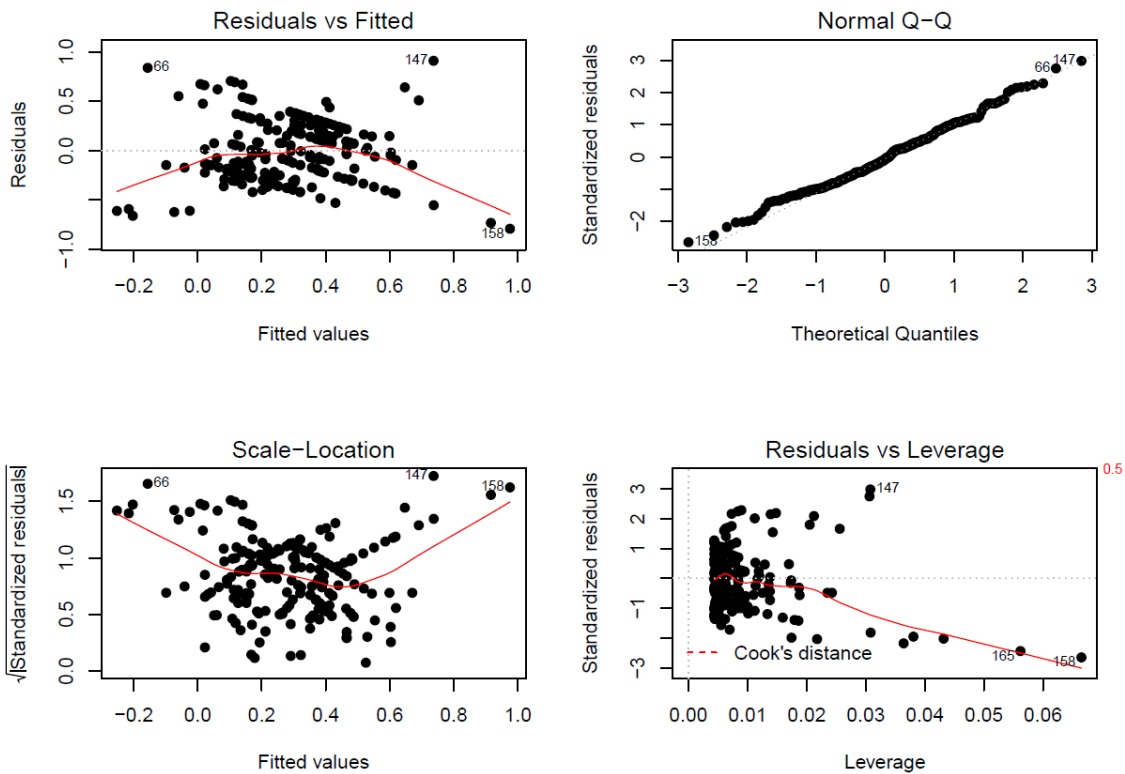
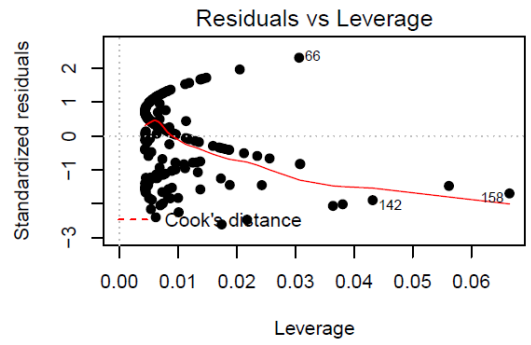
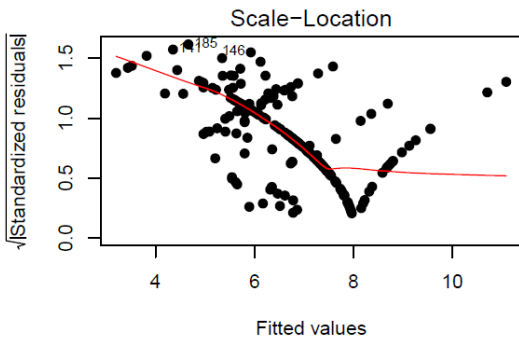
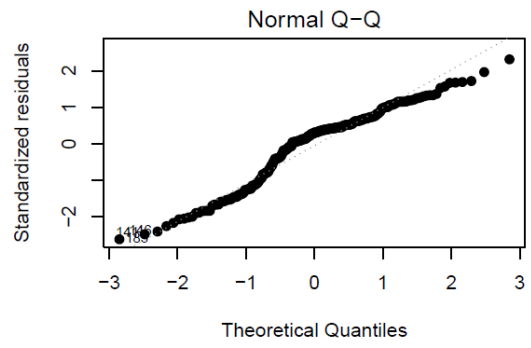
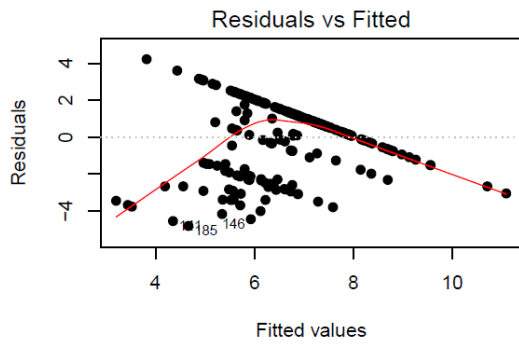


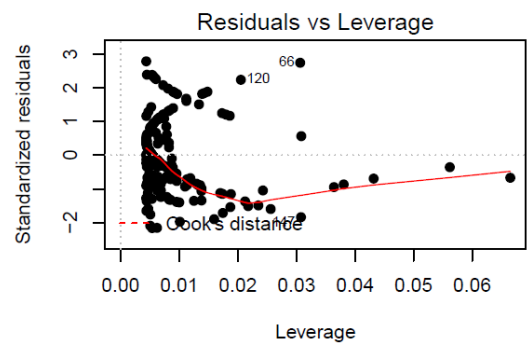
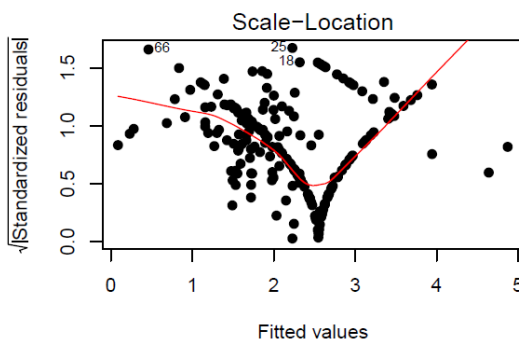
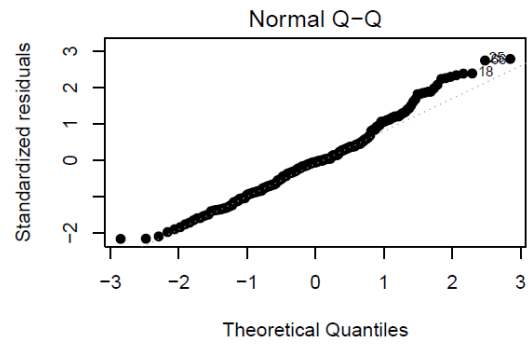
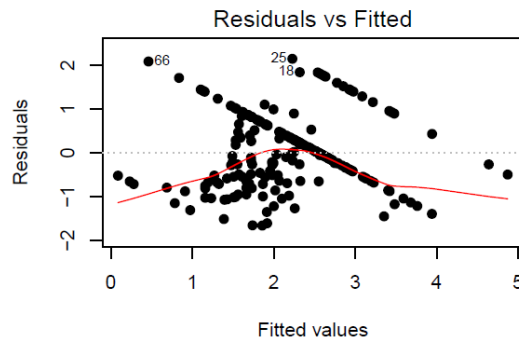
Figure 9: Estimation of parameter λ for (a) Wilson (1995) model, (b) Melville (1997) model, (c) HEC-18 (2012) model, (d) Briaud (2014) model, and (e) SC envelope (2018) model using laboratory live bed dataset (Data count: 229), (f) Wilson (1995) model, (g) Melville (1997) model, (h) HEC-18 (2012) model, (i) Briaud (2014) model, and (j) SC envelope (2018) model using field live bed dataset (Data count: 758).



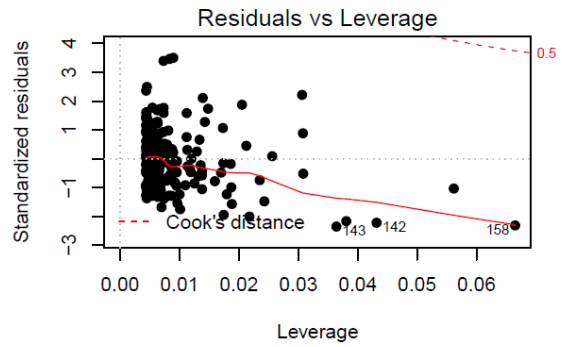
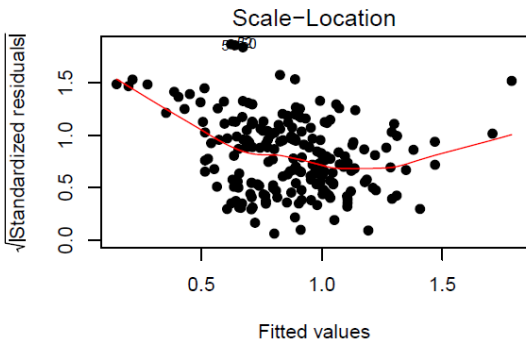
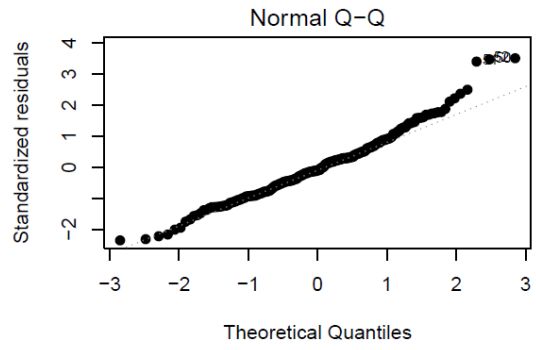
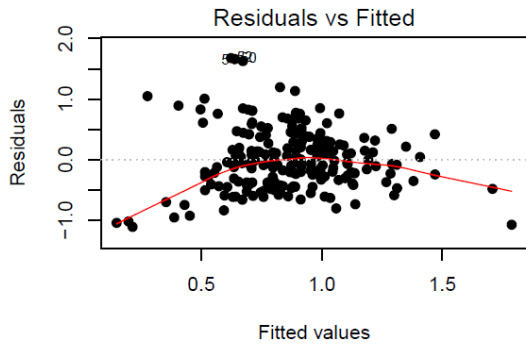
(a)



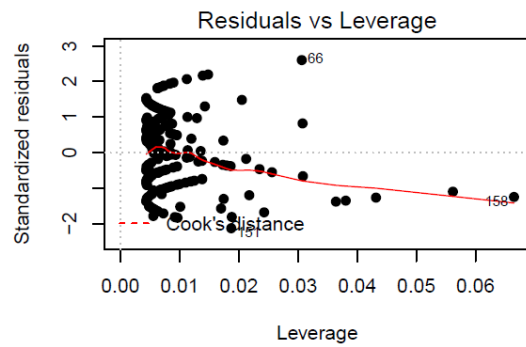
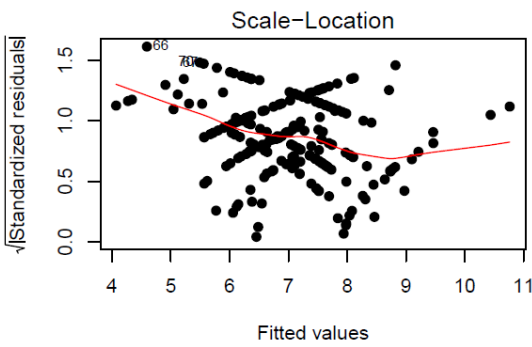
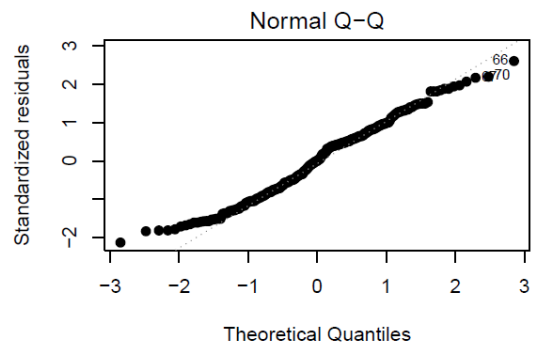
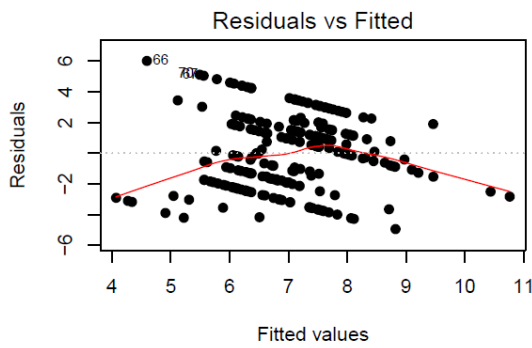
(b)



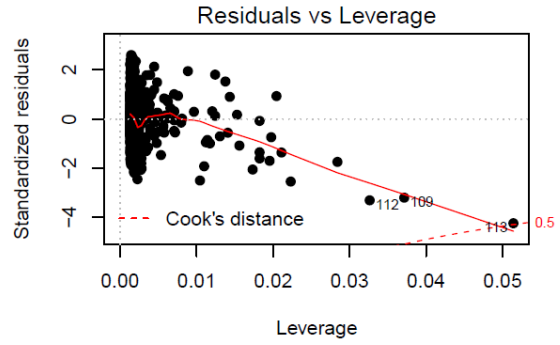
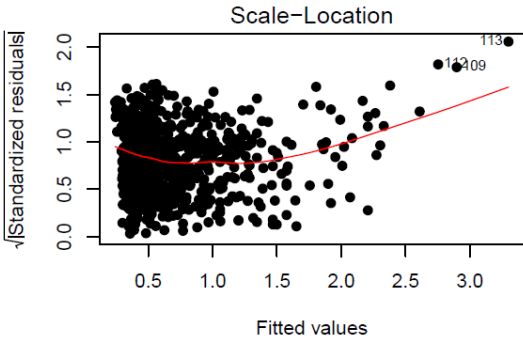
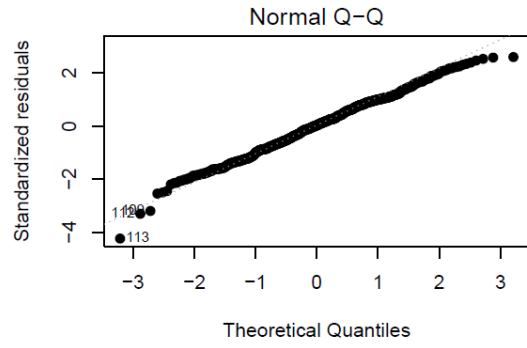
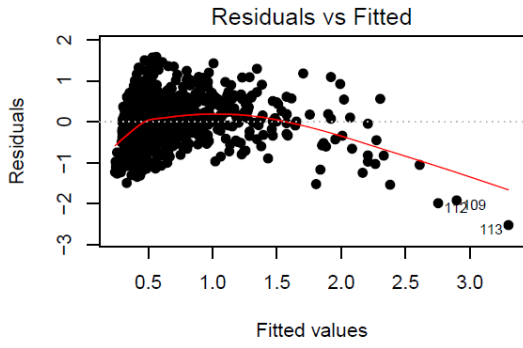
(c)



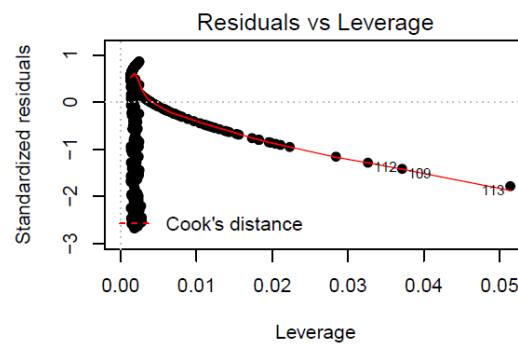
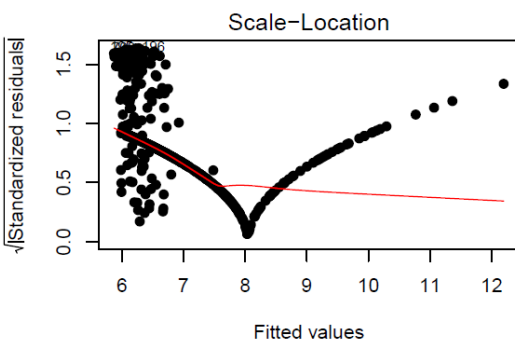
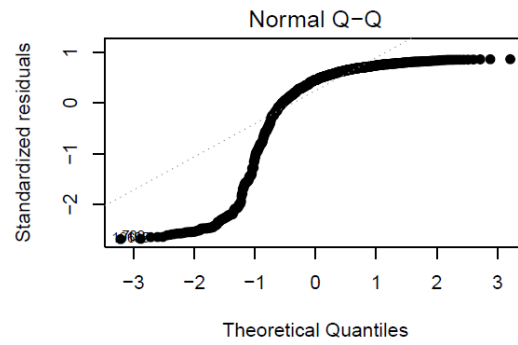
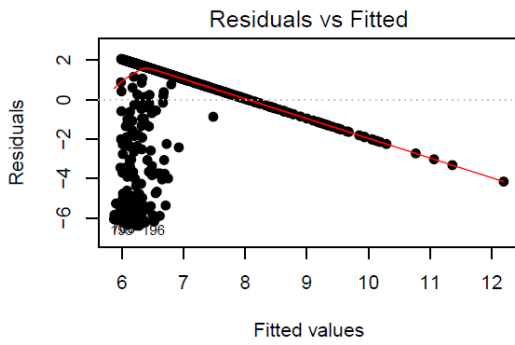
(d)



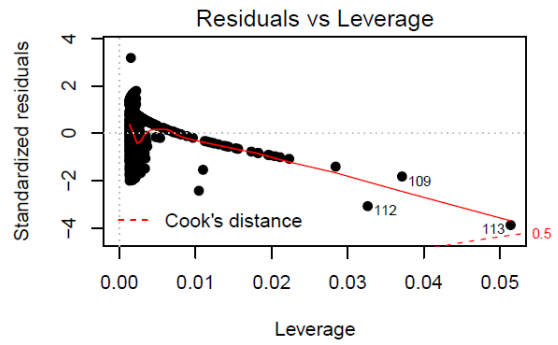
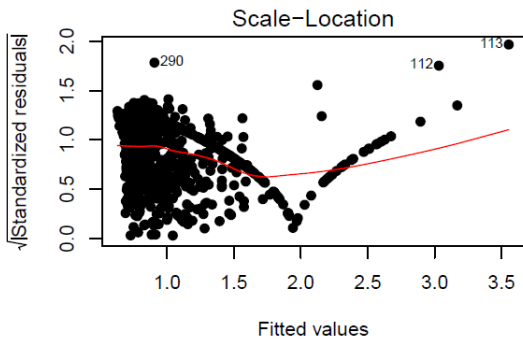
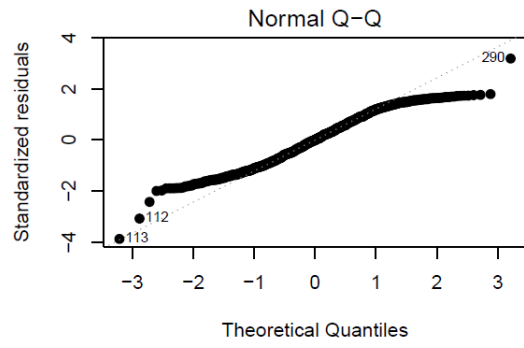
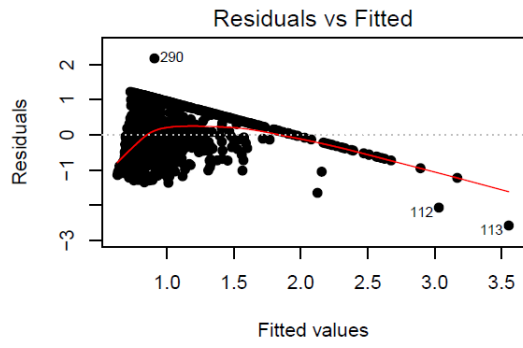
(e)



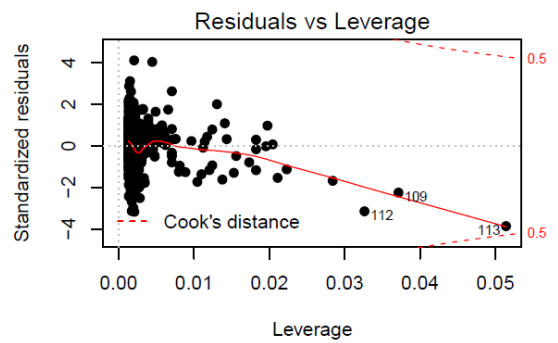
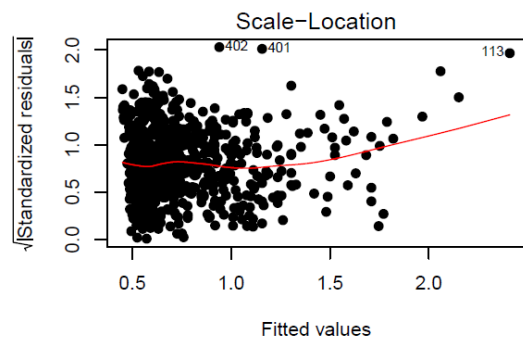
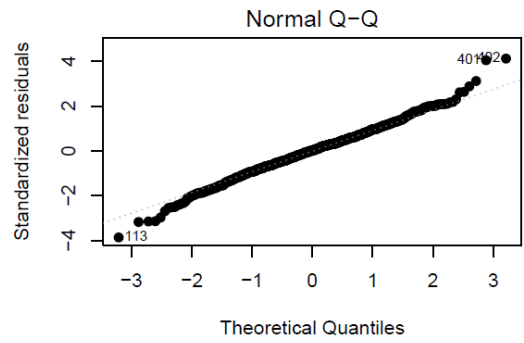
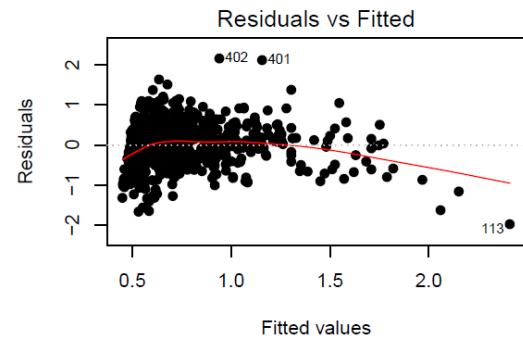
(f)



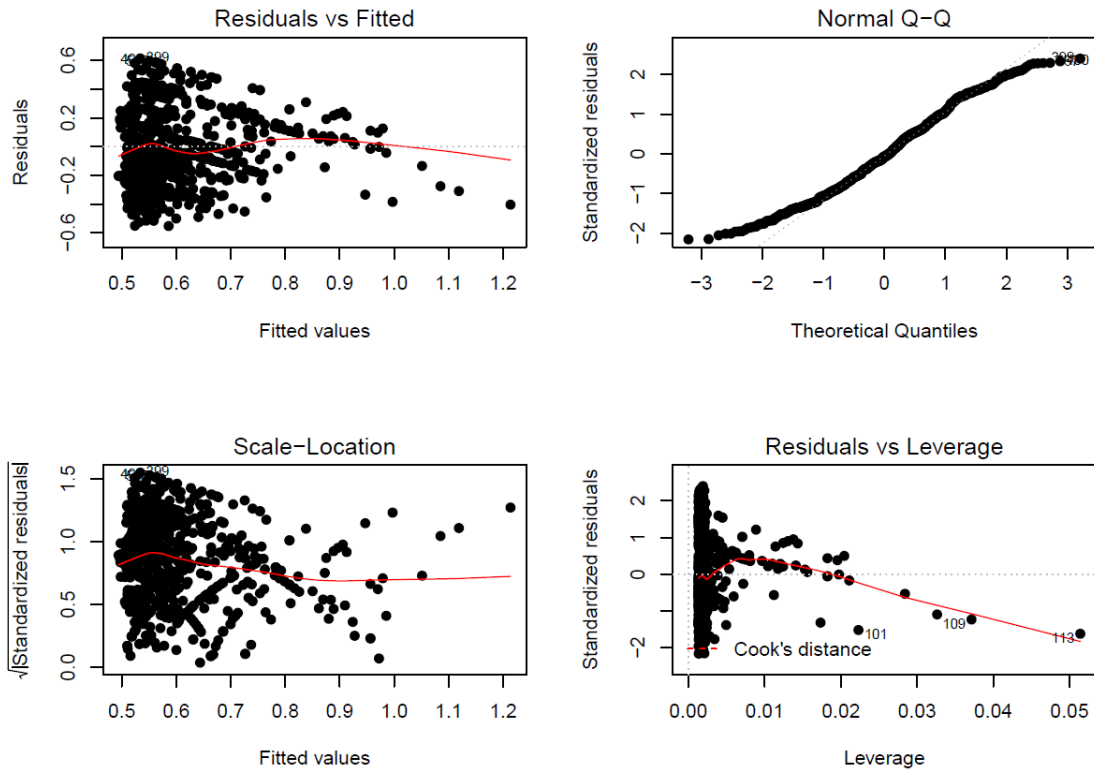
(g)



(h)

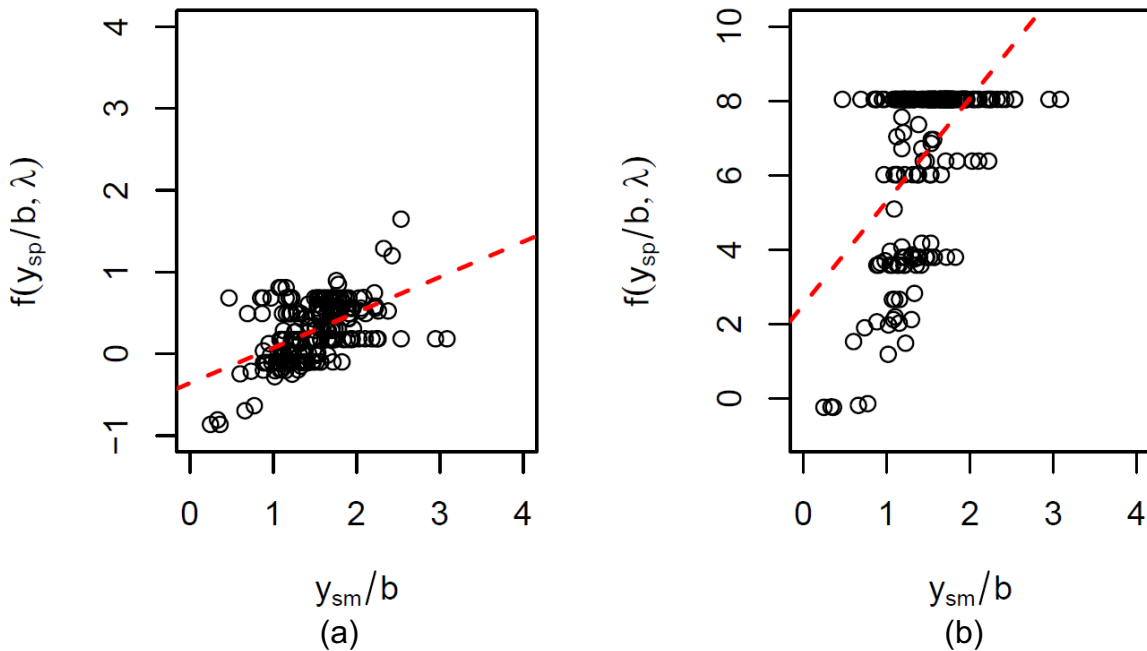


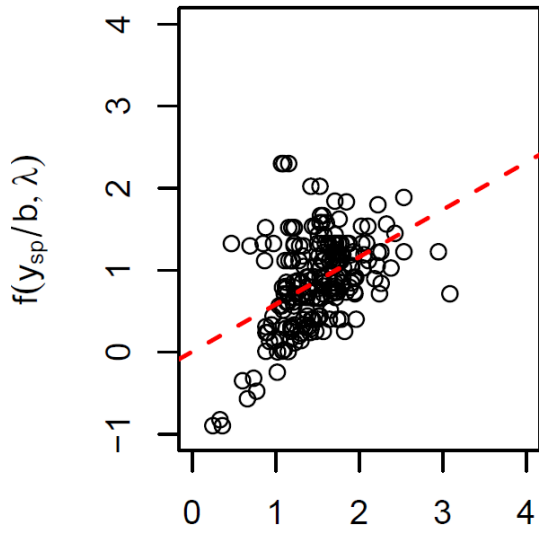
(i)



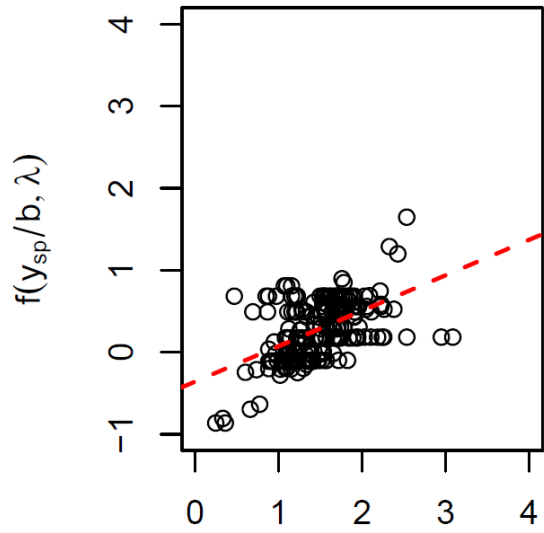
(j)

Figure 10: Residual diagnostics associated with model prediction for: (a) Wilson (1995) model, (b) Melville (1997) model, (c) HEC-18 (2012) model, (d) Briaud (2014) model, and (e) SC envelope (2018) model using laboratory live bed dataset (Data count: 229), (f) Wilson (1995) model, (g) Melville (1997) model, (h) HEC-18 (2012) model, (i) Briaud (2014) model, and (j) SC envelope (2018) model using field live bed dataset (Data count: 758).

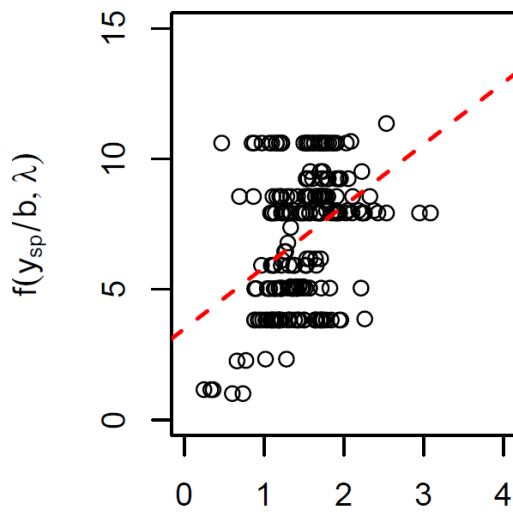




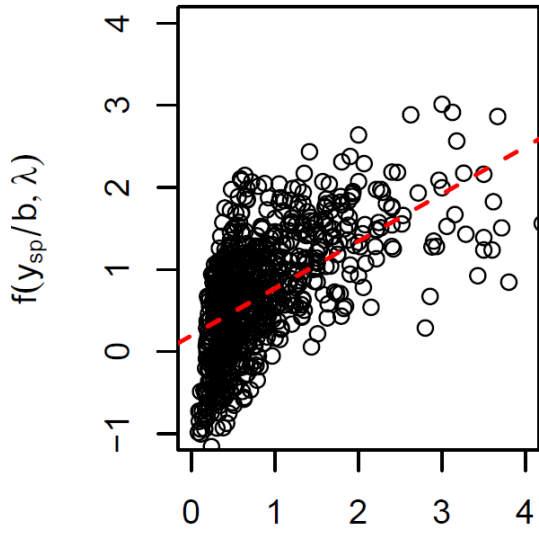
y_{sm}/b
(c)



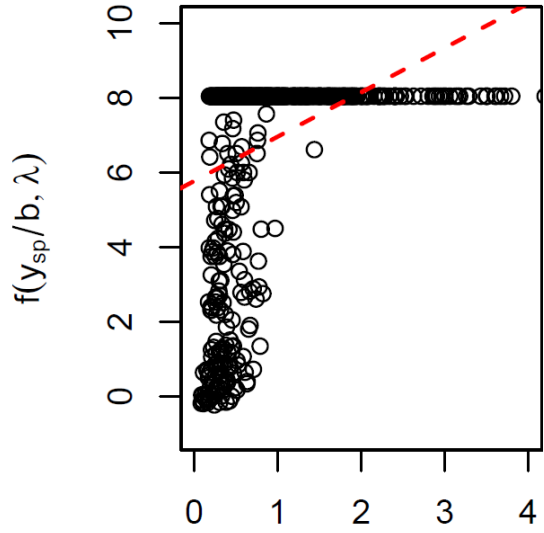
y_{sm}/b
(d)



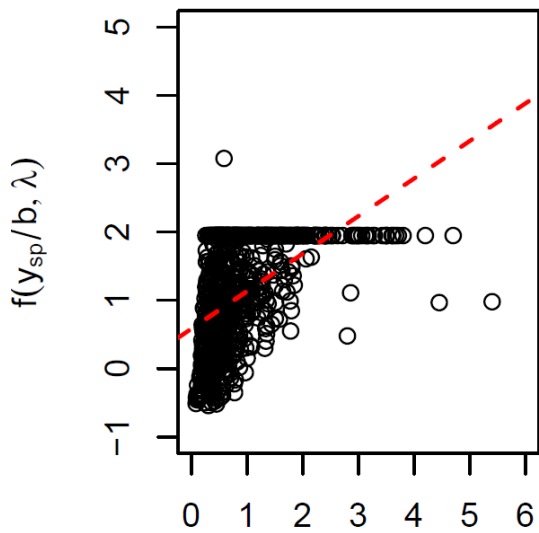
y_{sm}/b
(e)



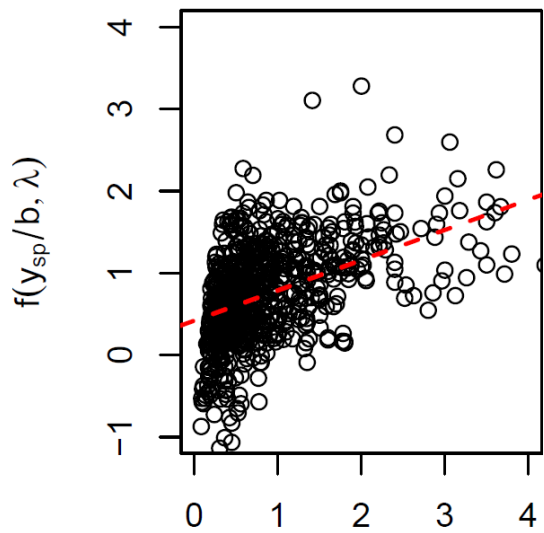
y_{sm}/b
(f)



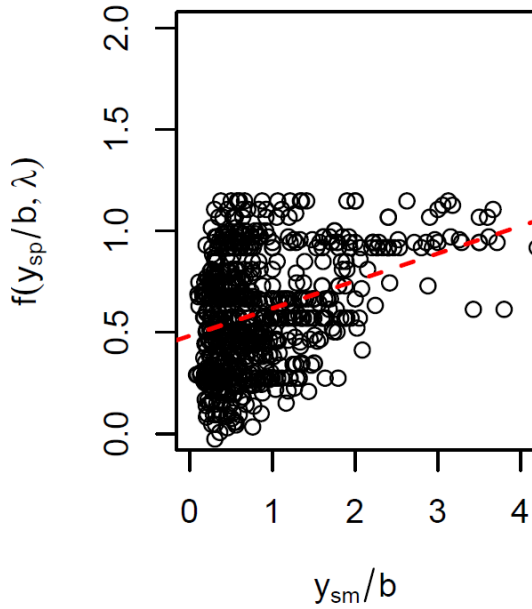
y_{sm}/b
(g)



y_{sm}/b
(h)

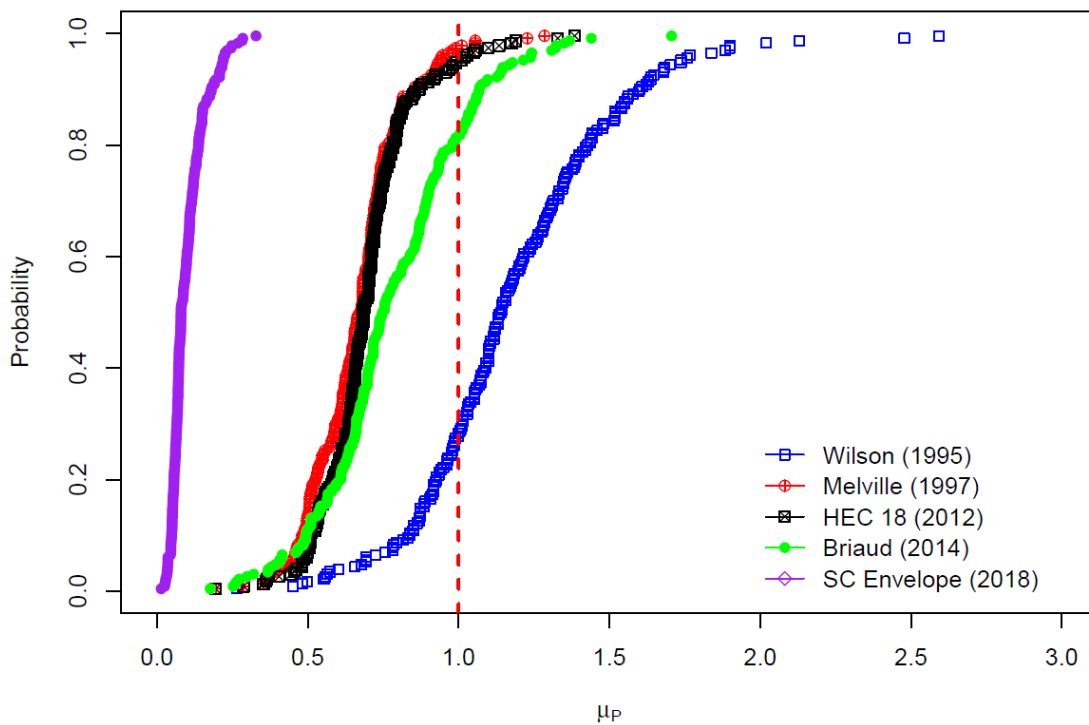


y_{sm}/b
(i)

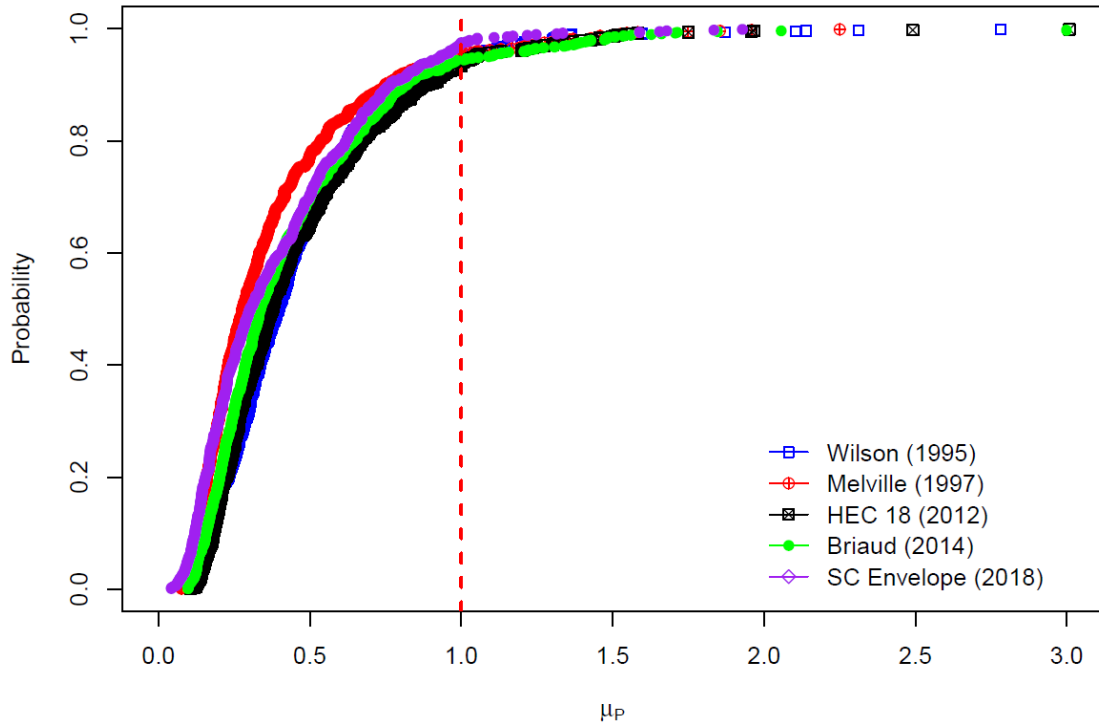


(j)

Figure 11: Variation of $f(y_{sp}/b, \lambda)$ with the measured normalized scour depth for: (a) Wilson (1995) model, (b) Melville (1997) model, (c) HEC-18 (2012) model, (d) Briaud (2014) model, and (e) SC envelope (2018) model using laboratory live bed dataset (Data count: 229), (f) Wilson (1995) model, (g) Melville (1997) model, (h) HEC-18 (2012) model, (i) Briaud (2014) model, and (j) SC envelope (2018) model using field live bed dataset (Data count: 758).

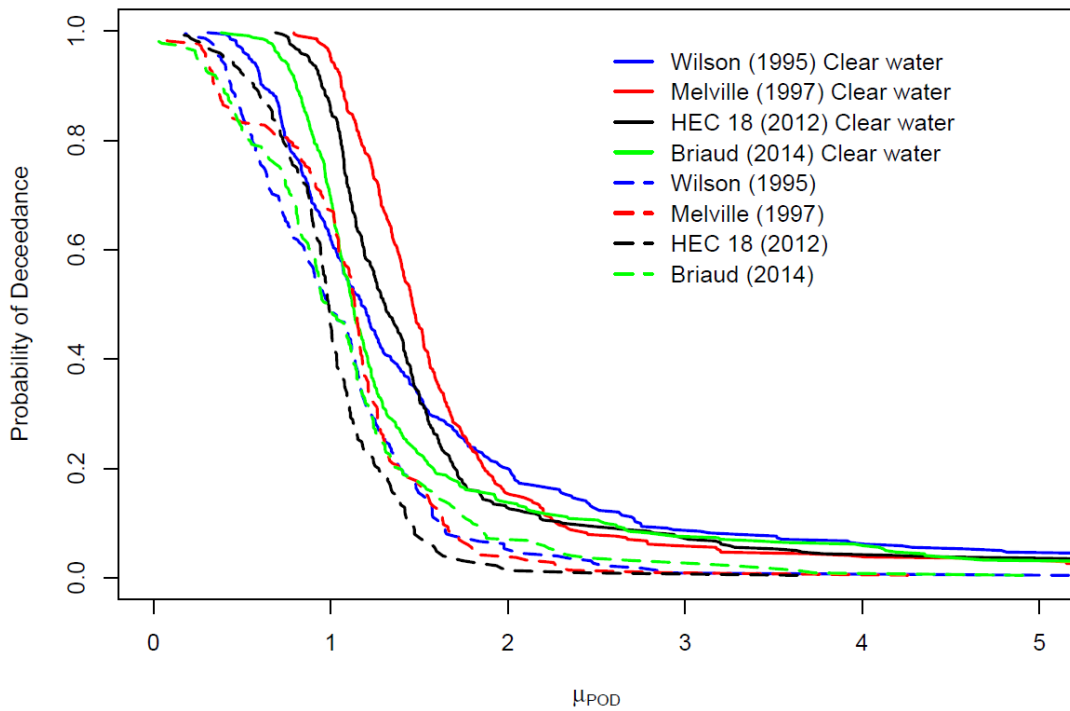


(a)

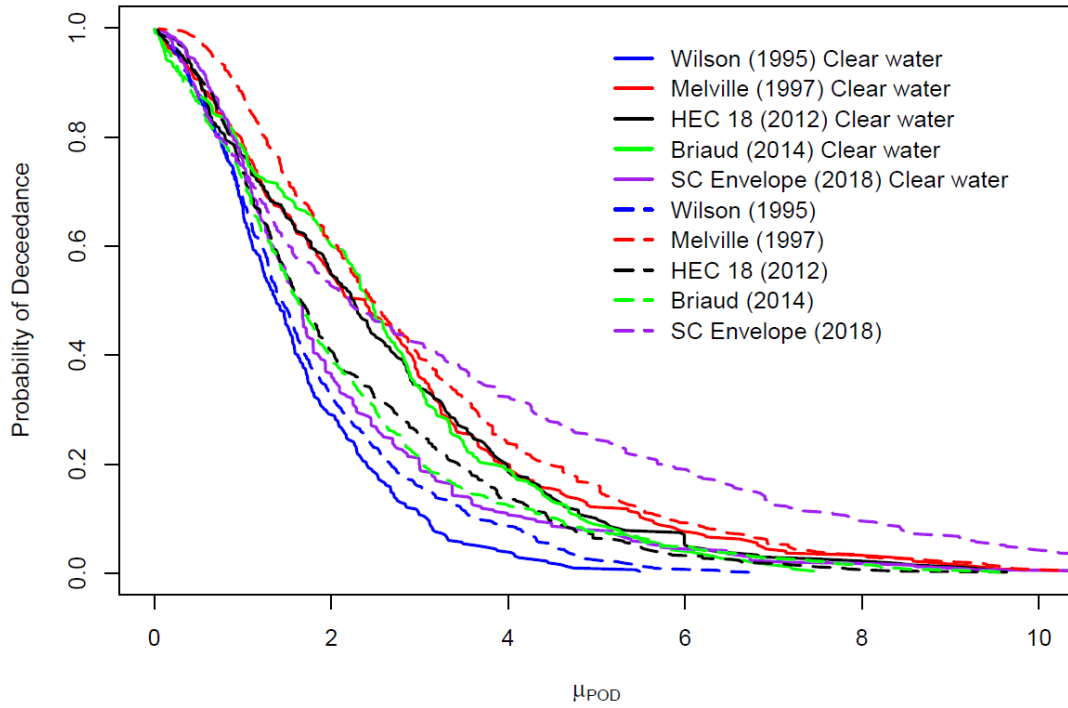


(b)

Figure 12: Probability-modification factor relation for different models using (a) laboratory live bed dataset (Data count: 229), (b) field live bed dataset (Data count: 758).



(a)



(b)

Figure 13: Probability of deceedance-modification factor relation for different models using (a) laboratory live bed dataset (Data count: 229), (b) field live bed dataset (Data count: 758). Clear water data points are from Shahriar et al. (2021b).

Appendix D: Development of Reliability Index based framework for Bridge Pier Scour Analyses

1. Introduction

Scour around existing bridges foundation has been a primary cause of bridge collapse in the United States and worldwide (Melville and Coleman, 2000; Liang et al. 2015; Qi et al. 2016). Records in National Bridge Inventory (NBI) suggests that more than 80% of the total 583,000 bridges in the United States are built over waterways. Support systems of structures crossing waterways are subjected to scour during their design life owing to the flowing water-induced bed shear stresses (Hong et al. 2012, Azmathullah 2013). Scour is amplified by extreme flooding due to increased baseflow and associate velocities; approximately 85% of the bridges fail due to externally triggered events like flood, collision, overload etc. (Wardhana and Hadipriono 2003). Johnson et al. (2015) noted that for the bridges under federal aid system, the average annual flood damage repair cost could be estimated at \$50 million.

Traditional practice of bridge scour estimation relies upon the use of deterministic models (Shahriar et al. 2021a). Although many pier scour prediction models are available in literature, the Hydraulic Engineering Circular No. 18 (Arneson et al. 2012) is one of the most commonly used in the United States (Johnson et al. 2015). There is a consensus that HEC 18 (Arneson et al. 2012) model often provides a conservative estimate of scour depth (Briaud et al. 2014; Yao 2013). However, the degree of inherent conservatism embedded in such models is unknown. A knowledge of the level of biasness of the scour prediction models is necessary to discern the extent of conservatism/un-conservatism in view of a given model's application to a wide range of site conditions.

Investigation into the scour prediction models suggests that pier scour estimation is predominantly influenced by flow depth to pier width ratio, pier width to median grain size ratio, pier face shape, pier aspect ratio, skew angle of pier, and upstream mean flow velocity to critical velocity ratio (Melville and Coleman 2000; Ettema et al. 2011). The majority of the input parameters related to flow and streambed are not deterministic in nature and can be random variables with a particular statistical distribution. This raises the necessity to assess input parameter uncertainty, along with the inherent biasness of the results from the deterministic model.

Multiple advancements have been made in probabilistic scour assessment front. Johnson (1992) developed a mathematical expression between probability of bridge failure and safety factors using data from Chee (1982) and Chiew (1984). A best-fit model to represent the databases used was considered as the basic deterministic model, thereby model uncertainty was not considered. Briaud et al. (2007) developed a probabilistic bridge scour model that considered the uncertainty of the hydrologic loading conditions. Bolduc et al. (2008) introduced a probabilistic model based on the bias in the HEC 18 (2012) model using three databases, which are the Gudavalli database (Gudavalli 1997), Landers-Mueller database (Landers and Mueller 1996), and Kwak database (Kwak 2000). Bolduc et al. (2008) suggested that a logarithmic transformation of the measured scour depth estimate is sufficient to remove heteroscedasticity. However, Shahriar et al. (2021b), using the Benedict and Caldwell (2014) database, demonstrated that Box-Cox transformation (Box and Cox 1964), rather than logarithmic transformation is necessary to remove heteroscedasticity and non-normal error associated with the measured scour depths, thereby, proposed a refined method to estimate model bias. Johnson et al. (2015) examined the hydraulic and hydrologic uncertainties associated with HEC-18 and Florida Department of Transportation (FDOT, 2011) scour

prediction models. A large number of simulations (10,000) in HEC RAS were considered to assess the hydraulic conditions at a bridge, given the hydrologic input variable uncertainties. Three levels of hydrologic uncertainties were considered, viz. low, medium, and high uncertainty. Johnson et al. (2015) showed that for different hydrologic uncertainty level, the estimated scour depth varies and reported “scour design factors” based on target scour non-exceedance. Contreras-Jara et al. (2021) utilized the first order reliability method to quantify the probability of exceedance of the estimated scour considering hydraulic and hydrologic parameter uncertainty. Contreras-Jara et al. (2021) reported that the probability of exceedance was dependent on uncertainties in annual maximum flow, Froude number, top width, and riverbed longitudinal slope, which agrees with the philosophy of Johnson et al. (2015). Briaud et al. (2014) developed a risk-based pier scour model through quantification of the “risk associated with failure”, where risk was defined as the product of the probability of occurrence times the value of consequence. Shahriar et al. (2021b) developed a statistical model that quantifies model uncertainty and bias, and suggested scour modification factors for target probability of deceedance. In summary, probabilistic aspects of scour estimation have been advanced to some extent to make a designer aware of model bias, hydraulic, and hydrologic uncertainties associated the model’s estimate and the associated risk.

The use of the reliability theory, in terms of reliability index, has been introduced through the concept of Load and Resistance Factor Design (LRFD) guidelines in the United States (Nowak 1999). Reliability index is a measure of the number of standard deviations that the mean margin of safety falls on the “safe” side (Paikowsky 2004), where the margin of safety is dependent on the limit state function representing the safety of a system. The calibration procedure of LRFD code is well documented in Nowak (1999) and Kulicki et al. (2007); while an example application procedure for driven pile axial capacity can be found in Kim et al. (2005). The reliability index values suggested in the AASHTO LRFD calibration procedure corresponds to acceptable risk against components failure. However, Ghosn and Moses (1998), and Liu et al. (2001) showed that if there were redundancy in the system, the overall system reliability index would be higher (compared to the target reliability index of the components), thereby suggested system factors to meet system reliability criteria instead of component criteria. ASCE 7-10 (2010) suggests the use of reliability targets based on the consequence of its failure. Lagasse et al. (2013) described that a commonly used calibration procedure is to achieve a consistent reliability level for the super- and sub-structure in a system. The concept of LRFD is yet to be applied to the realm of scour assessment. Lagasse et al. (2013) further reported that existing bridge design codes propose different levels of risk tolerance for different hazards. For example, for seismic hazard analyses, a 1000-year return period has been proposed (ATC/MCEER 2002), while for scour analyses, the return period is dependent on the bridge size, or the level of service expected. The return period in scour analyses ranges from 10 years to 500 years. This design proposition of using different return periods for different hazards might be owing to the fact that the vulnerability of bridge elements is different when subjected to different hazards. In addition, there are numerous deterministic scour prediction models that yield different magnitudes of scour estimates when the hydraulic, structural, and geotechnical input parameters are identical for each model. This indicates that the scour magnitude assessed during the design phase will depend on the specific model used for such assessment. And accordingly, unknown reliability level across the different scour prediction models. Given the uncertainties in scour estimates due to the input parameter uncertainties, a relationship between reliability index, and safety factor for deterministic scour prediction models needs to be devised.

Work herein is focused on developing a reliability-based pier scour assessment methodology by extending estimates from deterministic models. Four commonly used pier scour prediction models, namely

Wilson (1995) model, Melville (1997) model, HEC-18 (2012), and Briaud (2014) model are considered. The laboratory clear-water and live-bed databases documented by Benedict and Caldwell (2014) are utilized to quantify model bias and uncertainty. The relationship between probability of exceedance of the measured scour depth and scour factors for varying reliability levels is explored considering the effects of input parameter uncertainty. To advance the concept of LRFD application to the various components of hydraulic structures, scour factors were proposed relating to the reliability index. Responses for narrow pier, intermediate pier, and wide pier subjected to both clear water and live bed conditions are examined. Scour factors corresponding to various reliability levels are discussed in view of the deterministic scour evaluations.

2. Scour prediction models for analyses

Four pier scour prediction models, namely Wilson (1995) model, Melville (1997) model, HEC-18 (2012) model, and Briaud (2014) model are utilized herein. The model equations are provided in Table 1. Wilson (1995) developed the model based on the pier scour depth data collected from 22 bridges in Mississippi. The measured pier scour depth ranged from 0.6-20.4 ft. Melville (1997) developed the model based on the laboratory and field data collected over a period of 25 years. The tests were mostly administered in University of Auckland, New Zealand (Melville and Sutherland 1988). The US Federal Highway Administration (FHWA), for estimating equilibrium scour depth recommends HEC 18 model. The HEC 18 model was initially developed based on the scour reported in laboratory setup where the piers were installed on sandy deposits (Shen et al. 1966). Briaud (2014) model is based on data from 94 large scale laboratory flume testing (median grain size ranged from 0.10-0.60 mm), as well as dimensional analysis. Further details of the hydraulic and geotechnical data considered for developing the models are presented elsewhere (Shahriar et al. 2021b). In summary, these four models are chosen due to the differences in the groups of data on which each of these models was developed.

3. Database for analyses

Data reported in Benedict and Caldwell (2014), who compiled laboratory scour measurements conducted since 1956, are utilized herein. The database is comprised of both clear water (upstream mean flow velocity to sediment critical velocity ratio is less than one with mainly a sandy bed) and live bed (upstream mean flow velocity to sediment critical velocity ratio is more than one with the stream bed having appreciable percent fines) scour condition. Melville and Coleman (2000) identified that the upstream flow depth (y) to pier width (b) ratio is one of the most important parameters driving the maximum scour magnitude and suggested three classes of pier scour flow field. When $y/b > 1.4$, the vertical component of flow at the pier's leading face causes the deepest scour to occur at the pier face. When $0.2 \leq y/b \leq 1.4$, the main flow features get disrupted with the decrease of the normalized flow depth, leading to a reduced capacity of flow to erode bed material. For $y/b < 0.2$, the lateral movement of the flow contributes to cause the deepest scour to occur at the pier flanks. Ettema et al. (2017) presented information on the differences in the turbulence structures formed for the three pier classes. Subsequently, the database considered herein was classified into three pier categories per the suggestion of Melville and Coleman (2000). The ranges of the selected variables for both clear water and live bed laboratory data, including flow velocity, flow depth, median grain size, pier width to median grain size ratio, flow velocity to critical velocity ratio, and measured scour depth are presented in Tables 2 and 3 respectively. The standard deviation of the parameter and coefficient of variation are also respectively reported in Tables 2 and 3.

Important to note that, laboratory database, rather than field database was considered for analyses accounting for the uncertainties associated with the field scour measurements. Uncertainties of field scour measurements include the accuracy of measured scour (Ground Penetrating Radar versus Fathometer approach), the maturity of the scour depth (equilibrium versus non-equilibrium scour), and accuracy of the hydraulic attributes (historic flow-based approach versus one dimensional flow model-based approach). Mueller and Wagner (2005) and Sheppard et al. (2011) suggested that the laboratory scour models can well capture the scour mechanism occurring at a field condition, suggesting a platform to advance analyses using laboratory data-based statistics, thereby providing means to avoid the uncertainty associated with field-reported scour measurement.

3.1 Data screening

In the present study, two approaches were considered to identify the outliers within the database. It is important to note that the objective of data screening process was to identify data points that “most likely” are not representative of equilibrium scour depth since the deterministic models considered herein provide estimates of the equilibrium scour magnitude. Error in models’ estimation is the parameter that was considered to quantify the adequacy of a given deterministic model. Error is defined as the difference between the predicted, y_{sp} , and the measured scour depth, y_{sm} , expressed as a percentage of the measured scour depth, as shown in Equation (5):

$$Error, \% = \frac{y_{sp} - y_{sm}}{y_{sm}} \times 100\% \quad (5)$$

A positive error magnitude indicates that an over-prediction of the scour depth from a given deterministic model; conversely, a negative error indicates an under-prediction. The first approach to identify the outlier data points was to adopt a statistical outlier identification technique, commonly known as box plotting. Figure 1 shows the error-boxplot corresponding to narrow pier clear water data for the four deterministic models considered in the study. The outlier data points were identified and listed in Table 4. Observation of Table 4 suggest that 67% of the outliers has $b/D_{50} \leq 52$. Ettema et al. (2011) reported that for $b/D_{50} \leq 50$ the individual soil particles are so large compared to the groove carved out by the down flow, thereby erosion is impeded as the rough bed dissipates some of the energy. Data in Table 4 suggest that v/v_c ranged from 0.41 to 0.96, and 45% of the data points had a $v/v_c = 0.41 - 0.55$. Melville and Coleman (2000), based on the investigation on piers placed on uniform deposits in clear water condition, reported that scouring process initiates when $v/v_c \sim 0.4$, and the scour magnitude increases linearly with the increase of upstream mean flow velocity. As substantial data points presented $v/v_c < 0.55$ (refer to Table 4), it is expected that the scour rate was within the initial steep rising slope and has not reached equilibrium yet. Although the duration of flow was reported, whether such duration was sufficient for reaching the equilibrium state is not known.

The second method used to identify the outliers is estimating the standard deviation of the error from the data set and identifying the data points that presented an error beyond two standard deviations from the mean error. The outliers, along with the key parameter attributes are listed in Table 5. Data in Table 5 suggest that 56% of the data has a $v/v_c < 0.55$, while 50% of the outliers has $b/D_{50} \leq 52$. Therefore, the explanation presented before regarding the outliers and $v/v_c < 0.55$ is possibly applicable to justify the outlier nature of the data points.

The data screening process described herein eliminated 7% of the data points for narrow pier clear water condition, thereby reducing the coefficient of variation of the screened dataset. Using the similar methodology, the outliers for intermediate pier and wide pier corresponding to clear water and live bed cases were identified and removed from the dataset. Table 6 presents a summary of the percentage of the data points that are removed from the dataset corresponding to each category of pier investigated.

4. Methodology

The reliability theory incorporated in the Load and Resistance Factor Design (LRFD) methodology accounts for the uncertainties while evaluating the safety of a system as expressed by a level of reliability (e.g., Lagasse et al. 2013; Nowak and Collins 2000). The influence of different sources of uncertainties can be represented by considering the statistical attributes of a random variable. A random variable can take a specific value with a certain probability and the probabilities can be described by a distribution function. Safety is described where the capacity exceeds demand. Therefore, a limit state function, L , expressing safety can be expressed as shown in Equation (6).

$$L = D_p - D_s \quad (6)$$

Where, D_p is the depth from bed level to a depth that will lead to a foundation failure (as defined by geotechnical analyses), and D_s is the scour depth predicted from different scour prediction models.

Probability of exceedance is defined as the probability that a certain scour depth will be exceeded in a future time. The probability of exceedance, P_e for the limit state function can be expressed as in Equation (7).

$$P_e = P(L < 0) \quad (7)$$

Where, $P()$ symbolizes the probability. Considering Arneson et al. (2012) model, Equation (7) can be presented as shown in Equation (8).

$$P_e = P\left(D_p < \lambda 2K_1K_2K_3\left(\frac{y}{b}\right)^{0.35}F_r^{0.43}\right) \quad (8)$$

Where, λ is a bias factor equal to the ratio of the measured to the predicted scour depth from a given deterministic model, and the rest of the parameters in Equation (8) are defined in Table 1. Due to the nonlinear nature of Equation (8), a simulation technique needs to be used to compute the probability of exceedance; the Monte Carlo simulation approach was used herein.

If the limit state function follows normal probability distribution, then Equation (8) expresses the probability that L is less than 0.

$$P_e = \Phi\left(\frac{0 - \bar{L}}{\sigma_L}\right) \quad (9)$$

Where, Φ is a probability function representing the probability that the normalized random variable is below a given value, \bar{L} is the mean value of the limit state function, σ_L is the standard deviation of the limit state function, L . Therefore, reliability index, β , (which is a measure of the number of standard deviations that the mean margin of safety falls on the safe side), can be expressed as in Equation (10).

$$P_e = \Phi(-\beta) \quad (10)$$

Similar to “resistance factors” in the LRFD approach, the concept introduced herein seeks to develop “scour factors”. A scour factor, SF is defined as the ratio of the magnitude of depth from bed level to cause foundation system failure to the scour depth computed from different scour prediction models; expressed in Equation (11).

$$SF = \frac{D_p}{D_s} \quad (11)$$

The Monte Carlo simulation was run for scour factors, SF ranging from 1 to 3, and a relationship between the reliability index or the associated probability of exceedance and scour factor will be devised.

5. Deterministic and Random variables

To evaluate the probability of exceedance, a statistical distribution for the variables used in Equation (8), or its equivalent form when different scour prediction models (Equations 1-4) need to be considered. The pier width, skew angle, pier face shape, and aspect ratio were considered as deterministic, as these are not subjected to inherent temporal or spatial variability. Flow depth, flow velocity, median grain size, and bias factor are considered as random variables. A dimensionless measure of uncertainty is the coefficient of variation (COV), which is the ratio of standard deviation divided by the mean magnitude. The COV associated with flow depth, y , can be estimated based on the uncertainty analyses performed by U.S. Army Corps of Engineers (HEC 1986), as expressed in Equation (12).

$$COV_y = 0.76y^{0.6}S^{0.11}(5N)^{0.65} \quad (12)$$

Where, N is the reliable estimate of Manning’s coefficient, n . The distribution of n was considered lognormal as presented in HEC (1986) and Johnson (1992). The distribution of S , which is the slope of the channel bed, was considered lognormal based on the analyses of Johnson (1996). Discharge in a stream is a function of Manning’s roughness coefficient and channel bed slope. Johnson (1992), and Lagasse et al. (2013), based on hydrologic uncertainty analyses, considering the aforementioned distribution of Manning’s n and channel bed friction, S , showed that the distribution of flow velocity is lognormal, and suggested that the COV is 0.12 times the mean upstream flow velocity.

Lagasse et al. (2013) indicated that sediments’ gradation is normally distributed, as such, the median grain size herein was assumed to be normally distributed. The bias factor, λ , defined as the ratio of the measured to the predicted scour depth for the data set considered herein, was observed to be normally distributed as shown in Figure 2 for live bed condition (statistical Q-Q plot also warrants the observation). It appears that the distribution of λ is not purely symmetric, rather a mild positive skewness of 0.14-0.65 was noticed. Table 7 shows the list of deterministic and random variables and the associated statistical characteristics considered in the present study.

6. Analyses

6.1 Simulation cycles

To ascertain the minimum number of simulations needed to evaluate the probability of exceedance equilibrium pier scour magnitude with sufficient accuracy, various simulation counts are considered, and the corresponding probability of exceedance was computed. The procedure was repeated for two scour factors, e.g., 1.0 and 1.1, and the results are presented in Figure 3. Beyond a simulation cycle of 5,000, stability of the reported probability of exceedance is observed. However, to obtain a small probability of

exceedance, e.g., in the range of 0.0001, the number of simulation cycles should be greater than 5,000. Therefore, 10,000 simulation cycles were considered in the study.

6.2 Probability of exceedance-scour factor relation

Figure 4 shows the relationship between probability of exceeding the measured scour depth versus the scour factor using four scour prediction models considered in the study. The probability of exceedance decreases as the scour factor increases. The following is commentary on the results related to each deterministic model considered herein:

For Wilson (1995) model (Figure 4a-b), and above a probability of exceedance of 0.001, no discernible difference in the scour factor was noticed for narrow pier, intermediate pier, or wide pier cases. For narrow pier cases, a scour factor of 1.4 needs to be applied to the predicted scour depth to obtain a probability of exceedance in the range of 0.0001 (or 1 in 10,000.) Irrespective of the type of pier (narrow, intermediate, wide), a scour factor of 1.35 ensures a probability of exceedance of 0.001 for both clear water and live bed conditions when Wilson (1995) model is considered.

For Melville (1997) model, and in clear water condition (Figure 4c), the use of a scour factor of 1.0 corresponds to a 50% probability of exceedance for narrow, intermediate, and wide piers. For wide pier cases in clear water condition, the scour factor required to attain a given level of probability of exceedance is less than that required for narrow and intermediate piers. This is due to the fact that the Melville (1997) model, without the application of any factor, is providing a conservative estimate of the scour depth for wide pier compared to narrow and intermediate piers (under clear water conditions). Therefore, to achieve a certain probability of exceedance, the scour factor is less for wide pier compared to the narrow and intermediate piers. For Melville (1997) model, in live bed condition (Figure 4d), the use of a scour factor of 1.0 corresponds to 30% probability of exceedance for wide pier and 50% probability of exceedance for narrow, and intermediate piers.

Figure 4(e-f), for both clear water and live bed conditions, shows results for HEC 18 (2012) model. It appears that the highest scour factor is needed for the scour depth predicted for narrow piers, among the three categories of piers, to achieve the same level of probability of exceedance. This suggest that results from HEC 18 (2012) model provide the most conservative estimate for wide pier condition and the least conservative for narrow pier condition. It is important to note that HEC 18 (2012) model was developed mostly based on narrow pier ($y/b > 1.4$) data (Benedict and Knight 2017). Melville and Coleman (2000) reported that for a similar hydraulic condition, the use of HEC 18 for narrow piers will yield a higher scour depth compared to its use for intermediate and wide piers. Accordingly, the scour depth predicted from HEC 18 (2012) model is inherently conservative.

For Briaud (2014) model in clear water condition (Figure 4g), discernible differences in the scour factor for narrow and intermediate piers are not apparent. In this case, the scour factor corresponding to the wide pier condition is the lowest among the scour factors for narrow, intermediate and wide piers corresponding to a certain probability of exceedance. For Briaud (2014) model, and in live bed condition, the use of a scour factor of 1.0 corresponds to a 22% probability of exceedance for narrow pier and ~50% probability of exceedance for wide, and intermediate piers under both clear water and live bed conditions.

6.3 Reliability index-scour factor relation

The reliability index, β , has been used across structural and geotechnical engineering literature to represent a level of risk (AASHTO LRFD 2007; AISC 2005; ACI 2005). In general, a β value of 2 to 4 is specified for the various structural applications. For the design of new bridges, AASHTO LRFD specification (2007) suggests the use of a $\beta = 3.5$, while Moses (2001) suggests $\beta = 2.5$ for the load capacity evaluation of existing bridges.

Figure 5 shows the relationship between reliability index and scour factor for the four models considered in the study. As the target reliability index increases, the corresponding scour factor increases. Referring to Figure 5a-b, for the Wilson (1995) model, the scour factor corresponding to different reliability indices is almost identical. This is owing to the fact that Wilson model is empirical in nature and considered the upstream flow depth to pier width ratio as the primary variable controlling the magnitude of scour. Only the uncertainty of the upstream flow depth had an impact on the reliability index with the pier width considered deterministic in nature. This resulted in a maximum scour factor for the Wilson model to be the lowest (1.5) compared to the other three models, where a scour factor as much as 2.95 was computed to attain a reliability index of 3.7 as for the Melville model (clear water, intermediate pier- Figure 5c).

AASHTO (2007) bridge design specification suggests that a target reliability index, β_T , of 2.33 to be used for redundant systems, while 3.0 for a non-redundant system. For Wilson (1995) model (Figure 5a-b), the scour factor corresponding to a $\beta_T = 3.0$ is 1.34 for clear water case and 1.35 for live bed case. For Melville (1997) model in clear water condition (Figure 5c), the scour factor corresponding to a $\beta_T = 3.0$ is 2.24, 2.4, and 2.65 for wide pier, narrow pier, and intermediate pier respectively. However, for live bed condition (Figure 5d), the scour factor corresponding to a $\beta_T = 3.0$ varies within a narrow range (2.1-2.22). For HEC 18 (2012) model, irrespective of the clear water or live bed condition (Figure 5e-f), the scour factor corresponding to a $\beta_T = 3.0$ is lowest for wide pier (1.61 and 1.75 for clear water and live bed respectively), and highest for narrow pier (2.05 and 2.1 for clear water and live bed respectively). For Briaud (2014) model (Figure 5g-h), the scour factor corresponding to a $\beta_T = 3.0$ is identical (2.4) for narrow and intermediate piers under clear water condition, while for wide pier the scour factor is 1.9.

6.4 Sensitivity analyses

Sensitivity analyses were carried out to assess the effect of “mean value” magnitude of the random variables on the obtained reliability index. Figure 6 shows the relationship between reliability index and scour factors for different y/b and F_r . The responses from HEC 18 (2012) model under clear water narrow pier condition was presented. Investigation into the HEC 18 (2012) deterministic model (refer to Equation 3 for the mathematical expression) suggests that the reported scour magnitude is dependent on pier width, upstream mean flow velocity, and upstream flow depth, therefore although D_{50} is probabilistic in nature, its magnitude will not affect the computed reliability index-scour factor relation. Subsequently, the effect of non-dimensional terms y/b and F_r was explored. Figure 6(a) shows the 5% error bars from the suggested reliability index-safety factor magnitude (Figure 5e). It appears that differences in y/b magnitudes lead to insignificant impact on the computed reliability index-scour factor magnitudes, as the responses corresponding to different y/b fall within the bandwidth of $\pm 5\%$ from the base case value of $y/b = 2$ (For narrow pier condition). The effect of using a range of Froude number, F_r is minimal as well. As shown in Figure 6(b), irrespective of the Froude number (0.1-0.8), the error associated with the proposed reliability index-scour factor magnitude is less than 2% (The error bars correspond to $\pm 2\%$ in Figure 6b) from the base case value of $F_r = 0.25$.

7. Probability of deceedance-reliability index relation

The scour factor associated with a reliability index is correlated to the probability of deceedance obtained from the comparison of measured and the predicted scour depth reported in the Benedict and Caldwell (2014) database. A probability of deceedance (POD) is defined as the probability that the predicted scour depth will be less than the measured scour depth and can be expressed as in Equation (13).

$$POD = P(y_{sp} \leq y_{sm}) \quad (13)$$

Where, $P()$ symbolizes the probability, y_{sp} and y_{sm} denote the predicted and the measured scour depth respectively.

First, the frequency distribution of χ_{POD} , which is the ratio of predicted to the measured scour depth was developed. Using Kernel density estimation, the population probability density function for χ_{POD} was generated, followed by integration of the density function to obtain the cumulative density function. The POD is obtained by subtracting the cumulative density value from one. For illustration, HEC 18 (2012) model was applied to live bed local scour data reported in Benedict and Caldwell (2014). The POD estimates using HEC 18 (2012) model are presented in Figure 7. The reliability index and scour factor relation for narrow pier under live bed condition (Figure 4f) is presented on the same plot. For the data set in the database utilized herein, POD ranging from 1-0.0044 was estimated. As shown in Figure 7, the POD corresponding to a scour factor of one is 0.007, and the associated reliability index is zero (i.e., there is a 0.7% probability that the estimated scour depth from HEC 18 (2012) deterministic model would be less than the measured scour depth). The end point of the POD chart (POD = 0.0044) is corresponding to a scour factor of 1.3, and a reliability index of 0.90. To obtain a target reliability index of 3.0, the corresponding scour factor would be 2.09, and the extrapolated (by plotting a tangent; refer to Figure 7, the dashed-dot region) POD chart suggests the corresponding POD would be 0.0012. It implies that use of a scour factor of 2.09 can reduce the POD by 6 times (to 0.0012) compared to the POD corresponding to the unfactored scour depth estimation (0.007); whereby, a reliability index of 3 can be achieved.

8. Application example

The scour factors proposed herein can be applied to scour calculations as follows:

Step 1: Based on hydraulic and hydrologic studies, determine upstream flow depth and upstream mean flow velocity using the appropriate return periods as suggested by Arneson et al. (2012) (commonly referred to as HEC 18 (2012) manual).

Step 2: Compute the equilibrium scour depth using any of the four deterministic models (e.g., Wilson 1995, Melville 1997, HEC 18 2012, Briaud 2014; refer to Equations 1-4).

Step 3: Estimate the mean upstream flow velocity at the critical condition, referred to as critical velocity, using the expression suggested by Henderson (1966) and Melville and Sutherland (1988). Compare the critical velocity to the upstream mean flow velocity estimated in step 1 to assess the prevailing clear water versus live bed upstream condition.

Step 4: Specify the reliability index to be achieved. Use the appropriate chart from Figure 5 to estimate the scour factor based on: upstream flow depth to pier width ratio, the model used to compute scour, and the upstream flow condition. Multiply the scour factor by the scour depth computed in step 2 to obtain the design scour depth corresponding to the target reliability index.

For example, appropriate hydraulic and hydrologic modeling of a stream indicated that the upstream mean flow velocity and flow depth are 2 ft/sec and 6 ft respectively. The pier is circular in shape having a diameter of 2 ft, with a flow skew angle of 0 degree. The stream bed has median grain size is 0.7 mm. The use of HEC 18 (2012) model yields a normalized scour depth of 1.40. The critical velocity is estimated to be 1.50 ft/sec; therefore, live bed upstream condition is used. The upstream flow depth to pier width ratio is 3, indicating narrow pier condition. If the target reliability index is 3.0, then the corresponding scour factor from Figure 4(f) is obtained as 2.09. Therefore, the design normalized scour depth will be ~ 2.93 (scour depth will be ~ 5.9 ft). Figure 6 suggests that the POD corresponding to a reliability index of 3 is 0.0012 (from the extrapolated region); thereby suggesting in 12 out of 10,000 cases having the assumed parameters in the example, the scour depth of 5.9 ft would be exceeded.

9. Conclusion

Based on the results obtained herein, the following conclusions are advanced:

1. A reliability-based pier scour estimation methodology was presented accounting for input parameter uncertainty and inherent model bias. The methodology is applicable for local scour calculation in riverine flow under clear water and live bed condition using four deterministic scour prediction models: Wilson (1995) model, Melville (1997) model, HEC-18 (2012) model, and Briaud (2014) model.
2. A relationship between scour factor, which is the ratio of the depth from average bed level to the bottom of the footing, to the scour depth predicted from different scour prediction models and probability of exceedance of the measured scour depth is proposed. It was observed that the proposed relationship is dependent on the pier type (e.g., narrow pier, intermediate pier, and wide pier), upstream sediment transport condition (e.g., clear water and live bed), and the deterministic model being used (e.g., Wilson (1995) model, Melville (1997) model, HEC-18 (2012) model, and Briaud (2014) model).
3. AASHTO (2007) bridge design specification suggests different target reliability index, β_T , based on the redundancy and non-redundancy of the structure. A relationship between reliability index and scour factor is devised, enabling engineers to decide the level of reliability index desired per the importance of the structure. The proposed method will help mitigating the inconsistency posed by adopting a β -based approach for the design of various superstructure bridge components as opposed to a deterministic approach for assessing the scour magnitude at the foundation system. Having a uniform level in the reliability index of the bridge components will facilitate the development of integral risk-based design approach for bridge structures.

Data availability statement

All data, models, and code generated or used during the study appear in the submitted article.

Acknowledgements

Funding from North Carolina Department of Transportation (NCDOT) is gratefully acknowledged. Any conclusions, findings, opinions, and recommendations expressed in this article are those of the authors and do not necessarily reflect the views of NCDOT.

References

- AASHTO (2007). "AASHTO LRFD Bridge Design Specifications: Customary U.S. Units," 4th Edition, American Association of State Highway and Transportation Officials, Washington, D.C.
- ACI 318-05 (2005). "Building Code Requirements for Structural Concrete and Commentary," American Concrete Institute, Farmington Hills, MI.
- AISC 325-05 (2005). "Steel Construction Manual," Thirteenth Edition, American Institute of Steel Construction, Chicago, IL.
- ASCE (2010). "Minimum Design Loads for Buildings and Other Structures," ASCE 7-10, American Society of Civil Engineers, Reston, VA.
- ATC/MCEER Joint Venture (2002). "Comprehensive Specifications for the Seismic Design of Bridges," NCHRP Report 472, Transportation Research Board, National Academies of Science, Washington D.C.
- Arneson LA, Zevenbergen LW, Lagasse PF, and Clopper PE. (2012). "Evaluating scour at bridges." Hydraulic Engineering Circular No. 18, 5th edition, 1-340.
- Azamatullah HM, Yusoff MAM, and Hasan ZA (2014). "Scour below submerged skewed pipeline." *Journal of Hydrology*, 509(2014): 615-620.
- Benedict ST, and Caldwell AW. (2014). "A pier-scour database—2,427 field and laboratory measurements of pier scour." U.S. Geological Survey Data Series 845, 1-22.
- Benedict ST, and Knight TP. (2017). "Use of Laboratory and Field Data to Evaluate the Pier Scour Equation from Hydraulic Engineering Circular 18" *Transportation Research Record*. 2638(1):113-121.
- Bolduc LC, Gardoni P. and Briaud J-L. (2008). "Probability of exceedance estimates for scour depth around bridge piers." *Journal of Geotechnical and Geoenvironmental Engineering*; 134:2(175), 175–184.
- Box GEP, and Cox DR. (1964). "An analysis of transformations," *Journal of the Royal Statistical Society*, Series B; 26, 211-252.
- Briaud JL. (2014). "Scour depth at bridges: Method including soil properties. I: Maximum scour depth prediction." *Journal of Geotechnical and Geoenvironmental Engineering*; 141(2): 04014104.
- Briaud J-L, Gardoni P, and Yao C. (2014). "Statistical, risk, and reliability analyses of bridge scour." *Journal of Geotechnical and Geoenvironmental Engineering*; 140(2): 04013011.
- Briaud J-L, Brandimarte L, Wang J, and D’Odorico P. (2007). "Probability of scour depth exceedance due to hydrologic uncertainty." *Georisk: Assessment and Management of Risk for Engineered Systems and Geohazards*; 1(2), 77–88.
- Chabert J, and Engeldinger P. (1956). "Etude des affouillements autour des piles des ponts." Laboratoire d'Hydraulique, Chatou, France (in French).
- Chee, R.K.W., (1982), Live-bed scour at bridge piers: Auckland, New Zealand, School of Engineering, The University of Auckland, Report No. 290,
- Chiew, Y.M., (1984), Local scour at bridge piers: New Zealand, School of Engineering, The University of Auckland, Report No. 355,
- Contreras-Jara, M., Echaveguren, T., Chamorro, A., and Vargas-Baccheler, J., (2021), Estimation of Exceedance Probability of Scour on Bridges Using Reliability Principles: *Journal of Hydrologic Engineering*; 26(8), 04021029.

- Dey, S., Bose, S.K., and Sastry, G.L.N., (1995), Clearwater scour at circular piers—A model: *Journal of Hydraulic Engineering*; 121(12), 869–876.
- Ettema, R., (1976), Influence of bed material gradation on local scour: Auckland, New Zealand, School of Engineering, The University of Auckland
- Ettema, R., (1980), Scour at bridge piers: Auckland, New Zealand, School of Engineering, The University of Auckland, Report No. 216
- Ettema, R., Kirkil, G., and Muste, M., (2006), Similitude of large-scale turbulence in experiments on local scour at cylinders: *Journal of Hydraulic Engineering*; 132(1), 33–40,
- Ettema R, Constantinescu G, Melville BW. Evaluation of bridge scour research—Pier scour processes and predictions: Transportation Research Board of the National Academies, National Cooperative Highway Research Program Web Document 175 (Project 24–27(01)), 2011; 1-181.
- Ettema R, Constantinescu G, and Melville BW. (2017). “Flow-field complexity and design estimation of pier-scour depth: Sixty years since Laursen and Toch.” *Journal of Hydraulic Engineering*; 143(9), 03117006.
- Florida Department of Transportation (FDOT) (2011). “Bridge Scour Manual,” Tallahassee, FL.
- Ghosn, M. and Moses, F. (1998). “Redundancy in Highway Bridge Superstructures,” NCHRP Report 406, Transportation Research Board, National Academies of Science, Washington, D.C.
- Graf, W.H., (1995), Load scour around piers: Lausanne, Switzerland, Laboratoire de Recherches Hydrauliques, École Polytechnique Fédérale de Lausanne, Annual Report, p. B.33.1–B.33.8
- Gudavalli SR. (1997). “Prediction model for scour rate around bridge piers in cohesive soil on the basis of flume tests.” Ph.D. dissertation, Department of Civil Engineering, Texas A&M University, College Station, Texas.
- Henderson FM. (1966). *Open channel flow*. MacMillan Publishing Co. Inc., New York, N.Y.
- Hong, J-H, Goyal MK, Chiew, Y-M, and Chua LHC (2012). “Predicting time-dependent pier scour depth with support vector regression.” *Journal of Hydrology*, 468-469(2012): 241-248.
- Hydrologic Engineering Center (1986). "Accuracy of Computed Water Surface Profiles," U.S. Army Corps of Engineers, Davis, CA.
- Jain, S.C., and Fischer, E.E., (1979), Scour around circular bridge piers at high Froude numbers: Federal Highway Administration Report FHWA-RD-79-104, available from NTIS, 5285 Port Royal Road, Springfield, Virginia 22161
- Johnson PA. (1992). "Reliability-based pier scour engineering." *Journal of Hydraulic Engineering*; 118(10), 1344-1358.
- Johnson P.A. (1996). "Uncertainty of Hydraulic Parameters," *Journal of Hydraulic Engineering*; 122(2), 112-115.
- Johnson PA, Clopper PE, Zevenbergen LW and Lagasse PF. (2015). “Quantifying uncertainty and reliability in bridge scour estimations.” *Journal of Hydraulic Engineering*; 141(7), 04015013.
- Kim, K. J., M. S. Rahman, M. A. Gabr, R. Z. Sarica, and M. S. Hossain. (2005). “Reliability Based Calibration of Resistance Factors for Axial Capacity of Driven Piles.” In *Advances in Deep Foundations*, Geotechnical Special Publication 113, 1–12. Austin, TX: ASCE

- Kulicki J.M., Mertz D.R., and Nowak A.S. (2007). "Updating the Calibration Report for AASHTO LRFD Code," NCHRP Project 20-7/186, Transportation Research Board, National Academies of Science, Washington, D.C.
- Kwak K. (2000). "Prediction of scour depth versus time for bridge piers in cohesive soils in the case of multi-flood and soil systems." Ph.D. dissertation, Department of Civil Engineering, Texas A&M University, College Station, Texas.
- Lagasse P. F., Ghosn M., Johnson P. A., Zevenbergen L.W., and Clopper P. E. (2013). "Risk-based approach for bridge scour prediction." Final Rep., NCHRP Project 24-34, Transportation Research Board, National Academies of Science, Washington, DC.
- Landers MN, and Mueller DS. (1996). "Channel scour at bridges in the United States." *Report No. FHWA-RD-95-184*, Federal Highway Administration, Washington, D.C.
- Liang FY, Zhang H, and Huang MS. (2015). "Extreme scour effects on the buckling of bridge piles considering the stress history of soft clay." *Natural Hazards*; 77, 1143–1159.
- Liu, D., Ghosn, M., Moses F., and Neuenhoffer, A. (2001). "Redundancy in Highway Bridge Substructures," NCHRP Report 458, Transportation Research Board, National Academies of Science, Washington D.C.
- Melville BW. (1997). "Pier and abutment scour: Integrated approach." *Journal of Hydraulic Engineering*; 123(2), 125–136.
- Melville, B.W., and Chiew, Y.M., (1999), Time scale for local scour at bridge piers: American Society of Civil Engineering, *Journal of Hydraulic Engineering*; 125(1), 59–65,
- Melville BW. and Coleman SE. (2000). "Bridge scour." Highlands Ranch, USA: Water Resources Publications.
- Melville BW. and Sutherland AI. (1988). "Design method for local scour at bridge piers." *Journal of Hydraulic Engineering*; 114(10), 1210-1226.
- Moses, F. (2001). "Calibration of Load Factors for LRFR Bridge Evaluation," NCHRP Report 454, Transportation Research Board, National Academies of Science, Washington, D.C.
- Mueller, D.S., Wagner, C.R., (2005). "Field observations and evaluations of streambed scour at bridges," Report No. D-03-052, Federal Highway Administration, McLean, VA.
- National Research Council. (2000). *Risk Analysis and Uncertainty in Flood Damage Reduction Studies*. Washington, DC: The National Academies Press.
- Nowak A. (1999). "Calibration of LRFD bridge design code." NCHRP Rep. 368, Transportation Research Board, Washington, DC.
- Nowak A.S. and Collins K.R. (2000). "Reliability of Structures," McGraw-Hill, New York, NY.
- Paikowsky SG. (2004). "Load and resistance factor design (LRFD) for deep foundations." NCHRP Rep. 507, Transportation Research Board, Washington, DC.
- Qi M, Li J, and Chen Q. (2016). "Comparison of existing equations for local scour at bridge piers: parameter influence and validation." *Natural Hazards*; 82(3), 2089-2105.
- Shahriar AR, Ortiz AC, Montoya BM, and Gabr MA (2021a). "Bridge Pier Scour: An overview of factors affecting the phenomenon and comparative evaluation of selected models," *Transportation Geotechnics*, 28(2021), 100549. DOI: 10.1016/j.trgeo.2021.100549.

- Shahriar AR, Montoya BM, Ortiz AC and Gabr MA (2021b). “Quantifying probability of exceedance estimates of clear water local scour around bridge piers,” *Journal of Hydrology*; 597(2021):126177.
- Shen HW, Schneider VR, and Karaki SS. (1966). "Mechanics of local scour." *Report*, U.S. Dept. of Commerce, National Bureau of Standards, Inst. for Appl. Technol., Washington, D.C.
- Shen, H.W., Schneider, V.R., and Karaki, S.S., (1969), Local scour around bridge piers: *Journal of the Hydraulics Division*; 95(HY6), 1919–1940
- Sheppard, D.M., and Miller, W., (2006), Live-bed local pier scour experiments: *Journal of Hydraulic Engineering*; 132(7,) 635–642,
- Sheppard, D.M., Odeh, M., and Glasser, T., (2004), Large scale clear-water local pier scour experiments: *Journal of Hydraulic Engineering*; 130(10), 957–963
- Sheppard, M., Demir, H., Melville, B.W., (2011). “Scour at wide piers and long skewed piers,” NCHRP Report 682, Transportation Research Board of the National Academies, Washington D.C.
- Yanmaz, A.M., and Altinbilek, H.D., (1991), Study of time-dependent local scour around bridge piers: *Journal of Hydraulic Engineering*; 117(10), 1247–1268
- Yao C. (2013). “LRFD calibration of bridge foundations subjected to scour and risk analysis.” Ph.D. dissertation, Department of Civil Engineering, Texas A&M University, College Station, Texas.
- Wardhana K, Hadipriono FC. (2003). “Analysis of recent bridge failures in the United States.” *Journal of Performance of Constructed Facilities*; 17(3), 144-150.
- Wilson KV Jr. (1995). “Scour at selected bridge sites in Mississippi.” *Resources Investigations Report 94–4241*, Geological Survey Water, Reston, Virginia.

Table 1. Deterministic pier scour model equations considered in the present study (Shahriar et al. 2021b)

Reference	Model	Equation No.	Remarks
Wilson (1995)	$\frac{y_{sp}}{b'} = 0.9\left(\frac{y}{b'}\right)^{0.4}$	(1)	b' = projected pier width y_{sp} = predicted scour depth y = flow depth upstream of pier
Melville (1997)	$y_{sp} = K_{yb}K_IK_dK_sK_\theta K_G$	(2)	K_{yb} = pier depth-size factor K_I = flow intensity factor K_d = sediment size factor K_s = pier nose shape factor K_θ = pier alignment factor K_G = channel geometry factor (= 1 for pier)
Arneson et al. (2012)	$\frac{y_{sp}}{b} = 2K_1K_2K_3\left(\frac{y}{b}\right)^{0.35}F_r^{0.43}$	(3)	K_1 = pier nose shape factor K_2 = pier alignment factor K_3 = bed condition factor b = pier width F_r = Froude number
Briaud (2014)	$\frac{y_{sp}}{b'} = 2.2K_{pw}K_{psh}K_{pa}K_{psp}(2.6F_{pier} - F_{c(pier)})^{0.7}$	(4)	K_{pw} = water depth influence factor K_{psh} = pier shape influence factor K_{pa} = aspect ratio influence factor K_{psp} = pier spacing influence factor F_{pier} = pier Froude number $F_{c(pier)}$ = critical pier Froude number

Table 2. Mean, Standard deviation (SD) and Coefficient of variation (COV) of the parameters for clear water laboratory data considered in the study

Reference	Narrow pier																	
	v			y			D ₅₀			b/D ₅₀			v/v _c			y _s /b		
	Mean	SD	COV	Mean	SD	COV	Mean	SD	COV	Mean	SD	COV	Mean	SD	COV	Mean	SD	COV
Chabert and Engeldinger (1956)	0.9	0.3	0.3	0.8	0.3	0.4	0.8	0.6	0.8	166	111	0.7	0.7	0.1	0.2	1.5	0.4	0.2

Chee (1982)	0.8	--	--	0.3	--	--	0.4	--	--	134	--	--	0.9	--	--	1.2	--	--
Chiew (1984)	1.4	0.5	0.4	0.6	0.1	0.1	1.5	1.0	0.7	54	53	1.0	0.9	0.1	0.1	1.7	0.6	0.3
Ettema (1980)	2.0	0.9	0.4	1.2	1.0	0.8	1.8	1.9	1.1	145	310	2.1	0.8	0.1	0.2	1.4	0.5	0.4
Ettema and others (2006)	1.5	0.0	0.0	3.3	0.0	0.0	1.1	0.0	0.0	207	110	0.5	0.9	0.0	0.0	1.4	0.2	0.2
Ettema (1976)	1.8	0.7	0.4	2.0	0.0	0.0	1.5	1.2	0.8	106	60	0.6	1.0	0.0	0.0	1.4	0.6	0.4
Graf (1995)	2.0	0.0	0.0	0.7	0.1	0.1	2.1	0.0	0.0	57	10	0.2	0.9	0.0	0.0	1.8	0.2	0.1
Jain and Fischer (1979)	1.6	--	--	0.3	--	--	1.3	--	--	20	--	--	0.8	--	--	1.9	--	--
Jones	1.6	0.5	0.3	0.9	0.0	0.0	2.9	1.7	0.6	98	113	1.1	0.7	0.1	0.2	1.2	0.4	0.3
Melville (1997)	0.8	0.1	0.2	0.7	0.0	0.0	0.8	0.0	0.1	25	6	0.2	0.6	0.1	0.2	1.6	0.7	0.4
Melville and Chiew (1999)	0.8	0.2	0.2	0.5	0.2	0.4	1.0	0.0	0.0	55	13	0.2	0.6	0.1	0.2	1.2	0.7	0.6
Shen and others (1969)	0.5	--	--	0.7	--	--	0.2	--	--	635	--	--	0.5	--	--	0.2	--	--
Sheppard and Miller (2006)	0.9	0.2	0.3	1.5	0.1	0.1	0.6	0.3	0.5	373	192	0.5	0.7	0.1	0.2	1.2	0.3	0.3
Sheppard and others (2004)	6.0	0.5	0.1	4.7	1.0	0.2	0.9	0.9	1.1	1151	1403	1.2	0.8	0.1	0.1	1.5	0.3	0.2
Yanmaz and Altinbilek (1991)	0.8	0.1	0.1	0.4	0.1	0.2	1.0	0.1	0.1	60	10	0.2	0.7	0.0	0.1	1.5	0.2	0.2

Intermediate pier

Reference	v			y			D ₅₀			b/D ₅₀			v/v _c			y _s /b		
	Mean	SD	COV	Mean	SD	COV	Mean	SD	COV	Mean	SD	COV	Mean	SD	COV	Mean	SD	COV
Chabert and Engeldinger (1956)	1.1	0.4	0.3	0.4	0.1	0.3	1.1	0.8	0.7	172	114	0.7	0.8	0.1	0.1	1.3	0.2	0.14
Coleman (unpublished)	1.0	--	--	0.3	--	--	0.8	--	--	379	--	--	0.9	--	--	0.8	--	--
Dey and others (1995)	0.7	0.1	0.2	0.1	0.0	0.1	0.5	0.2	0.3	170	72	0.4	0.9	0.1	0.1	1.0	0.2	0.16
Ettema (1980)	1.5	0.6	0.4	0.3	0.1	0.3	2.8	2.1	0.8	153	183	1.2	0.9	0.0	0.1	1.2	0.3	0.22
Jain and Fischer (1979)	1.6	--	--	0.3	--	--	2.5	--	--	41	--	--	0.8	--	--	1.6	--	--
Melville (1997)	0.9	0.2	0.2	0.5	0.1	0.3	0.9	0.0	0.0	247	55	0.2	0.7	0.2	0.2	0.9	0.3	0.38
Melville and Chiew (1999)	0.8	0.1	0.2	0.2	0.0	0.1	1.0	0.0	0.0	73	0	0.0	0.7	0.1	0.2	1.1	0.6	0.52
Shen and others (1969)	0.8	--	--	0.4	--	--	0.2	--	--	635	--	--	0.9	--	--	0.8	--	--
Sheppard and others (2004)	1.8	0.5	0.3	2.8	1.2	0.4	2.1	1.0	0.5	647	406	0.6	0.8	0.1	0.1	1.2	0.2	0.14
Yanmaz and Altinbilek (1991)	0.6	0.1	0.1	0.2	0.0	0.2	1.0	0.1	0.1	62	12	0.2	0.5	0.1	0.1	0.9	0.2	0.28

Wide pier

Reference	v			y			D ₅₀			b/D ₅₀			v/v _c			y _s /b		
	Mean	SD	COV	Mean	SD	COV	Mean	SD	COV	Mean	SD	COV	Mean	SD	COV	Mean	SD	COV
Coleman (unpublished)	1.0	0.0	0.0	0.8	0.0	0.0	0.8	0.0	0.0	911	0.0	0.0	0.9	0.0	0.0	0.4	0.0	0.0
Ettema (1980)	1.0	--	--	0.1	--	--	1.9	--	--	53	--	--	0.8	--	--	0.7	--	--

Melville (1997)	1.1	--	--	0.3	--	--	0.9	--	--	901	--	--	0.9	--	--	0.6	--	--
Sheppard and others (2004)	1.6	--	--	0.6	--	--	2.9	--	--	316	--	--	0.7	--	--	0.8	--	--

Note: v , y , D_{50} , v_c , and y_s mean upstream mean flow velocity, flow depth, median grain size, sediment critical velocity, and measured scour depth respectively. v , y , and D_{50} has the units of ft/s, ft, and mm. SD has the same unit as the variable in question, while COV is unitless.

Table 3. Mean, Standard deviation (SD) and Coefficient of variation (COV) of the parameters for live bed laboratory data considered in the study

Reference	Narrow pier																	
	v			y			D_{50}			b/D_{50}			v/v_c			y_s/b		
	Mean	SD	COV	Mean	SD	COV	Mean	SD	COV	Mean	SD	COV	Mean	SD	COV	Mean	SD	COV
Chabert and Engeldinger (1956)	1.15	0.05	0.05	0.77	0.26	0.34	0.52	0.00	0.00	139	40	0.3	1.09	0.09	0.08	0.40	0.06	0.15
Chee (1982)	1.91	0.88	0.46	0.33	0.00	0.00	0.54	0.41	0.77	144	70	0.5	1.91	0.74	0.39	0.22	0.04	0.17
Chiew (1984)	2.11	0.67	0.32	0.58	0.07	0.12	0.78	0.66	0.84	76	46	0.6	1.83	0.56	0.30	0.21	0.06	0.27
Ettema (1980)	1.44	0.01	0.01	1.97	0.00	0.00	0.83	0.02	0.02	90	53	0.6	1.00	0.00	0.00	0.57	0.32	0.56
Jain and Fischer (1979)	3.01	0.94	0.31	0.41	0.16	0.40	1.61	0.85	0.53	66	74	1.1	2.04	1.00	0.49	0.34	0.08	0.22
Jones (unpublished)	1.77	--	--	0.87	--	--	1.20	--	--	127	--	--	1.09	--	--	0.66	--	--
Shen and others (1969)	1.19	0.16	0.13	0.79	0.08	0.10	0.24	0.00	0.00	635	0	0.0	1.28	0.17	0.13	0.53	0.07	0.14
Sheppard and Miller (2006)	4.26	1.53	0.36	1.21	0.15	0.13	0.62	0.28	0.45	330	187	0.6	3.53	1.20	0.34	0.82	0.10	0.12
Sheppard and others (2004)	1.31			4.00			0.22			1387			1.19			1.28		
Reference	Intermediate pier																	
	v			y			D_{50}			b/D_{50}			v/v_c			y_s/b		
	Mean	SD	COV	Mean	SD	COV	Mean	SD	COV	Mean	SD	COV	Mean	SD	COV	Mean	SD	COV
Chabert and Engeldinger (1956)	1.2	0.0	0.0	0.3	0.0	0.0	0.5	0.0	0.0	168	24	0.1	1.3	0.0	0.0	0.4	0.0	0.1
Chee (1982)	2.4	0.9	0.4	0.3	0.0	0.0	0.7	0.5	0.7	209	130	0.6	2.3	0.9	0.4	0.4	0.1	0.2
Dey and others (1995)	0.8	0.0	0.0	0.2	0.0	0.0	0.3	0.0	0.0	254	30	0.1	1.0	0.0	0.0	0.3	0.0	0.1
Jain and Fischer (1979)	2.8	0.8	0.3	0.3	0.0	0.0	1.4	0.9	0.6	157	158	1.0	2.1	1.0	0.5	0.5	0.1	0.1
Shen and others (1969)	1.8	0.6	0.4	0.7	0.5	0.7	0.3	0.1	0.3	777	448	0.6	1.9	0.8	0.4	0.7	0.5	0.7
Sheppard and Miller (2006)	2.1	0.3	0.1	0.7	0.0	0.0	0.3	0.0	0.0	565	0	0.0	2.3	0.3	0.1	0.7	0.1	0.1
Sheppard and others (2004)	1.0	--	--	0.6	--	--	0.2	--	--	1387	--	--	1.1	--	--	1.0	--	--
Reference	Wide pier																	
	v			y			D_{50}			b/D_{50}			v/v_c			y_s/b		
	Mean	SD	COV	Mean	SD	COV	Mean	SD	COV	Mean	SD	COV	Mean	SD	COV	Mean	SD	COV
Coleman (unpublished)	1.0	0.0	0.0	0.1	0.0	0.0	0.8	0.0	0.0	733	251	0.3	1.0	0.0	0.0	0.7	0.1	0.2
Melville (1997)	1.0	0.0	0.0	0.2	0.0	0.0	0.9	0.0	0.0	636	265	0.4	1.0	0.0	0.0	0.8	0.0	0.0

Note: v , y , D_{50} , v_c , and y_s mean upstream mean flow velocity, flow depth, median grain size, sediment critical velocity, and measured scour depth respectively. v , y , and D_{50} has the units of ft/s, ft, and mm. SD has the same unit as the variable in question, while COV is unitless.

Table 4. List of outliers that are identified using the concept of error boxplot

Data source	b (ft)	v (ft/s)	v_c (ft/s)	y (ft)	D_{50} (mm)	σ_g	Duration of flow (minutes)	y/b	F_r	v/v_c	b/ D_{50}	y_s/b
Chiew (1984)	0.15	1.6	1.7	0.56	1.5	4.3	--	3.8	0.39	0.96	31.1	0.5
Ettema (1980)	0.09	3.2	3.6	1.64	5.4	1.2	2864	17.4	0.44	0.90	5.4	0.7
Ettema (1980)	0.17	0.5	1.1	1.97	0.4	1.3	2733	11.8	0.07	0.50	134.0	0.3
Ettema (1980)	0.17	0.8	1.4	1.97	0.8	1.3	565	11.8	0.10	0.55	63.6	0.3
Ettema (1980)	0.17	1.1	2.4	1.97	1.9	1.3	580	11.8	0.13	0.44	26.8	0.3
Ettema (1980)	0.17	1.8	3.7	1.97	5.4	1.2	342	11.8	0.23	0.50	9.5	0.3
Ettema (1976)	0.33	1.2	1.2	1.97	0.6	4.6	--	6.0	0.14	0.95	181.8	0.5
Ettema (1976)	0.33	1.4	1.5	1.97	0.9	2.9	--	6.0	0.17	0.95	117.6	0.8
Ettema (1976)	0.33	1.4	1.5	1.97	0.9	3.3	--	6.0	0.17	0.95	117.6	0.4
Ettema (1976)	0.33	2.2	2.4	1.97	1.9	2.6	--	6.0	0.28	0.95	52.6	0.8
Jones (unpublished)	0.5	1.8	3.1	0.87	5	--	4320	1.8	0.33	0.56	30.4	0.6
Jones (unpublished)	0.5	1.8	3.1	0.87	5	--	5640	1.8	0.33	0.57	30.4	0.6
Melville (1997)	0.05	0.6	1.3	0.66	0.9	1.3	320	12.6	0.12	0.44	17.6	0.6
Melville (1997)	0.08	0.6	1.3	0.66	0.9	1.3	1235	8.0	0.12	0.44	27.8	0.7
Melville and Chiew (1999)	0.16	0.6	1.4	0.66	1	1.3	450	4.0	0.12	0.42	52.1	0.2
Melville and Chiew (1999)	0.23	0.6	1.4	0.66	1	1.3	1298	2.9	0.12	0.41	73.0	0.3
Melville and Chiew (1999)	0.23	0.6	1.4	0.66	1	1.3	1300	2.9	0.13	0.45	73.0	0.4
Shen and others (1969)	0.5	0.5	0.9	0.70	0.2	1.4	--	1.4	0.10	0.53	635.2	0.2

Note: b, v, v_c , y, D_{50} , σ_g , F_r , and y_s are pier width, upstream mean flow velocity, sediment critical velocity, median grain size, sediment non-uniformity, Froude number, and measured scour depth respectively.

Table 5. List of outliers that are identified using the concept of error standard deviation

Data source	b (ft)	v (ft/s)	v _c (ft/s)	y (ft)	D ₅₀ (mm)	σ _g	Duration of flow (minutes)	y/b	Fr	v/v _c	b/D ₅₀	y _s /b
Chiew (1984)	0.15	1.6	1.7	0.56	1.5	4.3	--	3.8	0.4	0.96	31.1	0.5
Ettema (1980)	0.17	0.5	1.1	1.97	0.4	1.3	2733	12	0.1	0.5	134	0.3
Ettema (1980)	0.17	0.8	1.4	1.97	0.8	1.3	565	12	0.1	0.55	63.6	0.3
Ettema (1980)	0.17	1.1	2.4	1.97	1.9	1.3	580	12	0.1	0.44	26.8	0.3
Ettema (1980)	0.17	1.8	3.7	1.97	5.4	1.2	342	12	0.2	0.5	9.52	0.3
Ettema (1976)	0.33	1.2	1.2	1.97	0.6	4.6	--	6	0.1	0.95	182	0.5
Ettema (1976)	0.33	1.4	1.5	1.97	0.9	3.3	--	6	0.2	0.95	118	0.4
Melville and Chiew (1999)	0.13	0.6	1.4	0.66	1	1.3	200	5.2	0.1	0.42	39.7	0.1
Melville and Chiew (1999)	0.16	0.6	1.4	0.66	1	1.3	450	4	0.1	0.42	52.1	0.2
Melville and Chiew (1999)	0.23	0.6	1.4	0.66	1	1.3	1298	2.9	0.1	0.41	73	0.3
Melville and Chiew (1999)	0.23	0.6	1.4	0.66	1	1.3	1300	2.9	0.1	0.45	73	0.4
Melville and Chiew (1999)	0.13	1.1	1.4	0.66	1	1.3	4530	5.2	0.2	0.79	39.7	2.5
Shen and others (1969)	0.5	0.5	0.9	0.7	0.2	1.4	--	1.4	0.1	0.53	635	0.2
Melville (1997)	0.08	1	1.2	0.66	0.8	1.3	2690	8	0.2	0.79	31.3	2.6

Note: b, v, v_c, y, D₅₀, σ_g, Fr, and y_s are pier width, upstream mean flow velocity, sediment critical velocity, median grain size, sediment non-uniformity, Froude number, and measured scour depth respectively.

Table 6. Percentage of data points eliminated for each category of pier

Pier type	Upstream flow condition	Percentage of data screened out
Narrow ($y/b > 1.4$)	Clear water	7.0
Intermediate ($0.2 \leq y/b \leq 1.4$)	Clear water	25.3
Wide ($y/b < 0.2$)	Clear water	0.0
Narrow ($y/b > 1.4$)	Live bed	9.3
Intermediate ($0.2 \leq y/b \leq 1.4$)	Live bed	24.2
Wide ($y/b < 0.2$)	Live bed	0.0

Note: y and b denote upstream flow depth and pier width respectively.

Table 7. Distribution properties of utilized deterministic and random variables

Variables		Clear water		Live bed		Distribution	
		Mean	COV	Mean	COV		
Pier width	Narrow pier	0.6 ft		0.6 ft		Deterministic	
	Intermediate pier	1.5 ft		1.5 ft		Deterministic	
	Wide pier	7 ft		7 ft		Deterministic	
Pier face shape		Circular		Circular		Deterministic	
Skew angle		0 degree		0 degree		Deterministic	
Aspect ratio (Length to width)		1		1		Deterministic	
Flow velocity		1.55 ft/s	0.186	1.55 ft/s	0.186	Log-normal	
Flow depth		1.24 ft	0.2	1.24 ft	0.2	Normal	
Median grain size		1.18 mm	0.081	0.3 mm	0.081	Normal	
Bias factor	Narrow pier	Wilson (1995)	0.75	0.45	1.11	0.3	Normal
		Melville (1997)	0.69	0.31	0.68	0.24	Normal
		HEC 18 (2012)	0.71	0.3	0.67	0.21	Normal
		Briaud (2014)	0.8	0.37	0.73	0.32	Normal
	Intermediate pier	Wilson (1995)	1.42	0.35	1.36	0.18	Normal
		Melville (1997)	0.66	0.27	0.61	0.18	Normal
		HEC 18 (2012)	0.95	0.26	0.71	0.19	Normal
		Briaud (2014)	1.1	0.3	0.89	0.22	Normal
	Wide pier	Wilson (1995)	2.051	0.1	1.33	0.29	Normal
		Melville (1997)	0.78	0.18	0.76	0.24	Normal
		HEC 18 (2012)	1.16	0.17	1.13	0.22	Normal
		Briaud (2014)	1.4	0.2	1.18	0.18	Normal

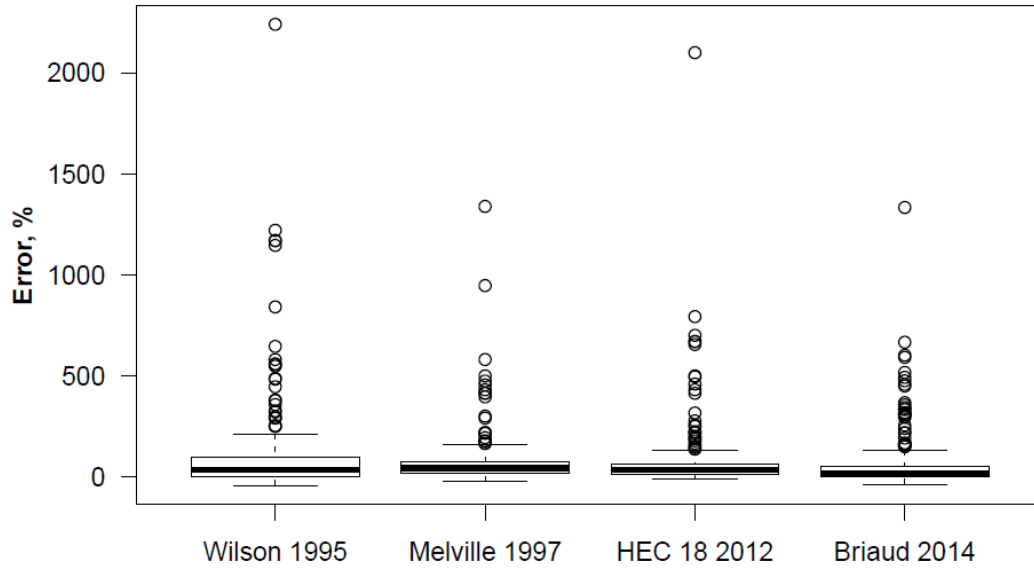


Figure 1. Error box plot for the four models considered in the study (Data: Narrow pier under clear water condition).

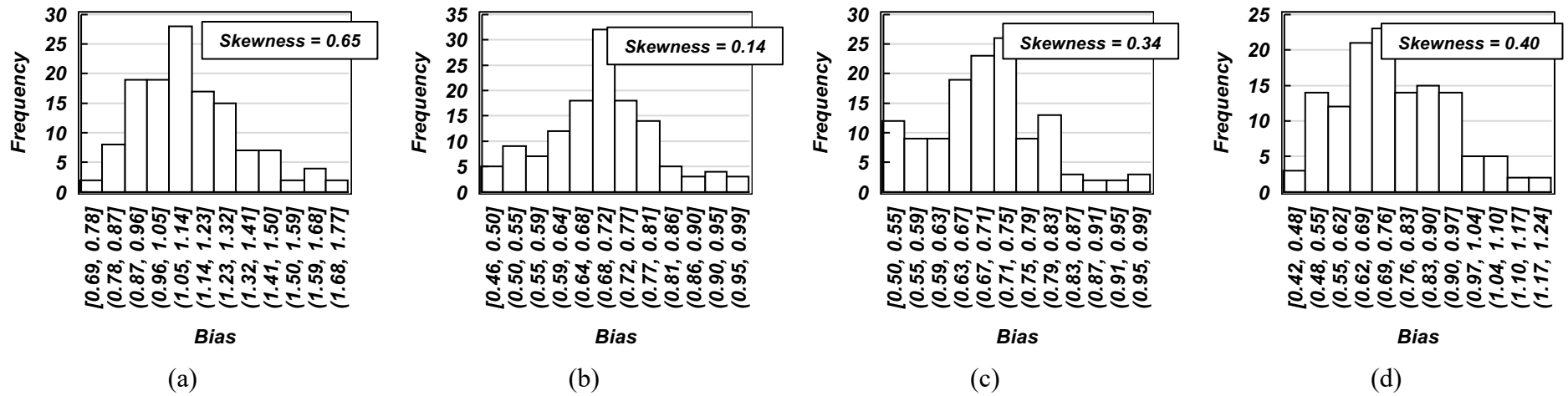


Figure 2. Statistical distribution of bias factor, λ for (a) Wilson 1995, (b) Melville 1997, (c) HEC 18, 2012 and (d) Briaud 2014 models for narrow pier under live bed condition

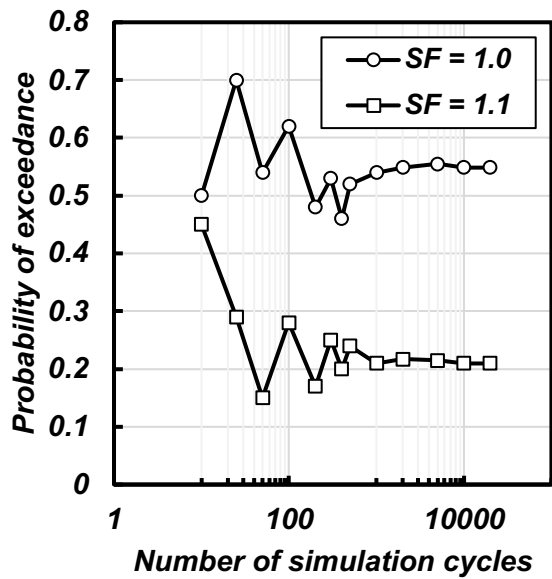
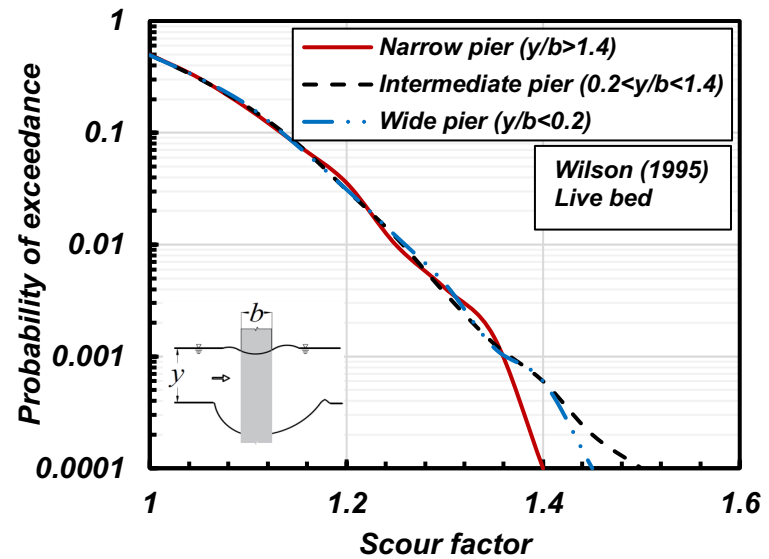
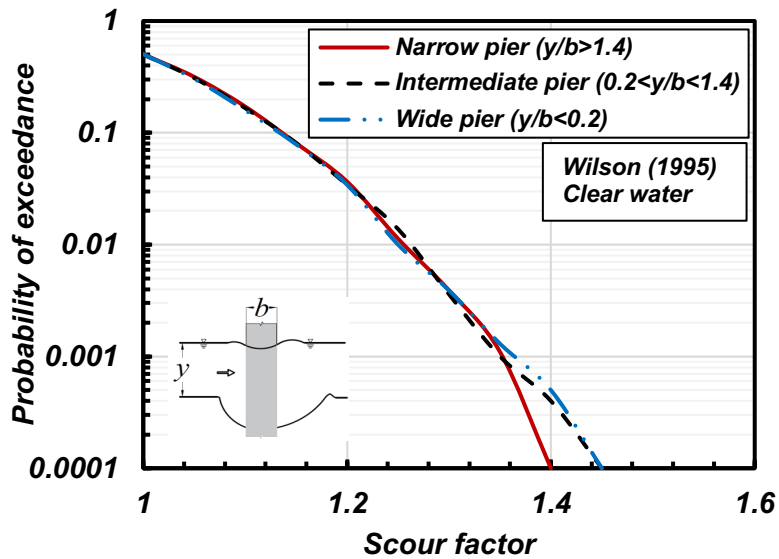
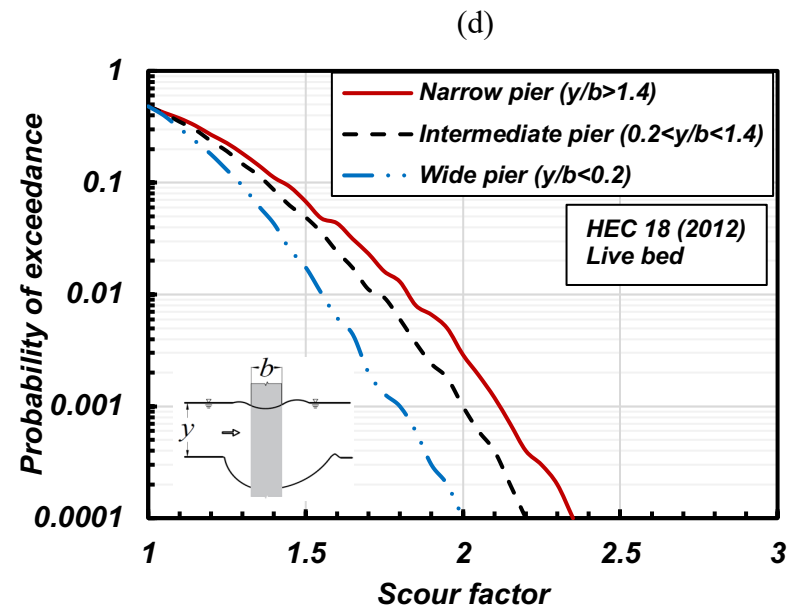
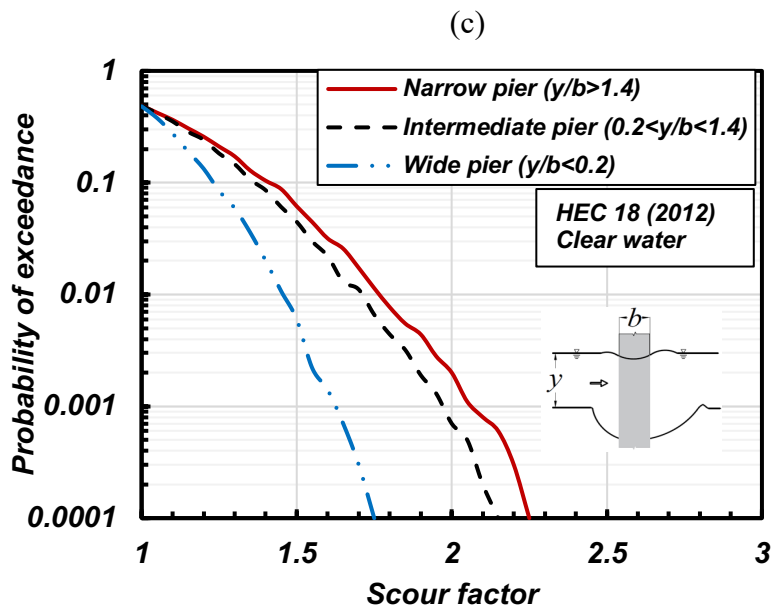
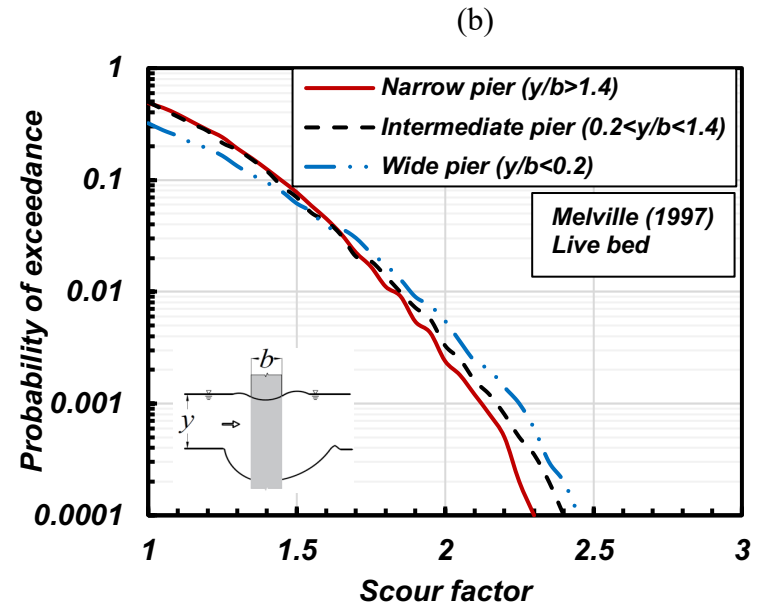
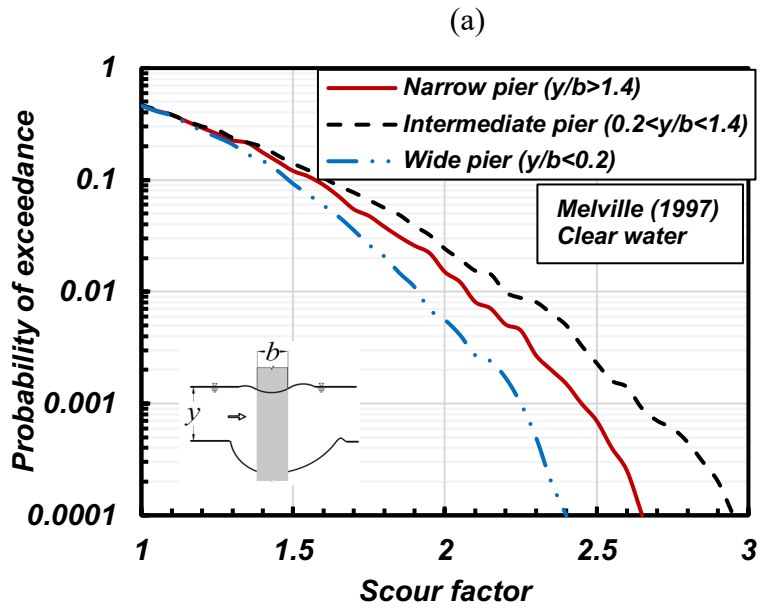


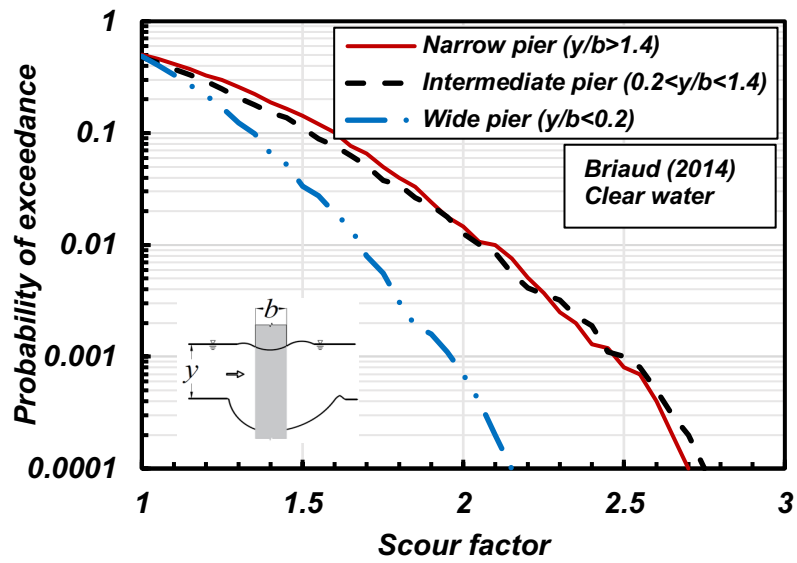
Figure 3. Relationship between probability of exceedance and number of simulation cycles when HEC 18 (2012) model is used (SF stands for scour factor, which is defined as the ratio of the depth from average bed level to the bottom of the footing to the scour depth predicted from different scour prediction models, in this plot which is HEC 18 model)



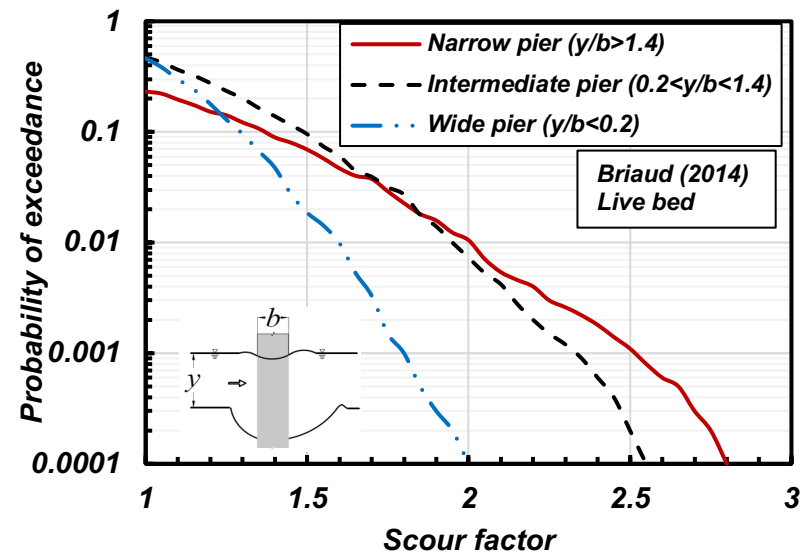


(e)

(f)

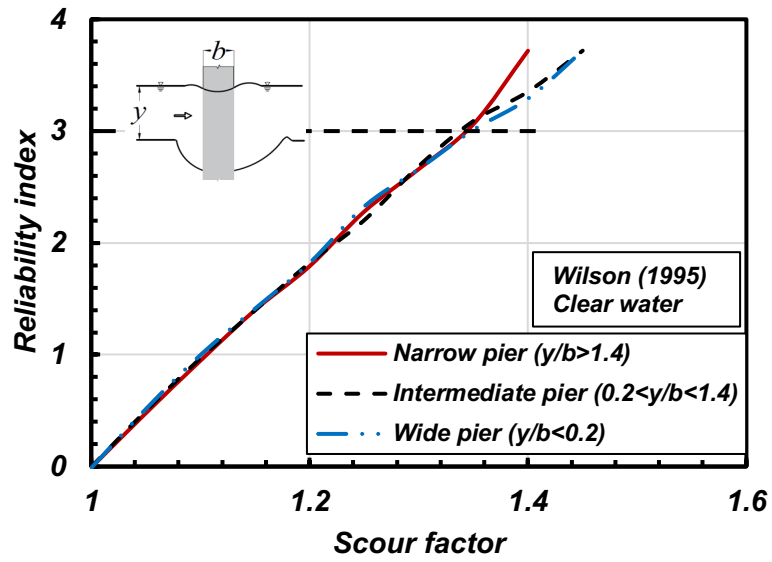


(g)

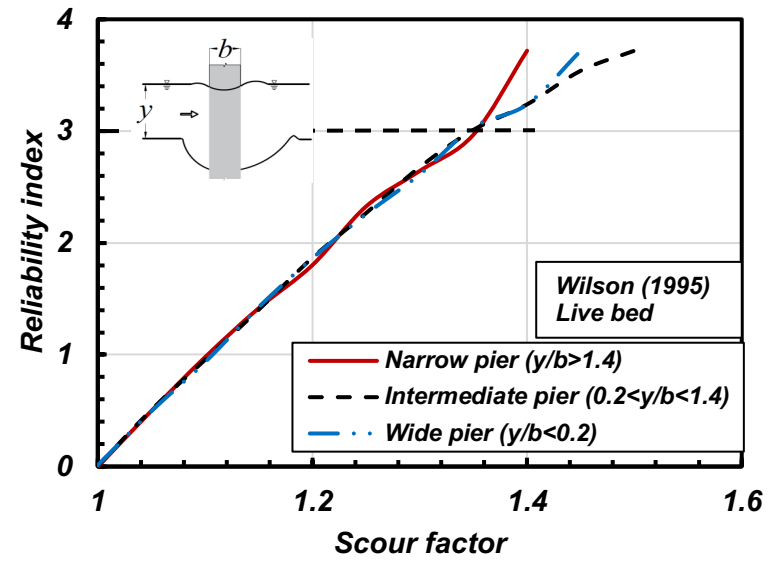


(h)

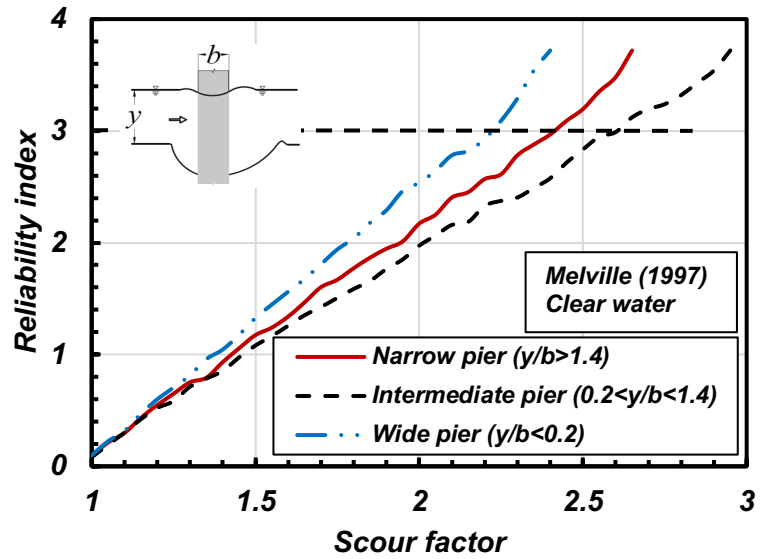
Figure 4. Relationship between probability of exceedance and scour factor for (a) Wilson (1995) clear water (b) Wilson (1995) live bed (c) Melville (1997) clear water (d) Melville (1997) live bed, (e) HEC 18 (2012) clear water (f) HEC 18 (2012) live bed (g) Briaud (2014) clear water (h) Briaud (2014) live bed. Note: y and b stand for upstream flow depth and pier width respectively.



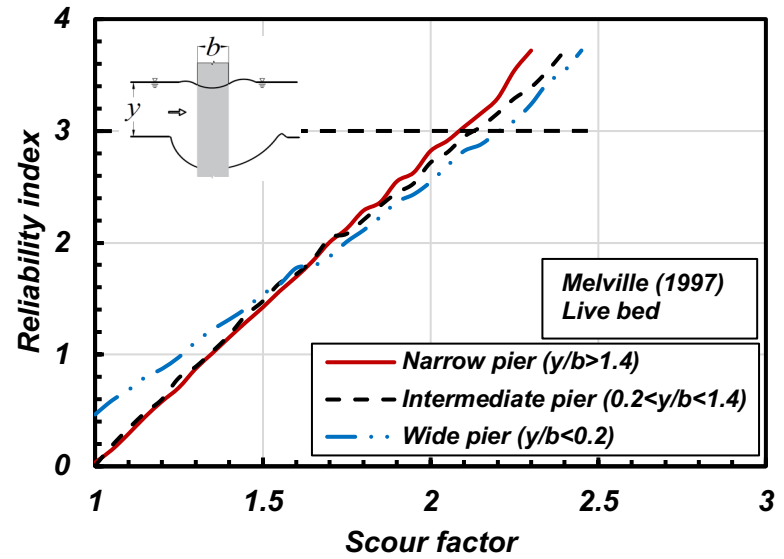
(a)



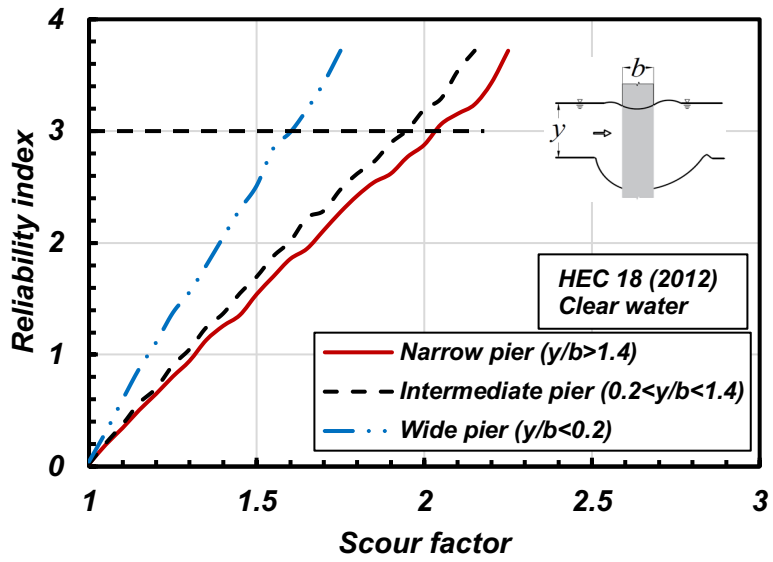
(b)



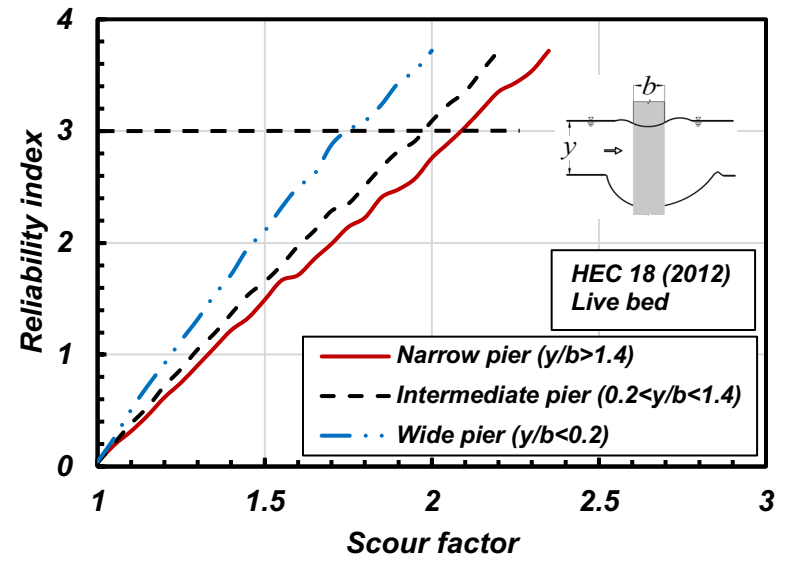
(c)



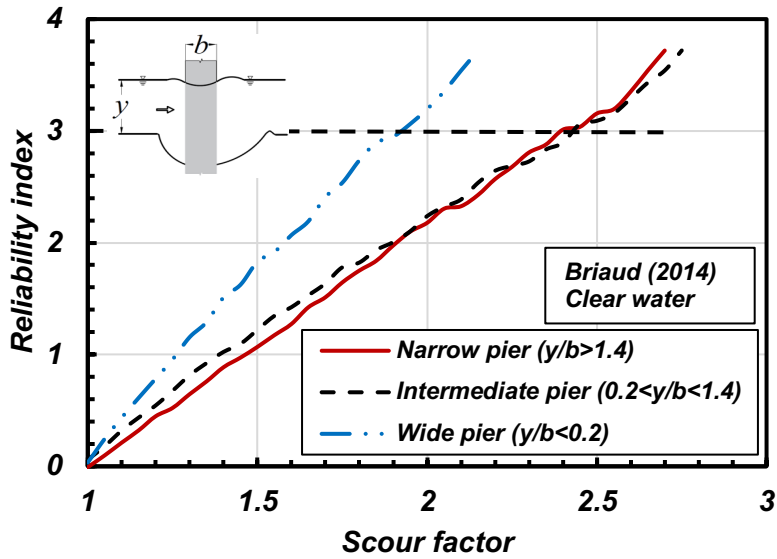
(d)



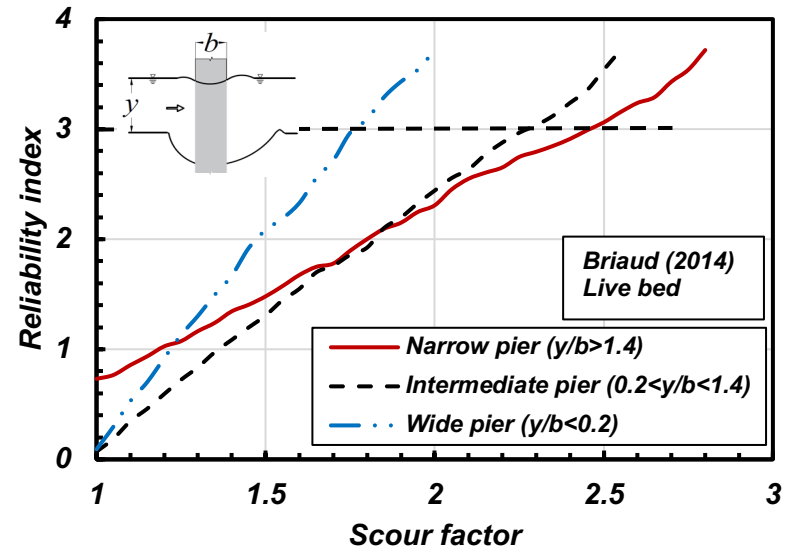
(e)



(f)



(g)



(h)

Figure 5. Relationship between reliability index and scour factor for (a) Wilson (1995) clear water (b) Wilson (1995) live bed (c) Melville (1997) clear water (d) Melville (1997) live bed, (e) HEC 18 (2012) clear water (f) HEC 18 (2012) live bed (g) Briaud (2014) clear water (h) Briaud (2014) live bed. Note: y and b stand for upstream flow depth and pier width respectively.

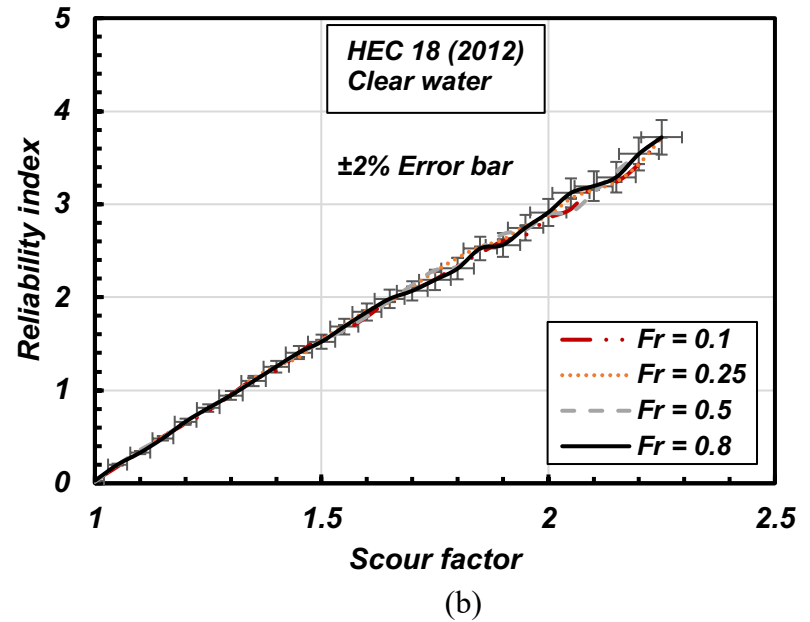
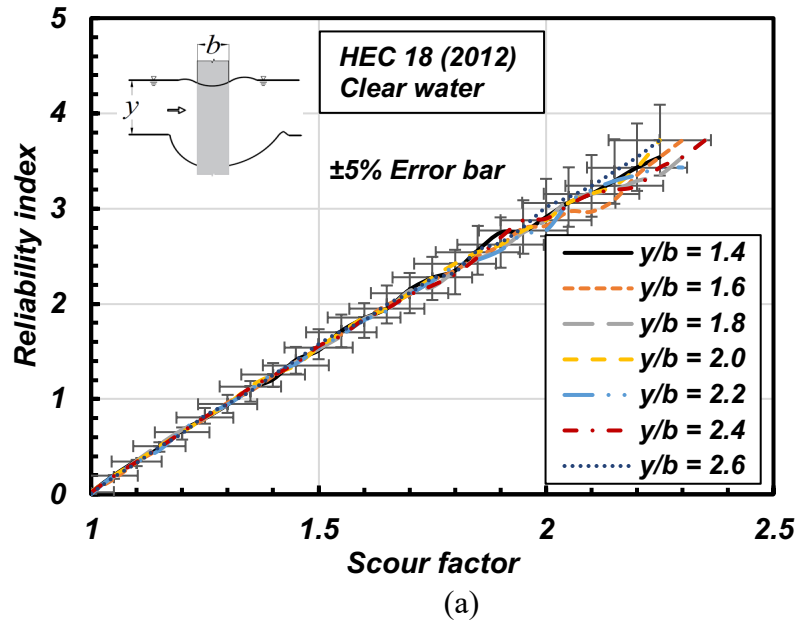


Figure 6. Sensitivity of reliability index when the Monte Carlo simulation is run under different (a) y/b , and (b) F_r for HEC 18 (2012) model in clear water narrow pier condition. Note: y , b and F_r stand for upstream flow depth, pier width, and Froude number respectively.

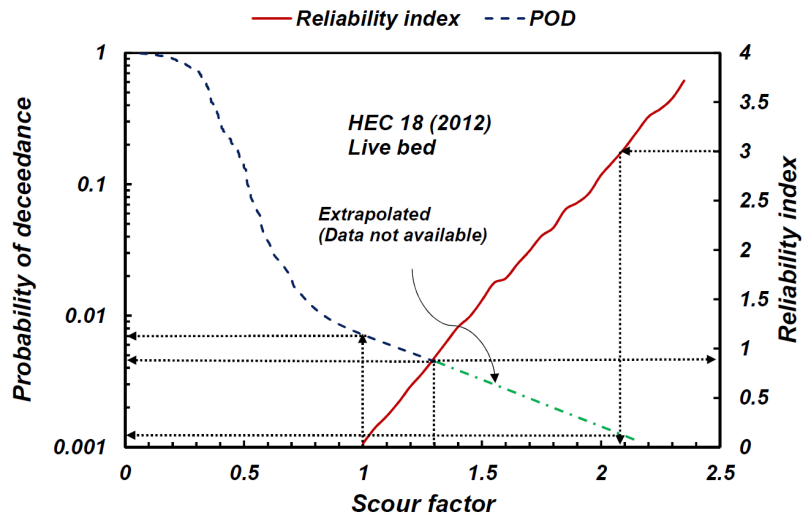


Figure 7. Relationship among probability of deceedance, reliability index, and scour factor when HEC 18 (2012) model is applied to estimate scour at narrow pier ($y/b > 1.4$) under live bed condition. Note: y , and b stand for upstream flow depth, and pier width respectively.

Appendix E: Application Assessment of Reliability-Index Based Scour Approach and Corresponding Impact on Pile Foundation System

Introduction

Bridge failures cause human life loss, disruption of commerce and enormous repair cost (Estes and Frangopol 2001; LeBeau and Wadia-Fascetti 2007; Deng et al. 2015). Bridge scour is one of the prime reasons for bridge failure in the United States and worldwide (Melville and Coleman, 2000; Briaud 2014; Liang et al. 2015; Qi et al. 2016). Wardhana and Hadipriono (2003) focused on 503 failures of bridge structures that occurred during the period 1989-2000 in the United States and estimated that 85% of the failure is associated with externally triggered events, of which flood-induced scour is the primary contributor. Arneson et al. (2012) reported that 493,473 highway bridges are built over waterways in the United States (which is more than 80% of the total number of bridges within the country). Scour, thereby, is a primary design consideration for the waterway bridges and similar transportation infrastructures. The evaluation of scour magnitude at bridge sites involves technical expertise from multiples disciplines, e.g., hydraulics, structural, and geotechnical engineering (Parkes et al. 2018). The Federal Highway Administration (FHWA) provides guidelines for assessing the potential maximum scour depth around bridge foundations using the Hydraulic Engineering Circular (HEC) No. 18 model. The HEC 18 model is deterministic (Arneson et al. 2012), and often provides a conservative estimate of scour depth (e.g., Briaud et al. 2014; Yao 2013). However, the degree of inherent conservatism embedded in deterministic models such as HEC 18 and others is unknown. The level of conservatism depends on the inherent model bias as well as the uncertainty of hydraulic, hydrologic, and geotechnical parameters (Johnson 1992, 1996; Lagasse et al. 2013; Johnson et al. 2015; Shahriar et al. 2021a-b).

On the other hand, the American Association of State Highway and Transportation Officials (AASHTO 2007) suggests that bridge foundation strength and serviceability limit states need to be assessed for the scour corresponding to the *design* flood (100-year flood) event, and the factored foundation resistance with scour-assessed soil removed should be greater than the factored load. Lin et al. (2014, 2015) showed that changes to the subsurface stresses occur owing to the removal of the soils in scour prism, with such change leading to reduced axial and lateral foundation resistance. The Load and Resistance Factor Design (LRFD) guidelines suggest achieving a certain level of reliability index (Nowak 1999) for the superstructure components, while for the design of foundation systems and considering scour, a deterministic HEC 18 approach is used. Reliability index, β is a measure of the number of standard deviations that the mean margin of safety falls on the “safe” side (Paikowsky 2004), where the margin of safety is dependent on the limit state function considered as “critical” for a system. Reliability index has been in use across structural and geotechnical engineering literature (AASHTO LRFD 2007; AISC 2005; ACI 2005). Current AASHTO LRFD (2007) bridge design specifications suggest different target reliability index depending on soil types, pile types, the various design methods, and the consequence of failure. AASHTO LRFD (2007) suggests the use of $\beta=2.33$ for redundant systems, and $\beta=3.0$ for non-redundant systems. In general, a β value of 2 to 4 is specified for the various structural applications. The calibration procedure of LRFD code is well documented in Nowak (1999) and Kulicki et al. (2007); and an example application procedure for driven pile axial capacity can be found in Kim et al. (2005). An inconsistency is posed by adopting a β -based approach for the design of superstructure components as opposed to a deterministic approach for assessing the scour magnitude at the foundation system. Subsequently, there is

a need to develop a reliability index-based model that considers the uncertainties of the parameters affecting the scour and that relates β with a multiplicative factor necessary to achieve a target β value.

Work herein is focused on demonstrating the implications of the β -based scour assessment approach on the response of pile groups supporting bridge piers. To facilitate illustrating the applicability of β based approach, parameters from the Woodrow Wilson bridge pier in Prince George County, Alexandria, Virginia carrying traffic of I-95 and I-485 was considered in the analyses. A relationship between the probability of exceedance over the design life and the scour depth is presented to demonstrate the risk associated with utilizing HEC 18 (Arneson et al. 2012) in the analysis. Scour depth was estimated using both traditional HEC 18 procedure and the β -based procedure. The estimated scour depth using both approaches was then applied to the Woodrow Wilson bridge foundation system and the corresponding displacement (transverse, longitudinal, axial) components and moments of the pile foundation under AASHTO loading condition were studied. The analyses were extended by conducting a parametric study by varying the pile length and pile diameter to explore the effect on the transverse, longitudinal, and axial displacement components of the pile foundation system. Finally, risk (the product of probability of failure and the cost of the consequences) analysis was presented to show how the consideration of β -based approach is advantageous in assessing the potential of economic loss.

The Woodrow Wilson Bridge Site

The Woodrow Wilson bridge on the Potomac River is located in Prince George County, Alexandria, Virginia, and crosses over to Washington D.C. The bridge carries traffic through I-95 and I-485 and the relatively recent construction was built due to the fact that the previous Woodrow Wilson bridge reached its capacity (75,000 vehicles per day) within 8 years of its construction in 1969. The overall cost of the project including the approach embankment, and interchanges was estimated at 2.2 billion dollars (Kwak 2000; Kwak and Briaud 2002). The drawbridge is supported by two bascule piers (Jones 2000), which are located on the main channel of the Potomac River. The foundation system of the bascule piers consists of exposed pile foundation that is capped near the water surface. The soil stratigraphy in the main channel is made of soft clay overlying on thin layer of loose sand. Below the loose sand layer, a clay layer persists. The profile view, and pile cap section along with the soil stratigraphy for the pier M1, which supports the drawbridge, is presented in Figure 1. The soil properties, pile and pile cap properties are from Kwak and Briaud (2002) and Briaud (2008).

Scour Estimation

The Woodrow Wilson bridge pier consists of three complex geometrical shapes of columns resting on a pile cap, supported by the pile groups. HEC 18 (2012) classifies such pier as complex pier and provides guidance on the calculation of scour depth. Jones and Sheppard (2000) suggested that a superposition of the scour depth component from the pier stem (y_{s-pier}), pile cap ($y_{s-pile\ cap}$) and the pile group ($y_{s-pile\ group}$) is necessary to estimate the total local scour depth, y_s (Equation 1).

$$y_s = y_{s-pier} + y_{s-pile\ cap} + y_{s-pile\ group} \quad (1)$$

The scour depth estimated from the HEC 18-suggested approach was 62.3 ft (19 m). Sheppard et al. (2004) reported experimental results of large-scale model bridge study in a 22 × 125 ft (6.7 × 38.1 m) long concrete channel at the USGS BRD Conte Research Center in Turners Falls, Massachusetts. The

geometric scale considered was 1:50, the sediment had a median grain size of $d_{50} = 0.8$ mm and sediment non-uniformity, $\sigma = \sqrt{d_{84}/d_{16}} = 1.3$ (d_{84} and d_{16} are particle diameters corresponding of 84% and 16% finer respectively). The sand bed was 6 ft (1.83 m) thick. The estimated scour depth was 54 ft (16.5 m). Jones and Davis (2007) further reported the results of small-scale flume study in a 6×70 ft (1.83×21.3 m) long flume at the FHWA hydraulics lab at the Turner Fairbanks Highway Research Center in McLean, Virginia. The geometric scale considered was 1:100, the used sediment had a $d_{50} = 0.30$ mm, the sediment standard deviation was not reported. The scour depth was estimated to be 53.2 ft (16.2 m).

Although large-scale and small-scale model experiments are important to understand the underlying scour mechanisms, Ettema et al. (2017) and Link et al. (2019) suggested that the incapability of the laboratory scale models to maintain a geometric similitude among the three length scales (pier width, flow depth, and bed sediment size) results in differences in scour estimations from laboratory test-based models and field observed scour magnitude. In addition, the uncertainty inherent in the hydraulic, hydrologic, and geotechnical parameters might result in a different scour depth compared to what has been observed in the flume experiments and estimated from deterministic models.

Jones and Davis (2007) computed the contraction scour in the main channel of the Potomac River using the Laursen (1960) model, and concluded that the contraction scour magnitude is insignificant, thereby suggesting that total scour entails only local scour around the bridge pier for the Woodrow Wilson bridge case. Subsequently, analyses in this study were conducted using a total scour magnitude of 62.3 ft (19 m), obtained from HEC 18 (2012) model (as currently FHWA suggests using HEC 18 (2012) model for scour assessment while designing bridge foundation).

Reliability Index-Based Scour Estimation

The reliability index incorporated in the LRFD methodology accounts for the uncertainties of loads and resistances while evaluating the safety of a system. In LRFD, safety is expressed by the level of desired reliability (e.g., Lagasse et al. 2013; Nowak and Collins 2000). The methodology to develop a reliability index based on scour estimation entails consideration of statistical attributes (mean, coefficient of variation, probabilistic distribution) of the input parameters in scour analyses (e.g., upstream flow velocity, upstream flow depth, median grain size of the bed material, Manning's roughness coefficient, channel bed slope) to analyze the limit state function that defines the foundation safety. The limit state function, L , can be expressed through Equation (2).

$$L = D_p - D_s \quad (2)$$

Where, D_p is the depth that will lead to a foundation failure from current bed level (as defined by geotechnical analyses), and D_s is the scour depth predicted from HEC 18 (2012) scour prediction model. The probability of exceedance of L when HEC 18 model is considered can be expressed as in Equation (3).

$$P_e = P \left(D_p < \lambda 2 K_1 K_2 K_3 \left(\frac{y}{b} \right)^{0.35} F^{0.43} \right) \quad (3)$$

Where, K_1 , K_2 , and K_3 are pier nose shape factor, pier alignment factor, and bed condition factor respectively; y , b , and F are flow depth upstream of the pier, pier width and Froude number respectively; λ is the bias factor. In Equation (3), flow depth, flow velocity, and bias factor are random variables, while pier width, skew angle, pier face shape, and aspect ratio are deterministic, as these parameters are not subjected to any inherent temporal or spatial variability. The Coefficient of Variation (COV) of y is

dependent on the statistical distribution of Manning's roughness coefficient, n and channel bed slope, S and can be estimated based on the uncertainty analyses presented by the U.S. Army Corps of Engineers (HEC 1986). The COV of flow velocity is also dependent on the distribution properties of n and S , and can be estimated based on the hydrologic uncertainty analyses presented in Johnson (1992), and Lagasse et al. (2013). The λ is defined as the ratio of the measured to the predicted scour depth; the estimation procedure of λ being dependent on the database being used. Data reported in Benedict and Caldwell (2014), who compiled laboratory scour measurements conducted since 1956, are utilized herein. Although the database entails a wide range of data, laboratory live bed data under narrow pier condition was considered for the estimation of λ since the site condition of the Woodrow Wilson bridge falls in such category. Based on the definition of Melville and Coleman (2000), if $y/b > 1.4$, then a narrow pier condition exists. The distribution of λ was observed to be normally distributed. Figure 2 shows the observed distribution of λ for the laboratory live bed data under narrow pier condition when the HEC 18 model is used. Table 1 shows the list of deterministic and random variables and the associated statistical characteristics considered herein.

Owing to the non-linear nature of Equation (3), a Monte Carlo simulation approach was considered to compute the probability of exceedance. A total of 10,000 simulation cycles were used to estimate P_e . If the limit state function follows normal probability distribution, β can be related to P_e using Equation (4).

$$P_e = \Phi(-\beta) \quad (4)$$

Where, Φ is a probability function representing the probability that the normalized random variable is below a given value. A *scour factor* is defined as the ratio of D_p to D_s . The Monte Carlo simulation was run for a scour factor ranging from 1 to 3, subsequently, a relationship between the reliability index and scour factor was devised. The concept is very similar to *resistance factors* in the LRFD approach as it develops *scour factors* to be applied to the deterministically-evaluated scour magnitudes.

The scour factor associated with a certain β can further be correlated to the Probability of Deceedance (POD). POD is defined as the probability that the predicted scour depth will be less than the measured scour depth, estimated from the Benedict and Caldwell (2014) database. To quantify POD, initially, the frequency distribution of χ_{POD} , which is the ratio of the predicted to the measured scour depth was developed. Using Kernel density estimation, the population probability density function for χ_{POD} was generated, followed by integration of the density function to obtain the cumulative density function. Finally, the POD is obtained by subtracting the cumulative density value from one. The relationship between the reliability index or the associated probability of deceedance and scour factor is presented in Figure 3.

For example, in Figure 3, if the target reliability index, β_T is 2.0, the corresponding scour factor is 1.70. Therefore, for the pier M1 of the Woodrow Wilson bridge, the scour depth corresponding to $\beta_T=2.0$ is 105.9 ft (32.3 m). Figure 3 further suggests that the use of a $\beta_T > 0$ causes the probability of deceedance (defined as the probability of having a predicted scour magnitude being less than the value occurring in the field) to decrease.

Probability of Exceedance over the Design Life of Structure

A flood event with a recurrence interval of T years has a $1/T$ probability of being exceeded in any given year. The 100-year flood is generally recommended in HEC 18 for hydraulic analyses. It has a probability of exceedance of $1/100$ in any year and this probability increases as the design life increases.

If the design life of a bridge is N years, the probability of exceedance in N years, $P_{cumulative}$, can be represented as a function of annual probability of exceedance, P_N , as expressed in Equation (5).

$$P_{cumulative} = 1 - (1 - P_N)^N \quad (5)$$

A 100-year flood has a 63.4% chance of being exceeded in a design period of 100 years. For a specific bridge, a chart relating the scour depth and the probability of exceedance in N years can be developed, allowing the engineer to select a scour depth corresponding to a target probability of exceedance in N years. Referring to Figure 3, the scour factors are corresponding to a certain annual probability of exceedance, which depending on the design life of the bridge, will provide the probability of exceedance in N years (Equation 5). The scour depth corresponding to a scour factor can be obtained by multiplying the HEC 18-predicted scour depth with the scour factor. Figure 4 shows the relationship between the probability of exceedance in N years and scour depth for different design life. For the pier M1 of Woodrow Wilson bridge, the HEC 18 (2012) suggested scour depth is 62.3 ft (19 m), which in turn has a 40%, 50%, and 76% probability of exceedance over a design life of 75, 100 and 200 years respectively. However, if the reliability index-based scour depth is considered with $\beta = 2$, the scour depth is 105.9 ft (32.3 m) and it has a 17%, 22%, and 38% probability of exceedance over a design life of 75, 100 and 200 years respectively. Therefore, it appears that the β based approach reduces the probability of exceedance by more than 23% over the design life investigated (75-200 years).

FB-MultiPier Modeling

Robinson et al. (2012) reported that FB-MultiPier can be chosen as a numerical tool to model bridge pier owing to multiple reasons, some of which are:- (i) has a built-in interactive bridge bent software wizard, (ii) automatically models the soil resistance (lateral and axial, single and group) using methods that represent the current state of practice, and (iii) allows for typical linear or nonlinear bent cap models to be utilized. Furthermore, FB-MultiPier produces similar results as commonly used finite difference program for pile analyses, LPILE with the additional benefit of modeling the superstructure (FB-MultiPier 2021).

The piles of the Woodrow Wilson bridge consist of 70 inch (1778 mm) diameter concrete filled pipe piles with a length of 210 ft (64 m) (Briaud 2008). The pile cap is 87 ft (26.5 m) wide and 129 ft (39.3 m) long. The flow depth was considered to be the water depth corresponding to the 100-year flood, which is 44.7 ft (13.6 m) (Kwak and Briaud 2002). The pile cap midplane is at an elevation of 19.3 ft (5.9 m) from the water level. For the top and bottom clay layer, lateral soil resistance was modeled using Matlock (1970) model, and axial resistance was modeled using API (2003) model. For the thin sand layer in between the clay layers, lateral soil resistance was modeled using Reese et al. (1974) model, and axial resistance was modeled using API (2000) model. The exact reinforcement detailing of the pier cap, and the pier were not provided in literature; as such a reinforcement ratio of 2% was assumed for the analysis.

FB-MultiPier facilitates generation of wind loads using the AASHTO LRFD design specification (2007) for pier. The generated wind pressure on structure, and wind pressure on live load were applied at the bearing location, which is at the center of the pier cap. Three wind angles (0, 30, 60 degrees) were considered to generate wind pressure in the transverse and longitudinal directions. In analysis settings, for both the pile and pier, the behavior was considered non-linear.

AASHTO Load Cases

FB-MultiPier, the modeling tool considered herein, allows for application of dead load, live load, impact load, braking load, vehicle collision load, and wind load among many other options (e.g., earth surcharge, locked in construction stresses, down drag, post tensioning, creep, shrinkage, temperature gradient etc.). In the present study, AASHTO strength (I-V) and serviceability (I-III) load cases were considered. Analyses were conducted using the aforementioned load cases and the results were synthesized considering the load case that governed in terms of yielding the most demand. Axial force, moment, transverse displacement, longitudinal displacement, and axial displacement generated on the pile foundation system were analyzed for “no scour,” and scoured cases. In FB-MultiPier, axial forces and moments, along with non-linear pile section properties are used to calculate Demand Capacity Ratio (DCR). The DCR is an estimate of the percentage of the cross-section capacity that has been reached for a particular loading state [due to a particular load case] (Robinson et al. 2012). A DCR of less than 1 implies that the section can sustain the range of AASHTO load cases considered for the analyses, while a DCR of more than 1 implies failure.

Modeling Results

The studied pier M1 of the Woodrow Wilson bridge has three pier columns with a complex cross-section placed on the pile cap. The “Pier” model type in FB-MultiPier does not allow modeling complex pier cross-section. Thereby, the analysis was divided into two phases. In the first phase, (Phase I), to represent the actual load transfer scenario, two cases with different pier count (on the same pile cap) were investigated. The first case consists of three piers transferring the load from the bridge deck to the pile cap. The base area of the pier was kept same as the base area of the pier M1. It is important to note that the cross section of the pier M1 changes along the depth, whereas a uniform cross-section was considered herein. The second case consists of equivalent single pier with the base cross-sectional area equal to the sum of the three piers (located centrally) with loads from the end piers transferred (as load, and moment) on the middle pier. The objective of the first phase analysis was to obtain similar results from both the 3-pier and equivalent single pier cases. Figure 5 shows a comparison of transverse, longitudinal, and axial displacement of the pile foundation along the depth from both model cases (Phase I). Considerable agreement in the displacement response can be obtained between the 3-pier case and the equivalent single pier case scenario. The maximum discrepancy in the displacement at any particular elevation was 4%. Figure 6 shows a comparison of the moments generated on the pile foundation around transverse and longitudinal axes. The maximum discrepancy of moments between 3-pier case and equivalent single pier case was 4.3%, which suggest that the equivalent single pier case is capable of replicating the load transfer mechanism of 3-pier case.

In the second phase (Phase II), scour analyses were conducted considering the equivalent single pier case as the base case model. Two further model cases are generated in FB-MultiPier to observe the difference in pile response when HEC 18-determined scour depth versus β based scour depth is used. For the HEC 18-determined scour depth case, the riverbed surface elevation near the vicinity of the pile group was lowered to the depth of total scour depth obtained from HEC 18 (62.3 ft). For the β -based scour depth case, the riverbed surface at the vicinity of the pile group was lowered to a depth of 105.9 ft (32.3 m). Per Richardson and Davis (2001), considering practical applications, a scour prism with a top width of 2 times the scour depth was considered on either side of the pile group.

Figure 7 shows the comparison among base case, HEC 18-predicted scour case, and β –based scour case in terms of transverse displacement, longitudinal displacement, and axial displacement. Results

show the pile head deflections for β –based scour depth case is considerably higher than the HEC 18-computed scour depth case. The second edition of AASHTO LRFD placed a limit of 1.5 inches allowable deflection for bridge piles at the pile head. However, the limit was removed in the subsequent versions of AASHTO LRFD specifications. Nevertheless, researchers (e.g., Robinson et al. 2006; Robinson et al. 2012) consider 1 inch (25 mm) as an acceptable allowable deflection for bridge piles at the pile head.

Figure 8 shows the comparison among base case, HEC 18-computed scour case, and β -based scour case in terms of transverse and longitudinal moments generated on the piles. The point of contraflexure for the β based scour depth case is at a lower elevation than the HEC 18-computed scour depth case. The maximum positive and negative moments generated also increases for β based scour depth case than the HEC 18-predicted scour depth case. The maximum Demand to Capacity Ratio (DCR) for the pile was 0.148, 0.153, and 0.165 for the base case, the HEC 18- computed scour depth case, and the β – based scour depth case respectively. Figure 9 shows the interaction diagram for pile 3, which governed for the moment capacity. Referring to Figure 1-pile cap section, pile 3 is the center pile in the first row that is parallel to the “87 ft (26.5 m)” side (black shaded). With the increase of the considered scour depth, the moment generated on the pile tends to reach the envelope, although the capacity of the section is significantly higher than the generated moment on the pile.

Parametric Analysis

FB-MultiPier analyses were performed to explore the mitigation measures of the increased scour magnitude with the use of the scour factor approach. Subsequently, the effect of variation of pile length and pile diameter on the transverse, longitudinal, and axial displacement of the pile was investigated. While performing the parametric analyses, the center-to-center distance between the piles was kept same as the base case.

Effect of pile length variation

The variation of transverse displacement, longitudinal displacement, axial displacement, and DCR with the changes in pile length is presented in Figure 10. The pile length of the base case model is 210 ft (64 m). The pile length was increased from 210 ft (64 m) to 250 ft (76.2 m) (19%). It appears that an increase of pile length by 40 ft (12.2 m) decreased the transverse and longitudinal displacement by 4.4% and 6.2% respectively, while the axial displacement was reduced by 41.4%. Nevertheless, if the pile length is increased to 220 ft (67.1 m) (increasing length by 4.8%), the axial displacement can be lowered to an acceptable displacement limit of 1 inch (25 mm). It is also apparent that increase of pile length is effective in reducing the axial displacement of the pile.

Effect of pile diameter variation

Figure 10 further shows the variation of pile displacement components with the changes in pile diameter. The pile diameter of the base case model is 70 inches (1778 mm). The pile diameter was increased from 70 inch (1778 mm) to 75 inch (1905 mm). As shown in Figure 10, and for an increase in pile diameter from 70 inches (1778 mm) to 74 inches (1880 mm), the transverse and longitudinal displacement was reduced by 13.2% and 14.4% respectively, while for axial displacement, the reduction was 7.8%. However, as the pile diameter was increased further to 75 inches (1880), the displacement tends to increase. This could be due to the center to center spacing between the piles that was kept same as the base case, which resulted in a reduction of the effective volume surrounding the pile to mobilize the complete foundation

resistance. However, it is evident that increase in pile diameter is effective in reducing transverse and longitudinal displacement of the pile.

Scour Risk

Annual risk, R is defined as the product of the annual probability of failure, POF , times the cost of the consequences, C , as expressed in Equation (6) (Baecher and Christian 2003).

$$R = POF \times C \quad (6)$$

In respect to bridge scour study, the probability of exceedance is the probability that a certain scour depth will be exceeded in any future time. Any such event will be considered as a failure event, although failure in this case does not imply a true “collapse” of the foundation system.

Briaud et al. (2014) described that the target risk level for the civil engineering structures in the United States is 1000 dollars/year and 0.001 fatalities/year. Referring to Figure 3, the HEC 18 (2012) model, without the application of any scour factor, is associated with an exceedance probability of 0.007. Therefore, in the typical frequency-severity chart suggested by Baecher and Christian (2003), the accepted associated cost of consequence will be \$142,900 (1000/0.007). With the target reliability index, β_T of 2.0, the scour factor will be 1.70, and the associated exceedance probability will be 0.0024. For the same cost of consequence = \$142,900, the target risk level will be approximately reduced by a factor of 2/3 and be 343 dollars/year (142,900×0.0024).

Statistics presented in HEC 18 (2012) suggest that in the United States, 493,473 bridges are built over waterways. In a given year, if HEC 18 (2012) suggested approach is used to estimate scour depth, there is a possibility that the scour depth will be exceeded in 3,454 bridges. Whereas, if the scour factor corresponding to the β_T of 2.0 is used, annually, the scour depth would be exceeded in 1,184 bridges, reducing the affected number of bridges by 2,270.

We present herein an example to illustrate the advantage of the proposed approach. Briaud et al. (2014) reported that if the economic loss entails the bridge repair cost, detour cost, and time cost, then the economic loss for one bridge failure can be estimated at \$13,180,158 US Dollars. However, based on the repair cost data reported in California DOT (2011), Briaud et al. (2014) estimated that the average repair cost of one bridge is 560,100 Dollars. For the 2,270 bridges, the economic loss considering only the bridge repair would be 1.27 billion Dollars. Therefore, adopting the scour depth corresponding to the β_T of 2.0 will help to preventing a loss of 1.27 billion Dollars annually. Nevertheless, as presented in the *parametric analyses* section, consideration of β based scour depth might cause the transverse, longitudinal, or axial displacements of the pile to exceed the allowable limit, thereby, requiring a need to optimize pile diameter, pile length, or pile spacing, which might increase the construction cost.

Summary and Conclusion

Based on the results presented, following conclusions are advanced:

1. FHWA suggests use of HEC 18 (2012) model to estimate the scour depth around bridge foundations. For the studied site, pier M1 of Woodrow Wilson bridge, HEC 18 procedure predicts the scour depth to be 62.3 ft (19 m). During the design life of 100 years, there is a 50% chance that this scour depth will be exceeded.

2. Reliability index-based procedure considers the hydraulic, hydrologic, geotechnical parameter uncertainty in addition to inherent model bias. For the studied site, pier M1 of Woodrow Wilson bridge, for a target reliability index of 2.0, the scour depth will be 105.9 ft (32.3 m). During the design life of 100 years, there is a 22% chance that this scour depth will be exceeded, reducing the exceedance probability by 28% compared to the HEC 18 suggested scour depth case.
3. FB-MultiPier modeling results suggest that for the studied site, consideration of reliability index-based scour depth causes the longitudinal and axial displacement to exceed the allowable displacement limit of 1 inch (at pile head), while for the HEC 18 suggested scour depth case, the transverse, longitudinal, and axial displacements remained within the 1-inch (25 mm) allowable limit.
4. FB-MultiPier modeling results further reveal that the point of contraflexure for reliability index-based scour depth case is at a lower elevation than the HEC 18 predicted scour depth case. The maximum positive and negative moments generated on the pile also increases for reliability index-based scour depth case compared to the HEC 18 predicted scour depth case. Subsequently, the moments generated on the piles tend to reach the envelope of interaction, although the section moment capacity is significantly higher than the generated moments on the pile.
5. Parametric analyses were performed to explore the mitigation measures of the increased scour magnitude with the use of the scour factor approach. It was apparent that increase of pile length is effective in reducing axial displacement of the pile, while increase of pile diameter is effective in reducing transverse and longitudinal displacement of the pile.
6. In the United States, 493,473 highway bridges are built over waterways. Based on the repair cost data reported in California DOT (2011) and the estimated average repair cost of one bridge by Briaud et al. (2014), it was showed that the use of reliability index-based scour depth in foundation design will help to prevent risking a loss of 1.27 billion Dollars annually.

Data availability statement

All data, models, and code generated or used during the study appear in the submitted article.

Acknowledgements

Funding from North Carolina Department of Transportation (NCDOT) is gratefully acknowledged. Any conclusions, findings, opinions, and recommendations expressed in this article are those of the authors and do not necessarily reflect the views of NCDOT.

Declaration of interests

The authors declare that they have no known competing financial interests or personal relationships that could have appeared to influence the work reported in this paper.

References

- AASHTO (2007). "AASHTO LRFD Bridge Design Specifications: Customary U.S. Units," 4th Edition, American Association of State Highway and Transportation Officials, Washington, D.C.
- ACI 318-05 (2005). "Building Code Requirements for Structural Concrete and Commentary," American Concrete Institute, Farmington Hills, MI.

- AISC 325-05 (2005). "Steel Construction Manual," Thirteenth Edition, American Institute of Steel Construction, Chicago, IL.
- American Petroleum Institute (API) (2003). "Recommended Practice for Field Testing Water-Based Drilling Fluids," API RP 13B-1/ISO 10414-1, 3rd Ed., American Petroleum Institute, Washington, D.C., 1-82.
- ASCE (2010). "Minimum Design Loads for Buildings and Other Structures," ASCE 7-10, American Society of Civil Engineers, Reston, VA.
- Arneson LA, Zevenbergen LW, Lagasse PF, and Clopper PE. (2012). "Evaluating scour at bridges." Hydraulic Engineering Circular No. 18, 5th edition, 1-340.
- Baecher, G. B., and Christian, J. T. (2003). Reliability and statistics in geotechnical engineering, Wiley, New York.
- Benedict ST, and Caldwell AW. (2014). "A pier-scour database—2,427 field and laboratory measurements of pier scour." U.S. Geological Survey Data Series 845, 1-22.
- Briaud J-L. (2008) Case histories in soil and rock erosion: Woodrow Wilson Bridge, Brazos River Meander, Normandy Cliffs, and New Orleans Levees, *Journal of Geotechnical and Geoenvironmental Engineering, ASCE*; 134(10): 1425-1447.
- Briaud JL. (2014). "Scour depth at bridges: Method including soil properties. I: Maximum scour depth prediction." *Journal of Geotechnical and Geoenvironmental Engineering*; 141(2): 04014104.
- Briaud J-L, Gardoni P, and Yao C. (2014). "Statistical, risk, and reliability analyses of bridge scour." *Journal of Geotechnical and Geoenvironmental Engineering*; 140(2): 04013011.
- California DOT. (2011). "Construction statistics." http://www.dot.ca.gov/hq/esc/estimates/Construction_Stats_2011.pdf (May 1, 2012).
- Deng L., Wang W., and Yu, Y. (2007). "State-of-the-Art Review on the Causes and Mechanisms of Bridge Collapse." *Journal of Performance of Constructed Facilities*; 10.1061/(ASCE)CF.1943-5509.0000731, 04015005.
- Estes A. C., and Frangopol, D. M. (2001). "Bridge lifetime system reliability under multiple limit states." *Journal of Bridge Engineering*, 10.1061/(ASCE)1084-0702(2001)6: 6(523), 523–528
- Ettema R, Constantinescu G, and Melville BW. (2017). "Flow-field complexity and design estimation of pier-scour depth: Sixty years since Laursen and Toch." *Journal of Hydraulic Engineering*; 143(9), 03117006.
- FB-MultiPier Version 5.9 [Computer software]. Bridge Software Institute, Gainesville, FL.
- FB-MultiPier Version 5.9 [Help Manual], (2021). Bridge Software Institute, Gainesville, FL.
- Hydrologic Engineering Center (1986). "Accuracy of Computed Water Surface Profiles," U.S. Army Corps of Engineers, Davis, CA.
- Johnson PA. (1992). "Reliability-based pier scour engineering." *Journal of Hydraulic Engineering*; 118(10), 1344-1358.
- Johnson P.A. (1996). "Uncertainty of Hydraulic Parameters," *Journal of Hydraulic Engineering*; 122(2), 112-115.

- Johnson PA, Clopper PE, Zevenbergen LW and Lagasse PF. (2015). "Quantifying uncertainty and reliability in bridge scour estimations." *Journal of Hydraulic Engineering*; 141(7), 04015013.
- Jones, J.S. (2000). "Hydraulic testing of Wilson bridge designs" Public Roads, March/April, U.S. Department of Transportation, FHWA, Washington, DC, USA, 40-44.
- Jones, J.S. and D.M. Sheppard, (2000). "Local Scour at Complex Pier Geometries," Proceedings of the ASCE 2000 Joint Conference on Water Resources Engineering and Water Resources Planning and Management, July 30 - August 2, Minneapolis, MN.
- Jones JS, and Davis SR. (2007) "Evaluating Scour for the Piers on the New Woodrow Wilson Bridge." World Environmental and Water Resources Congress 2007, 1-10.
- Kim, K. J., M. S. Rahman, M. A. Gabr, R. Z. Sarica, and M. S. Hossain. (2005). "Reliability Based Calibration of Resistance Factors for Axial Capacity of Driven Piles." In *Advances in Deep Foundations*, Geotechnical Special Publication 113, 1–12. Austin, TX: ASCE
- Kulicki J.M., Mertz D.R., and Nowak A.S. (2007). "Updating the Calibration Report for AASHTO LRFD Code," NCHRP Project 20-7/186, Transportation Research Board, National Academies of Science, Washington, D.C.
- Kwak K. (2000). "Prediction of scour depth versus time for bridge piers in cohesive soils in the case of multi-flood and soil systems." Ph.D. dissertation, Department of Civil Engineering, Texas A&M University, College Station, Texas.
- Kwak KS, and Briaud JL (2002). "Case Study: An Analysis of Pier Scour Using the SRICOS Method." *KSCCE Journal of Civil Engineering*, 6(3), 243-253.
- Lagasse P. F., Ghosn M., Johnson P. A., Zevenbergen L.W., and Clopper P. E. (2013). "Risk-based approach for bridge scour prediction." Final Rep., NCHRP Project 24-34, Transportation Research Board, National Academies of Science, Washington, DC.
- Laursen, E.M., (1960). "Scour at Bridge Crossings," *Journal Hydraulic Division, ASCE*, 86 (HY 2).
- LeBeau K. H., and Wadia-Fascetti S. J. (2007). "Fault tree analysis of Schoharie Creek Bridge collapse." *Journal of Performance of Constructed Facilities*;10.1061/(ASCE)0887-3828(2007)21:4(320), 320–326.
- Liang FY, Zhang H, and Huang MS. (2015). "Extreme scour effects on the buckling of bridge piles considering the stress history of soft clay." *Natural Hazards*; 77, 1143–1159.
- Lin, C., J. Han, C. Bennett, and R. L. Parsons. (2014). "Analysis of laterally loaded piles in sand considering scour hole dimensions." *Journal of Geotechnical and Geoenvironmental Engineering*; 140 (6): 04014024.
- Lin, C., Bennett, J. Han, C. and R. L. Parsons. (2015). "Effect of Soil Stress History on Scour Evaluation of Pile-Supported Bridges." *Journal of Performance of Constructed Facilities*; 04014178.
- Link et al. (2019) "Physical scale modelling of scour around bridge piers". *Journal of Hydraulic Research*, 57(2), 227-237.
- LPILE V5.0 [Computer software]. Austin, TX, Ensoft.
- Matlock, H. (1970). "Correlation for Design of Laterally Loaded Piles in Soft Clay," in Proceedings, Second Offshore Technology Conference, Dallas, Texas, pp. 577 - 594.

- Melville BW. and Coleman SE. (2000). "Bridge scour." Highlands Ranch, USA: Water Resources Publications.
- Nowak A. (1999). "Calibration of LRFD bridge design code." NCHRP Rep. 368, Transportation Research Board, Washington, DC.
- Nowak A.S. and Collins K.R. (2000). "Reliability of Structures," McGraw-Hill, New York, NY.
- Paikowsky SG. (2004). "Load and resistance factor design (LRFD) for deep foundations." NCHRP Rep. 507, Transportation Research Board, Washington, DC.
- Parkes J, Castelli R, Zelenko B, O'Conner R, Montesi M, and Godfrey E (2018). "Design, Analysis, and Testing of Laterally Loaded Deep Foundations that Support Transportation Facilities." FHWA-HIF-18-031, 1-296.
- Qi M, Li J, and Chen Q. (2016). "Comparison of existing equations for local scour at bridge piers: parameter influence and validation." *Natural Hazards*; 82(3), 2089-2105.
- Reese, Lymon C., Cox, William R., and Francis D. Koop. (1974) "Analysis of Laterally Loaded Piles in Sand." Paper presented at the Offshore Technology Conference, Houston, Texas.
- Richardson EV, and Davis SR. (2001). Hydraulic Engineering Circular No. 18, Fourth Edition, FHWA NHI 01-001, Federal Highway Administration, Washington, D.C.
- Robinson B, Suarez V, Gabr M, and Kowalsky M (2012). "Configuration Optimization of Drilled Shafts Supporting Bridge Structures: Three Case Studies." *Practice Periodical on Structural Design and Construction*; 17(3), 93-101.
- Robinson, B., Suarez, V., Robalino, P., Kowalsky, M., and Gabr, M. (2006). "Pile bent design criteria." NCDOT Research Project 2005-19, North Carolina Department of Transportation, Raleigh, NC.
- Shahriar AR, Ortiz AC, Montoya BM, and Gabr MA (2021a). "Bridge Pier Scour: An overview of factors affecting the phenomenon and comparative evaluation of selected models," *Transportation Geotechnics*, 28(2021), 100549. DOI: 10.1016/j.trgeo.2021.100549.
- Shahriar AR, Montoya BM, Ortiz AC and Gabr MA (2021b). "Quantifying probability of deceedance estimates of clear water local scour around bridge piers," *Journal of Hydrology*; 597(2021):126177.
- Sheppard, D.M., Odeh, M., and Glasser, T., (2004), Large scale clear-water local pier scour experiments: *Journal of Hydraulic Engineering*; 130(10), 957–963.
- Sheppard, D.M., Jones JS, Odeh, M., and Glasser, T., (2004). "Local Sediment Scour Model Tests for the Woodrow Wilson Bridge Piers" Joint Conference on Water Resource Engineering and Water Resources Planning and Management 2000, 1-9.
- Yao C. (2013). "LRFD calibration of bridge foundations subjected to scour and risk analysis." Ph.D. dissertation, Department of Civil Engineering, Texas A&M University, College Station, Texas.
- Wardhana K, Hadipriono FC. (2003). "Analysis of recent bridge failures in the United States." *Journal of Performance of Constructed Facilities*; 17(3), 144-150.

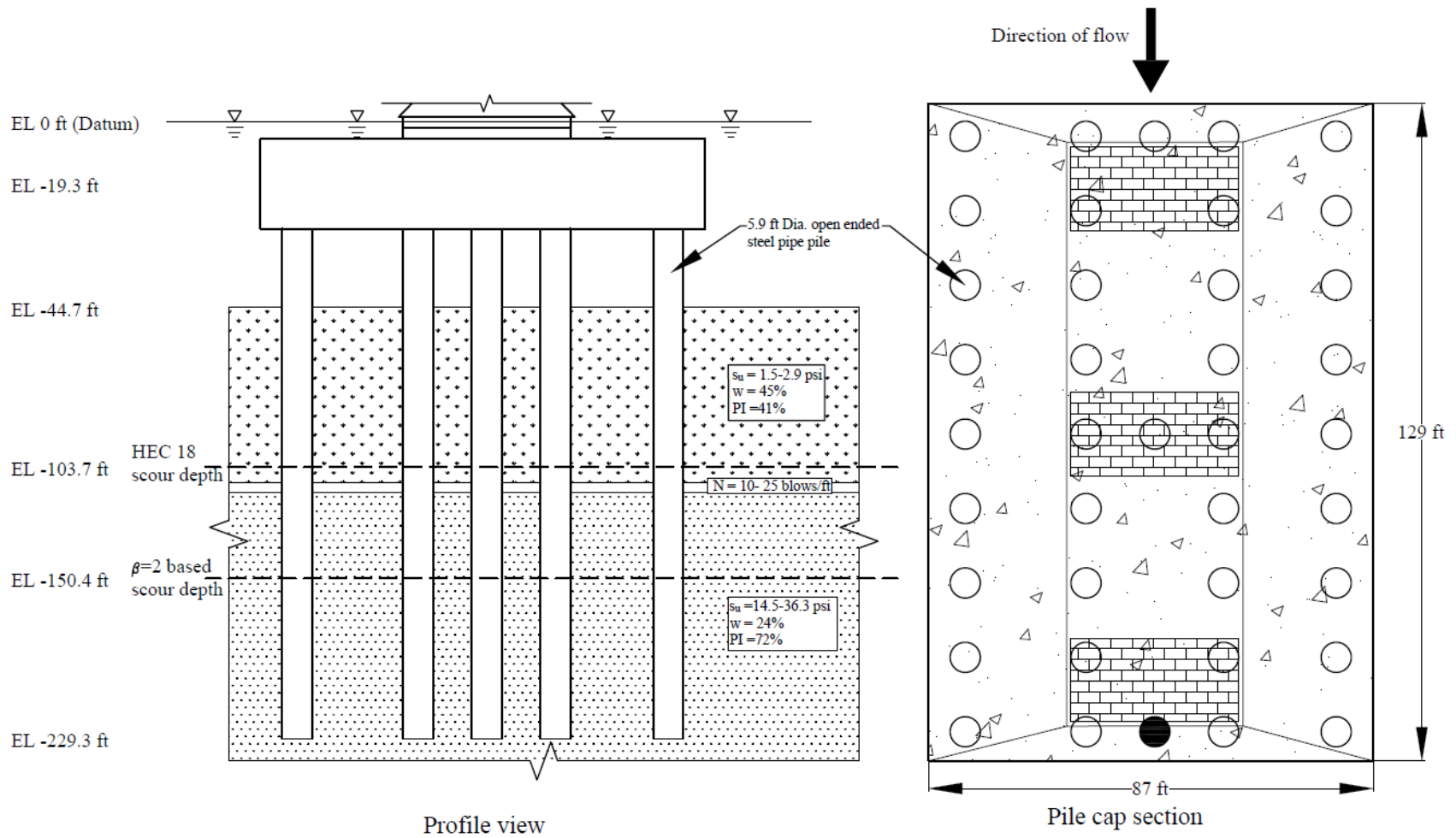


Figure 1: Profile view and pile cap section along with the soil stratigraphy for the bascule pier M1 of Woodrow Wilson bridge (After Kwak and Briaud 2002; Briaud 2008).

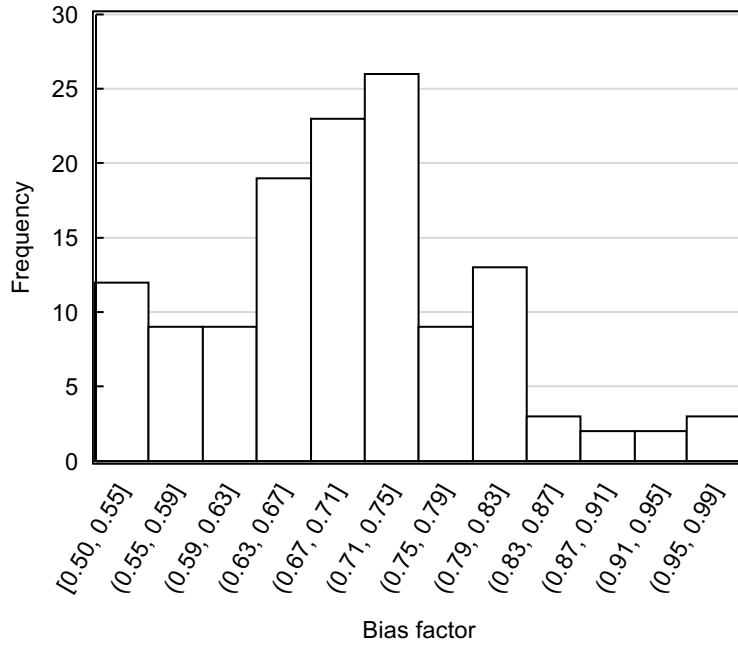


Figure 2: Statistical distribution of bias factor, λ for narrow pier under live bed condition when HEC 18 (2012) model is used. (Normally distributed with skewness = 0.34)

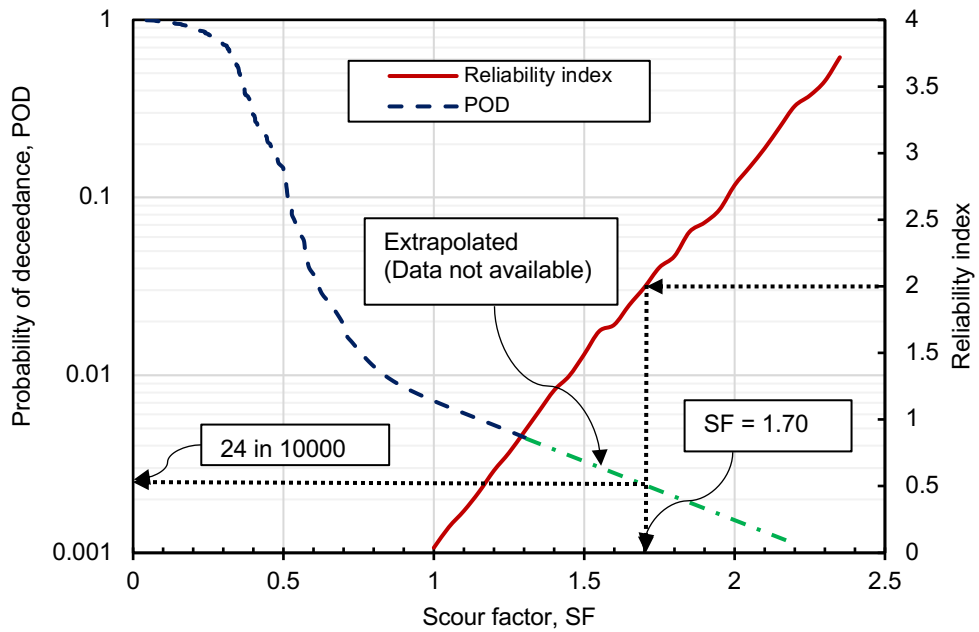


Figure 3: Relationship among probability of deceedance, reliability index and scour factor. (Note: The POD chart has been developed based on HEC 18 model applied to live bed laboratory data)

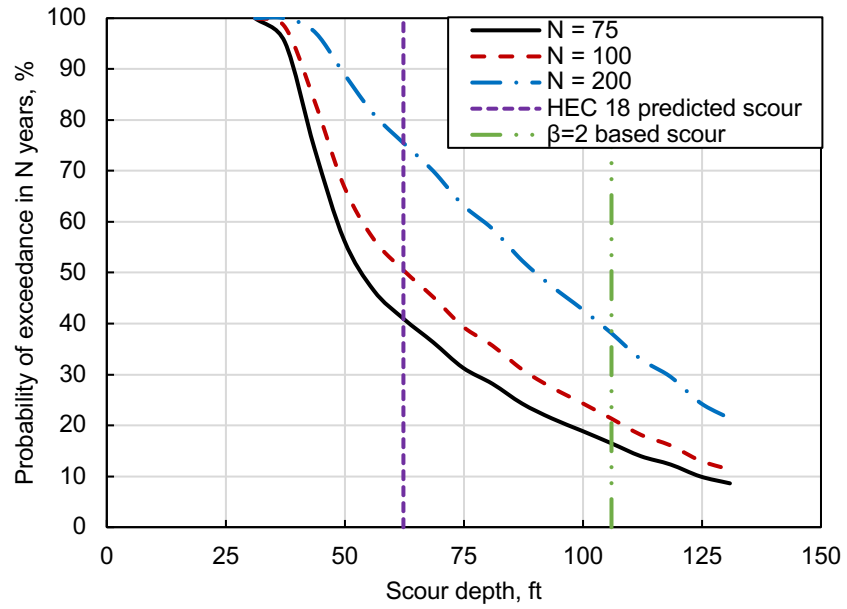


Figure 4: Relationship between probability of exceedance and scour depth for different design life of the bridge when HEC 18 model is used. (Scour depths are for pier M1 of the Woodrow Wilson bridge)

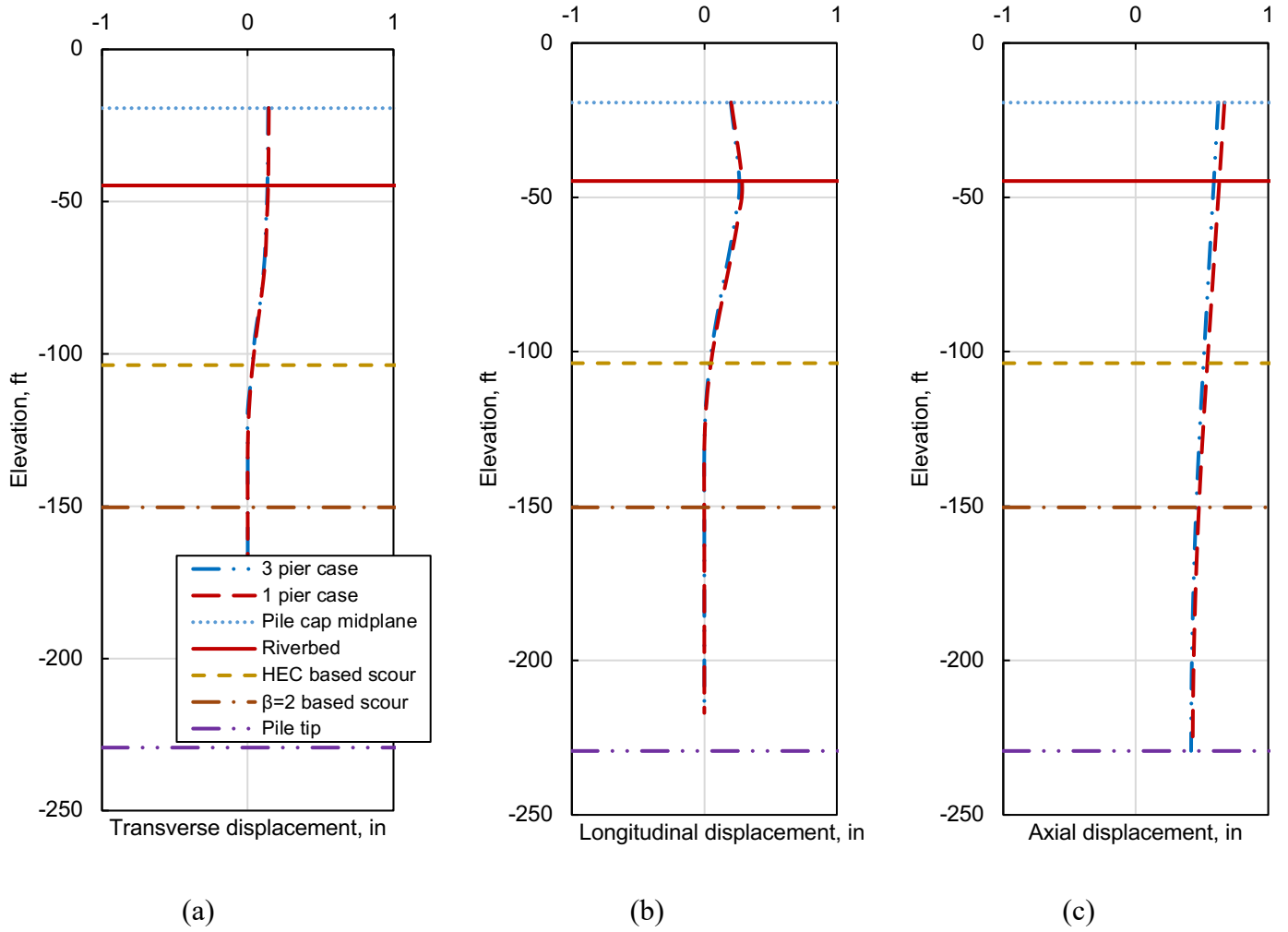
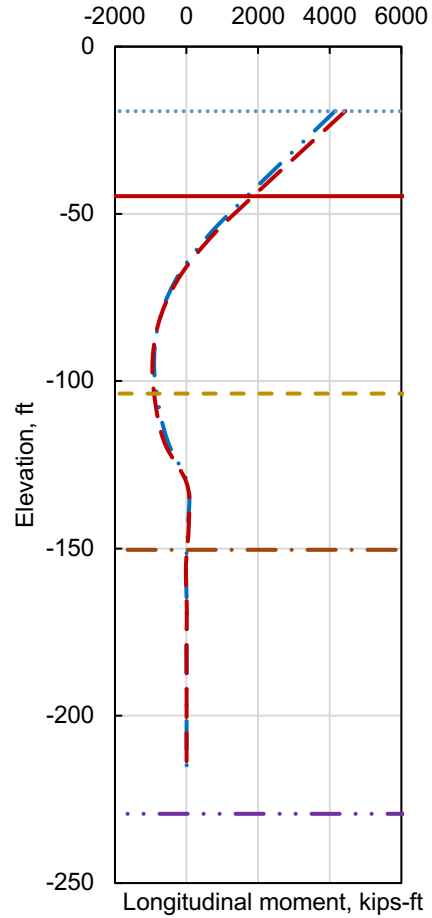
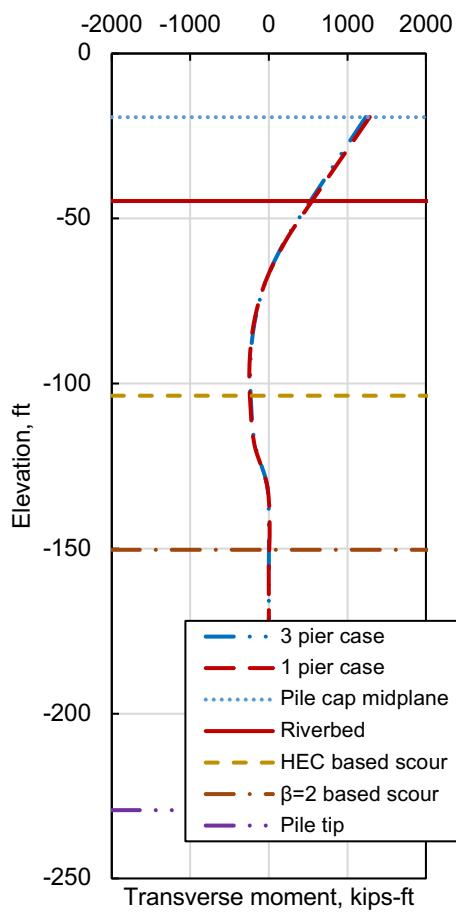


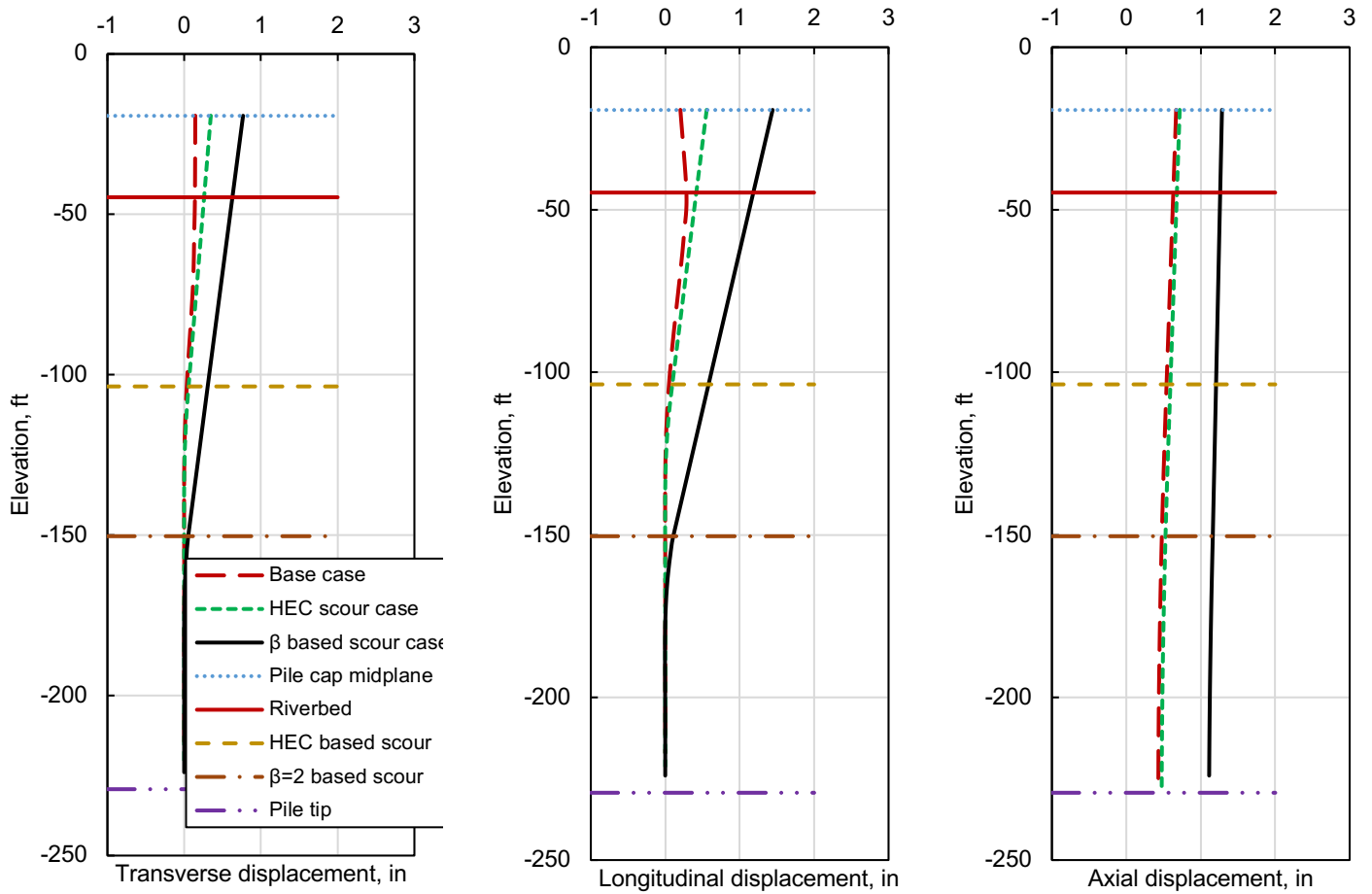
Figure 5. Comparison between the 3-pier case and equivalent 1 pier case in terms of (a) transverse displacement, (b) longitudinal displacement, and (c) axial displacement of the pile. (Maximum among the investigated strength and serviceability limit states is plotted; Datum is at an elevation of 0 ft)



(a)

(b)

Figure 6: Comparison between the 3-pier case and equivalent 1 pier case in terms of (a) transverse moment, and (b) longitudinal moment generated on the pile. (Maximum among the investigated strength and serviceability limit states is plotted; Datum is at an elevation of 0 ft)



(a)

(b)

(c)

Figure 7: Comparison among base case, HEC 18 predicted scour case, and reliability index-based scour case in terms of (a) transverse displacement, (b) longitudinal displacement, and (c) axial displacement. (Maximum among the investigated strength and serviceability limit states is plotted; Datum is at an elevation of 0 ft)

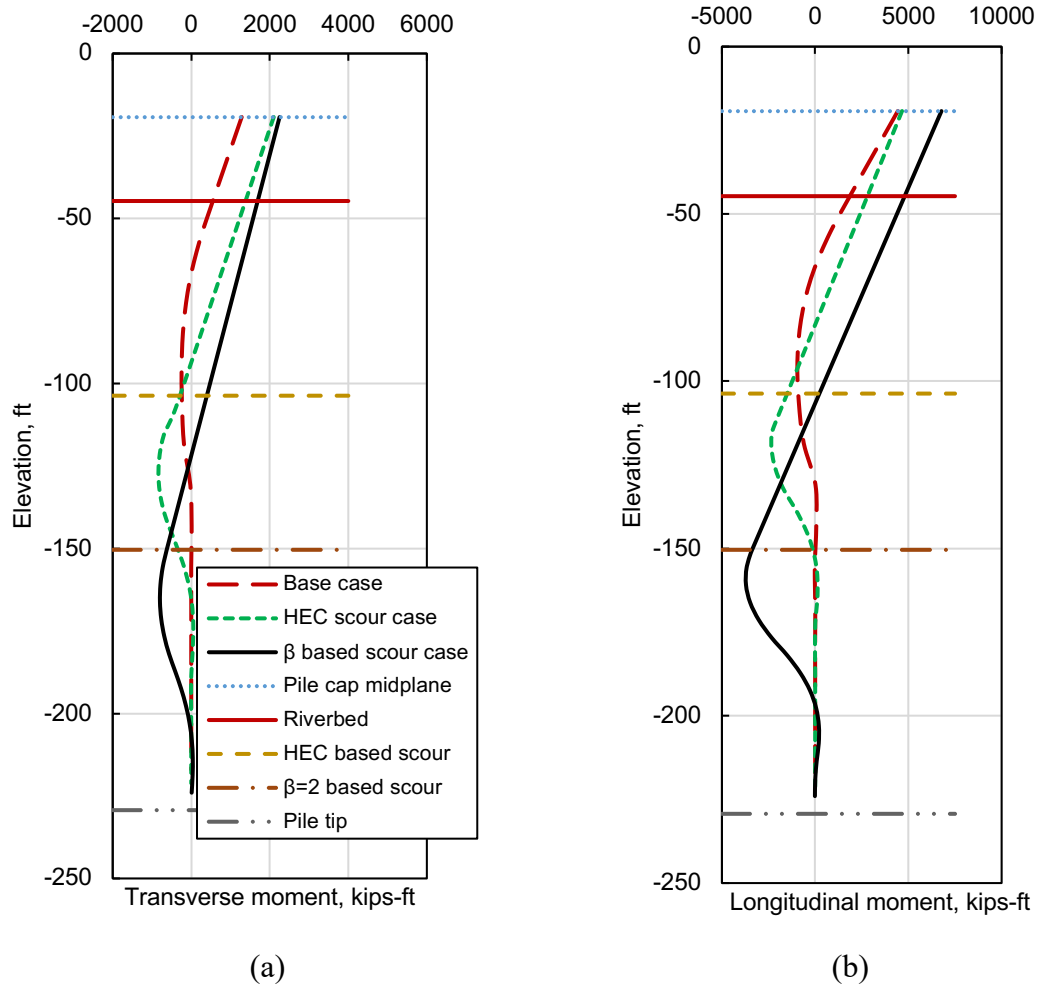


Figure 8: Comparison among base case, HEC 18 predicted scour case, and reliability index-based scour case in terms of (a) transverse moment, and (b) longitudinal moment generated on the pile. (Maximum among the investigated strength and serviceability limit states is plotted; Datum is at an elevation of 0 ft)

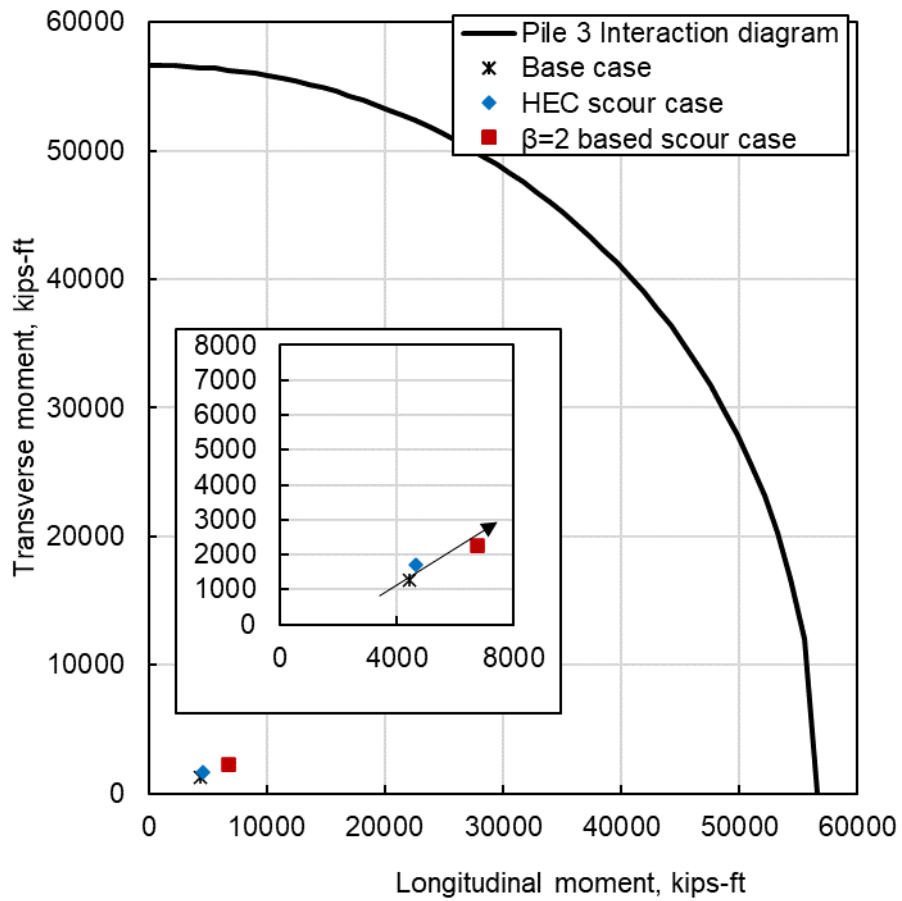
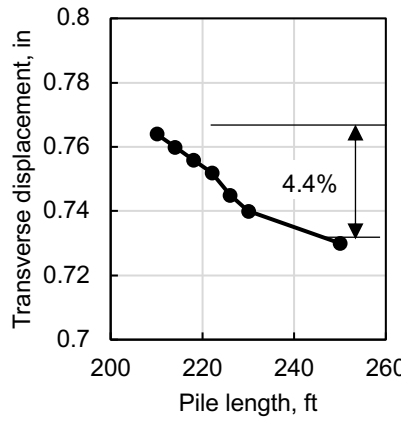
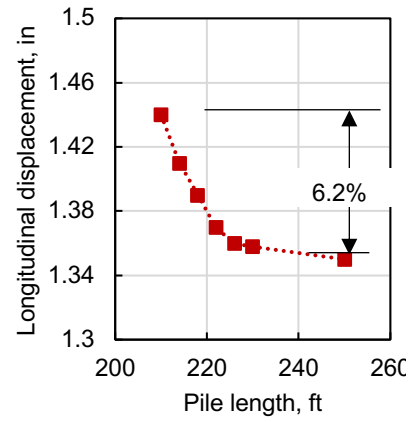


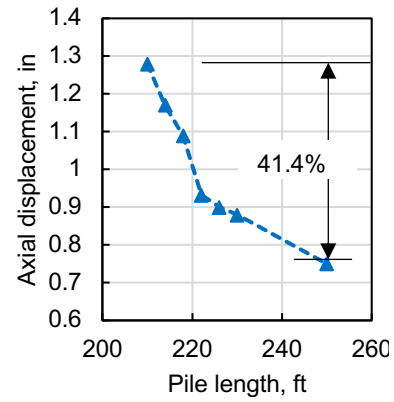
Figure 9: Interaction diagram for pile 3 of pier M1, which governed for moment capacity. (Referring to Figure 1-pile cap section, pile 3 is the center pile in the first row parallel to the 87 ft side—black shaded)



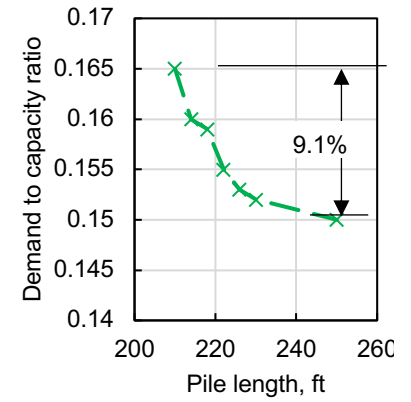
(a)



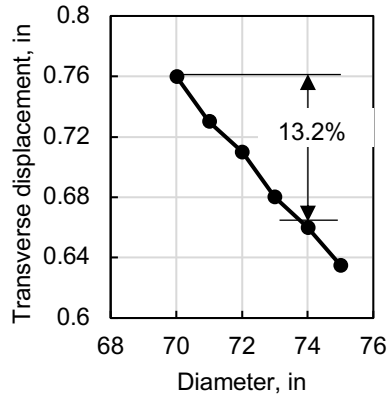
(b)



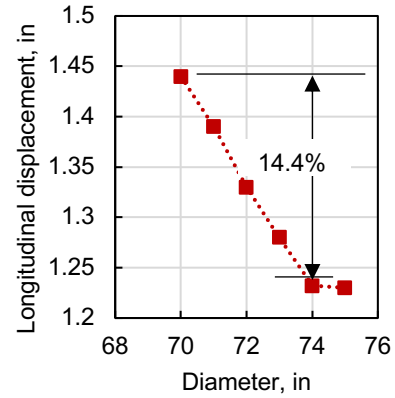
(c)



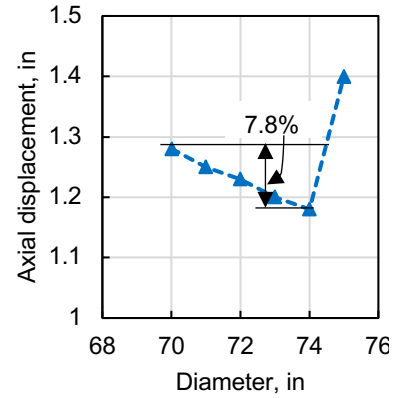
(d)



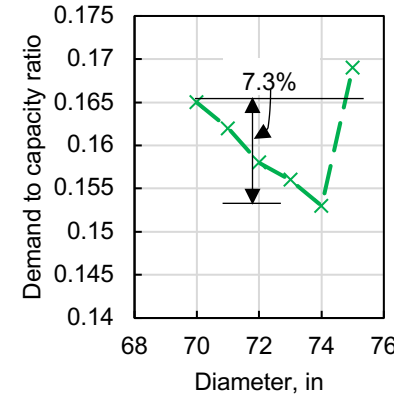
(e)



(f)



(g)



(h)

Figure 10: Variation of (a) transverse displacement, (b) longitudinal displacement, (c) axial displacement, (d) demand to capacity ratio with pile length, and (e) transverse displacement, (f) longitudinal displacement, (g) axial displacement, (h) demand to capacity ratio with pile diameter.

Table 1. Distribution properties of utilized deterministic and random variables in Monte Carlo simulation

Variables	Live bed		Distribution
	Mean	COV	
Pier width	0.6 ft		Deterministic
Pier face shape	Circular		Deterministic
Skew angle	0 degree		Deterministic
Aspect ratio (Length to width)	1		Deterministic
Flow velocity	1.55 ft/s	0.186	Log-normal
Flow depth	1.24 ft	0.2	Normal
Median grain size	0.3 mm	0.081	Normal
Bias factor – HEC 18 (2012)	0.67	0.21	Normal

Appendix F: Bridge abutment scour: Analyses using Sturm (2004) data

Introduction

Scour around existing bridge foundation has been a primary cause of bridge collapse in the United States and worldwide (Melville and Coleman, 2000; Liang et al. 2015; Qi et al. 2016). Records in National Bridge Inventory (NBI) suggests that more than 80% of the total 583,000 bridges in the United States are built over waterways. Support system of structures crossing the waterways are subjected to scour during their design life owing to the flowing water-induced bed shear stresses. Two types of local scour processes are predominantly observed, viz. pier scour and abutment scour. Abutment scour occurs when the abutment and roadway embankment obstruct the flow. The flow obstructed by the abutment and roadway embankment accelerates and forms vortex at the upstream side of the embankment that runs through the tow of the abutment, followed by wake vortex formation at the downstream end of the abutment. Several research has been conducted to comprehend the vortex formation steps and resulting effect on the scour magnitude (Arneson et al. 2012, Ettema et al. 2011). The National Bridge Inspection Standards (NBIS) regulation suggests that bridge owners identify bridges that are scour susceptible and further suggests preparing the plan of action to address potential deficiencies. Despite such stringent regulations, in 10 years (from 2001 to 2011), the percentage of scour critical bridges has reduced by merely 0.5% (from 5.2 to 4.7%). Bridge scour evaluation program, in 2011 reported that there are 23,034 bridges that are scour critical (Arneson et al. 2011).

Ettema et al. (2011) explained that the state-of-the-art of abutment scour prediction is less advanced than pier scour prediction. Pier scour studies have focused on deterministic (e.g., Melville 1997, Arneson et al. 2012), probabilistic (e.g., Lagasse et al. 2013, Shahriar et al. 2021a), and observational (e.g., Govindasamy et al. 2013) aspect, while abutment scour analyses are still deterministic in nature. Ettema et al. (2011) and Arneson et al. (2012) suggested that the abutment scour prediction models do not take into account the physical processes involved. Although deterministic scour prediction models seem lucrative in a sense that it is easy to apply, however, the designer while applying the model does not possess the understanding of degree of conservatism/un-conservatism inherent in the abutment scour prediction model. On top of it, there are more than 15 abutment scour prediction models available in the literature. Therefore, there is a necessity to develop a probabilistic scour prediction model that accounts for inherent model bias and uncertainty of a specific model.

Work herein is focused on comparing the predicted and the measured scour depth using a database collected from the literature. In addition to the SC envelope curve model, three abutment scour prediction models suggested by Hydraulic Engineering Circular No. 18 (HEC 18 2012), namely Froehlich (1989) model, Highway in the River Environment (HIRE) (FHWA 2001) model, and National Cooperative Highway Research Program (NCHRP 2010) model are considered. The database documented by Sturm (2004) is utilized herein.

Scour prediction models

For estimating scour at bridge abutments, HEC 18 (2012) suggested use of three models, such as Froehlich (1989) model, HIRE (2001) model, and NCHRP (2010) model. Froehlich (1989) model (Equation 1) is developed based on 170 abutment scour measurements in laboratory flumes. HIRE (2001) model was developed based on field data of scour at the end of spurs in the Mississippi river. HEC 18 (2012) suggested that the HIRE (2001) model (Equation 2) is applicable mostly for abutments where the abutment length (L) to the flow depth (y) ratio is greater than 25. The abutment scour assessment procedure developed by Ettema et al. (2010) as a part of NCHRP 24-20 (2010) argue the importance of considering how abutments are built. All the abutment scour prediction formulae developed except Ettema et al. (2010) consider that the abutment is a pier-like structure, extending as solid forms deeply into the bed. Ettema et al. (2010) suggested that the maximum scour depth that is attainable at an abutment is limited by the geotechnical stability of the embankment at the abutment. Ettema et al. (2010) developed the abutment scour model for a range of abutment types, abutment locations, and sediment transport conditions. One of the basic differences between Ettema et al. (2010) model and the other models available for abutment scour calculation is that Ettema et al. (2010) consider that the potential maximum scour depth near an abutment due to scour can be expressed in terms of an amplified contraction scour. Ettema et al. (2010) also identified three scour conditions (e.g., scour conditions A, B, and C) depending on the flow field developed at an abutment. Scour condition A happens when the abutment is in or close to the main channel, scour condition B occurs when the abutment is set back from the main channel, and scour condition C occurs when the approach embankment is breached. Specific site conditions necessary to identify the scour condition can be found in Ettema et al. (2010) and HEC 18 (2012). The Ettema et al. (2010) model can be expressed as in Equations (3-6). The SC envelope model proposes two sets of scour prediction models, one based on embankment length, the other based on geometric contraction ratio. Please refer to Equations (7-8) for the SC envelope models considered herein.

An investigation into the parameters influencing abutment scour calculation suggest that abutment scour is influenced by multiple factors. Ettema et al. (2011) classified the factors affecting abutment scour into five categories. Table 1 shows the parameter group and associated parameter names as suggested by Ettema et al. (2011). Different deterministic scour prediction models focused on different datasets, thereby, the performance of any model to a common set of data will be different. Table 2 presents the models suggested by HEC 18 (2012) and list of parameters considered in developing those models. Important to note that the scour prediction models considered in the study assume that the first deck span is not short, i.e., there is no effect of the abutment being close to the first pier. However, there are scarce studies (e.g., Croad 1989) on the effect of pier proximity to the abutment scour. Croad (1989) investigated the effect of pier scour when abutment is located in close proximity and concluded that the scour depth at the pier can be calculated by multiplying the abutment scour depth by 0.9. Nevertheless, how the abutment scour location and its magnitude is affected by short first deck is yet to be investigated.

Database for analyses

The database collected by Sturm (2004) is utilized herein. Sturm (2004) conducted the experiments in a 4.2-m-wide by 24.4-m-long flume of a fixed slope in the Hydraulics Laboratory of the School of Civil and Environmental Engineering at the Georgia Institute of Technology. Scour depths were measured as a function of discharge, sediment size, and abutment shape and length for two different compound-channel configurations constructed. Although there are numerous data sources available in the literature focusing on abutment scour analysis, most of them are focused on tests conducted in a rectangular channel. The tests performed by Sturm (2004) focuses on compound channel hydraulics, a more representative scenario compared to the rectangular channel hydraulics, as such was the focus in the current study.

Melville (1992) suggested that abutment scour can be classified into three categories based on the abutment length (L) to flow depth (y) ratio. These are (a) Long abutment ($L/y > 25$), where scour depth is proportional to flow depth, (b) Intermediate abutment ($1 \leq L/y \leq 25$), where scour depth is dependent on both flow depth and embankment length, and (c) Short abutment ($L/y < 1$), where scour depth is proportional to embankment length. The Sturm (2004) database was classified and analyzed separately for long, intermediate and short abutments.

Analyses

Predicted-measured scour depth relation

Figure 1 presents the relationship between the predicted and the measured scour depth for the Vertical Wall abutments using the four models considered in the study. Figure 1 suggests that in general for long abutments, Froehlich (1989) model provides a more conservative estimate of scour depth compared to HIRE (2001) model. Although Froehlich (1989) model did not underpredict the measured scour depth, the HIRE (2001) model underpredicted the measured scour depth in two occasions. The underpredicted two occasions were corresponding to long abutment in clear water condition (Figure 1d). HEC 18 (2012) suggested that HIRE (2001) model be only used for estimating scour of long abutments, as such only for long abutments, the scour estimations were compared. The application of NCHRP (2010) model is based on the location of embankment in relation to the floodplain. Ettema et al. (2010) suggested that if the projected embankment length (L) is 75 percent or greater than the floodplain width (B), live bed conditions prevail, while for the cases when $L/B < 75\%$, clear water conditions exist. Figure 1(f) suggest that for $L/B \geq 75\%$ cases, NCHRP (2010) model under-predicted the scour depth for 2 out of 10 data points. Observation of Figure 1(g) suggest that for $L/B < 75\%$ cases, NCHRP (2010) model significantly under-predicts the scour depth. Referring to Figure 1(g), on an average, the predicted scour depth is 0.45 times the measured scour depth for $L/B < 75\%$ case. Comparison of Figures 1(f) and 1(g) suggest that most data points (80%) are in $L/B < 75\%$ category, while the rest 20% sites have $L/B \geq 75\%$.

The SC envelope curves has two sets of models to estimate the abutment scour depth, one based on the embankment length, the other based on the geometric contraction ratio. Figure 1 (h-i) suggests that the geometric contraction ratio based scour depth estimation model over-predicts

the scour depth by 2.5 times the measured scour depth. However, when the embankment length based scour estimation model is used, the SC envelope curve model seems to under-predict the measured scour depth. Such underprediction is owing to the fact that the SC envelope curve model is based on the field scour measurements, while the database considered herein is a laboratory compound channel scour measurements.

References

- Arneson LA, Zevenbergen LW, Lagasse PF, and Clopper PE. (2012). "Evaluating scour at bridges." Hydraulic Engineering Circular No. 18, 5th edition, 1-340.
- Benedict, S.T., Deshpande, Nikhil, Aziz, N.M., and Conrads, P.A., 2006, Trends of abutment-scour prediction equations applied to 144 field sites in South Carolina: U.S. Geological Survey Open-File Report 2003-295, 150 p
- Croad RN. Investigation of the pre-excavation of the abutment scour hole at bridge abutments, Report 89-A9303, Central Laboratories, Works and Development Services Corporation (NZ) Ltd., Lower Hutt, New Zealand, 1989.
- Federal Highway Administration, 2001, "River Engineering for Highway Encroachments - Highways in the River Environment," FHWA NHI 01-004, Federal Highway Administration, Hydraulic Design Series No. 6, Washington, D.C. (Richardson, E.V., D.B. Simons, and P.F. Lagasse).
- Froehlich, D.C. (1989). "Local scour at bridge abutments," Proc. ASCE National Hydraulic Conference, Colorado Springs, Colorado, pp. 13-18.
- Govindasamy AV, Briaud J-L, Kim D, Olivera F, Gardoni P, Delphia J. Observation method for estimating future scour depth at existing bridges. Journal of Geotechnical and Geoenvironmental Engineering, ASCE, 2013; 139(7):1165-1175.
- Johnson PA. (1992). "Reliability-based pier scour engineering." *Journal of Hydraulic Engineering*; 118(10), 1344-1358.
- Lagasse P. F., Ghosn M., Johnson P. A., Zevenbergen L.W., and Clopper P. E. (2013). "Risk-based approach for bridge scour prediction." Final Rep., NCHRP Project 24-34, Transportation Research Board, National Academies of Science, Washington, DC.
- Liang FY, Zhang H, and Huang MS. (2015). "Extreme scour effects on the buckling of bridge piles considering the stress history of soft clay." *Natural Hazards*; 77, 1143-1159.
- Melville, B.W. (1992). "Local scour at bridge abutments." *Journal of Hydraulic Engineering*, ASCE, Vol. 118, No. 4, p. 615.
- Melville BW. Pier and abutment scour: Integrated approach. Journal of Hydraulic Engineering, ASCE, 1997; 123(2), 125-136.
- Melville BW. and Coleman SE. (2000). "Bridge scour." Highlands Ranch, USA: Water Resources Publications.

- National Cooperative Highway Research Program, 2011, "Estimation of Scour Depth at Bridge Abutments," NCHRP Project 24-20, Transportation Research Board, National Academy of Science, Washington, D.C., (Ettema, R., Nagato, T., and M. Muste).
- Qi M, Li J, and Chen Q. (2016). "Comparison of existing equations for local scour at bridge piers: parameter influence and validation." *Natural Hazards*; 82(3), 2089-2105.
- Richardson, E.V., and Davis, S.R. (2001). "Evaluating Scour at Bridges." *Hydraulic Engineering Circular* No. 18, 4th Ed., Federal Highway Administration, Arlington, VA.
- Shahriar AR, Montoya BM, Ortiz AC and Gabr MA (2021a). "Quantifying probability of deceedance estimates of clear water local scour around bridge piers," *Journal of Hydrology*, 597(2021):126177. DOI: 10.1016/j.jhydrol.2021.126177.
- Shahriar AR, Ortiz AC, Montoya BM, and Gabr MA (2021b). "Bridge Pier Scour: An overview of factors affecting the phenomenon and comparative evaluation of selected models," *Transportation Geotechnics*, 28(2021), 100549. DOI: 10.1016/j.trgeo.2021.100549.

Table 1. Deterministic abutment scour model equations considered in the present study

Reference	Model	Equation No.	Remarks
Froehlich (1989)	$\frac{y_{sp}}{y_a} = 2.27K_1K_2\left(\frac{L'}{y_a}\right)^{0.43} Fr^{0.61} + 1$	(1)	y_{sp} = predicted scour depth y_a = average depth of flow on the floodplain K_1 = coefficient for abutment shape K_2 = coefficient for angle of embankment to flow L' = length of active flow obstructed by the embankment Fr = Froude number
HIRE (2001)	$\frac{y_{sp}}{y_a} = 4Fr^{0.33} \frac{K_1}{0.55} K_2$	(2)	
NCHRP (2010)	$y_{max} = \alpha y_c$	(3)	y_{max} = Maximum flow depth resulting from abutment scour α = amplification factor depending on clear water/live bed condition y_c = Flow depth including live-bed or clear-water contraction scour
	$y_{sp} = y_{max} - y_o$	(4)	y_o = flow depth prior to scour
	$y_{cLB} = y_1 \left(\frac{q_2}{q_1}\right)^{6/7}$	(5)	q_2 = unit discharge in the constricted opening
	$y_{cCW} = \left(\frac{q_2}{K_u D_{50}^{1/3}}\right)^{6/7}$	(6)	q_1 = upstream unit discharge y_{cLB} = flow depth including live bed contraction scour y_{cCW} = flow depth including clear water contraction scour D_{50} = median grain size
SC envelope (2018)	$y_s = -0.000009L^2 + 0.0276L$	(7)	y_s = Scour depth in feet
	$y_s = 3.27m^2 - 1.12m$	(8)	L = length of active flow obstructed by the embankment, in feet m = geometric contraction ratio

$$+1.29 \quad (0 \leq L \leq 100 \text{ ft}; \\ 0.136 \leq m \leq 0.85)$$

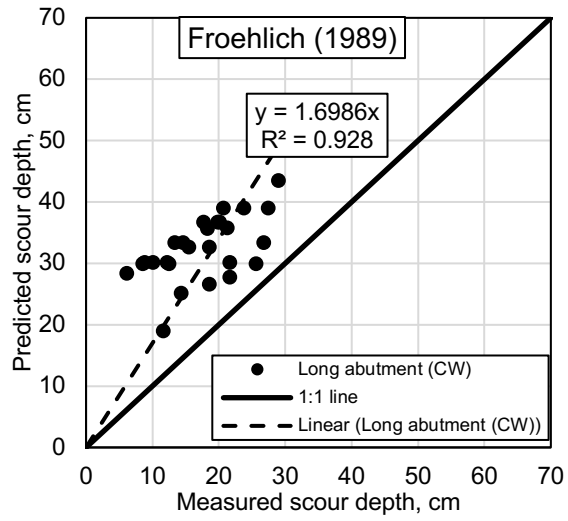
Table 2. Classification of abutment scour parameters (summarized from Ettema et al. 2011)

Parameter group	Parameter names
Flow/ Sediment	Flow intensity, Froude number, Reynolds number
Abutment/ Sediment scale	Relative sediment size
Abutment/ Flow geometry	Floodplain aspect ratio, relative contraction length, abutment shape, skewness
Abutment flow distribution	Abutment, channel, and flow length scales
Geotechnical aspect	Abutment stability parameter

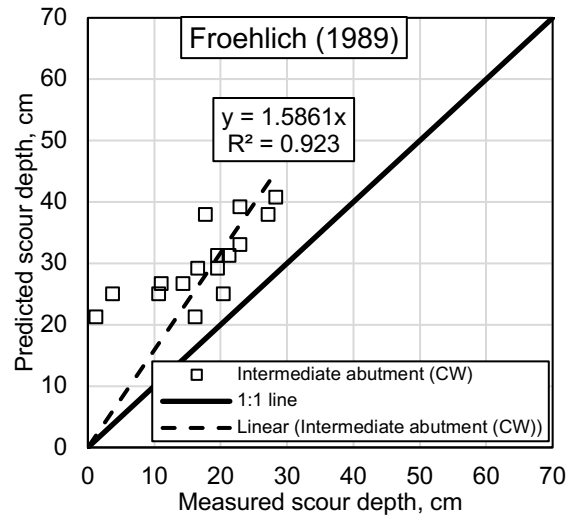
Table 3. Consideration of abutment scour influencing parameters in HEC 18 (2012) suggested deterministic models

Model	Parameter group				
	Flow/ sediment	Abutment/ sediment scale	Abutment/ flow geometry	Abutment/ flow distribution	Geotechnical aspect
Froehlich (1989)	C	NC	C	NC	NC
HIRE (FHWA 2001)	C	NC	C	NC	NC
NCHRP (Ettema et al. 2010)	C	NC	NC	NC	C

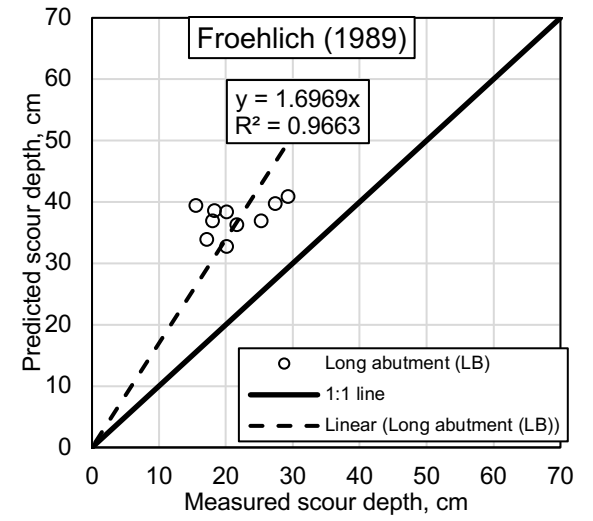
Note: C means *Considered* in the respective model, while NC means *Not Considered* in the respective model.



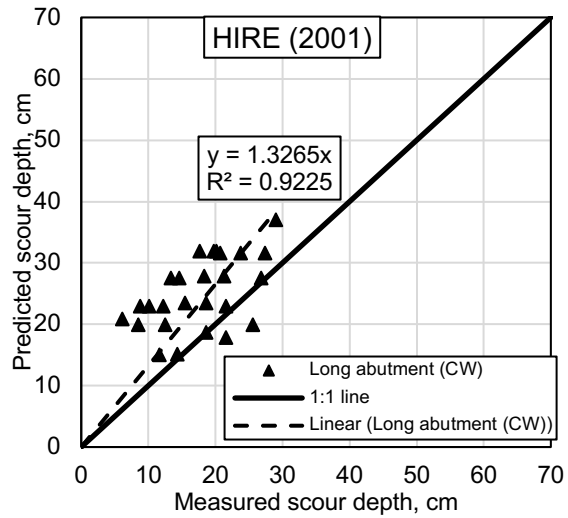
(a)



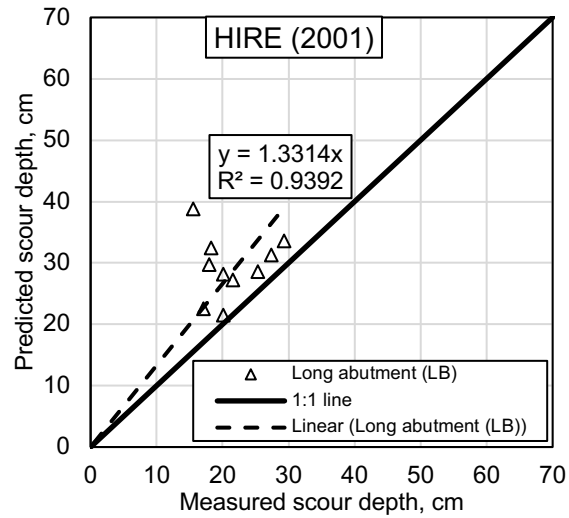
(b)



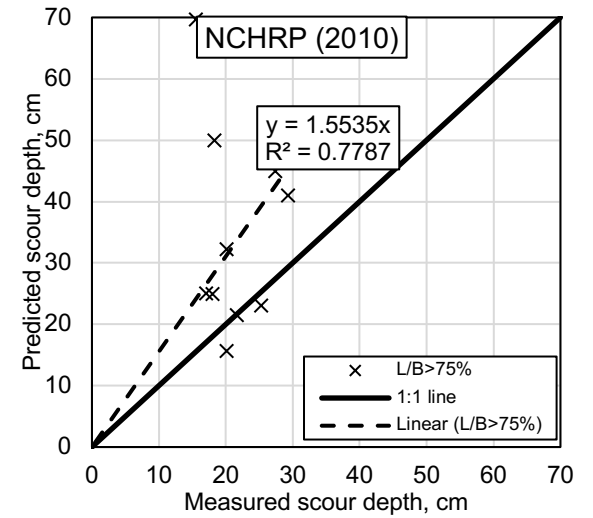
(c)



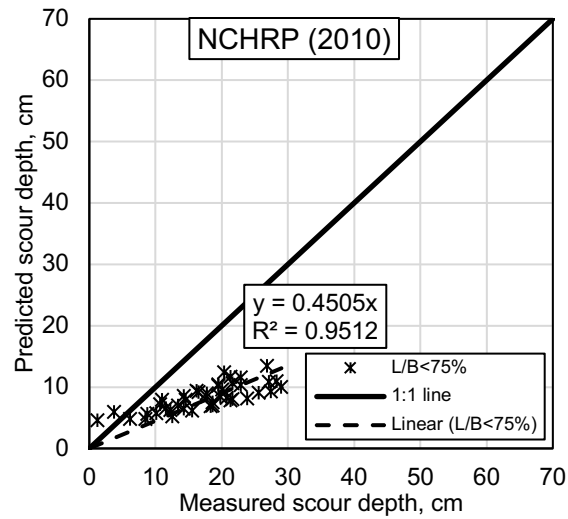
(d)



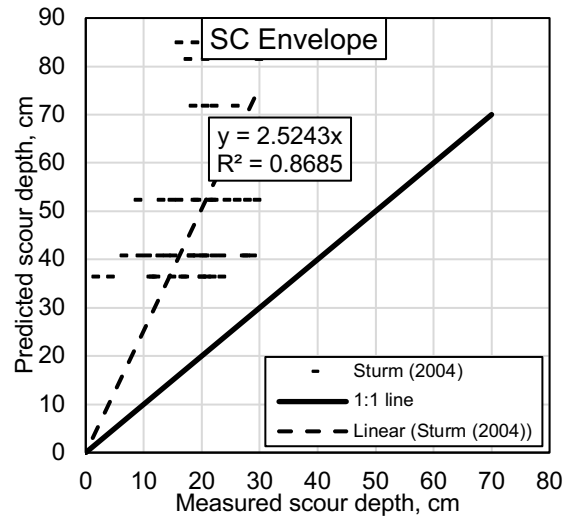
(e)



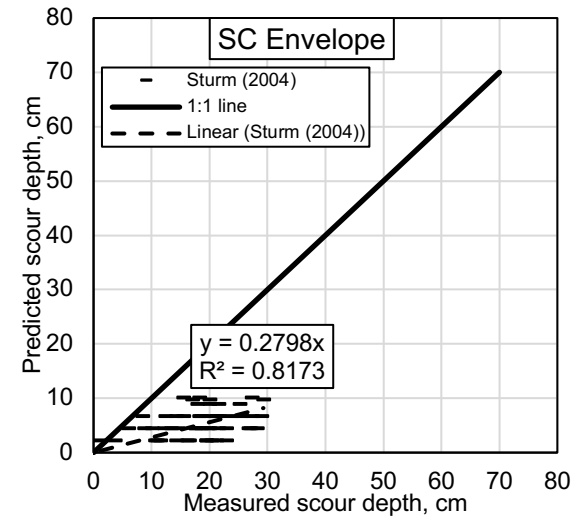
(f)



(g)



(h)



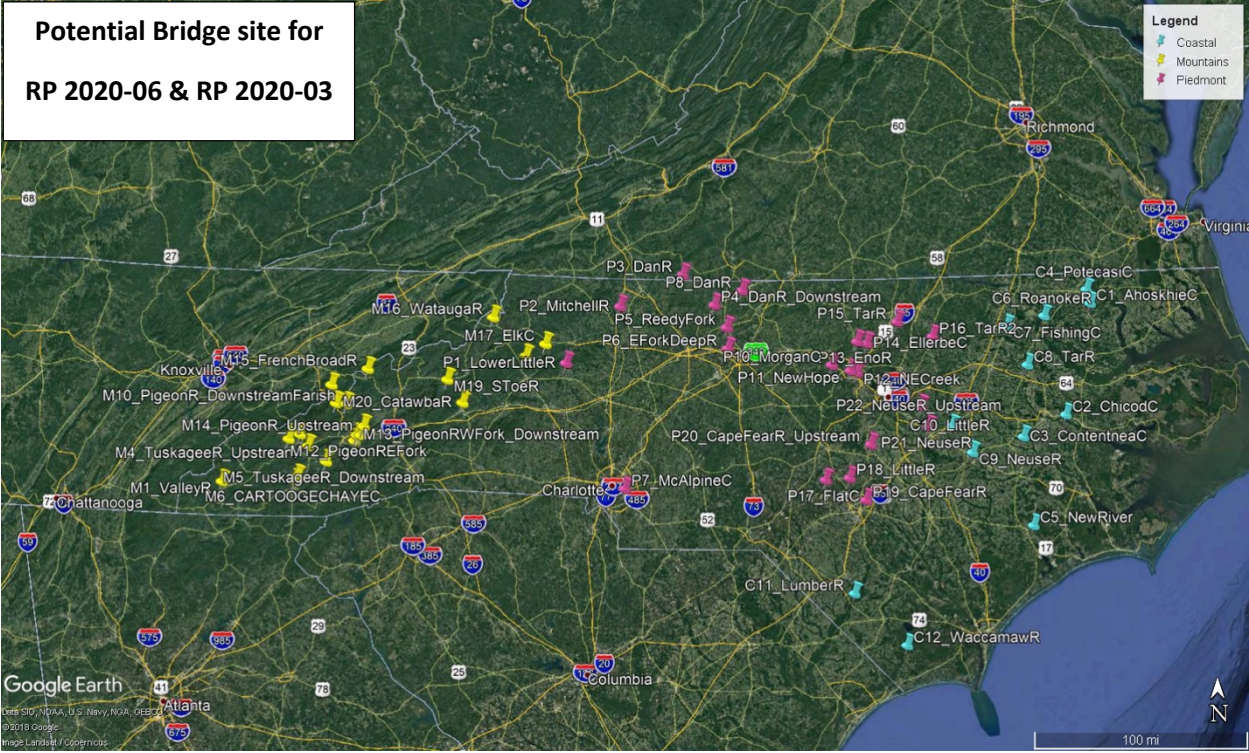
(i)

Figure 1. Relationship between the predicted and measured scour depth for (a) Froehlich (1989) model- Long abutment- Clear water condition, (b) Froehlich (1989) model- Intermediate abutment- Clear water condition, (c) Froehlich (1989) model- Long abutment-Live bed condition, (d) HIRE (2001) model Long abutment- Clear water condition, (e) HIRE (2001) model Long abutment- Live bed condition, (f) NCHRP (2010) model $L/B > 75\%$, (g) NCHRP (2010) model $L/B < 75\%$ (h) SC envelope contraction ratio based model, and (i) SC envelope embankment length based model. (Note: L and B stand for length of the embankment and width of the floodplain respectively)

Appendix G: Preliminary list and map of potential bridge sites to study in collaboration with RP 2020-03

	ns1:name4	ns1:latitude	ns1:longitude	Bridge Name	USGS Gage Number
1	M1_ValleyR	35.138052	-83.9785345	190057	03550000
2	M2_TuskageeR	35.428837	-83.4451567	860129	03513000
3	M5_TuskageeR_Downstream	35.287839	-83.1438097	490078	03508050
4	M6_CARTOOGECHAYEC	35.159463	-83.3912449	550025	03500240
5	M7_LittleTennesseeR	35.187266	-83.3743038	550349	03501500
6	M10_PigeonR_DownstreamFarish	35.664417	-82.9905885	430142	03459500
7	M11_PigeonRWFork_UpstreamFar	35.428169	-82.9186223	430136	0345577330
8	M12_PigeonRWFork	35.462585	-82.8692257	430132	03456500
9	M13_PigeonRWFork_Downstream	35.464855	-82.8974376	430464	03456100
10	M14_PigeonR_Upstream	35.522272	-82.8478254	430164	03456991
11	M15_FrenchBroadR	35.893614	-82.820165	560067	03454500
12	M16_WataugaR	36.237764	-81.8226346	940214	03479000
13	M17_Elkc	36.06976	-81.4027836	960022	02111180
14	M18_YadkinR	35.990891	-81.5565854	130007	02111000
15	M19_SToeR	35.832863	-82.1831423	990079	03463300
16	M20_CatawbaR	35.68574	-82.060625	580025	02137727
17	P1_LowerLittleR	35.946176	-81.2357216	10077	02142000
18	P2_MitchellR	36.311363	-80.8056425	850007	02112360
19	P3_DanR	36.514447	-80.3029254	840008	02068500
20	P4_DanR_Downstream	36.31897	-80.0501962	840115	02069000
21	P5_ReedyFork	36.173079	-79.952615	400106	02093800
22	P8_DanR	36.412889	-79.8257064	780119	02071000
23	P9_CaneC	35.985165	-79.2028635	670189	02096846
24	P11_NewHope	35.882521	-78.9625523	310111	02097314
25	P12_NECreek	35.872492	-78.9136084	310107	0209741955
26	P13_EnoR	36.071112	-78.9050707	310035	02085070
27	P14_EllerbeC	36.05571	-78.8300077	310034	02086849
28	P15_TarR	36.192891	-78.5798186	380010	02081500
29	P16_TarR2	36.094033	-78.2962706	340033	2081747 & 02081740
30	P18_LittleR	35.192974	-78.9857914	250182	02103000
31	P19_CapeFearR	35.047624	-78.8554045	250219	02104000
32	P20_CapeFearR_Upstream	35.407671	-78.8090614	420045	02102500
33	P21_NeuseR	35.512976	-78.3485807	500040	02087570
34	P22_NeuseR_Upstream	35.648217	-78.4034391	500075	02087500
35	C1_AhoskhieC	36.280893	-76.9997839	450033	02053500
36	C2_ChicodC	35.561188	-77.2296407	730010	02084160
37	C3_ContentneaC	35.427985	-77.5827014	390023	02091500
38	C4_PotecasiC	36.365612	-77.0240429	450021	02053200
39	C5_NewRiver	34.848345	-77.5181752	660039	02093000
40	C6_RoanokeR	36.206692	-77.3798651	410023	02081000
41	C7_FishingC	36.150789	-77.691808	320023	02083000
42	C8_TarR	35.891271	-77.5354906	320024	02083500
43	C9_NeuseR	35.339328	-77.9963945	950018	02089000
44	C10_LittleR	35.508129	-78.1587238	500224	02088500
45	C11_LumberR	34.439472	-78.961337	770118	02134500
46	C12_WaccamawR	34.094717	-78.5480047	230072	02109500

Potential Bridge site for
RP 2020-06 & RP 2020-03



Appendix H: Numerical Modeling of Monitored Sites Data

In this appendix, we use Delft3D Flexible Mesh, a finite volume hydrodynamic and morphodynamic model, to simulate the hydrodynamic condition around bridge piers for Tar River, Ellerbe Creek, and Middle Creek. Then, the scour depth and hydrodynamic characteristics for 25-, 50-, 100-, and 200-year flood conditions for each site will be computed and compared with the results of FHWA HEC-18 procedure and the SC scour envelope curves. The modeling details are as follows.

Tar River

In this section, we summarize the steps taken to find the hydrodynamic conditions around bridge number 340033 piers (Tar River). First, we analyzed the records of USGS gage number 02081747 to find the 25-, 50-, 100-, and 200-year flood characteristics for this location. By applying extreme value analysis on the 56 years of data (1964 – 2020) the flood conditions were obtained (Figure 1). The computed values were in good correlation with the USGS StreamStats application outputs (Table 1).

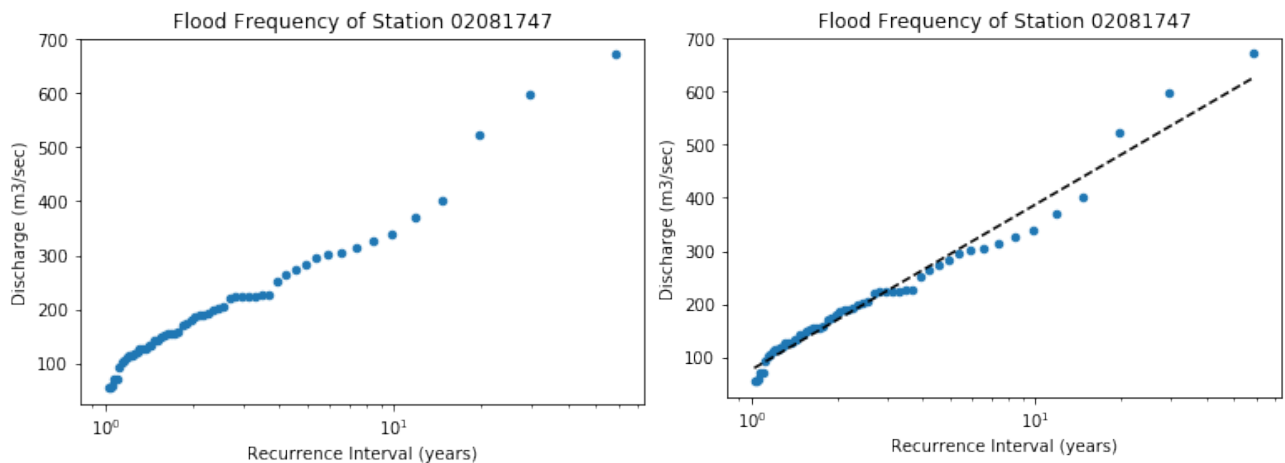


Figure 1. Extreme Value analysis applied to USGS gage number 02081747 records from 1964 to 2020

Table 1. Computed flood conditions vs. USGS StreamStats application (Tar River)

Tar River/Gage 02081747	years of data	mean Discharge (m ³ /s)	10-yr flood (m ³ /s)	25-yr flood (m ³ /s)	50-yr flood (m ³ /s)	100-yr flood (m ³ /s)	200-yr flood (m ³ /s)
StreamStats application	42 (1973 -2015)	11	354	467	561	660	770
Research Team Analysis	56 (1964 - 2020)	6	387	510	604	697	790

We used Delft3d Flexible Mesh Suite to make a high-resolution Tar River unstructured mesh with 50,000 elements (Figure 2). The grid cell sizes vary from 2m near the bridge piers to 8m into the floodplain area. The bathymetry was made by the river profiles taken from the latest NCDOT Scour Inspection reports and the floodplain DEM was obtained from NC Risk Management most recent LiDAR data. Bridge number 340033 has two rectangular piers stacks that are indicated in the Figure 2 by four black rectangles.

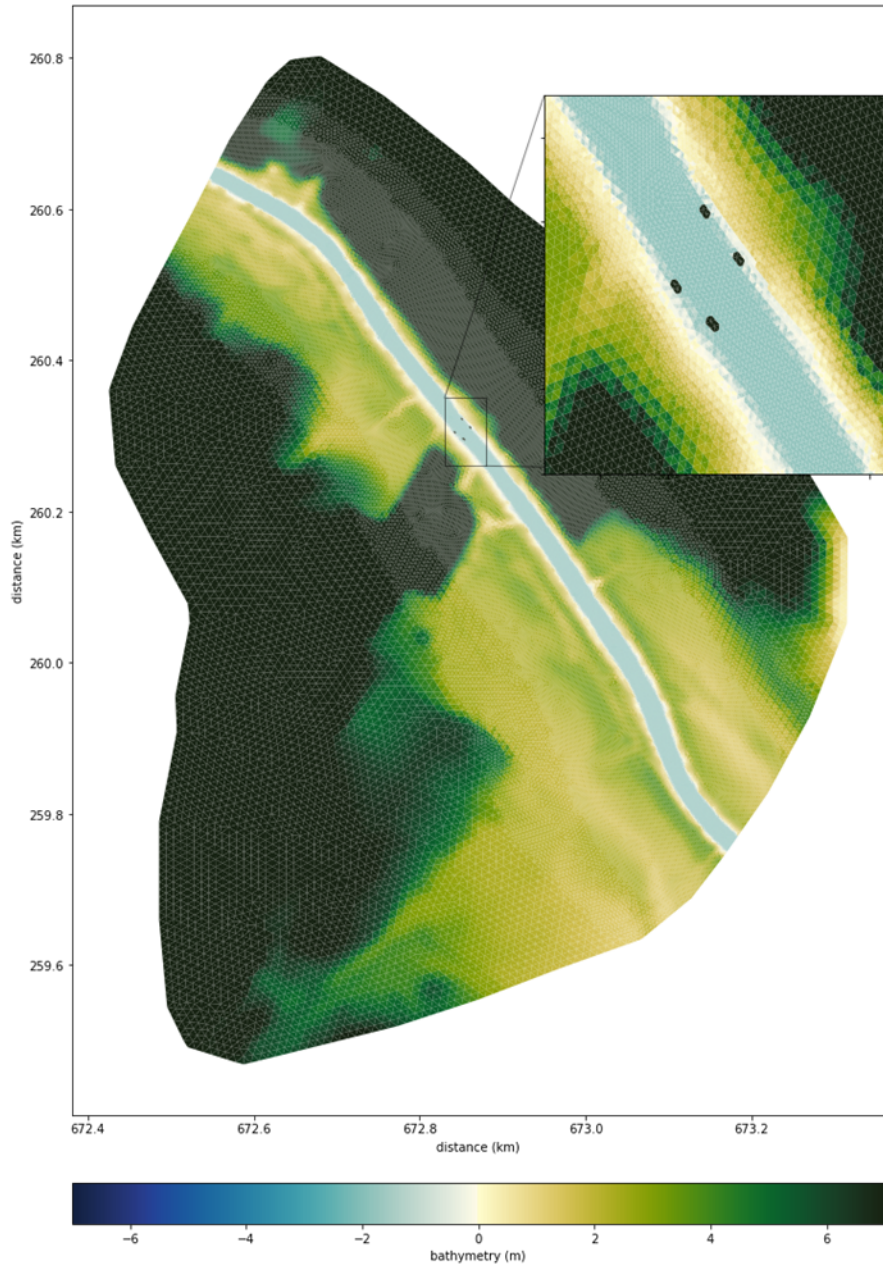


Figure 2. Tar River model mesh and bathymetry, Bridge piers are indicated by four black rectangles

We calibrated the model by applying the discharge of the day of field work (June 7th, 2021) taken from the adjacent USGS Gage (4.36 m³/s). Given this condition, the simulated velocity at the

location of the deployed ADCP is ~0.15 m/s which is in an excellent correlation with the ADCP measured velocity (0.15-0.16 m/s). After calibration the computed flood discharges were applied and the resultant velocities and water depths were extracted for further scour depth calculations (Figure 3, Table 2).

Table 2. The modeled approach velocity and approach flow depth for flood condition in Tar River

Tar River	Discharge (m ³ /s)	Approach mean flow velocity (m/s)	Approach flow depth (m)
10-yr flood	387	2.2	5.1
25-yr flood	510	2.5	5.5
50-yr flood	604	3	5.9
100-yr flood	697	3.6	6.4
200-yr flood	790	3.8	6.9

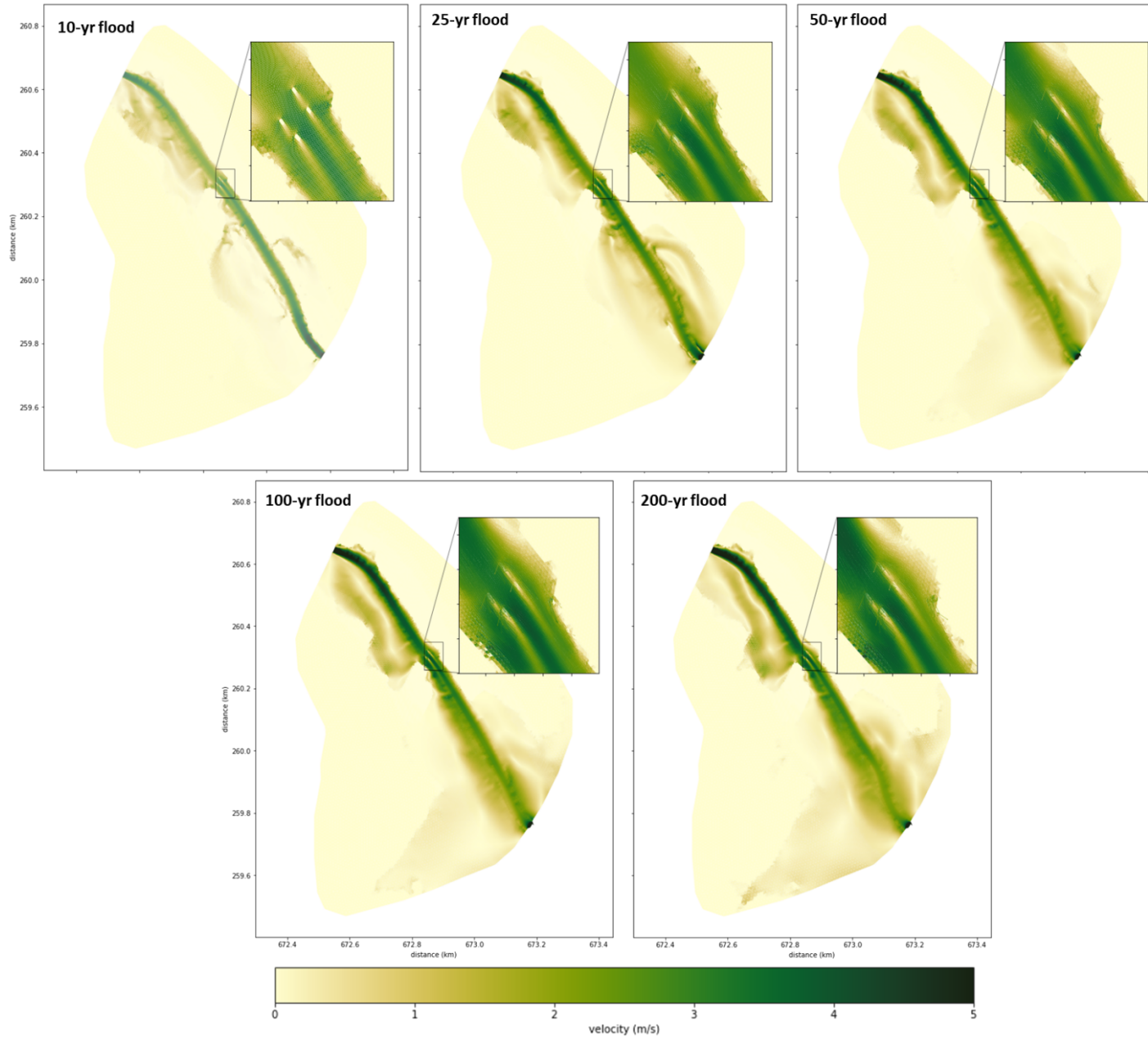


Figure 3. Flow velocity distribution over the spatial domain of Tar River in flood conditions

Ellerbe Creek

In this section, we summarize the steps taken to find the hydrodynamic conditions around bridge number 310034 piers (Ellerbe Creek). The same as the procedure for Roanoke River and Tar River, we analyzed the records of USGS gage number 02086849 to find the 25-, 50-, 100-, and 200-year flood characteristics for this location (Figure 4). We used the available 30 years of data (1982 - 2022) and our computed flood discharges were 30-40% less than the StreamStats application outputs which were derived from 18 years of data (1982 -2015), (Table 3).

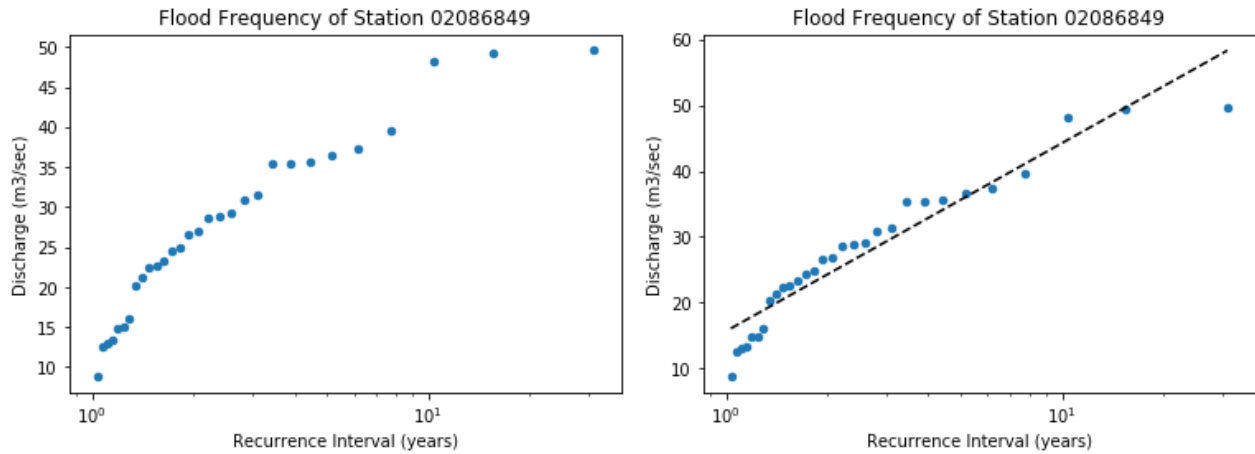


Figure 4. Extreme Value analysis applied to USGS gage number 02086849 records from 1982 to 2022

Table 3. Computed flood conditions vs. USGS StreamStats application (Ellerbe Creek)

Ellerbe Creek/Gage 02086849	years of data	mean Discharge (m ³ /s)	10-yr flood (m ³ /s)	25-yr flood (m ³ /s)	50-yr flood (m ³ /s)	100-yr flood (m ³ /s)	200-yr flood (m ³ /s)
StreamStats application	18 (1982 -2015)	1.1	74	81	86	90	94
Research Team Analysis	30 (1982 - 2022)	1.2	44	55	64	73	81

The same as Tar River model, we used Delft3d FM to make a high-resolution Ellerbe Creek unstructured mesh. The spatial domain is ~370 m x 400 m and the cell grid sizes range from 0.6 m around the bridge piers to 8 m into the floodplain (Figure 5). We used the ADCP data that we took in October 2020 to calibrate the model. The flow discharge from the gage for those dates were applied to the model and the simulated velocity compared to the ADCP measurements (Figure 6). After calibration the computed flood discharges (Table 3) were applied and the resultant velocities and water depths were extracted for further scour depth calculations (Figure 7, Table 4).

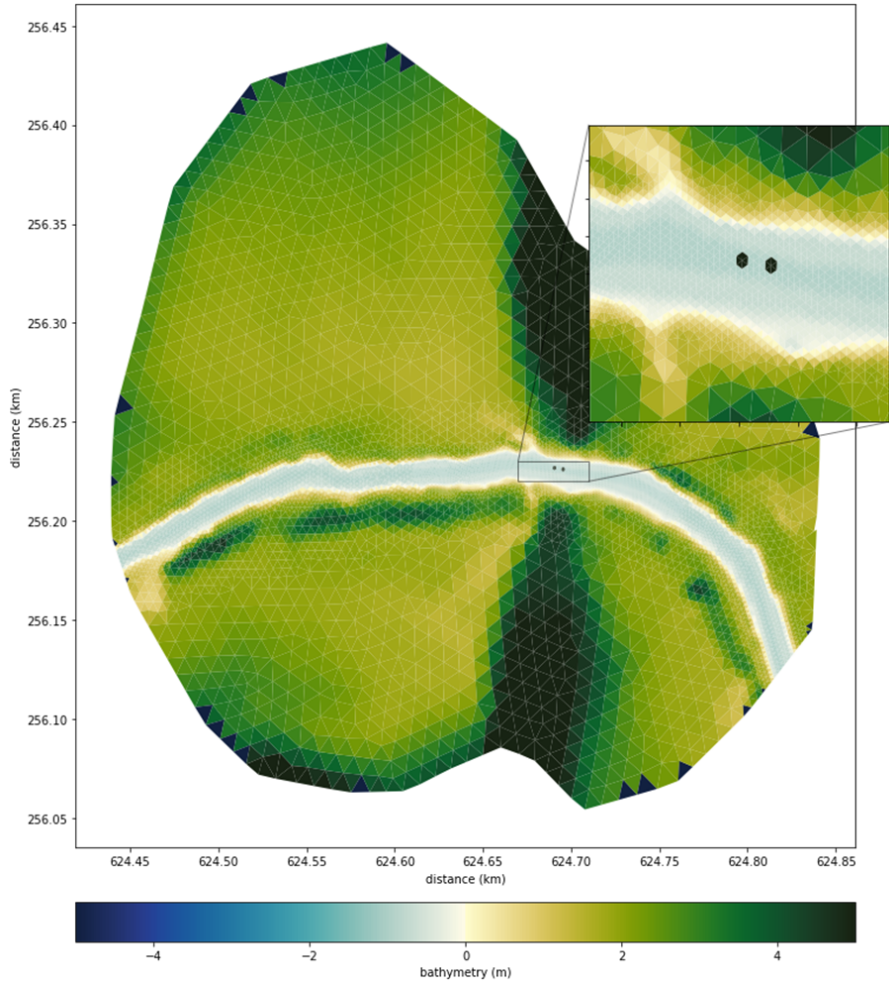


Figure 5. Ellerbe Creek model mesh and bathymetry, Bridge piers are indicated by two black circles

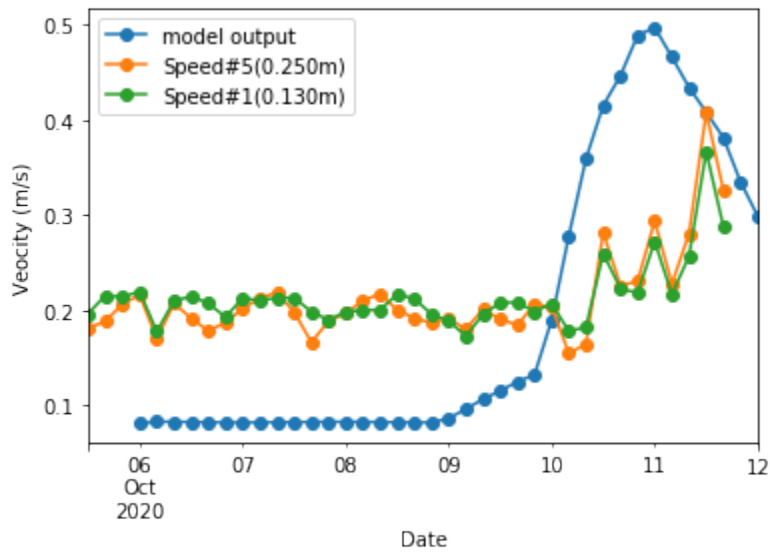


Figure 6. Time series of flow velocity measured by ADCP (green and orange) vs. model output (blue)

Table 4. The modeled approach velocity and approach flow depth for flood condition in Ellerbe Creek

Ellerbe Creek	Discharge (m ³ /s)	Approach mean flow velocity (m/s)	Approach flow depth (m)
10-yr flood	44	1.22	2.5
25-yr flood	55	1.12	3.2
50-yr flood	64	1.02	3.8
100-yr flood	73	0.95	4.2
200-yr flood	81	0.90	4.7

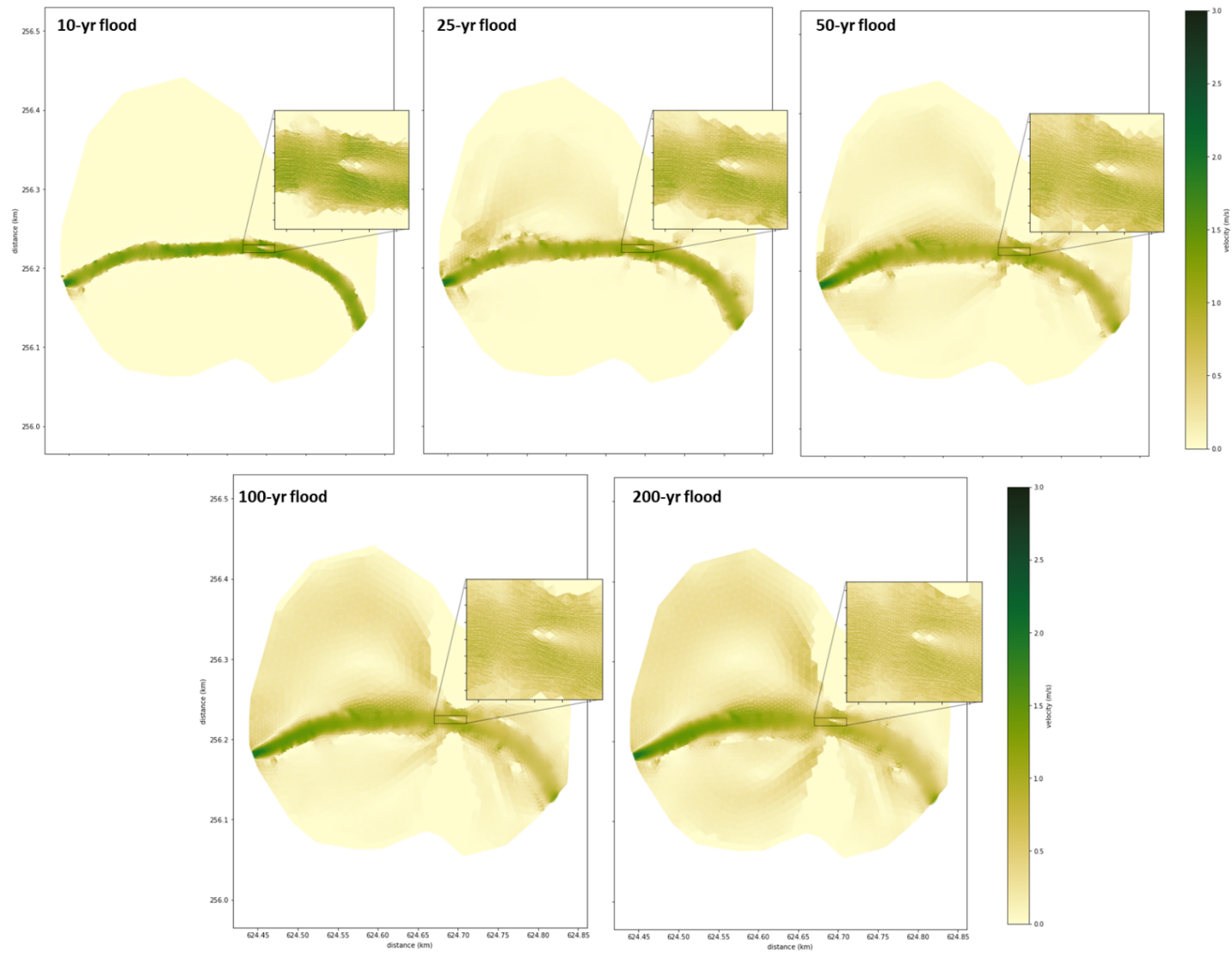


Figure 7. Flow velocity distribution over the spatial domain of Tar River in flood conditions

Middle Creek

In this section, we summarize the steps taken to find the hydrodynamic conditions around bridge number 500092 piers (Middle Creek). The same as the procedure for other selected sites, we analyzed the records of USGS gage number 02088000 to find the 25-, 50-, 100-, and 200-year flood characteristics for this location (Figure 8). We used the available 78 years of data (1940 - 2018) and our computed flood discharges were higher than the StreamStats application outputs which were derived from 72 years of data (1940 -2012), (Table 5). Due to computational issues and Delft3D limitations during Middle Creek modeling, we couldn't model flood conditions for this site.

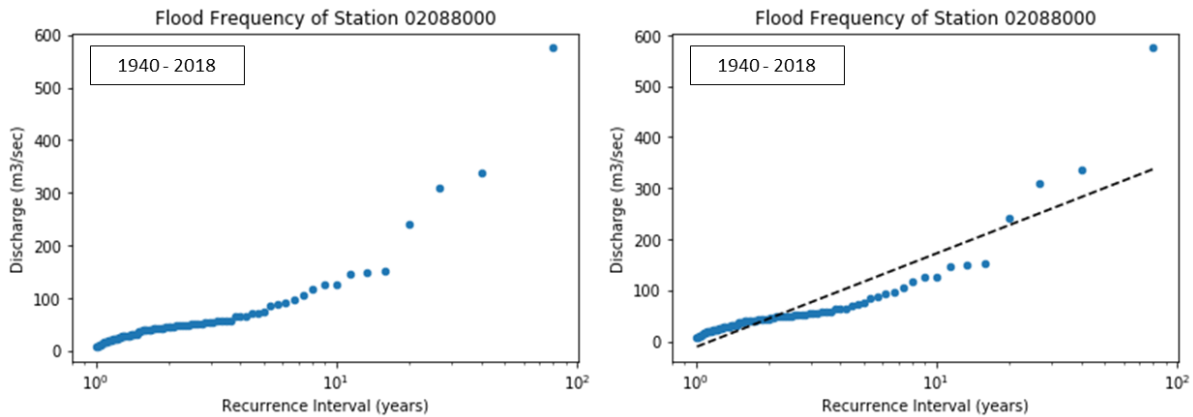


Figure 8. Extreme Value analysis applied to USGS gage number 02086849 records from 1982 to 2022

Table 5. Computed flood conditions vs. USGS StreamStats application (Ellerbe Creek)

Middle Creek/Gage 02088000	years of data	mean Discharge (m ³ /s)	10-yr flood (m ³ /s)	25-yr flood (m ³ /s)	50-yr flood (m ³ /s)	100-yr flood (m ³ /s)	200-yr flood (m ³ /s)
StreamStats application	72 (1940 - 2012)	2.6	114	169	218	276	345
Research Team Analysis	78 (1940 - 2018)	2.6	172	245	300	355	410

We set up an unstructured high-resolution mesh (cell sizes from 25 cm to 5m) for Middle Creek, bridge number 500092. After analyzing and smoothing LiDAR data in ArcMap and MATLAB, we used these data as the initial bed level for land area in our model. For river area, we used the latest river channel information from NCDOT Inspection Reports and integrated the river channel profile into the existing LiDAR topography. For input flow conditions, we have used data from USGS gage 02088000 to assess mean conditions (2.634 m³/s) in our initial hydrodynamic modeling. To isolate the impact of bridge piers, we have developed two models. One without the bridge piers (control case) and one with the piers.

The results of the initial hydrodynamic models suggest a decrease of upwards of 75% immediately downstream and behind the piers (the red area, Figure 9). However, in the contracted flow between the piers there is an increase in flow velocity, ~20% (from ~17 cm/s to ~23 cm/s), which suggests a higher bed shear stress and consequently, more potential erosion (Figure 9 and 10). This change in velocity from the piers under mean discharge only lasts about 50 m upstream and downstream of the piers. Middle Creek simulations have consistently crashed when running in morphodynamic mode. Dr. Castro-Bolinaga's team also had significant issues with modeling Middle Creek. We have run hydrodynamic mode only as a result.

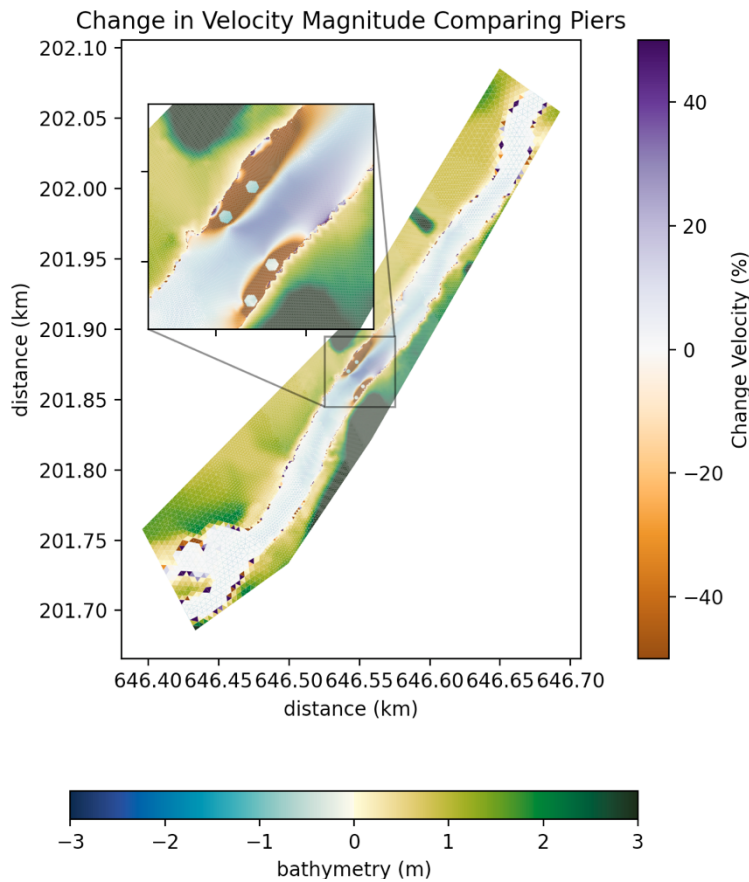


Figure 9. Percent change of velocity (red to blue colorbar on right) for mean discharge when adding in the piers superimposed on the underlying bathymetry of the model (blue to green colors see colorbar at bottom) with a zoomed in insert around the bridge location.

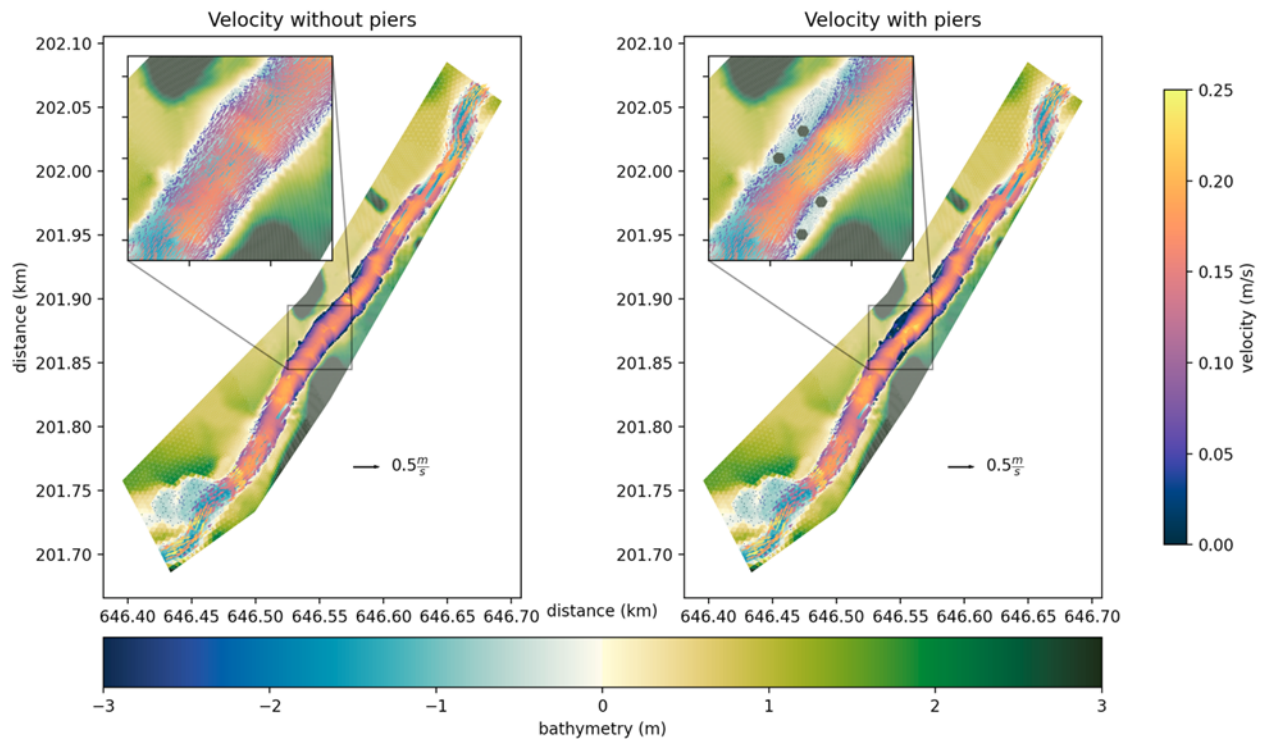


Figure 10. Quiver plots of depth averaged velocity (where the length and color of the arrows indicate velocity, see purple to yellow colorbar on right) superimposed on the underlying initial idealized bathymetry (see bottom colorbar with blues to greens for magnitude of bed elevation) for our mean discharge ($2.634 \text{ m}^3/\text{s}$) for both the control case (no piers) on the left and the experiment case (with piers) on the right. Insets showing zoomed in view of bridge location with piers visible on right image. All color and length scales are the same for all graphs.

Appendix I: Scour depth analysis by numerical modeling for Roanoke River

The computed maximum scour depth during the 10-yr, 25-yr, 50-yr, 100-yr, and 200-yr flood conditions at 1D, 2D, and 4D around the bridge piers on the outside and inside bend of the Roanoke River are as follows:

Table 1. The computed maximum scour depth during the **10-yr flood** at 1D, 2D, and 4D around the bridge piers on the outside and inside bend of the river

The pier closer to the outside bend of				The pier closer to the inside bend of			
Max scour depth (cm)	1D	2D	4D	Max scour depth (cm)	1D	2D	4D
Upstream	2.67	2.7	1.1	Upstream	4.1	1.8	1.5
Downstream	13.6	11.0	5.0	Downstream	18.3	8.6	6.8
Right side (inner bank)	0	0.1	0.1	Right side (outer bank)	0.2	0.5	0.5
Left side (outer bank)	0.1	0.8	0	Left side (inner bank)	0	0.1	0.5

Table 2. The computed maximum scour depth during the **25-yr flood** at 1D, 2D, and 4D around the bridge piers on the outside and inside bend of the river

The pier closer to the outside bend				The pier closer to the inside bend of			
Max scour depth (cm)	1D	2D	4D	Max scour depth (cm)	1D	2D	4D
Upstream	2.9	3.1	1.2	Upstream	4.5	2.0	1.7
Downstream	16.1	13.8	6.1	Downstream	22.7	10.3	8.7
Right side (inner bank)	0	0.2	0.3	Right side (outer bank)	0.6	0.1	0
Left side (outer bank)	0.3	0.8	0	Left side (inner bank)	0	0.1	0.2

Table 3. The computed maximum scour depth during the **50-yr flood** at 1D, 2D, and 4D around the bridge piers on the outside and inside bend of the river

The pier closer to the outside bend of				The pier closer to the inside bend of			
Max scour depth (cm)	1D	2D	4D	Max scour depth (cm)	1D	2D	4D
Upstream	3.3	3.7	1.4	Upstream	5.4	2.3	2.1
Downstream	19.2	17.4	7.7	Downstream	28.5	13.2	11.0
Right side (inner bank)	0.1	0.3	0.4	Right side (outer bank)	0.8	0.1	0
Left side (outer bank)	0.3	0	0	Left side (inner bank)	1.4	0.2	0.3

Table 4. The computed maximum scour depth during the **100-yr flood** at 1D, 2D, and 4D around the bridge piers on the outside and inside bend of the river

The pier closer to the outside bend of the river				The pier closer to the inside bend of the river			
Max scour depth (cm)	1D	2D	4D	Max scour depth (cm)	1D	2D	4D
Upstream	3.2	2.2	1.3	Upstream	5.1	3.5	1.8
Downstream	19.6	14.1	8.2	Downstream	28.8	17.4	10.9
Right side (inner bank)	0.1	0.5	.8	Right side (outer bank)	0.5	0.1	0.1
Left side (outer bank)	0.2	0.1	0.2	Left side (inner bank)	0	0.6	1.0

Table 5. The computed maximum scour depth during the **200-yr flood** at 1D, 2D, and 4D around the bridge piers on the outside and inside bend of the river

The pier closer to the **outside** bend

Max scour depth (cm)	1D	2D	4D
Upstream	3.8	3.4	1.7
Downstream	26.7	16.1	9.9
Right side (inner bank)	0.2	0	1.6
Left side (outer bank)	0	1.2	0.8

The pier closer to the **inside** bend of

Max scour depth (cm)	1D	2D	4D
Upstream	5.0	2.4	2.2
Downstream	27.2	17.3	10.1
Right side (outer bank)	0.2	1.0	1.2
Left side (inner bank)	0.5	0.5	1.7

This analysis indicates that the largest scour depths appear on the downstream of the piers in case of a flood condition. Also, we realized the further we go from the bridge piers the less the effect of the flood condition on scour depth will be.